A STUDY OF THE ROTATIONAL MOULDING OF LINEAR LOW DENSITY POLYETHYLENE

Vibhooti Ellis, B.Sc., Cert. Ed.

Submitted in partial fulfilment of
the requirements for the degree of
DOCTOR OF PHILOSOPHY

DE MONTFORT UNIVERSITY
in collaboration with
JOHN ORME COMPANY LIMITED

June 2004

ABSTRACT

Rotational Moulding of Linear Low Density Polyethylene – V Ellis, 2004

The aim of this investigation was to increase understanding of the rotational moulding process by studying the rotational moulding of linear low density polyethylene, and to thus contribute to the optimisation of the process.

A test moulding was selected as the standard. It was established that the heating cycle of the moulding can be divided into three well defined phases; mould induction, polymer fusion and melt densification. The processing conditions to give optimal physical properties in the moulding were determined as 1 ± 0.5 minute mould induction time, 5 ± 0.5 minutes fusion time, 7 ± 0.5 minutes densification time and a cooling cycle of 5 ± 0.5 minutes using a water spray. The optimum oven set temperature during the heating cycle was determined as 220° C. A quantitative study of the effects of oven set temperature and polymer mass on the three phases of the heating cycle was then made.

The oven set temperature was found to have the greatest effect on the melt densification phase. Increasing the temperature from 220° C to 330° C reduced the melt densification time from 6 ± 0.5 minutes to 1 ± 0.5 minutes. The oven set temperature of 330°C was found to be significant, in that the melt densification time was found to remain constant after this temperature, even for increasing polymer mass.

Increasing the oven set temperature from 220° C to 440° C reduced the heating cycle from 12 ± 0.5 minutes to 4 ± 0.5 minutes, without loss in yield stress. At 220° C oven set temperature, the melt densification phase was found to be the longest and hence the rate determining step of the heating cycle. At 440° C the fusion phase was measured as the longest phase.

The fusion time of the moulding was found to be directly proportional to the polymer mass. However, contrary to expectation, the overall heating cycle did not show a linear relationship with increasing polymer mass.

During the fusion process particle boundaries were found to be completely eliminated, contrary to some reports that complete boundary elimination is not possible in low density polyethylene. The yield stress at oven set temperatures of 220° C and 330° C was found to be unaffected by the presence of bubbles in the moulding wall. However, elongation at break was reduced at the higher temperature.

The degree of crystallinity and spherulitic size were found to increase at the higher processing temperature of 440° C, and a slower cooling rate (achieved by rotating mould in ambient air conditions for 15 ± 0.5 minutes.)

A description of polymer fusion processes in a typical heating cycle has been made. A statement of the heat transfer processes in a typical moulding cycle, was made for any future mathematical modelling of the process. The thermal properties of linear low density polyethylene and mould necessary in heat transfer calculations were also established, and the thermal conductivity of the polyethylene measured. A method for measuring the thermal conductivity of polyethylene powder under steady state conditions was developed.

Finally, the isotropy of physical properties of rotational mouldings (in the plane of the wall), until now only assumed but not proven, was established by measuring stress at yield of rotationally moulded samples cut at right angles to each other.

DECLARATION

The work carried out in this thesis, unless otherwise stated, is original and was carried out in De Montfort University and John Orme Company.

The material included in this dissertation has not been submitted wholly or in part for any academic award or qualification other than that for which it is now submitted.

During the period of registered study in which this thesis was prepared, the author has not been registered for any other academic award or qualification.

V. Ellis

June 2004

ACKNOWLEDGMENTS

I would like to record my sincere thanks to the following people, without whose help this project would not have been possible.

Dr. B. C. Cope and Dr. J. Comyn for their guidance and encouragement as supervisors throughout this work.

Professor R. Linford for his understanding and support.

John Orme Company for their support, funding assistance and use of their facilities for the practical work.

CONTENTS

Chapter 1. Introduction

		Page
1.1.	The rotational moulding process	2
1.2.	Description of the rotational moulding process	4
	1.2.1. Rotational moulding criteria	4
1.3.	Basic steps of the rotational moulding process	5
1.4.	Polymers suitable for rotational moulding	7
1.5.	Rotational moulding equipment	10
	1.5.1. Rotational moulds	14
	1.5.2. Mould heating systems	17
	1.5.3. Mould cooling	18
	1.5.4. Mould venting	18
	1.5.5. Mould rotation	19
	1.5.6. Mould release agents	19
1.6.	Advantages and disadvantages of rotational moulding	21
1.7.	Background	25
1.8.	Literature survey	31
	1.8.1. Polymer particle fusion and melting	38
	1.8.1.1. Polymer sintering and melt densification models	43
	1.8.1.2. Surface levelling	57
	1.8.2. Bubbles in rotational moulding	58
	1.8.3. Thermal conductivity of polyethylene	61
	1.8.3.1 Thermal conductivity of polyethylene powder	65
1.9.	Aim of research programme	66

Chapter 2. Technical analysis of the rotational moulding process

Page

2.1. Polymer parameters 70

2.1.1 Polyethylene powder characteristics 70
2.1.2 Bulk density and dry flow 71
2.1.3 Melt flow index 72

2.2. The heating cycle 72

2.2.1 Effect of process variables on the heating cycle 74

2.3. The cooling cycle 75

2.4. Heat transfer in the rotational moulding process 76

2.4.1. Thermal properties 77

2.5. Effect of processing conditions on physical properties 78

2.5.1. Crystallinity in rotational mouldings 79
2.5.2. Isotropy in rotational moulding 79

Chapter 3. Experimental Procedure

		Page
3.1.	Programme of work	82
3.2	Materials and equipment	84
	3.2.1. Linear low density polyethylene	84
	3.2.2. Rotational moulding machine	84
	3.2.3. Rotational mould	86
	3.2.4. Release agent	86
3.3	Assessment techniques	88
	3.3.1. Sieve analysis	88
	3.3.2. Apparent density and flow of powder	88
	3.3.3. Melt flow properties	89
	3.3.4. Temperature measurement using a thermocouple	89
	3.3.5. Thermal imaging with infra red	89
	3.3.6. Mechanical testing of polymers	92
	3.3.7. Transmitted light microscopy	92
	3.3.8. Degree of crystallinity by density measurement	93
	3.3.9. Thermal conductivity of polyethylene	94

Chapter 4. Results and Discussion

	Page
4.1. Physical properties of the polymer	97
4.1.1. Particle shape	97
4.1.2. Particle size distribution	97
4.1.3. Bulk density and rheology	97
4.2. Heating cycle of standard moulding	102
4.2.1. Examination of mouldings with scanning electron microscopy	102
4.2.2. Apparent density	102
4.3. Process variables in the heating cycle	102
4.3.1. Mould induction phase	117
4.3.2. Polymer fusion phase	121
4.3.3. Melt densification phase	125
4.4. Crystallinity in mouldings	132
4.4.1. Effect of cooling rate on spherulitic size	132
4.4.2. Degree of crystallinity	135
4.4.2.1. Effect of cooling rate	135
4.4.2.2. Effect of oven set temperature	135
4.4.2.3. Variation with moulding surface	135
4.5. Tensile properties	135
4.5.1. Isotropy in rotational mouldings	139
4.6. Thermal conductivity of polyethylene	145

Chapter 5. Discussion

Page

5.1. Physical properties of polymer 148

5.1.1. Particle shape 148
5.1.2. Particle size distribution 150
5.1.3. Bulk density and rheology 153

5.2. Heating cycle of the standard moulding 156

5.2.1. Effect of process variables on the heating cycle 162

5.2.1.1. Mould induction phase 166
5.2.1.2. Fusion phase 167
5.2.1.3. Melt densification phase 169

5.3. Heat transfer in the rotational moulding process 172

5.3.1. The heating cycle 174

5.3.1.1. The mould induction phase 174
5.3.1.2. The polymer fusion phase 179
5.3.1.3. The melt densification phase 189

5.3.2. The cooling cycle 189
5.3.3. Other heat transfer models 196

5.4. Crystallinity in rotational moulding 200

5.4.1. Spherulitic morphology 200
5.4.2. Degree of crystallinity 207

5.4.2.1. Effect of crystallisation temperature and cooling rate 207
5.4.2.2. Variation of crystallinity with moulding surface 211

5.5. Effect of processing conditions on tensile properties 213

5.5.1. Isotropy in rotational mouldings 216

5.6. Principal sources of error 219

5.7. Conclusions 221

5.7.1. Physical properties of the polymer 221
5.7.2. Heating cycle 222
5.7.3. Crystallinity 223
5.7.4. Tensile properties 224
5.7.5. Thermal properties 225

5.8 Further work 225

References 227

CHAPTER 1

INTRODUCTION

1.1. The rotational moulding process

Rotational moulding is a unique and an important polymer processing method for producing hollow, seamless mouldings. In 1998, Spence [201] reported its growth rate as phenomenal. It is currently one of the fastest growing of all polymer processing techniques; in 2001 its annual growth rate was estimated to be in the region of 10 to 12%. [225].

Advances in process control [228] reported in 1992, mean that rotational moulding now offers a very competitive alternative to other established polymer processing methods, such as injection and blow moulding. The process is widely believed to have the most exciting potential for further development and improvement.

The process is capable of producing complex, thin-walled hollow mouldings in small sizes (e.g. a doll's eye) and extremely large sizes (e.g. 21,000 litre storage tanks), otherwise impossible to produce by other methods [148]. Complex geometries not possible by other polymer processes are widely produced by rotational moulding [148].

Rotational moulding has several unique features that separates it from other major processing techniques. The first is that the moulding is formed by heating the polymer in a rotating mould. The mould is heated from room temperature up to the melt temperature range of the polymer and then back again. Mould rotation is continued

throughout the cycle and is bi-axial, in two perpendicular planes and distributes the polymer completely and evenly over the inner mould surface.

The second unique feature of this process is that the moulding, unlike other major plastics processing techniques, is achieved without using high pressure to inject the polymer melt into the mould. No pressure is used at any stage of the moulding, and even centrifugal forces are avoided by keeping the mould rotation speeds low. The polymer experiences only low atmospheric pressures and low shear rates, which have been estimated to be as low as 1×10^{-4} s^{-1} [170]. Mould rotation speeds are typically four to twenty revolutions per minute and, depending on the shape of the moulding, are set at differing values along the two axes. Typical examples are given in Table 1.

The third unique feature of the rotational moulding process is that the polymer is used in powdered form, not as pellets. The powder usually contains a range of particle sizes from below 149μm up to 500μm.

Examples of rotationally moulded products include large tanks, water and other large containers, medical equipment, cleaning equipment, lawn and garden equipment, automotive (including the car body), aeroplane parts, toys, playground equipment, displays, boats, child care products, military equipment, insulated containers and protective packaging [187].

1.2. Description of the rotational moulding process

Finely ground polymer is loaded and heated in a biaxially rotating mould. The polymer starts as a pool of powder at the bottom of the mould cavity. As the mould rotates through the two axes, all surfaces of the cavity repeatedly come into contact with the powder pool. As the mould temperature increases to the polymer melt temperature range, the polymer particles adhere, sinter and melt onto the cavity wall. When the melting is complete, the rotating mould assembly is cooled to room temperature and the moulding removed. The processing cycle can now begin again. Typically, the mould is cooled using a combination of high-speed air fans and water mist to solidify the polymer.

Polymers used are mainly thermoplastic, but some thermosets have also been tried [see Section 1.4]. If liquid polymers such as vinyl plastisols are used, the process is then known as slush moulding.

1.2.1. Rotational moulding criteria

Commercially, the general criteria for selecting the rotational moulding process are:

- Fabrication of hollow moulding with a large surface area which would require extensive tool design and complicated moulds [227].
- Fabrication of hollow items having complex shapes such as convoluted wall sections , undercuts, or similar irregularities that would make mould design difficult,

and present production problems.

- The manufacture of relatively large items subject to widely varying production schedules such as those related to seasonal cycles, or uncertain contracts.
- When the volume of production is too small to warrant sizeable investment in expensive tooling.
- When the item is subject to unpredictable changes in styling.
- When identical mouldings or different parts of a moulding are required in different colours.

1.3. Basic steps of the rotational moulding process

Four basic steps are involved in the rotational moulding process, see Figure 1.

1. Loading

The mould is treated with a release agent and filled with a measured mass of the polymer. This is known as 'charging' the mould. The mass of the polymer is determined by the volume and the wall thickness of the moulding. The mould is now allowed to rotate.

2. The heating cycle

After loading, the rotating mould is transferred to a heated isothermal oven, set at a temperature above the melting point of the polymer. Typical oven set temperatures are

FIGURE 1

SCHEMATIC REPRESENTATION OF THE ROTATIONAL MOULDING PROCESS

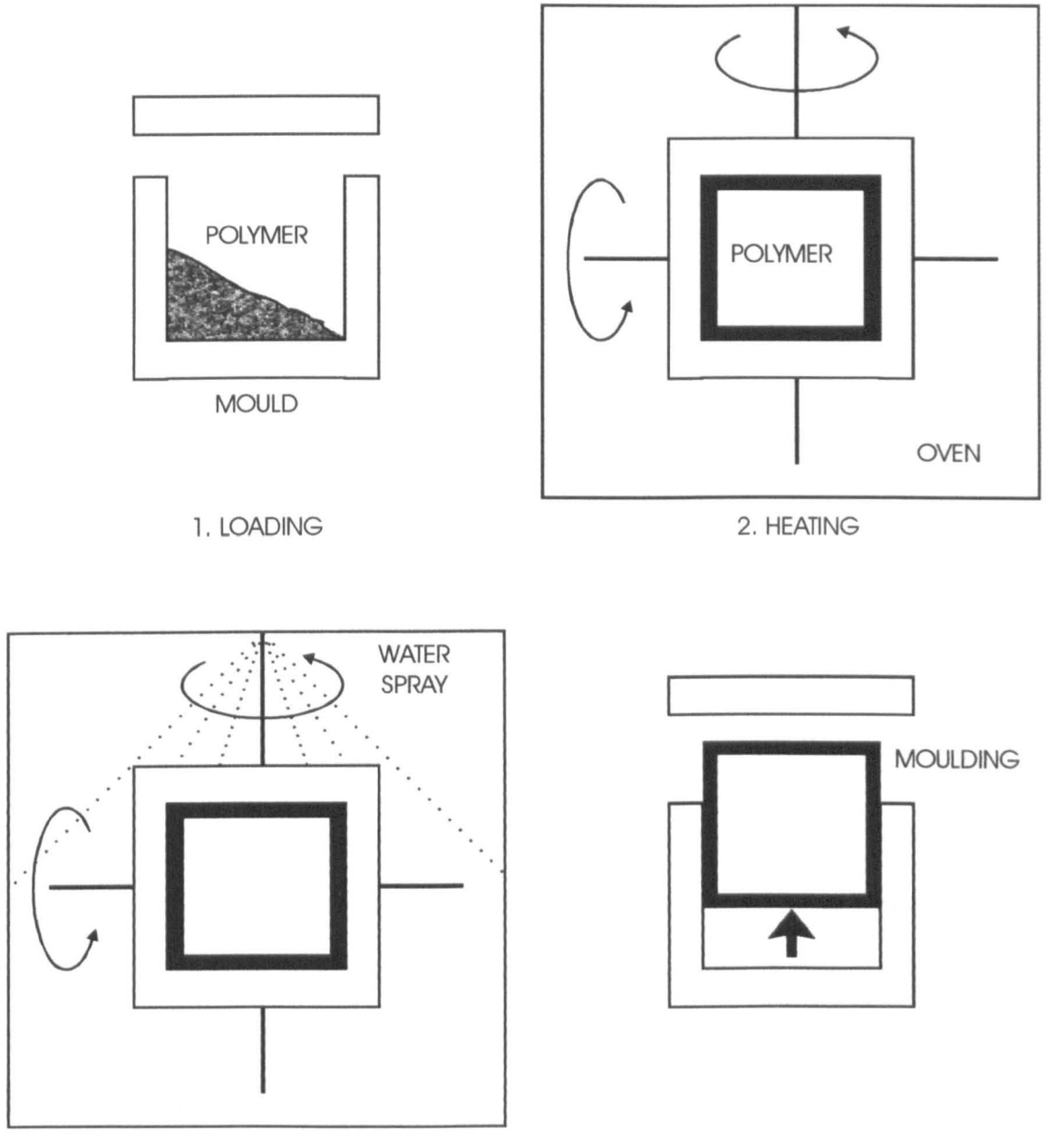

between 200° C and 400° C.

3. The cooling cycle

When the polymer has melted into a homogeneous layer covering the inner walls of the mould, it is removed into the cooling chamber and allowed to cool. The rotation of the mould is continued until the polymer has solidified.

4. Unloading

Unloading is usually accomplished manually. Compressed air is sometimes used to eject the moulding.

1.4. Polymers suitable for rotational moulding

Two criteria have to be met before a polymer can be rotationally moulded. First the polymer must be available in a powdered form and the flow properties of both powder and melt must allow it to coat the inner mould surface evenly. Secondly, because the polymer is subject to high temperatures and long heating cycles, it must also be thermally stable at the high processing temperatures [229]. Thermal degradation effects have limited the use of some polymers [229].

At present the most commonly used polymer is polyethylene [2, 41, 56, 73, 82, 83, 84], and it accounts for over 90% of the total tonnage of plastics used in the rotational

moulding industry [211].

The first rotational moulding grades of polyethylene were produced in the 1950's. This was the result of development in two areas; polyethylene with suitable chemical and rheological properties, and a grinding process for producing polyethylene powder with suitable particle size and particle size distribution [230].

All types of polyethylenes including crosslinkable polyethyene [10] are moulded. However, linear low-density polyethylene (LLDPE) contributes the largest volume now being moulded. This is because polyethylenes easily meet the criteria set out at the beginning of this section. In addition, they have good impact strength and excellent environmental stress crack resistance. The disadvantage of mechanical properties such as a low elastic modulus (stiffness) can be compensated through the use geometric factors, some of which are unique to rotational moulding [159, 211]. Work on high density polyethylene [1] and foamed polyethylene is also reported [15, 38], including metallocene polyethylene foams [232]. Normally chemical blowing agents are used to generate the cellular structure in foamed polymers. However, work on using microspheres for creating the foam structure is also reported [233]. Microspheres are very small hollow glass or ceramic based beads which, when used in foaming, results in microcellular structure.

Polyvinyl Chloride (PVC) in plastisol and rigid form, [43, 85, 86, 242] is reported to be the second largest volume material, followed by Nylon 6,11 and 12 [40, 42] with polycarbonate as the fourth largest volume polymer used in rotational moulding.

Other polymers being investigated include polystyrene and high impact polystyrene [36] ethylene vinyl acetate, crosslinked high density polyethylene [4, 41, 74] and crosslinked medium density polyethylene [52]. Work on glass reinforced polyethylene is also reported [14].

Other materials used in smaller quantities are ionomers, acetal [5, 173], ABS [37] polyurethane [221], polyester, polycarbonate [247], polypropylene, chlorinated polyether, epoxy and acrylonitrile based polymers [213]. The latest additions are fluoropolymers [39, 44], caprolactams [75], glass reinforced polymers [14], including short fibre reinforced thermoset polymers.

Some work on linear polyethylene modified with elastomers and fillers is reported by Vasudeo [196] and Robert et al [172]. The use of wood fibres as potential fillers in the rotational moulding of polyethylene has also been investigated [190].

The limitations of some fillers (e.g. uneven distribution of short glass fibres) in rotational moulding has been highlighted by Martin et al [229]. In this and another paper [231], the authors report work on polymer-clay nanocomposites as possible new materials that overcome the limitations of glass fibres and other mineral fillers for rotational moulding. Nanocomposites are polymers to which silicate clays have been added to manipulate the structure of the polymer at a nanoscopic scale.

Wang et al [179] and Takacs et al [180] report that metallocene grades of polyethylene 'offer exciting opportunities for the rotational moulding industry'. These new

generation grades of polyethylene are produced by metallocene catalyst systems and are of great interest to the plastics industry. This is because of their unique characteristics such as a narrower molecular weight distribution (MWD). Polymers with a narrow MWD are not sensitive to shear rate giving them poor processability, except for rotational moulding where only zero shear rate viscosity is important, and the variation of viscosity with shear rate is irrelevant.

Although powdered polymers remain the main form of raw material used, in recent years interest has also grown in the rotational moulding of reactive liquid polymers [81, 235]. Reactive rotational moulding is the moulding of a liquid, which undergoes a chemical reaction to form the solid polymer. This method makes it possible to mould polymers, which have been otherwise difficult to rotationally mould.

1.5. Rotational moulding equipment

The equipment, which constitutes a rotational moulding system, includes the necessary machinery required to transport the mould(s) through the four basic steps of the process, shown diagrammatically in Figure 2.

The simplest type of rotational moulding machine is the single spindle machine and this is normally used for moulding prototypes or for small production runs. Two designs are possible; the pivot type, Figure 3, and the straight-line machine, Figure 4. Figure 13 (Section 3.2.2) is a photograph of the straight-line, single spindle machine used in the study.

FIGURE 2

SCHEMATIC REPRESENTATION OF THE ROTATIONAL MOULDING MACHINE

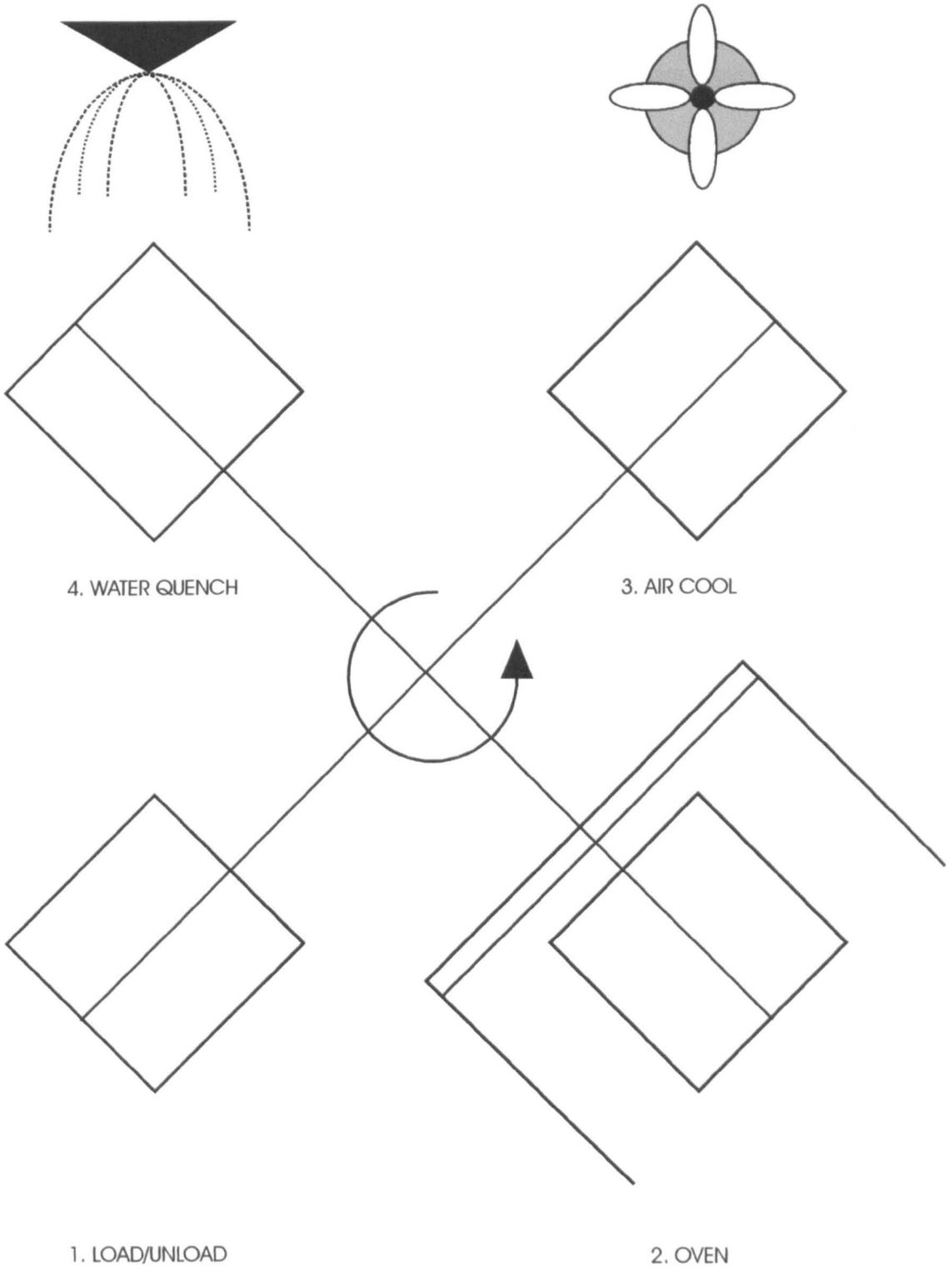

FIGURE 3

THE PIVOT TYPE SINGLE SPINDLE ROTATIONAL MOULDING MACHINE

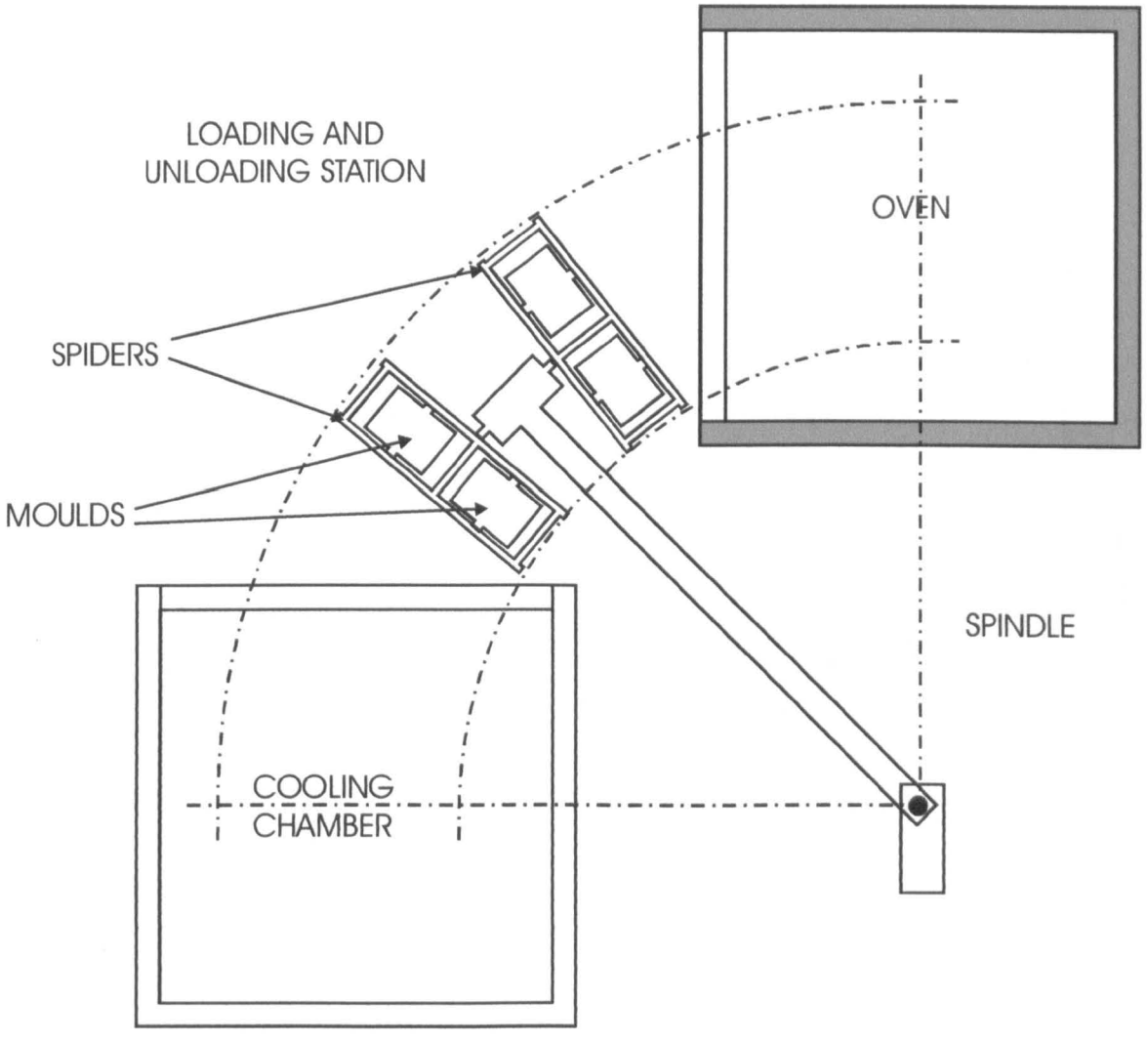

FIGURE 4

THE STRAIGHT-LINE TYPE SINGLE SPINDLE ROTATIONAL MOULDING MACHINE

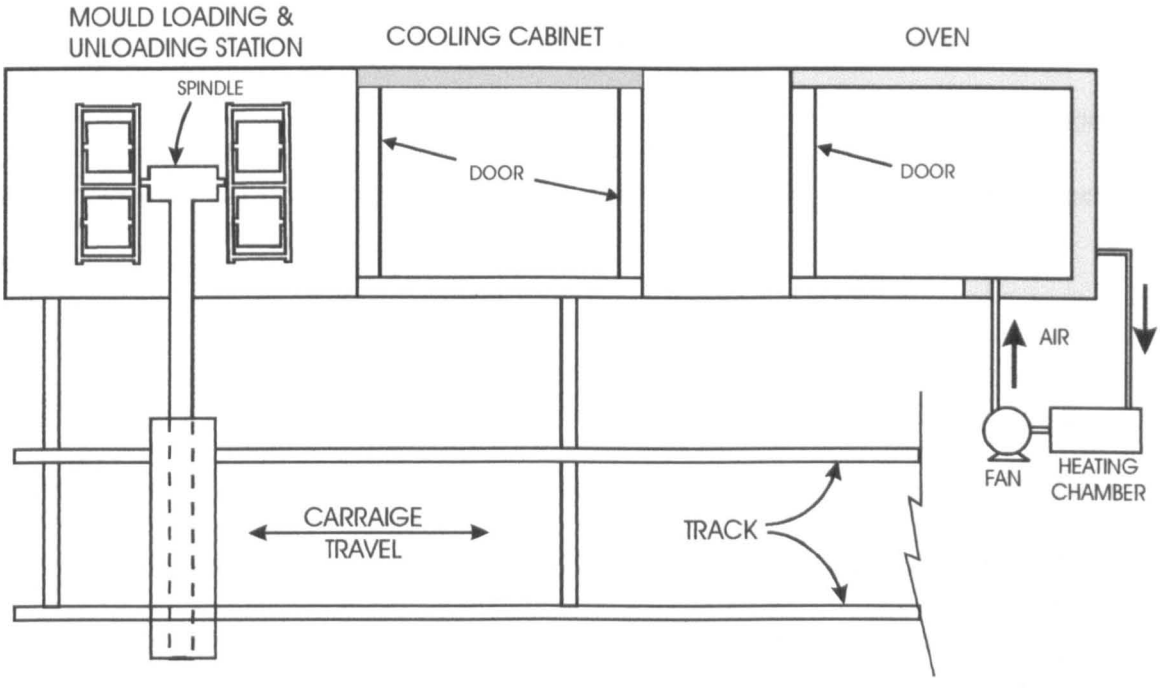

Machines (except straight-line machines) used commercially have two or more spindles to allow four steps of the rotational moulding process to take place simultaneously [19]. These machines are of either a carousel or a ferris wheel type. A three spindle machine is the most popular rotational moulding machine [69]. Here, a three-position cycle is used: the first spindle in the oven, the second in the cooling station and the third for loading and unloading. Figure 5 and Figure 6 show examples of a commercial three arm carousel machine and a Ferris wheel machine.

Rotational moulding machinery is sometimes classified as continuous or batch type [24]. In the batch type, the moulds are pushed manually from oven to cooling chamber over roller conveyers. In the continuous type, the moulds move automatically between the various stations.

The open flame or 'rock and roll' machine, uses a combination of uniaxial rotation in one direction and a rocking motion in the other. The mould is heated by a gas-fired burner, which is applied directly to the mould. This type of equipment is simple; operation and control are normally manual and the processing conditions crude. However, the low equipment cost makes the rotational moulding of some products economical.

1.5.1. Rotational moulds

Rotational moulds are of simple construction because little internal pressure develops during the cycle, and coring of the mould walls for water cooling channels is

FIGURE 5

THE THREE ARM CAROUSEL ROTATIONAL MOULDING MACHINE

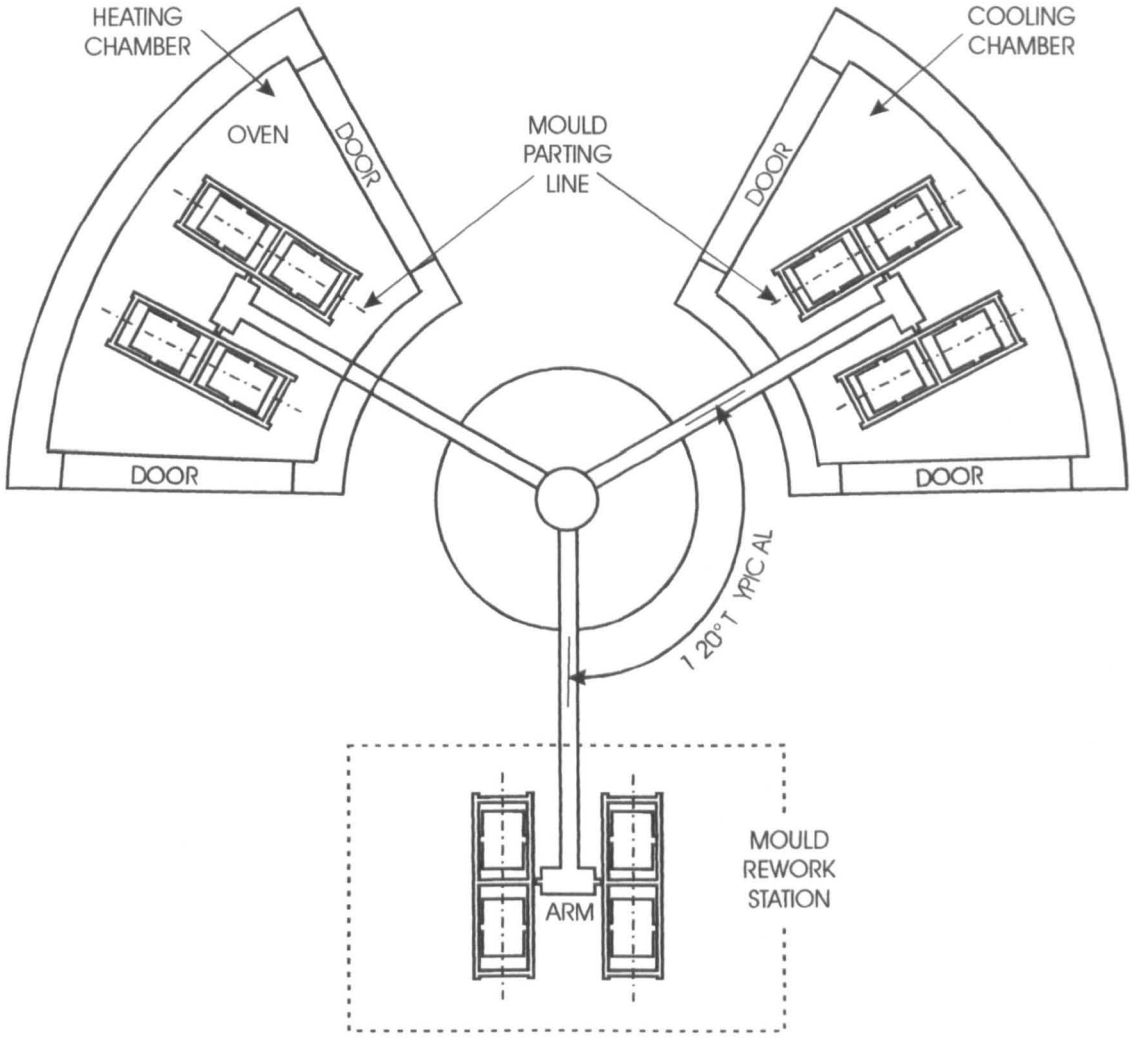

FIGURE 6

THE FERRIS WHEEL ROTATIONAL MOULDING MACHINE

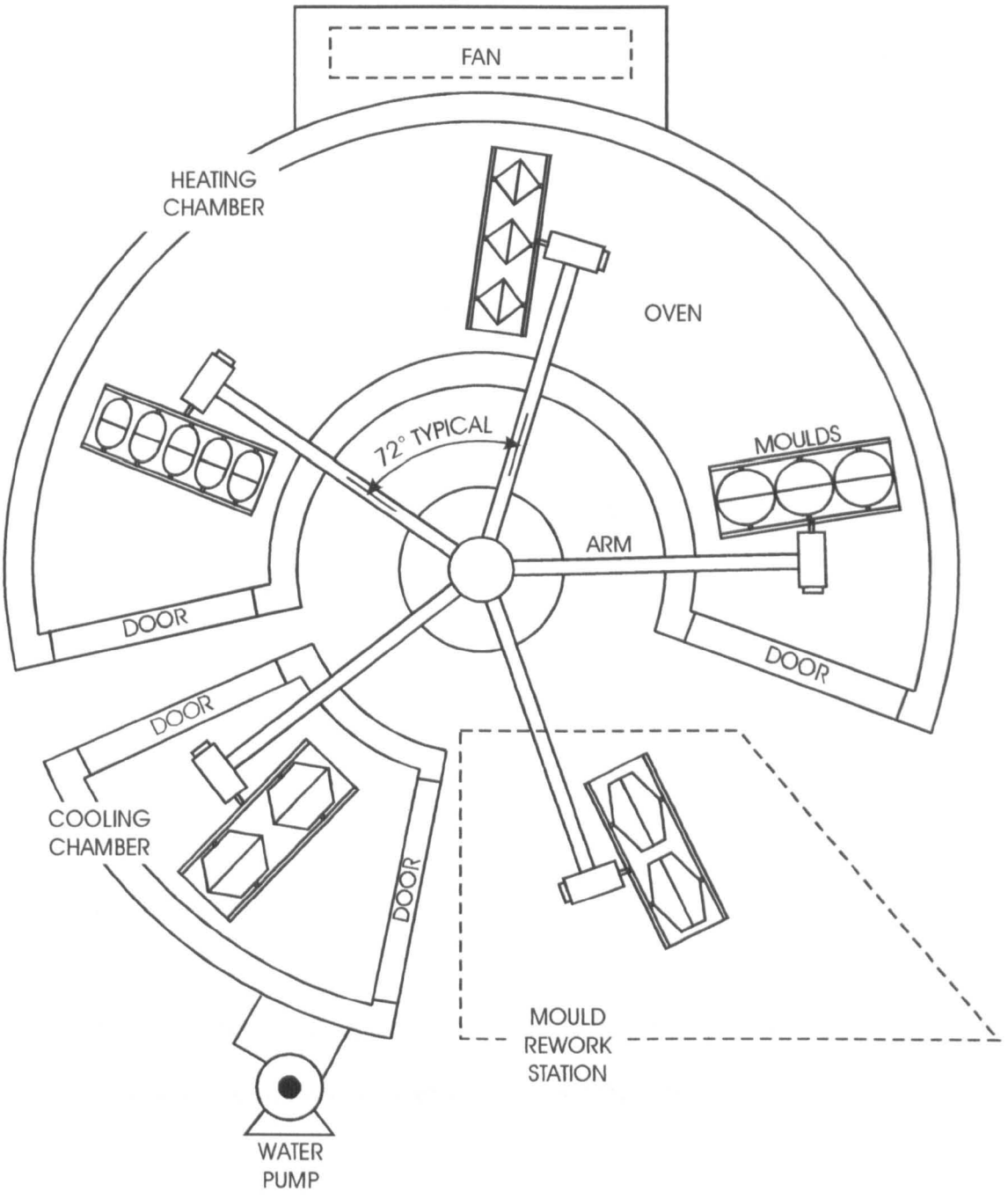

unnecessary [71].

Rotational moulds are made of low density, non porous metals to prevent water or air being drawn into the polymer through the pores. Metals are used because of their high thermal conductivity and high resistance to thermal shock. This is important as the mould temperature can vary from room to above 400° C in a typical moulding cycle.

The most widely used metals are cast aluminium, welded sheet aluminium, mild steel, electroformed nickel and copper lined with nickel [7]. The advantages of each material are widely reported [7, 24, 25]. Some work on glass fibre reinforced epoxy mould is also reported [32].

The surface finish of the moulding can be varied from high gloss to matt by polishing or sand blasting the mould surface.

The development of a latch for moulds to make the loading and unloading easier and quicker is reported [76].

1.5.2. Mould heating systems

Four main heating methods have been developed; hot air convection, hot liquid conduction, infra red radiation and direct gas jet flame [18, 20, 28, 69].

Hot air convection is the most widely used method [24, 11]. Hot air produced by a

flame is directed over the rotating mould in the oven. Most ovens use gas as the basic fuel [17]. For efficient heat transfer and to achieve uniform wall thickness in the moulding, the air velocity must be high and airflow directed accurately over the mould [69]. An analysis of heating efficiency in rotational moulding is reported by Crawford [149].

1.5.3. Mould cooling

Uniformity of mould cooling is important and the three most commonly used methods are water spray, highly atomised water spray and air-cooling [11, 31]. Internal cooling is also used for polymers that are susceptible to oxidative degradation at low temperatures [25, 11]. A possible internal coolant is carbon dioxide and this has been successfully used in blow moulding. A thin walled moulding can be cooled in a few seconds by this method [1].

1.5.4. Mould venting

Rotational moulds are usually vented so that atmospheric pressure is maintained inside the mould during the processing cycle [11]. An increase in pressure could result in uneven distribution of the melt. Venting also prevents the formation of a partial vacuum during the cooling cycle, which may cause air to be drawn into the polymer melt at the parting line and become entrapped as bubbles in the wall of the moulding. However, very low pressure inside the mould can cause the moulding to detach from the mould wall and collapse, and hence thermal contact is lost.

The mould vent is thin and is made from a stainless steel or a fluorocarbon polymer tube. It is designed to enter the mould where the opening will not detract from the appearance or function of the moulding, see Figure 14 (Section 3.2.3).

1.5.5 Mould rotation

The axis along which the spindle turns and the axis along which the mould turns are termed respectively the major and minor axes. Separate drive systems allow independent control of each axis so that different ratios of the major to minor can be set.

Rotational speed and ratio are important variables in the moulding process; proper rotational speeds are necessary to achieve a uniform wall distribution [25]. Generally the speed is a function of the polymer flow properties and the ratio is a function of the moulding shape [23]. Accurate control of mould rotation is reported as especially important for thin walled or unusually shaped mouldings [53, 23]. The two speeds of rotation are set so that one is four times greater than the other [3, 53]. This ratio has been found to be successful for most regularly shaped mouldings [23, 24]. Typical examples of rotational speeds set for common mouldings are given in Table 1.

1.5.6. Mould release agents

Mould release agents are important in the rotational moulding process, as they facilitate the removal of the moulding from the mould, unlike for example, in the injection moulding process where ejector pins may be present to expel the moulding. No such

TABLE 1.

TYPICAL ROTATION SPEEDS OF MAJOR AND MINOR AXIS

Shapes	Speed rpm	
	Major axis	**Minor Axis**
Oblongs (horizontal mounted), straight tubes	8	9
Some defroster ducts	5	6
Balls or globes	8	9.75
Any shape showing over-lapping lines of rotation at 4 to 1.	10 12	12.25 14.5
Cubes, balls, odd shapes Rectangular boxes, horses with bent legs	8 10	10 12.5
Rings, tyres, balls. Any rectangle which shows two or more thin sides when run at 4 to 1. Picture frames, manikins, round flat shapes. Horses with straight legs Auto crash pads (vertically mounted.)	6 8 10 12	9 12 15 18
Parts which should run at 2 to 1 but show thin side walls.	5 7	15 21
Flat rectangles (gas tanks, suitcases, tote bin covers.)	4 6 9.6	15 22.5 36
Tyres, curved air ducts. Pipe angles, flat rectangles. Balls whose sides are thin at 4 to 1.	4 5 6	20 25 30
Vertical mounted cylinders.	4	24

mechanism can be built into rotational moulds.

Reference 226 is a discussion of the relative merits of various commercially available release agents.

1.6. Advantages and disadvantages of rotational moulding

Advantages

(i) Wall thickness

The nature of the polymer fusion process is reported to result in unusually uniform wall thickness [33, 58, 211]. Dimensional tolerances of walls are also easily controllable. This is in contrast to, for example blow moulding, where significant variation in wall thickness is well known [77]. Another main advantage of the rotational moulding process is that the wall thickness of a moulding can be changed without changing the mould.

Wall thickness within a moulding can be varied by insulating relevant areas of the mould. Radiussed corners of the moulding are filled by polymer melt to a greater thickness, increasing the strength of the moulding [24,33]. This is an important characteristic of the process [34].

(ii) Design freedom

The rotational moulding process is reported to allow greater design freedom than any other processing technique [24]. For example, draft, a critical factor in the design of blow and injection mouldings is unnecessary in rotational moulding [32].

Rotational moulding is also applicable to mouldings of complex shapes, multiple parts and other configurations such as undercuts and inserts [11, 24, 70, 216]. Also possible are double walled parts [11, 31], that can be foam filled to decrease thermal conductivity and increase the load bearing properties of the moulding. Double walled mouldings, where each wall is made of a different polymer, are also possible [9, 16].

The development of the rotational moulding of inert fluorocarbon polymers overcomes limitations set by other methods in the prevention of corrosion [39].

(iii) Size and economics

Rotational moulding is reported to be the most economic method for producing large mouldings [2, 4, 9, 23, 32, 42]. In addition, the size of the moulding that can be produced by rotational moulding, exceeds any other forming process in operation today [2], and no upper limit on the size has yet been set [2, 33].

(iv) Rotational moulds

Low processing pressures mean the mould design is simple, and cheap materials such as sheet metal or cast aluminium may be used [9]. Moulds are manufactured with shorter lead-time [79] and prototype moulds are cheap to produce [9, 11]. In fact, initial capital investment in both equipment and moulds is significantly smaller than with other processing techniques, even for small production volumes [1, 2, 45]. For example, compared to injection moulding, mould costs are typically one-fifth of the cost. Additionally, the cost difference between the two moulds becomes much more significant as the moulding size increases [211]

(v) Miscellaneous advantages

Other miscellaneous advantages are listed as follows:

- Very little flow of the polymer during forming means an absence of flow lines, which improve the appearance of the moulding. Lack of weld lines adjacent to inserts or openings also improve the strength of the moulding.
- Mouldings are frequently produced in one step, which also eliminates the need for secondary operations such as part trimmings [11, 25]. Enclosed parts, like tanks, can be produced in one piece [46,45]
- Moulds of different size and shape may be run simultaneously on the same equipment and multicavity moulds may be used to produce small items individually [2, 11, 31].

- Plastic and metal inserts often can be moulded as integral parts of the item.
- Little or no waste scrap is produced.
- There is minimal cross sectional deformation and warpage in moulding.
- Mouldings are relatively stress free (see Section 2.1.1.)
- The process is ideally suited to economic short production runs, with an increasing role in prototype work for other processes.
- A recent development is the production of a moulding with different, but compatible materials. This is done with a 'dump box' inside the mould. This is a container holding a second (or third) polymer inside the mould. The second is then released partway through the moulding cycle; this produces a moulding with different, but compatible polymers [211]
- Finally, mouldings with colour and special effects are possible [218]

Disadvantages

The disadvantages of rotational moulding are briefly summarised as follows:

- Moulding cycles are longer than other processes
- Labour is intensive due to manual loading and unloading of moulds, although automation is slowly being introduced
- It is difficult to mould parts with varying wall thickness.

1.7. Background

It is believed that the origin of rotational moulding can be traced back to the Egyptian times [80]. In the 18th century, the process was believed to be used in the production of hollow Chinese figures.

The first recorded mention of the use of heat and biaxial rotation to produce a hollow part, is an 1865 British patent that describes the forming of hollow metal artillery projectiles [148].

Another patent was applied for in 1895 by an Englishman named Peters [222]. This patent describes a hollow mould rotating along two axes at 90°, connected by a pair of barrel gears, in which a metal or other substance in a fluid or semi fluid state is poured.

Two more patents followed; one by Voelke in 1905 describing the use of the process to mould wax and the other in 1910 by Baker and Perks, involving the rotational casting of chocolate eggs. The first patent to mention the now accepted 4 to 1 ratio between speeds of primary and secondary axes was Powell in 1920. He also stressed the importance of avoiding centrifugal force by keeping the speed of the mould rotation low.

With reference to rotational moulding equipment, the first mention of a machine that resembles the currently used rotational moulding machinery appears in a 1935 British patent. This patent relates to the production of hollow latex objects and forms the basis

of modern rotational moulding machines [148].

However, despite developments in rotational moulding machinery, at this time there were no suitable plastic materials and the process was used and refined by the rubber industry.

In the 1940's vinyl plastisols were introduced as suitable materials and this marked the origin of rotational moulding of thermoplastics. The first mention of this was made in 1941 in a patent issued to Clewell and Fields. This patent (except for minor differences) covers all elements of rotationally moulding vinyl plastisols. The period from the 1940's to the late 1950's saw the true development of vinyl plastisol moulding, with many patents being filed.

However, due to the inherent low strength and stiffness of vinyl plastisols, the process was considered to be specialised and limited to non-technical or non-engineering applications, such as consumer products (e.g. toys and advertising displays) [11, 34]. Another common application then was the moulding of road cones.

The potential of rotational moulding for wider industrial applications was not considered until the development of powdered thermoplastics, and the development of more accurate rotational moulding equipment. After this, the process began to be considered with the other major thermoplastics processing techniques available for forming hollow objects: blow moulding, injection moulding and thermoforming. Since then, its application has reached a phenomenal growth, with product emphasis turning

to more technical applications [29]. As stated in Section 1.1, in 2001 the rotational moulding industry was reported to be growing at a rate of approximately 10% per annum [225].

There is some contradiction in the literature concerning the exact beginning of vinyl plastisol moulding. The period is quoted by Throne as being late 1930's to early 1940's [54]. Beall [148] states it began in 1946 with introduction of vinyl plastisols by the Union Carbide Company.

However, more important to the present discussion, and something all sources agree on, is that rotational moulding of powdered thermoplastics did not begin until the 1960's, when two symposia by USI Chemicals (now the Quantum Corporation)[223, 224] highlighted the potential of rotationally moulding low density polyethylene powders.

This marked the beginning of the rotational moulding of powdered polymers. Since then the application of the process has grown to include other polymers, (Section 1.4.), and by the mid-1970s, rotational moulding had become a primary plastics processing technique [148]. In the following twenty years, the growth of the rotational moulding industry in terms of the number of moulders setting up, was on average faster than the growth of the rest of the plastics industry [148].

Despite this growth and, as stated in Section 1.1, that rotational moulding has the greatest potential for development [24, 25, 26, 72], compared to other processes,

systematic investigation or technical development of the process has been slow. For a number of complex reasons, the rotational moulding industry has not realised its full potential [148].

The main reason for this lack of progress is that the initial non-technical applications of rotational moulding obviously demanded no particular properties of the finished moulding. This did not require much experimental work towards an understanding of the process and meant that basic technical information, such as the effect of processing conditions on the polymer and the physical properties of the rotational moulding was limited.

After this initial 'unscientific' start, the rotational moulding process did progress to more engineering applications. This led to substantial advances being made in the design of rotational moulding machines [11, 32, 16, 198, 199, 246]; in the rates of output that could be achieved, and in the sizes of the mouldings which could be produced.

However, even at this stage, very little work was done on understanding the principles behind the process. Added to this was the fact that, commercially, installing a rotational moulding plant required only a small capital investment [24]. This resulted in the industry becoming fragmented with individual moulders being too small to contemplate fundamental research and development. Hence in contrast to other polymer moulding processes, such as injection moulding and blow moulding which have been, and continue to be scientifically investigated and optimised, rotational moulding initially,

developed only empirically.

Liu [150] states the optimisation of the rotational moulding process has essentially been based on trial and error. Cramez et al [182] state that the process offers major advantages to the designer, but it is hampered by a strong dependence on trial and error to achieve good part quality at economic production rates.

In the 1970's, some polymer manufacturers encouraged a better understanding of the fundamentals behind the process. Celansese Ltd. in conjunction with the Society of Plastics Engineers sponsored educational seminars on rotational moulding of polymer powders [4, 5, 21, 29, 88, 107] but the subjects treated were general with only some quantitative work reported [1, 6, 113, 173, 207, 245, 243].

At this time, there was also some data available relating to the physical properties of rotationally moulded polymers, but this was largely published by raw material manufacturers in the form of data sheets or booklets [3, 2, 12, 51, 68]. Some detailed discussion is found in Paquette's 'Guide For Selecting Rotational Moulding Powders' [21].

The need for further academic research is emphasised by several authors [148].
Xu [152] comments on the complex powder flow, transient heat transfer, and melt sintering processes, which make the prediction of product quality difficult.

One reason cited by Crawford [156] as hampering the growth of RM, is the long heating

cycle; the challenge to the industry is to reduce cycle times.

The need for establishing rules is not just of scientific interest, it also has economic advantages. 'The economics of a process can be drastically affected by the control of the heating cycle' [22]. Commercially, there is a great need for faster cycles and high production rates. The major disadvantage of rotational moulding compared to blow moulding, is that output rates for rotational moulding are lower [57]. This is due to the long heating cycles [22].

Sanada [60] has investigated general ways to reduce the final product cost in relation to the annual production rate. He concludes that other factors which affect the final product cost are relatively unimportant compared to the effects of cycle time and labour cost.

Reduction in cycle times can only be achieved by scientific study of the processing variables in a typical cycle. However, apart from the work by Rao, Throne, Scott and Crawford, for rotational moulding, these have not been fully investigated. Very little information is available as a guide and the industry relies on trial and error to arrive at optimal conditions [22, 24, 50, 55]. Thus, the present development of the process is such that the processing conditions for a particular mould/polymer combination are set as a result of experience rather than rules, and the quality of mouldings is often determined by visual examination.

1.8 Literature survey

The following is a literature survey of some research and development that has taken place in rotational moulding since the introduction of powdered thermoplastics in the 1960's.

Zimmerman [222] published one of the first descriptions and analysis of rotational moulding, based on the technology and applications of the day. As such, this paper illustrates how the theories of rotational moulding relate to the plastics technology and scientific thought of the late 1960's to early 1970's.

An updated general overview of the state of rotational moulding in the 1990's is made by Metha and Crawford [211, 230].

Metha briefly sums up the current technology, materials and specifications for mould construction and rotational moulding machines. Advantages and applications of the process are also discussed, although applications are limited to within India.

Crawford [211, 230] makes a much more detailed analysis of the principles behind rotational moulding in the technological environment of the 1990's. This paper provides a clear picture of how rotational moulding as a technique has evolved since Zimmerman's description [222].

The first attempt at examining the principles behind the rotational moulding process

was made by Rao and Throne in 1972 [55]. A series of papers were published and covered heat transfer, fluid flow, and sinter melting and degradation. In 1976, Throne published a paper documenting further research into heat transfer [113].

Later, a study of heat transfer in the rotational moulding process was carried out by Crawford and Scott in 1985 [214]. This study took advantage of new developments in technology, which allowed for example, temperature changes in the mould to be continuously monitored during a processing cycle. The aim of this study was to determine the optimum processing conditions for the rotational moulding of plastics. The experiments were carried out using a number of different heating methods; propane gas, electrical and air heating. The efficiency of these systems is compared and a computer model developed to predict temperature change through the wall thickness of moulding during heating. The influence of processing conditions on the physical properties of plastics was then studied. The results of this study indicated that impact strength, tensile strength and creep behaviour are affected to varying extent by the degree of fusion in the polymer. The cold impact strength was found to be particularly affected by over fusion.

In 1987, Scott [125] furthered the above study to include an investigation of the processing conditions that result in the formation and removal of bubbles in the polymer melt. The conclusions were that bubbles are formed as powder particles sinter and melt. Once formed, because of the high polymer melt viscosity, the bubbles remain virtually stationary in the melt until diffusion of gases out of the bubble causes its collapse.

In 1999, Kontopoulou and Vlachopoulos [147] reported a study of bubble dissolution in polymer melts. It was concluded that the process is controlled by the diffusion of air from the bubbles to the melt. Bubble dissolution was found to depend significantly on initial bubble size, surface tension and air concentration in the polymer melt, but not significantly affected by the melt viscosity in the ranges recommended for rotation moulding.

In a paper published in the same year, Gogos [166] supports the above conclusion that surface tension contributes substantially to bubble dissolution.

Liu and Chen [215] in 2000 reported that the main factors affecting bubbles in rotational moulding are the particle size of the polymer powder and the cooling conditions of the polymer melt. The bubble size was also found to increase with increasing viscosity of the polymer melt.

Bellehumeur and Tiang's work in 2000 [183] and 2001 [191] led to the development of a numerical simulation which describe the formation and evolution of bubbles in polymer melt during the rotational moulding process. The simulation can be used for quantitative studies on the effect of moulding conditions and material properties on the moulding cycle and moulded part density.

Crawford [211] has studied mechanical properties and processing behaviour of plastics, where the effect of processing conditions on the physical properties of plastics was

investigated. This study was not confined to rotational moulding, but also included injection moulding and solid phase compaction.

Crawford et al [203, 204] have proposed different models to simulate the rotational moulding cycle and have good correlation between the simulation and the experimental data.

Further work on the relationship between microstructure and properties was reported in 1988 by Cramez et al [161]. The effect of cooling rate on the mechanical properties was investigated by Callan et al [216] in 1997. The effect of fillers on the properties of rotationally moulded polyethylene was reported in 1999 by Robert and Crawford [172]. Dodge and Perry [192] in 2001 studied the effect of the density of a rotational moulding on its impact strength, tensile strength and the flexural modulus. Their work showed that the tensile strength and the flexural modulus increased with increasing density, while the impact strength increased only up to a certain value of the density. After this critical value of the density, the impact strength began to decrease again.

Van Hooijdonk et al [194] in 2001 have examined the influence of different processing parameters on the properties of polypropylene for rotational mouldings. Their main conclusions were that the toughness of rotational mouldings is determined by the degree of crystallinity. A higher degree of crystallinity (achieved by slow cooling or using a Teflon mould) results in decreasing toughness.

Also in this year Kissick et al [195] report falling weight impact testing analysis of

rotationally moulded polyethylene. One conclusion is that the processing temperature affects the impact properties of rotational mouldings. Low temperatures result in excessive bubble formation, which reduces the impact strength of the moulding. The addition of pigments is reported to affect the impact strength; compounded pigments showed a 14% increase in the impact strength compared to turboblended pigments.

Kohlman has specifically looked at the effect of processing variables on the environmental stress crack resistance (ESCR) of rotationally moulded polyethylenes. She has correlated ESCR to the moulding parameters and chemical properties of linear low density polyethylene and crosslinkable polyethylene. She concludes that a combination of long fusion times and a slow cooling cycle produced the worst ESCR for the polymers. Optimum ESCR was achieved by a short fusion time, and a fast cooling cycle.

In 1994, Liang and Crawford [217] reported work on the computer simulation of the rotational moulding process which has resulted in a computer program that can accurately predict the air temperature profile inside the mould during a typical moulding cycle.

In 1997, two more papers on the computer simulation of rotational moulding and rotational moulding of thermoplastics were presented by Attaran et al [153] and Gogos et al [154]. At this stage numerical modelling of the process was reported to be difficult.

A later study on computer simulation in 1999 by Wright and Crawford [167]

concentrated on predicting and displaying the wall thickness distribution in a rotational moulding for given variables such as mould rotation speeds and speed ratios, bulk density of the polymer etc.

Advances in rotational moulding equipment have also been made. Machines are now built with microprocessor controls and facilities for gas injection. Crawford [248] reports the development of the 'ROTOLOG' will allows the measurement of polymer temperature during an actual rotational moulding cycle. This is a major development towards the optimisation of the process and has the potential to provide feedback for controlling a typical rotational moulding cycle.

Syler [202] has developed a technique for mounting an insulated video camera and light source inside the mould. This allows the observation of polymer sintering in the heating cycle.

Another development reported by Spence [201] is a hybrid of rotational and blow moulding (roto-blow moulding) where the internal atmosphere of the mould is pressurised. This can reduced warpage and improve the wall thickness distribution of the finished moulding.

As already stated in Section 1.6, one advantage of rotational moulding is that it is the ideal process for moulding-in inserts. The Graphics Systems Company [206] has further developed this technique to include multi-coloured labels and decorative inlays that become a permanent part of the product, and eliminates secondary operations.

Liu and Ho [163] have studied the shrinkage and warpage mechanisms in rotational mouldings. They have compared the warpage, shrinkage and residual stress of various polymers subject to different cooling conditions and have concluded that all three conditions increase with increasing cooling rate. For the polymers studied, they also observed an increase in the above three with increasing extent of crystallisation. A mould pressurisation method to minimise warpage has also been proposed.

Liu and Lin [150] have successfully used the Taguchi method in their study to optimise the rotational moulding process. This method presents an organised approach, employing statistics, to investigate the many possible factors that affect the tensile and impact strengths of rotational mouldings. The findings are discussed in detail in Section 5.5., but generally, the impact strength was found to be primarily affected by the cooling method and to a lesser extent, by the particle size of the polyethylene powder. The particle size of the polymer powder however, was found to have a significant effect on the tensile strength of the moulding; the correct choice of particle size distribution was found to increase the tensile strength several times. The heating time and the cooling method are also reported to be important roles in achieving the maximum tensile strength.

Cramez et al [182] in 2002 have reported a study into the optimisation of rotational moulding of polyethylene by predicting antioxidant consumption. During the heating cycle, the polymer is subject to relatively high temperatures for long periods of time. Because of the presence of oxygen in the mould, the polymer becomes susceptible to thermal and oxidative degradation. Cramez et al have proposed a method to predict the

onset of degradation on the basis that this occurs when the concentration of anti-oxidant in the polymer reaches zero. Good agreement between experimental and predicted optimum processing temperature is reported, for the two grades of polyethylene stabilised with two different anti-oxidant systems.

In the 1940's, when the rotational moulding of plastics was first developed, open flames were used to heat the mould. In the 1950's, hot air ovens were developed as cleaner, more efficient methods of mould heating. However, it is widely recognised that hot air ovens are relatively inefficient at mould heating. Kearns et al [184] in 2000 carried out an experimental investigation to assess the relative merits of open flame and hot air oven rotational moulding machines, and found that significant cost savings are possible using the open flame heating method. A previous study on the forced air convection heating method in 1997 by Wright et al [149] revealed that the convection method is very inefficient, with only around 1.7% of the heat generated going to heat the polymer.

1.8.1. Polymer particle fusion and melting

There is very little discussion in the literature concerning the stages a polymer powder goes through in a typical rotational moulding cycle. The following is a discussion of the possible methods of particle fusion and melting in the heating and cooling stages of a typical rotational moulding cycle.

Initially, as the mould rotates, some particles that are in contact with mould wall are carried with it until the gravitational force on the particles exceeds the frictional force.

At this point, the particles drops back into the powder pool, see Figure 52 (Section 5.3.1.2). As the mould temperature increases however, the particle start to stick to the mould surface.

During mould rotation, the polymer particles also come into contact with each other. At high temperatures the conditions are ideal for the sintering process (discussed in Section 1.8.1.1.) The particles thus coalesce at the points of contact and melt, Figure 7(i) and Figure 7(ii). Continued rotation of the mould causes further particles to melt, Figure 8(iii) until fusion is complete, Figure 8(iv).

Thus at any point during the heating cycle, there are three distinct zones inside the mould, Figure 9. Zone 1 is the molten polymer containing many air bubbles, Zone 2 consists of partially fused powder particles which adhere to the melt during mould rotation and sinter as the particles reach the melting point of the polymer. The remaining unfused polymer powder comprises Zone 3 [98].

The end of particle fusion is signified by the removal of particle boundaries resulting in the formation of a layer polymer melt containing many air bubbles, Figure 8(iv). The bubbles are removed during the melt densification process.

It is apparent from this discussion that the conversion of polymer particles into a uniform melt involves a number of discreet phases. The consensus of opinion seems to be that there are three stages:

FIGURE 7 (i) & (ii)

SCHEMATIC REPRESENTATION OF POLYMER FUSION AND MELT DENSIFICATION

(i) Start of fusion phase

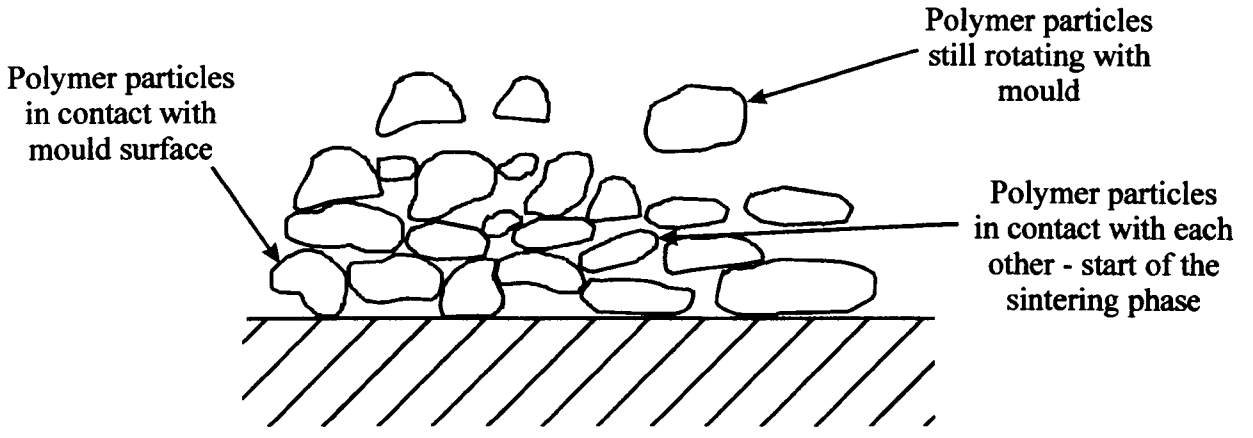

(ii) Fusion phase continued

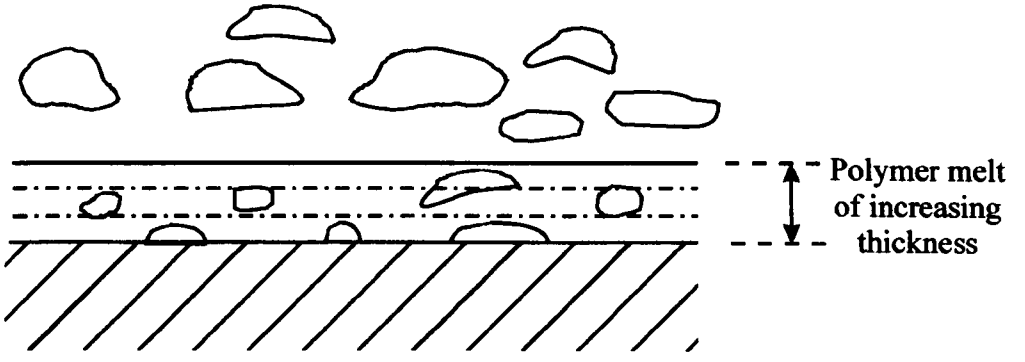

FIGURE 8 (iii) & (iv)

SCHEMATIC REPRESENTATION OF POLYMER FUSION AND MELT DENSIFICATION

(iii) Fusion phase continued

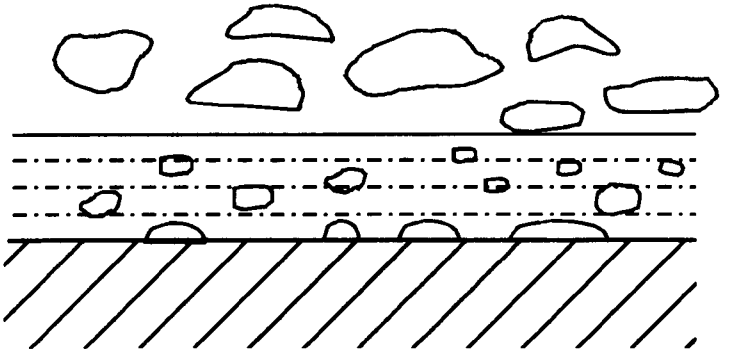

(iv) End of Fusion Phase

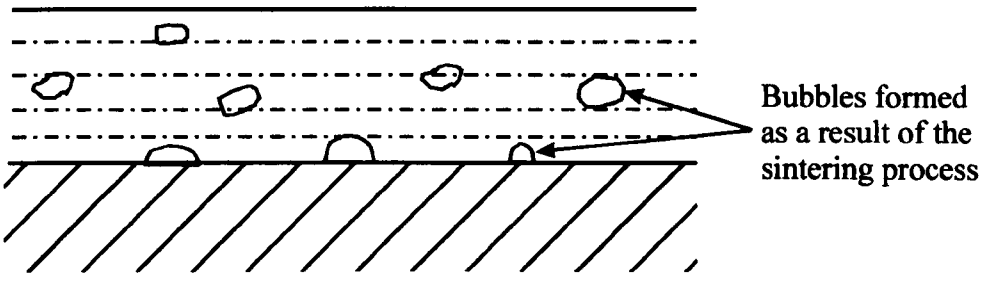

FIGURE 9

SCHEMATIC REPRESENTATION OF THE FUSION PHASE

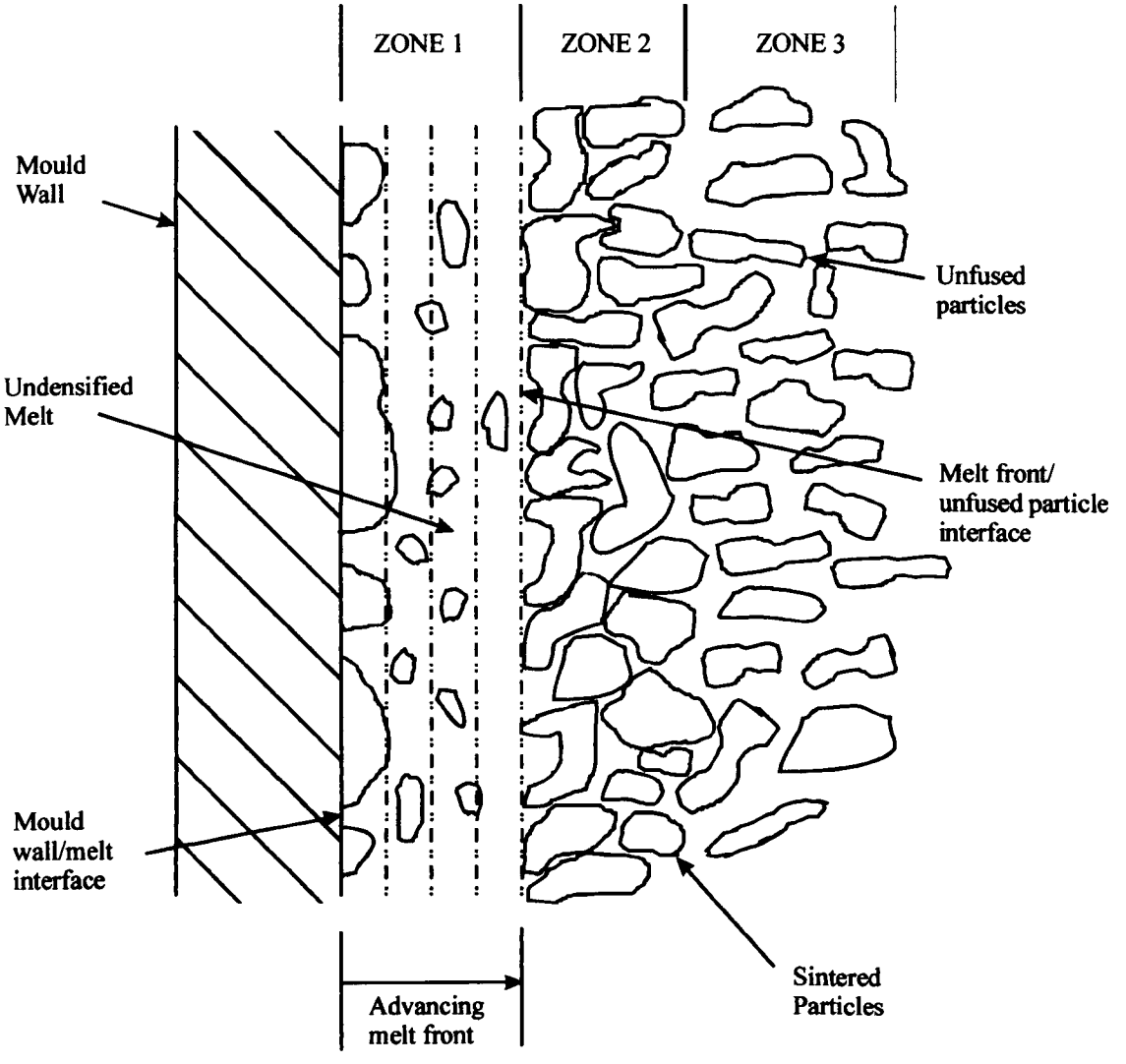

(1) A sintering type mechanism

(2) Bubble formation and removal.

(3) Surface levelling.

In order to understand bubble formation and removal, it is first necessary to discuss the processes of polymer sintering and melt densification. This is done in Section 1.8.1.1 and Section 1.8.1.2 that follows.

1.8.1.1 Polymer Sintering and Melt Densification Models

Polymer Sintering

As already stated in Section 1.8.1, sintering is a process in which solid particles, when in contact with each other at elevated temperatures, decrease the total surface area by coalescence. Decrease in the surface area results in a decrease in the surface free energy. Surface tension is thus the driving force of the coalescence process.

The sintering process proceeds in two distinct stages. First, interfaces and bridges develop between two adjacent particles, with little change in density, see Figure 7(i). This is followed by melting in which the inter particle boundaries are eliminated.

The sintering process in relation to plastic particles has been reviewed by Lontz [91], Rosenzweig and Narkis [92, 93, 94, 95], Throne and Rao [96], Tadmor and Gogos [99], Gogos [160, 241] and more recently, by Bellehumeur at al [127].

The concept of viscous sintering was first developed by Frenkel [100] who derived an expression for the rate of coalescence of adjacent spheres under the action of surface tension, see Figure 10. This model predicts the sintering progress with time for two identical spheres and takes the form:

$$x^2 = \frac{3\ a_s\ s\ t_c}{2\ \eta} \qquad \text{Equation 1.8.1.1.1.}$$

Where x is the radius of the interface between the two twin spheres, a_s is the radius of the spheres, s is the surface tension, t_c is the time of contact and η is the viscosity at zero shear.

The Frenkel equation was confirmed by Kuczynski [101] and Kingery [102] using glass sintering experiments, and by Rosenweig and Narkis [92, 93] using polystyrene and PMMA.

However, Kuczynski et al [123] found Equation 1.8.1.1.1 inadequate for describing the sintering of PMMA. They used an empirical relationship to curve fit their experimental data.

FIGURE 10

FRENKEL MODEL FOR SINTERING

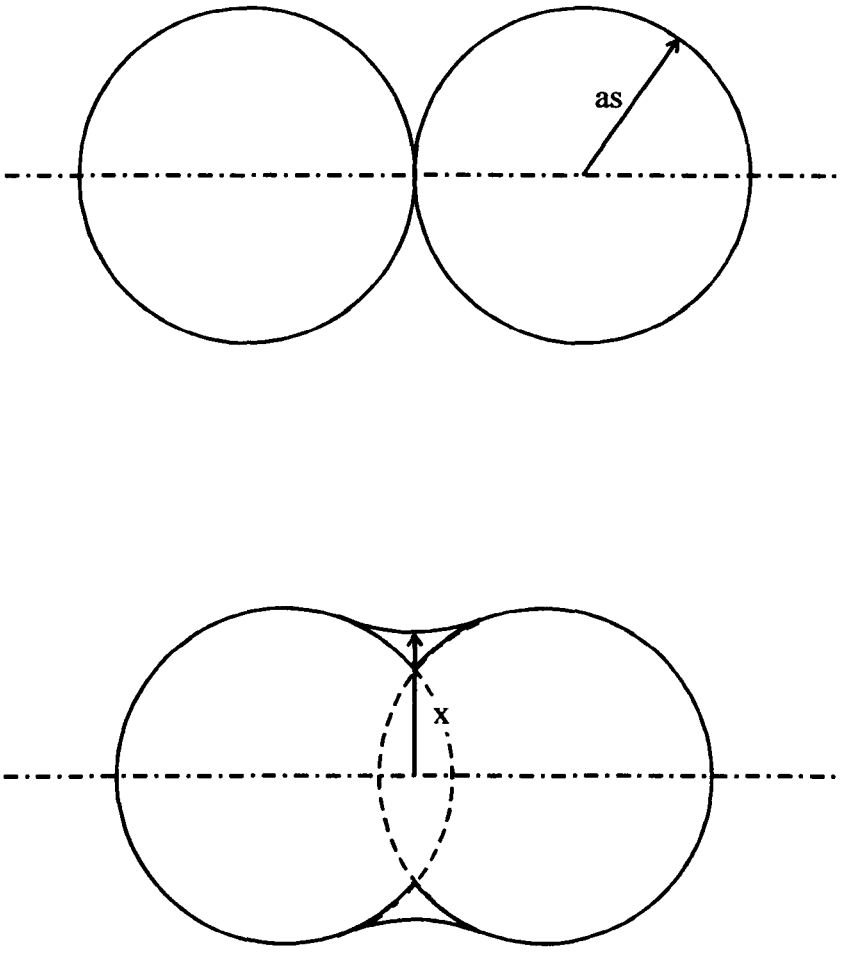

The resulting equation is:

$$\left(\frac{x^2}{a_s^{1.02}} \right)^n = K(T_s)\, t_s \qquad \text{Equation 1.8.1.1.2.}$$

Where K is an experimental constant, T_s is the temperature, t_s is the sintering time, x is the radius of the interface and a_s is the radius of the PMAA sphere. The exponent n decreases from approximately 5 to 0.5 as the sintering temperature increases from 127°C to 207°C. The relevance of Equation 1.8.1.1.2 to this study is discussed in Section 5.2.1.2.

Lontz [124] modified this equation to include a term $\frac{t_s}{\tau}$ where τ is the relaxation time to reflect the viscoelastic nature of plastics.

$$\frac{x^2}{a_s} = \frac{3}{2} \left(\frac{\tau\, t_s}{\eta_o (1 - e^{-t_s/\tau})} \right) \qquad \text{Equation 1.8.1.1.3.}$$

τ = apparent relaxation constant to be assigned from experimental determinations to account for both inherent and stress-induced retardation.

η_o = viscosity of melt at zero shear.

Throne picked up on this concept and in his work on the rotational moulding of ABS, observed that the very long relaxation time for the material drastically altered the web growth rate. He suggested an equation of the form:

$$x^2 = \frac{3\ a_s\ s\ \tau}{2\ \eta_o}$$ Equation 1.8.1.1.4.

where s = surface tension

He proposed that isothermal sintering would stop when X reached the value given by the equation. An interesting conclusion from this equation is that increasing the temperature in an attempt to increase X and reduce the size of the voids may be detrimental since S and η_o both increase with temperature, which may counteract the decreasing value of viscosity with temperature.

Cogswell [259] took a different approach to the phenomenon of sintering. Using Stoke's Law for describing the force on a sphere as it passes through viscous fluid, he equated this with the surface tension, giving:

$$2\ \pi\ a\ s = 6\ \pi\ \eta_o\ a\ v$$ Equation 1.8.1.1.5.

where s is the surface tension, η_o is the viscosity of the polymer at zero shear, a is the particle radius and v the velocity. Each particle is sucked into the melt in a time $\frac{2a}{v}$ and a depth of melt, x_m is formed in a time t, given by

$$t = \frac{3\ \eta_o\ x_m}{s}$$ Equation 1.8.1.1.6.

The relevance of Equation 1.8.1.1.6 to the present study (on polymer fusion) is discussed in Section 5.2.1.2.

Bellehumeur et al in 1996 [127] report that the validity of Frenkel's model, Equation 1.8.1.1.1, is limited to Newtonian flow and only in the early stages of sintering, when

the particle diameters remain relatively constant. This paper also reports other polymer sintering models. These are briefly summarised as follows.

Hornsby and Maxwell [128] experimentally studied the sintering of polypropylene beads and found that using the Trouton viscosity (three times larger than the shear viscosity) in the Frenkel model produced good agreement between predicted and experimental results.

Eshelby [129] corrected the Frenkel model for an incompressible fluid and proposed the following Frenkel/Eshelby model:

$$\frac{x}{a_s} = \left(\frac{s\, t_c}{\eta_o^{\,r}} \right)^{1/2}$$

$$x^2 = \frac{s\, t_c\, a_s}{\eta_o} \qquad \text{Equation 1.8.1.1.7.}$$

Hopper [130] presents the following sintering model:

$$\frac{x}{a_f} = (1 - \alpha)\,(1 + \alpha^2)^{-1/2} \qquad \text{Equation 1.8.1.1.8.}$$

a_f = final particle radius at the completion of coalescence

α = parameter of the inverse ellipse of constant area

when $\alpha = 0$ the curve is one circle

$\alpha = 1$ the curve approaches the shape of two circles

The late stage of sintering has been modelled analytically by MacKenzie and Shuttleworth [131], Cosgrove et al [132] and by Hopper [130]. Scherer [133] modelled the densification of particle agglomerates, and more recently, Jagota and Scherer [134] numerically modelled the composite packing of spheres.

Numerical solutions for two-dimensional sintering systems have also been proposed by Ross et al [135], Kuiken [136], Van der Vorst [137] and Martinez-Herrera [138]. The model presented by the latter author enabled the study of the effect of initial particle geometry on the flow and sintering rate. Martinez-Herrera and Derby [138] also showed that their numerical results were in good agreement with the prediction from Hopper's model, Equation 1.8.1.1.8. Reported data for the coalescence of two spheres by Jagota and Dawson [139, 140] is also reported to be in close agreement to the Hopper's model.

The role of mechanisms other than Newtonian viscous flow in sintering and melting have been suggested by some authors [123, 141, 142, 143, 144]. Mazur [141] reviews the various aspects of polymer coalescence. Kuczynski et al [123] proposed the use of a shear dependent viscosity in Frenkel's model, although it is widely assumed that the development of shear rates in rotational moulding must be very small or negligible.

Siegmann et al [143] compared the sintering rates of polyethylenes of various molecular weights. They found that the coalescence rate for ultra high molecuar weight polyethylene (UHMWPE) was surprisingly higher than for the high molecular weight polyethylene (HMWPE), although HMWPE has a smaller viscosity than UHMWPE. This was explained in terms of morphological differences between the polymers. This is

supported by Barneston and Hornsby [144] who report a study of the effect of morphology on the sintering behaviour of several grades of UHMWPE.

Bellehumeur et al [127] report a quantitative assessment of the Frenkel and Hopper models for polymer powders, cylindrical particles and micropellets. The conclusions were that powder particles for both HDPE and LLDPE sinter at the same rate as cylindrical particles, and the rate of coalescence increases with decreasing molecular weight and viscosity.

In 1998, Bellehumeur derived [145] a further viscoelastic model based on Frenkel [100] and modifications proposed by Pokluda et al [146], and confirmed that both polymer viscosity and viscoelasticity are important factors in polymer sintering.

Melt Densification

Bubble formation and removal is unique to rotational moulding, and not a problem encountered in other major processing techniques. There is therefore, very limited literature concerning the removal of bubbles from polymer melts.

Kontopoulou and Vlachopoulos [147] have proposed a model for the dissolution of bubbles by considering a single spherical bubble in an infinite polymer melt, see Figure 11 and Equation 1.8.1.1.9.

FIGURE 11

SINGLE SPHERICAL BUBBLE SURROUNDED BY AN INFINITE AMOUNT OF POLYMER MELT

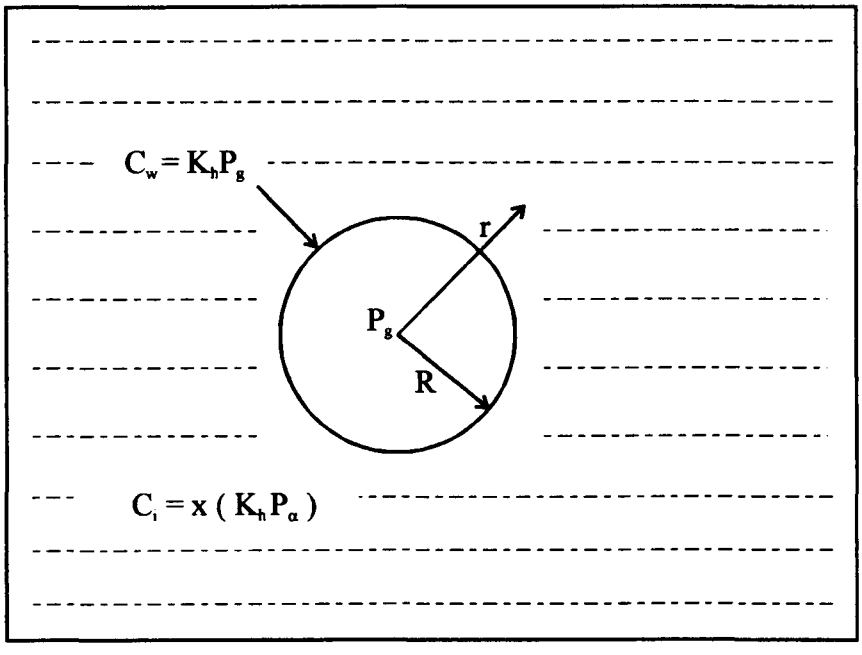

$$\dot{R} = \frac{1}{4\eta_o}\left[(P_g - P_f)R - 2\delta\right]$$ Equation 1.8.1.1.9.

P_g = gas pressure inside bubble

C_w = concentration of gas at bubble/liquid interface

K_h = Henry's Law constant

R = bubble radius, $\dot{R}$ = rate of bubble dissipation

r = radial co-ordination

C_i = concentration of gas in bulk polymer melt

P_f = pressure in the bulk polymer melt

δ = surface tension

η_o = melt viscosity at zero shear

This equation relates the rate of dissolution of the bubble to the pressure inside the bubble. This model gives some understanding of the mechanism of bubble dissolution. As the bubble forms, the air pressure, P_g, inside the bubble is slightly higher than the ambient pressure, because of the action of surface tension. Henry's Law shows that the higher pressure inside the bubble results in a higher concentration of air, C_w, in polymer/air interface (bubble walls) compared with the concentration C_i in the rest of the polymer melt, which is exposed to ambient pressure.

The difference in concentration results in a driving force, which forces the air to diffuse out of the bubble to the surroundings. As the air is removed, the bubble diameter decreases and the air pressure inside the bubble increases further, see Figure 11. This Figure shows the change in P as the bubble diameter decreases. The initial bubble diameter is 0.25 mm. The bubble is in a PE melt which is close to saturated conditions and has a viscosity of 3000 Pa., at 190° C. At long times, P_g increases dramatically as $R \rightarrow 0$, and this accelerates the rate of bubble dissolution. This is a result of increase in

P_g inside the bubble, hence increase in c and predicted by Henry's law and subsequently and an even larger concentration difference between the bubble/air interface and the polymer melt. This accelerates diffusion.

Crawford and Scott [125, 126] studied polymer melting using hot plate tests and video to record the formation and dissolution of bubbles.

Following a force analysis on a typical bubble, it was concluded that the apparent viscosity of molten polyethylene was so large, that the buoyancy forces acting on it can be assumed to be insignificant. The authors also stated that trapped air will diffuse into the surrounding polymer mass, and reported bubble measurements to support this theory. The initial bubble size was found to have a significant effect on the rate at which it dissolves. This is because the surface area to volume ratio is inversely proportional to the diameter. The removal of bubbles from the polymer melt was modelled as follows:

$$\left(\frac{\emptyset}{\emptyset_o} \right)^2 = K_3 - K_2 t \qquad \text{Equation 1.8.1.1.10.}$$

Where $\emptyset$ = diameter of bubble at time t

$\emptyset_o$ = original diameter of bubble

t = time

K_2 and K_3 = experimental constants

Crawford and Xu [121] modified Equation 1.8.1.1.10 to increase its accuracy . This model includes two more experimental constants: K_s and K_c

$$\left(\frac{\emptyset}{\emptyset_o} \right)^2 = K_s - K_2 t + K_c t^2 \qquad \text{Equation 1.8.1.1.11.}$$

In 1996, Crawford and Spence [122] used Equation 1.8.1.1.11 to graphically illustrate how the removal of gas bubbles from the polymer melt was influenced by the melt temperature.

Throne [54, 55] used the Frenkel model, Equation 1.8.1.1.1, as the only basis for his analysis. He first differentiated between a void and a bubble. He defined a void as an interstitial space in the sintered lattice structure and a bubble as the resulting encapsulation of air as the void fills up by capillary action.

Throne related the Frenkel analysis to voids but not to bubbles. He used the Frenkel equation to calculate the time taken to fill a void in the sintered material.

$$Z^2 = \left(\frac{r}{2} \right)_{t_1} \int^{t_2} \left\{ s(t) / \eta_o(t) \right\} \partial t \qquad \text{Equation 1.8.1.1.12.}$$

Where Z = depth of void

r = radius of void

This is the differential form of the Frenkel equation. The surface tension for most plastic polymers is linear with respect to temperature, and the viscosity is exponential

with respect to temperature. Thus:

$$s(T) = s_0 - \frac{\partial_s}{\partial_t}(T - T_o) \qquad \text{Equation 1.8.1.1.13.}$$

and

$$\eta = \eta_0 \exp\left[- \frac{E}{R} (T - T_o) \right] \qquad \text{Equation 1.8.1.1.14.}$$

Throne explained the transition from a void to a bubble by suggesting that, if the sintered material does not remain strong enough to allow the Frenkel forces to fill the void area, the sintered material can collapse above the melt front and encapsulate air voids. Thus a plane of encapsulated bubbles would appear, which is parallel to the melt surface in the interior of the final moulding.

Throne used the word densification to describe the filling of the voids with melt by capillary action, not to the dissipation of bubbles in the melt, as it is in this study. He verified that the rate of Frenkel filling, or densification, increased with increasing temperature. However, he suggested that if the temperature is too high, the sintered material would collapse too quickly and encapsulate air bubbles. He suggested the obvious solution to this problem was to densify at low oven set temperature, to reduce the rate of melting and the rate of softening of the three dimensional structure above the planar melt front.

Once the bubbles were formed, flat plate simulator experiments performed by Throne [96] showed the bubbles migrate to the free surface where they dissipated. From this

study, Throne also found that the bubbles formed on the mould surface, although with time they diminished in size.

Kelly [98] used a similar approach to Kontopoulou and Vlachopoulos [147] and explained the formation and removal of bubbles in terms of surface tension forces and vapour pressures in the bubble. When a spherical gas bubble is enclosed in a liquid medium, the pressure forces of the liquid and vapour must be balanced by the surface tension forces at the vapour/liquid interface. If $\emptyset$ is the diameter of the bubble, then the pressure acts on an area $\Pi\emptyset^2/4$ and the surface tension acts on the circumferential interface length $\Pi\emptyset$. Hence the equilibrium:

$$\frac{1}{4}\Pi\emptyset^2(P_V - P_L) = \Pi\emptyset S_{VL} \qquad \text{Equation 1.8.1.1.15.}$$

Where P_V is the vapour pressure inside the bubble, P_L is the liquid pressure, and S_{VL} is the surface tension of the vapour/liquid interface.

This equation may be simplified to the form:

$$P_V - P_L = \frac{4 S_{VL}}{\emptyset} \qquad \text{Equation 1.8.1.1.16.}$$

Kelly's argument related to this simple pressure balance. For example, consider a bubble which is in pressure equilibrium, i.e. one which is not growing or collapsing, and assuming that the temperature of the vapour inside the bubble is the saturation temperature corresponding to the pressure. If the liquid is at the saturation temperature corresponding to the pressure it is below the temperature inside the bubble and so heat

must be conducted out of the bubble, the vapour inside must condense and the bubble must collapse. In contrast, in order for the bubble to grow and escape from the surface, it must receive heat from the liquid.

An essential part of Kelly's theory is that the gases in the bubble dissolve in the plastic melt. This phenomenon has been confirmed by a number of other workers [104, 105] and Kline [106] supported Kelly's view that oxygen permeates into the polyethylene more rapidly than nitrogen does. This is contrary to the US Army report [227] which states that bubbles migrate to the surface.

Investigations of bubble dissipation in Section 4.3.3 of this study, show that up to a critical temperature, dissipation of bubbles is time controlled. At temperatures higher than this critical temperature, dissipation of bubbles appear to be almost instantaneous

1.8.1.2. Surface levelling

There has been relatively little work done on this aspect of rotational moulding, although it has important practical significance in industry.

Progelhof et al [97] observed that there was a time lag between the final melting and the time when the surface had levelled off. It was suggested that this phenomenon might be similar to the levelling time of ink or paint, in which case an equation of the following would apply:

$$t_L = \frac{(2a)^4}{(x_m)^3 s}$$

Where t_L is the levelling time, **a** is the radius of the powder particle, X_m is the depth of the melt layer and **s** is the surface tension.

1.8.2. Bubbles in rotational moulding

Bubble formation in the melt in other major polymer processes is not a problem; this is unique to rotational moulding. The detrimental effect of bubbles in rotational mouldings is discussed in Section 5.5.

Literature on the possible mechanisms of bubble formation and dissipation was reviewed in Section 1.8.1.1. Other, more general discussions on bubbles in rotational moulding, are reported here.

McKenna [260, 261] discusses the effect of particle shape on air entrapment. Particles with hairs or tails give rise to a low packing density and hence greater air entrapment. This theory is supported by the US Army report [227]. Paquette [21] in contrast, emphasises particle shape as a factor in void content. It is suggested that as a result of mould rotation, finer particles work their way to the inner mould surface and are the first to melt. An excess of small particles, due to the build up electrostatic charge, would clump together and not melt uniformly, creating voids. A further explanation is given in terms of the hygroscopic nature of thermoplastic polymers. A polymer powder with

small particle size will have a larger surface area across which moisture can be absorbed. This moisture then vapourises during the heating cycle, creating bubbles.

Throne [54, 55, 96] classifies the bubbles into two types; surface bubbles on the mould surface of moulding, and bulk bubbles formed in the wall of the moulding. He has also suggested that during the cooling cycle, water can lodge in the parting line, and this trapped moisture can then expand and blow through the part or enter the wall and form a bubble.

Ramazzotti [50] suggests that surface bubbles are caused by the oven temperature being too high and that the bulk bubbles are caused using large particles of the polymer powder.

Throne [54, 55] has stated that surface bubbles can never be completely eliminated. This is supported by Paquette [21] who reports that surface bubbles can only be eliminated by a highly polished inner mould surface. ICI [2] state there is a critical length of heating time after which most bubbles disappear, and that any further increase in the heating time does not remove any remaining bubbles. However, these statements are contrary to findings of this research and other studies (discussed in previous Sections) where complete elimination of surface and bulk bubbles is reported.

Hot plate tests carried out by Crawford et al [199] showed that the initial size of the bubble had a significant effect on the rate at which it dissipates. This is explained in

terms of the surface area-to-volume ratio of a sphere being inversely proportional to the diameter.

Spence and Crawford [122] have identified the following parameters as contributing to the formation and removal of bubbles:

- Powder particle shape, size and distribution.
- Viscosity, measured as the MFI, of the melt.
- Additives e.g. pigments.
- Mould surface.
- Temperature.
- Time.
- Atmosphere inside the mould.
- Surface tension.
- Vacuum.
- Pressure.

The bubbles were found to diminish in size with increasing melt temperature and the rate is increased in lower viscosity materials. A low viscosity polymer, MFI 25 g min^{-1}, was shown to contain no surface or bulk bubbles when rotationally moulded.

The inclusion of carbon black was shown to increase the viscosity of the melt, and hence slow down bubble dissipation. Other pigments were not found to have any effect.

Increasing the percentage of finer particles in the polymer powder was shown to produce more, smaller bubbles. Particles with tails were also shown to produce more bubbles.

The number of surface bubbles was also found to increase with the use of a release agent. This was explained in terms of surface tension, which is reduced by the release agent. This in turn reduces the attractive force that causes the polymer to wet and spread evenly over the mould surface.

Thermal imaging revealed 'hot spots' on the mould surface and explained the absence of surface bubbles on the mouldings in these areas.

Crawford et al [199] report conclusive experimental evidence that internal mould pressure can be used to eliminate bubbles. The pressure needs to be applied after the polymer has melted.

1.8.3. Thermal conductivity of polyethylene

Published data on the thermal properties of polymers is very inconsistent. Hands [249] reviews the available data using the reported values of the thermal conductivity of polystyrene as an example, see Figure 12. Not only do the values differ at some temperatures by more than 300%, but different trends are indicated throughout the temperature range. Discrepancies of this magnitude cannot be attributed to sample

FIGURE 12

LITERATURE VALUES FOR THE THERMAL CONDUCTIVITY OF POLYSTYRENE

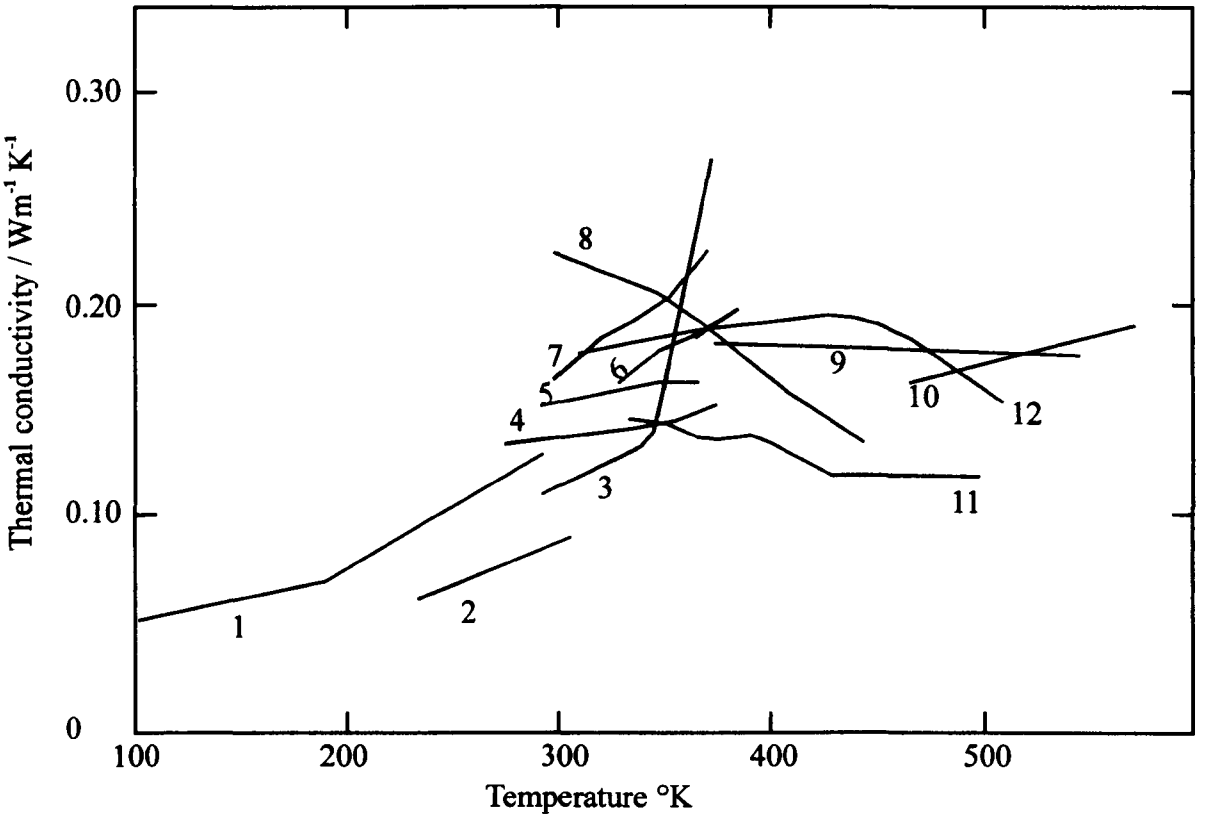

Curve: 1 - Hagar (1960); 2- Chen (1971); 3 - Hatten (1960); 4 - Kline (1961); 5 - Pasquino and Pilsworth (1964); 6 - Ho (1964); 7 - Cherkasova (1959); 8 - Holzmuller and Lorenz (1961); 9 - Lohe (1965); 10 - Fuller and Fricke (1971); 11 - Uberreiter (1967); 12 - Hands (1976).

variation, and they give some indication of the experimental difficulties associated with thermal property measurement.

Majurey [250] also reviews the data available on thermal conductivity, and attributes the wide variation in data as being due to the thermal conductivity of polymers being relatively low.

This means that only very small quantities of heat flow are involved, making measurement difficult. In addition, relatively small heat losses can introduce significant errors in the measured value.

Apart from the temperature, the thermal conductivity of polymers is also affected by the polymer and processing variables, such as degree of crystallinity, molecular weight, crosslinking, orientation, additives and pressure. The effect of these properties on the thermal conductivity is summarised by Hands [249] and Eiermann [257].

The process and polymer variables important to this study are, temperature and the degree of crystallinity of polyethylene. Although precise values of thermal conductivity are unavailable, some work on the effect of these variables on the thermal conductivity of polyethylene is reported [254, 255, 256].

Sheldon and Lane [254] have measured the variation of thermal conductivity with density for polyethylene between 20° C and 100° C. The thermal conductivity was found to decrease with increasing temperature.

Sheldon and Lane [254] also report an increase in thermal conductivity of polyethylene with increasing density, or crystallinity. This indicates the superior mechanism of conduction in crystalline materials. This is supported by Hansen and Bernier [255] who reports an increase in the thermal conductivity with increasing lamellar thickness of polyethylene.

Since polymers are not 100% crystalline, it is generally assumed that they can be regarded as two phase systems with the resultant conductivity obtained by combining the conductivity of the crystalline and the amorphous phase. Sheldon and Lane [254] have discussed methods for combining the two phases, and methods for obtaining values for completely crystalline and completely amorphous polymers, by extrapolation from the results for polymers with different degrees of crystallinity.

Conductivity is conceptually easier to understand than diffusivity, and it has received more attention. However, diffusivity is the essential parameter for the transient heat flow calculations. It is easier to determine than thermal conductivity, mainly because it is only necessary to measure the temperature, compared to thermal conductivity where the heat flux, which cannot be measured directly, has to be calculated as well [251]. However, although thermal diffusivity is easier to determine, its measurement has received very little attention until 1963, when Schoulberg [252] reported diffusivity measurements for some polymers such as PMMA and polystyrene. Hands [253] reviews basic principles and methods of diffusivity measurements.

1.8.3.1. Thermal conductivity of polyethylene powder

In a powder, heat transmission occurs by a number of mechanisms, see Figures 53 and 54 (Section 5.3.1.2).

a) Conduction through the solid particles.

b) Conduction across the contact surfaces between the solid particles.

c) Conduction through the gas film near contact points.

d) Conduction in the gas phase.

e) Radiation between solid surfaces.

f) Radiation between neighbouring voids.

Heat transfer through particulate solid polymeric systems is slower compared to homogeneous polymeric systems, because the thermal conductivity of most gases is considerably less e.g. air (0.026 W m^{-1} k^{-1}) than those of polymers (0.15-0.45 W m^{-1} k^{-1}) and the contact area between the particles is small.

Yagii and Kunii [258] have suggested a mathematical model for the thermal conductivity of the bed, k_e, which for fine particles and low temperatures simplifies to:

$$k_e = \frac{k_p (1 - \epsilon)}{1 + (k_p \varnothing / k_g)}$$ Equation 1.8.3.1.1.

Where k_p = thermal conductivity of polymer

k_g = thermal conductivity of air occupying the voids

ϵ = bed porosity

$\emptyset$ = correlation factor dependent on the bed porosity and determined experimentally for each material.

1.9. Aim of research programme

The aim of this study was to increase knowledge of the rotational moulding process and to contribute towards a general understanding of the process that will eventually predict optimum cycle times for a given mould/polymer combination.

The polymer chosen for the study is linear low density polyethylene as it is the most widely used polymer in the rotational moulding industry. Test mouldings of cubic shape and sides 0.17m were moulded on a small rotational moulding machine (see Section 3.2.)

Optimisation of any industrial process is best done by a quantitative study of the effects of design and process variables and material parameters on the process.

In rotational moulding of powdered polymers the polymer parameters relate to geometrical factors of the powder; particle shape, particle size, and particle size distribution, and also to the physical and thermal properties of the polymer. The latter include the melting point, the melt viscosity, thermal/oxidative degradation and thermal conductivity of the polymer.

The process variables relate to:

- Mould and part design
- Heating temperature and the length of the heating time of polymer (the heating cycle)
- The rate of cooling of the polymer melt (the cooling cycle)

The heating cycle is slowest and hence the rate determining step in the rotational moulding process. Limitations are imposed on attainable rates by the thermal and physical properties of the polymer, in particular, low thermal conductivity and thermal degradation. Thermal conductivity limits the rate of heat transfer, and the degradation properties reduce the temperature and the time the polymer can be exposed to in the heating cycle.

A study of the effects of processing variables on the heating cycle was therefore made, with the aim of achieving the highest possible rates of polyethylene powder particle fusion without thermal or oxidative degradation.

In rotational moulding the cooling cycle is also critical in that it determines the physical properties of the processed polymer by affecting the crystalline morphology of the processed sample.

Crystalline morphology relevant to linear low density polyethylene and the processing conditions, is spherulitic growth. Spherulitic size and density varies with the melt crystallisation temperature and the cooling rate of the polymer. Thus, finally, the effect

of the rate of polyethylene melt cooling on the spherulitic morphology and the physical properties of the processed polymer was investigated.

The specific aims of the research programme were to:

- Investigate the effect of process variables on the mould induction, polymer fusion and melt densification phases of the heating cycle.
- Study the effect of cooling rate on the degree of crystallinity and the spherulitic size in linear low density polyethylene.
- Investigate the effect of processing conditions on the tensile properties of the polymer.
- Examine the polymer fusion process during the heating cycle.
- Summarise the heat transfer processes taking place in a typical rotational moulding cycle and establish what thermal property data is necessary for heat transfer calculations.
- Measure the thermal conductivity of the polymer powder.
- Establish the isotropy of mechanical properties in rotational mouldings.

CHAPTER 2

TECHNICAL ANALYSIS OF THE ROTATIONAL MOULDING PROCESS

2.1. Polymer parameters

The quality of a rotational moulding depends not only on the physical properties of the polymer, but also on the characteristics of the polymer powder. These are the particle shape, particle size, and particle size distribution.

The ideal polymer particle is one that flows easily into sharp angles, undercuts or ribbing within the mould and melts to a bubble free state with the minimum of heat.

2.1.1. Polyethylene powder characteristics

The shape of the rotational moulding powder particle can be shown to be significant during the heating cycle [227].

Heat transfer to a particle takes place by conduction through contact with other particles, contact with the mould surface and by convection from the air inside the mould (see Section 5.3.)

The surface to volume ratio of a particle relates to the efficiency by which heat transfer through the particles takes place. For air convection, and for a flat particle of thickness R, the surface to volume ratio is 1/R. For a cube of side R this becomes 6/R, and for a sphere of radius R, it is 3/R. For contact conduction, however, if only a small surface

area of the particle is in contact with a heated surface, the surface to volume ratio becomes 1/(2R) for a flat sheet, 1/R for a cube, and zero for a sphere. This means that as the particle becomes more spherical, the area for conductive heat transfer is reduced. The conclusion is that the rate at which a polymer powder melts, is determined by the shape of the powder particle.

In addition to its role in heat transfer, the shape of the polymer particle is also important in the flow of the powder during rotation – the more spherical the shape, the better the flow.

Finally, the particle size and size distribution can also be shown to affect the rate of heat transfer. The argument used for particle shape can be used again. The smaller the characteristic dimension R, the larger the surface to volume ratio and the more efficient the contact or conductive heat transfer becomes. Thus the heat transfer improves with decreasing particle size.

2.1.2. Bulk density and dry flow

Bulk density of the polymer powder and its dry-flow or pourability are two closely related properties which, as well as particle shape, size and distribution, affect the flow characteristics of the powder.

Inefficient grinding of the powder results in the formation of hairs and tails on the powder particles. The presence of these particles reduces bulk density of the powder and

results in poor dry flow. During rotation, these particles can also agglomerate as a result of the build of static charge. This causes an uneven inner surface and bridging in sharp corners, angles and undercuts of the moulding. To produce high quality rotationally moulded products with uniform wall thickness, it is therefore essential to have a free flowing powder of high bulk density.

2.1.3. Melt flow index

The ease with which a polymer powder melts and forms a continuous layer in the mould during the heating cycle is determined by the molecular weight, or the melt viscosity of the polymer at low rates of shear. This is usually represented by the melt flow index (MFI). This is the measurement of a melt viscosity test carried out under standardised rates of shear at 190°C. Polymer melts with low melt viscosity have a high value of MFI; the value of the MFI decreases with increasing melt viscosity. Most polymers used for rotational moulding have a an MFI within the range 2 – 20.

2.2. The heating cycle

The function of the heating cycle is to convert the polymer from powder to a homogeneous melt. It is important to achieve the correct degree of fusion of the polymer; underfusion or overfusion has been reported to result in a detriment in the physical and chemical properties of the moulding [26].

As well as rotational moulding, the study of polymer fusion is also important to other

forming processes such as extrusion and calendering. However, in rotational moulding, the mechanism of polymer fusion should be unique compared to other processes, since unlike other processes, particle fusion in rotational moulding is achieved at atmospheric pressures and in the absence of shear stresses. Fusion is therefore controlled only by temperature [1].

In rotational moulding three conditions are reported to be identifiable in the fusion cycle of any polymer: underfusion, optimum fusion and overfusion [98]. Underfusion occurs when the heating stage is terminated before the fusion process is complete; the particles are still identifiable and separable. The finished moulding has a rough or powdery inside surface and a large number of air bubbles throughout the wall of the moulding. The presence of these bubbles is undesirable in the moulding as they can act as stress concentrators to initiate both impact and stress crack type failures [98].

Continued heating beyond the underfused state results in a formation of a smooth inner surface and a complete absence of air bubbles, with the inner surface appearing dull and the same colour as the outer surface, indicating absence of any surface oxidation. This is the condition that is recognised in the rotational moulding industry as the condition of optimum polymer fusion and one which is accepted as resulting in the best physical properties [98], although little experimental evidence is reported to support this assumption.

A heating stage that is longer than that required for the optimum fusion leads to the thermal and oxidative degradation of the polymer resulting in an overfused moulding

showing the characteristic signs of oxidative degradation e.g. glossy or discoloured inner surface. Overfused mouldings are reported to show a drastic reduction in low temperature impact strength [98], mainly due to the oxidation of the polymer.

In rotational moulding therefore, the surface finish of the moulding is not only of aesthetic importance, but can also indicate whether a polymer has been processed to achieve the best physical and chemical properties of the polymer [3]. To allow the optimum degree of fusion in the polymer, the temperature of the heating medium must be set at the optimum value and the length of the heating cycle accurately determined to avoid underfusion or degradation [31]. The rate at which the polymer melts is also an important factor in the determination of the length of the overall processing cycle [22, 28], and also in the design of the heating system in the processing equipment [109].

However, at this stage in the development of the rotational moulding process, the length of the heating cycle and the oven temperature, for most polymers, are widely set as a result of experience rather than any scientific study [22, 53]. A number of references give 'rules of thumb' or empirical data represented graphically, to help in the prediction of the time required for the mould in the oven to give a good quality finished product [23, 54, 55].

2.2.1. Effect of process variables on the heating cycle

For a given mould/polymer combination, the length of the heating cycle will be determined primarily by the following factors:

- The oven set temperature
- The heat transfer medium
- The heat medium velocity
- The moulding thickness

2.3. The cooling cycle

The method used to cool the mould is determined by the rate of cooling desired in the melt. Slow cooling rates are achieved by rotating the mould in ambient conditions; fast cooling by spraying the mould with cold water. Intermediate cooling rates are obtained by either using a combination of the two [25] or by forced air convection.

In rotational moulding the rate of cooling of the polymer melt is critical in that it determines the final physical properties of the moulding by affecting the morphology of the processed sample, see Section 2.4. Accurately controlled cooling cycles are reported to result in better physical properties [1, 27] and good dimensional stability [25] in the moulding. However, at present the control of the cooling cycle is reported to be largely neglected in the rotational moulding industry [23, 28, 50].

The rate of cooling is also important in rotational moulding because no pressure is used to hold the part against the mould wall. This can result in the moulding warping during the cooling cycle [163].

The mould cooling process is thus important to the end use properties of the moulding

and needs to be studied and controlled [49].

2.4. Heat transfer in the rotational moulding process

In most polymer processing techniques, the accurate correlation of heat transfer to the polymer and the rate at which the polymer melts is important during the heating cycle [112]. In rotational moulding, the optimum rate of heat transfer to the polymer is not necessarily the maximum rate, as a limit is set on the rate by the thermal oxidative degradation of the polymer when exposed to oxygen at high temperatures [2, 53].

The time temperature relationships (for all processing techniques) are also widely known to affect the economics and physical properties of the moulding. Thus to optimise cycle times and to achieve uniform heating of the polymer are the major aims of the rotational moulding process [17, 156].

The optimisation of any process is best done by the mathematical modelling of the process. Of the three stages of a polymer processing cycle (melting, shaping, cooling), in major processing techniques such as blow moulding and injection moulding, the mould is associated with only shaping and cooling of the polymer. Hence, generally, many heat transfer studies have concentrated on the cooling cycle. In rotational moulding however, the mould is also involved in the heating of the polymer as well, and although many polymer processing techniques have been and continue to be analysed, to date only a few attempts at mathematically modelling rotational moulding have been made. These have been summarised by Tiang and Bellehumeur [188]. The first attempt at mathematical

modelling was made by Rao and Throne in 1972 [55]. Since then several reports have been published to improve the model and these are discussed in Section 5.3.

For any moulding technique, it is first necessary to establish the heat transfer processes that take place in a typical moulding cycle. This is the first stage in the mathematical modelling of the process. However, detailed heat transfer analysis of rotational moulding has not yet been done. Throne's [55] approach is only approximate and only considers the main heat transfer processes. An attempt is thus made in Section 5.3 to identify the heat transfer processes taking place in the heating and cooling cycles of the rotational moulding process.

2.4.1. Thermal properties

Discussion of heat transfer in the rotational moulding process in Section 5.3 shows how heat transfer analysis and calculations for linear low density polyethylene and mild steel mould combination require the following thermal property data:

- Specific heat capacity of LLDPE and mild steel.
- Thermal conductivity or thermal diffusivity of LLDPE in the powdered state, with and without voids in the solid state and finally, in the melt state.
- Thermal conductivity or thermal diffusivity of mild steel.

The thermal properties of metals and their alloys have been measured accurately and extensively and reliable data is widely available in standard data books.

A lot of work has also been done on the measurement of thermal properties of polymers, especially thermal conductivity. However, a look through the literature indicates that the published data is very inconsistent (see Section 1.8.3.1), with no work reported (before completion of this study) on the thermal conductivity of linear low density polyethylene in the powdered state.

2.5. Effect of processing conditions on physical properties

For a given polymer, the physical and chemical properties of the moulding will depend on the interaction between the polymer properties and process variables. The effects of processing techniques on polymer properties can sometimes be so small as to be insignificant. However, often the effects are large and cannot be ignored. This area of the effects of processing conditions on the polymer and hence the properties of the moulding, is a growing area of research and is becoming increasingly documented for most processing techniques. However, for rotational moulding this is a relatively new area of research.

The main reason why the effect of processing conditions on the physical and chemical properties of the mouldings needs to be examined, is that a knowledge of these factors can help determine the choice of polymer and processing conditions for an optimum balance of properties in the final moulding.

2.5.1. Crystallinity in rotational mouldings

In polymer processing, the crystallisation of polymers is of significant technological importance, because crystallinity in the processed polymer is widely known to affect the physical and chemical properties of the polymer.

The morphology of crystalline regions in the polymer can vary according to the conditions under which the regions develop. Polyethylene crystallised from the melt results in the formations of small units called spherulites. Spherulitic size and the degree of crystallinity are affected by the processing conditions of the polymer and are important parameters in determining the physical properties of the moulding.

Since polyethylene is the most widely used polymer for rotational moulding, and because it is crystallisable, it is necessary to understand the effect of process variables on the crystallinity of processed polymer. The characteristic features of rotational moulding make the microstructure of the processed polymer unique. Slow rotation speeds with the resulting low shear rates in the polymer, slow rates of heating and cooling and the presence of air inside the mould lead to unique morphologies in the moulding when compared to other processes using high pressures and high shear rates [161].

2.5.2. Isotropy in rotational mouldings

One potential change found in most processing technique where the polymer melt is sheared, is molecular orientation. On being sheared in the melt, the polymer molecules

become disentangled and orientated along the streamlines. This orientation may occur within, for example, an extruder or between the time when the polymer is extruded and finally cooled to the solid state. Unless this orientation is relaxed first, some of it may be 'frozen-in' in the solid polymer.

The effects of 'frozen-in' orientation in the solid can lead to molecular orientation, which can cause anisotropy of mechanical properties such as tensile strength.

In rotational moulding, as already discussed previously, because plastisation of the polymer is achieved through high temperatures only and not by using high pressures, the polymer is not sheared at any stage during its processing. This means that there should be no molecular orientation in the melt and hence no ' frozen-in' stress in the moulding. The absence of molecular orientation should also result in isotropy of mechanical properties.

The absence of stress in rotational mouldings is widely assumed in the rotational moulding industry, but to date no supporting experimental evidence has been reported.

CHAPTER 3

EXPERIMENTAL PROCEDURE

3.1. Programme of work

The first step was to select a moulding as the standard test moulding, to establish the length of its heating and cooling cycles using the trial and error method of the rotational moulding industry, and to check the results by examining the moulding surfaces for complete fusion and melt densification using scanning electron microscopy.

The next step was to investigate the effect of selected process variables on:

1. The mould induction, polymer fusion and melt densification phases of the heating cycle.
2. The crystallinity of linear low density polyethylene, LLDPE
3. The mechanical properties of the moulding.

Finally, the particle size distribution, melt flow index, and thermal conductivity of LLDPE were measured.

In the investigation of the heating cycle, the process variables examined were the oven set temperature and the moulding wall thickness.

In the measurement of the mould induction time, the first problem encountered was measuring the temperature of the rotating mould during heating. One solution was to

stop the rotation periodically, remove the mould from the oven and measure the temperature using a surface probe. To minimise errors in this method (discussed in Section 5.6), a second method of temperature measurement was used where mould rotation was stopped during the mould induction phase and any effects of rotation on the heating rate were ignored. This allowed the mould to be kept in the oven and a copper/constantin thermocouple to be attached to the mould surface so that the temperature could be continuously recorded. Finally, the mould temperature was measured using infra red thermography. This method also allowed the mould to be kept in the oven during induction, and for the mould to rotate between temperature measurements.

In the study of crystallinity, the effect of the crystallisation temperature and the cooling rate on the degree of crystallinity and spherulitic size was investigated. The variation of the degree of crystallinity within the moulding wall was also examined. The crystallisation temperature was varied by changing the oven set temperature. The two cooling methods (rates) investigated were the cooling of mould and polymer in ambient air conditions and by water spray.

In the investigation of tensile properties, the effect of the degree of fusion and melt densification, and the degree of crystallinity on the tensile properties of the moulding was examined. The isotropy of tensile properties of the mouldings was also investigated.

Finally, an analysis of polymer fusion during the heating cycle was made, the heat transfer processes taking place in a rotational moulding cycle summarised and the

thermal conductivity of polyethylene measured in the solid and the powdered state.

3.2. Materials and equipment

3.2.1. Linear low density polyethylene

The polymer chosen for the study is linear low density polyethylene, LLDPE, with a narrow molecular weight distribution and density in the range 0.920 to 0.940 kg m^{-1}. This polymer is widely used in the rotational moulding industry [2, 24, 29, 211] and is sold by Du Pont of Canada as Sclair 8307 [212].

The melt temperature range of the polyethylene was measured as commencing at 120° C.

3.2.2. Rotational moulding machine

The rotational moulding machine used for the study was a straight-line shuttle type machine shown in Figure 4 and Figure 13. The machine was believed not to be commercially available, but built on site for prototype moulding. The spindle and drive are mounted on a carriage that moves the track through three loading and cooling and heating stations. No other information concerning the machine was available.

The oven was heated by hot-air convection where air is first heated by passing it over a gas flame. The heated air is then blown into the oven and over the mould by a fan. The air is then directed out of the oven and over the gas flame again for reheating and

FIGURE 13

ROTATIONAL MOULDING MACHINE USED IN STUDY

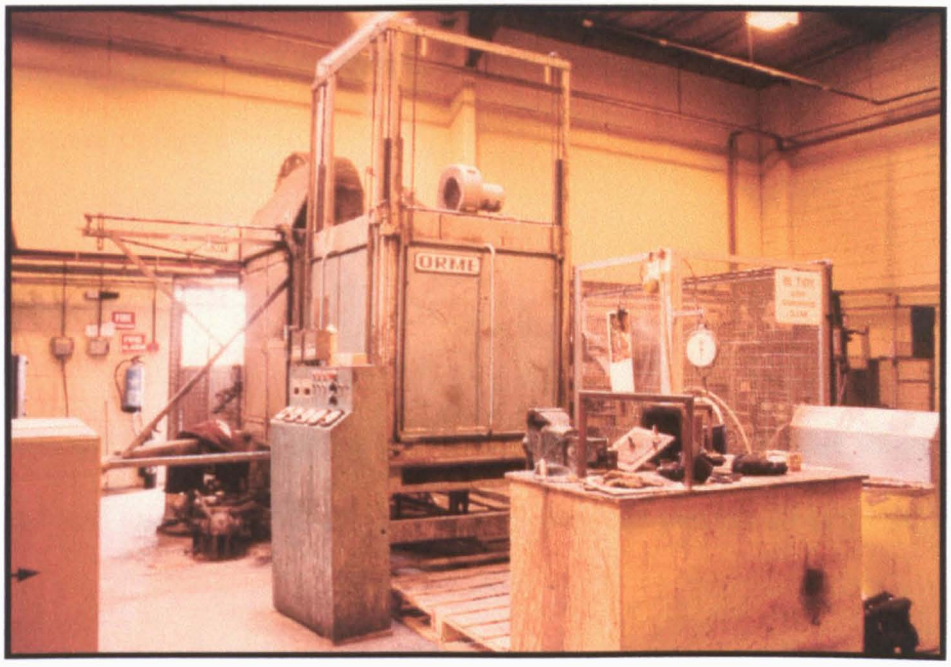

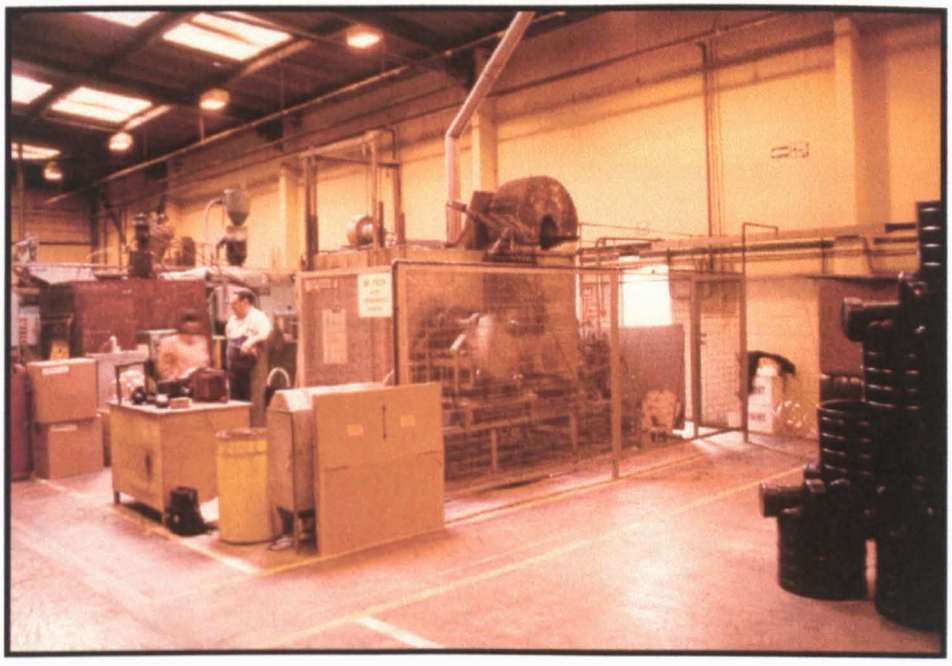

reintroduced into the oven and so on, as shown in Figure 4. The temperature of the air is controlled by varying the temperature of the flame. The velocity of the air is determined by the speed of the fan, which for this machine was fixed by the manufacturer.

Three methods for cooling the mould were available; water quench, cooling in air or a water spray. No control over the temperature of the cooling medium was available for any of the three methods.

3.2.3. Rotational mould

The mould used for the study was a mild steel sheet metal mould of cubic shape, of side 0.23 m and wall thickness 0.004 m. The air vent was built into the lid of the mould, see Figure 14.

3.2.4. Release agent

The release agent was silicone based and sold under the trade name of Freekote 44. When applied to the mould surface, the release agent polymerises to form a clear continuous microthin film stable at temperatures up to 500° C.

FIGURE 14

ROTATIONAL MOULD USED IN STUDY

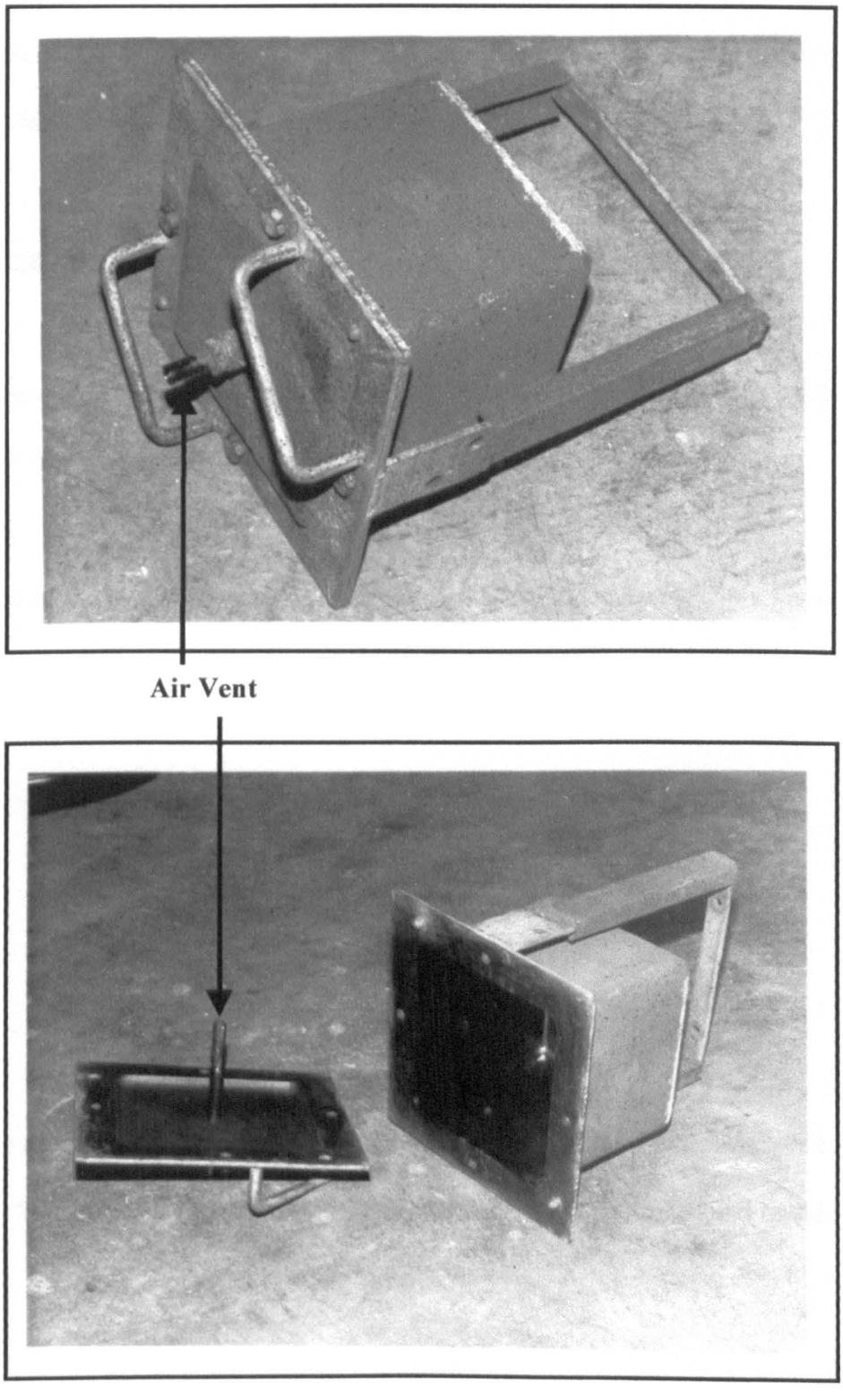

3.3. Assessment techniques

3.3.1. Sieve Analysis

The particle size distribution of polyethylene was determined by sieve analysis similar to the ASTM Test Method D 1921 - 62 (1970).

3.3.2. Apparent density and flow of powder

The apparent or bulk density of the powder was measured by ASTM Test Method D 1895-69, Method A, a standard test used in the rotational moulding industry.

The flow of the powder particles was measured by the time required for a given amount of powder to flow by gravity through a standard funnel of the following dimensions:

Throat diameter	=	125 mm
Included angle	=	60°
Stem	=	100 mm
Opening I.D.	=	10.5 mm

The end of the funnel is kept closed while 90g of the polymer powder is placed into the funnel. The sample is then allowed to flow freely through the funnel and timed.

3.3.3. Melt flow properties

The method used to measure the melt flow index of polyethylene was B.S. 2782. This method is restricted to polyethylene compounds and three variants are described.

Method A recommended for polymers with a MFI in the range 1 to 25 was selected.

3.3.4. Temperature measurement using a thermocouple

The material combination was copper/constantin with an automatic converter to convert the EMF to a digital readout.

For temperature measurement during the mould induction phase, the junction bead was attached to the mould surface with a high temperature resistant adhesive. In another method of temperature measurement, a surface probe with a built in junction bead was used.

3.3.5. Thermal imaging with infrared

The thermovision camera used was the AGA thermovision 700 system. The camera is based on the principle of electronic thermography. This is the name associated with a group of infrared imaging systems that employ some intermediate means of converting variations in infrared radiation into a visual display that may be photographed by conventional methods.

The camera scans the target point by point and collects the infrared radiation emanating from a target. This is then directed on to a supercooled photodetector, see Figure 15, which converts the incoming energy into a proportionate electrical signal.

The detector is a photon detector made of indium antimonide. For the scanning rates used in the AGA thermovision camera, the indium antimonide has a response time shorter than a microsecond.

The detector converts the incoming energy from the scanner into a proportionate electrical signal that may be used to modulate the input of the cathode ray tube. The image displayed on the face of the cathode ray tube is a temperature profile, where variations in image density correspond to temperature differences in the original subject. This image may be visually observed, photographed in the conventional manner, or analysed using a digital format. The hardware and software to do this has been developed by AGA. Several methods to represent the difference in temperature are available; one is the use of different colours.

The mould induction time was measured by setting the oven temperature to 220° C and placing the mould initially at room temperature into the oven. The oven door was opened after 1 ± 0.5 minute and a thermal image of the mould taken. The procedure was repeated for an oven set temperature of 440° C.

FIGURE 15

ARRANGEMENT OF ELECTRO-OPTICAL COMPONENTS IN THE INFRA-RED SCANNER OF THE AGA THERMOVISION SYSTEM

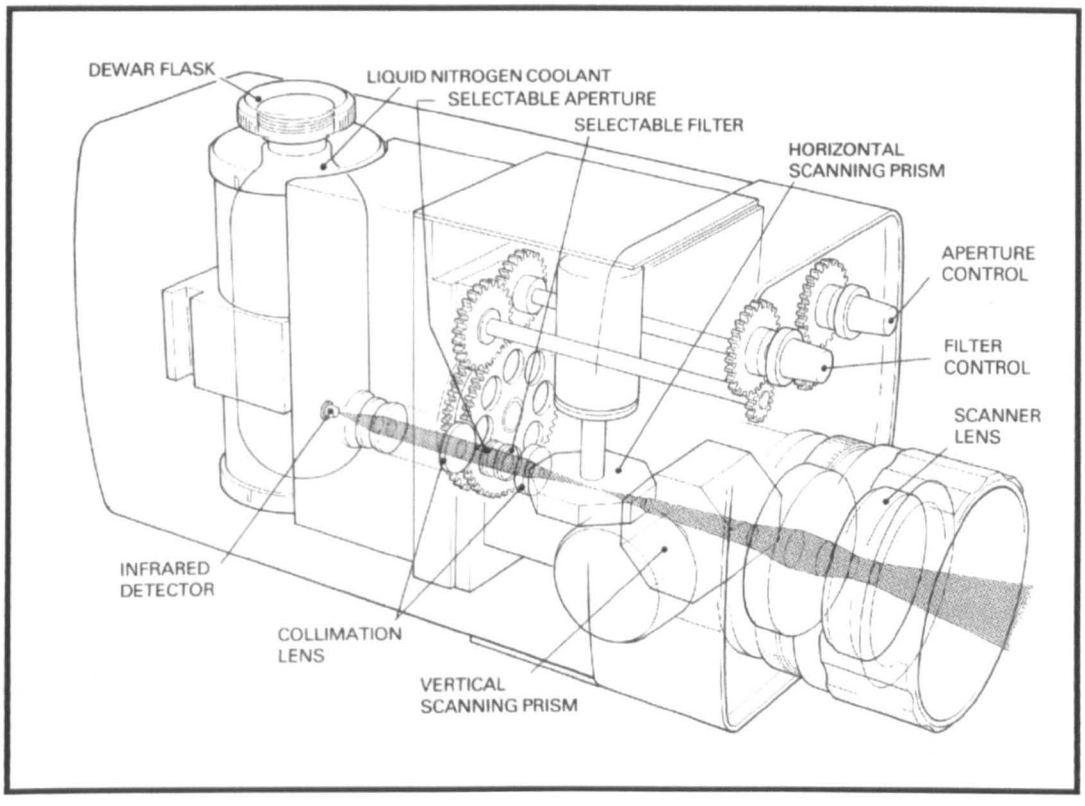

3.3.6. Mechanical testing of polymers

Tensile tests were carried out on elongated specimens that can be gripped at both ends.

Four basic types of test piece are described in the standards literature: the narrow-waisted dumbell, the broad-waisted dumbell, the 'dog-bone' dumbell and the parallel-side strip. The type used in this study is the narrow-waisted dumbell shape standardised in ISO R527 (1970) as the type 2 test piece, in ISO/DIS 527 as the type A test piece, in BS 2728, Method 320A (1976), in ASTM D638 (1977) as the type II or IV test piece and DIN 53455 (1978) as the type 3 test piece.

The tensile tests were carried out on a constant rate traverse type machine, where the test is controlled by the straining of the specimen and the resulting force measured.

In the investigation of isotropy, two sets of test samples at right angles to each other were cut from the moulding walls.

3.3.7. Transmitted light microscopy

The design, construction and use of various types of optical microscopes are discussed in standard texts.

Polarised light microsopy

In polarised light microscopy, the illuminating source is plane polarised before it illuminates the sample and passes through a second polariser or analyser. In most cases the polariser and analyser are crossed at 90° to each other which means that only materials which cause a partial depolarisation of the light are visible.

Preparing specimens for light microsopy

High ductility of linear low-density polyethylene initially made it difficult to microtome thin samples (3 μm to 4 μm) without shearing the polymer. This was resolved by freezing the polymer in liquid nitrogen prior to sectioning, and by allowing liquid nitrogen to 'drip over' the sample during sectioning. The specimens were mounted in Canada balsam.

3.3.8. Degree of crystallinity by density measurement

The density of polyethylene was measured by floatation in a density-gradient column. This is a long vertical tube containing a mixture of liquids of different densities (mixture of isopropanol and water.) The column was set up with a low density liquid at the top and a steady increase in density downwards. The column was then calibrated with a series of floats of known density. Samples of thickness 5 μm were cut from mouldings and the density determined from the position the samples adopted when dropped into the column.

3.3.9. Thermal conductivity of polyethylene

The thermal conductivity of polyethylene was measured using a method based on the unguarded hot plate method specified in BS 874 (1973.) The apparatus consists of heat sinks controlled at a given temperature, see Figure 16. Thermocouples are embedded on either side of the heater and on the surface of the heat sinks.

Two polyethylene samples are placed on sides of the heat source and heated at a known rate. The temperature of the heater is adjusted so that the temperature difference between T_1 and T_2, and T_3 and T_4 is approximately 10° C.

The apparatus is placed in a constant temperature environment and allowed to reach steady state. The temperature drop across the sample is then measured.

Sample size

The samples were square of sides 10 cm cut from moulding walls. To measure the thermal conductivity of polyethylene powder, square frames filled with equal quantities of powder were placed on either side of heater.

FIGURE 16

STEADY STATE APPARATUS FOR MEASURING THE THERMAL CONDUCTIVITY OF POLYETHYLENE

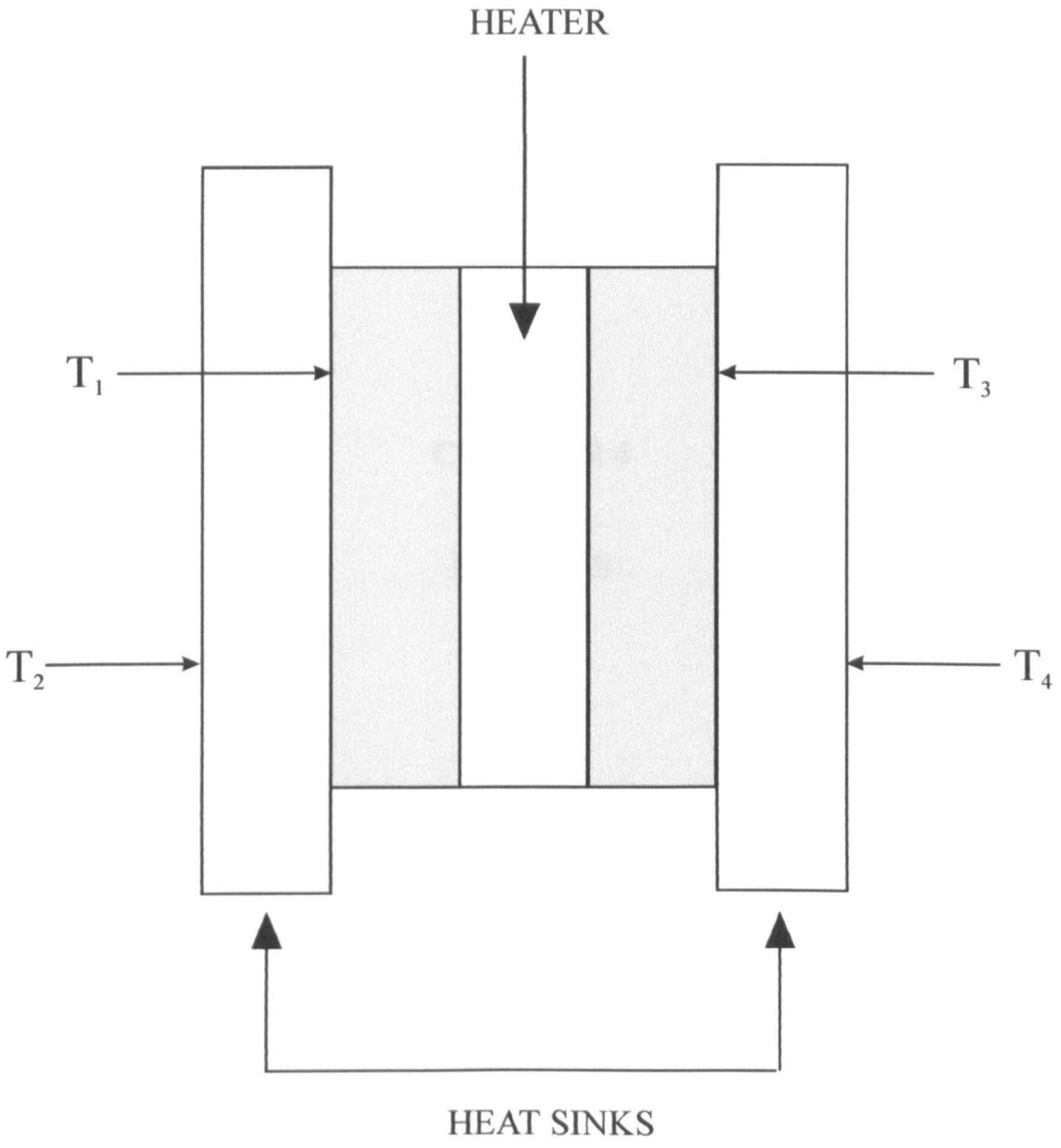

CHAPTER 4

RESULTS

4.1. Physical properties of the polymer

4.1.1. Particle shape

Figure 17 shows microscopic examination of the polyethylene powder at x100 magnification. The photomicrographs reveal the presence of elongations on the polymer particles.

4.1.2. Particle size distribution

The particle size distribution of the polyethylene powder was measured as between 149 μm to 500 μm, see Figure 18.

4.1.3. Bulk density and rheology

The melt flow index of the polyethylene was measured as 3.37 g m^{-1}, see Table 2.

As expected for a semicrystalline polymer, the melt temperature range of polyethylene was found to be wide, with melting beginning at 120° C and ending at 140° C.

Table 2 shows that the bulk density of the unfractionated powder is higher

FIGURE 17

MICROSCOPIC EXAMINATION OF POLYETHYLENE POWDER (MAGNIFICATION x100)

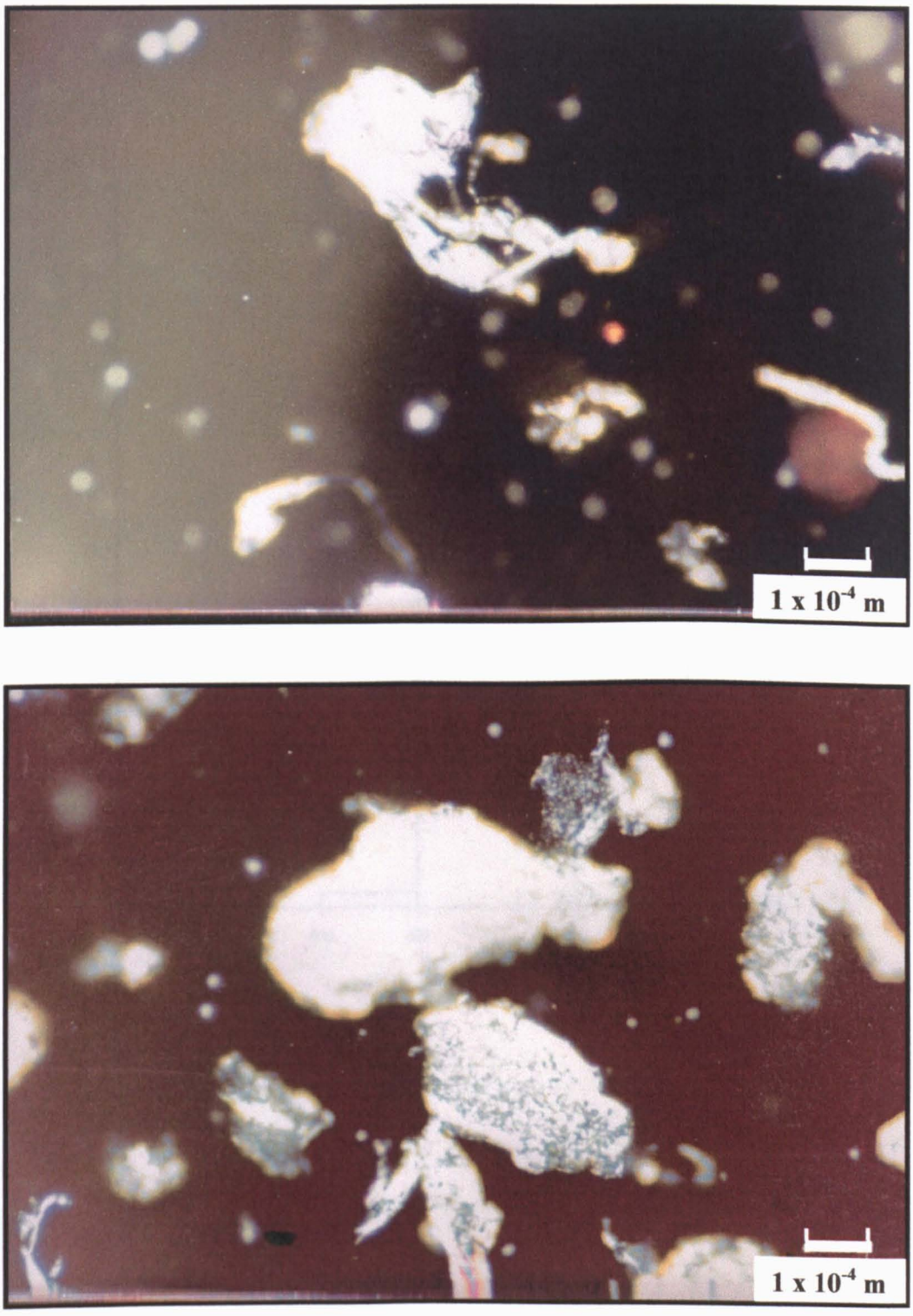

FIGURE 18

PARTICLE SIZE DISTRIBUTION IN POLYETHYLENE POWDER

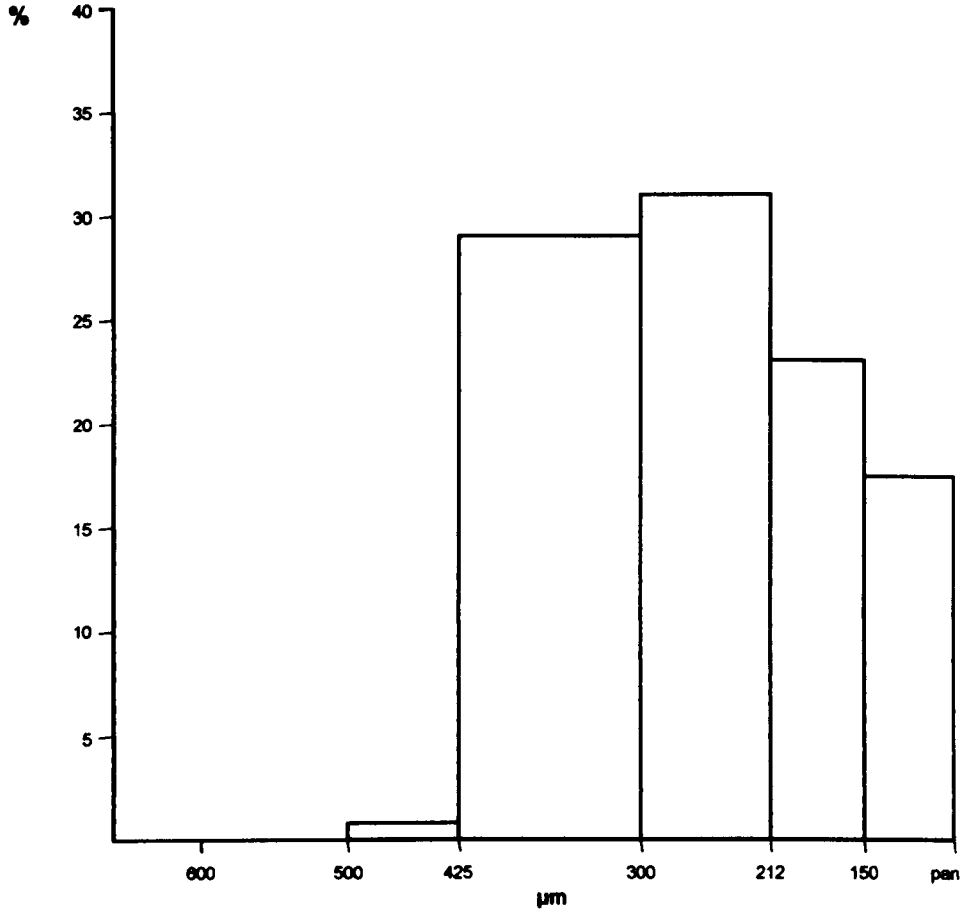

TABLE 2

PHYSICAL PROPERTIES OF POLYETHYLENE

Particle Size (m)	Average Bulk Density x 10^3 (kg m^{-3})	Rate of Flow (g min^{-1})
Unfractionated Powder > 150 – 500	0.33	635.2
425 – 300	0.33	Rate of flow decreasing ↓
300 – 212	0.30	
212 – 150	0.30	
< 150	0.29	Very little flow

Melt Flow Index	3.37 g min^{-1}
Melt Temperature Range	120 – 140 °C

than the bulk density of the fractions below 300 μm. This demonstrates the closer packing expected in a powder with a wider size distribution - the smaller particles occupy the spaces between the larger particles.

Comparison of the bulk density of individual fractions however, shows the results are contrary to the expected. Due to the closer packing of smaller particles, the bulk density of the fractions would be expected to increase with decreasing particle size. However, the results show a decrease in bulk density with decreasing particle size. One explanation is that a greater number of smaller particles have tails or hairs, which reduce the degree of packing. This is supported by the fact that the flow of particles below 300 μm is poor - hairs and tails must reduce the flow properties of the polymer. The results also show that the flow of particles decreases with decreasing particle size, with particles below 150 μm having no flow properties at all. This suggests that the percentage of particles having tails and hairs increase with decreasing particle size.

Du Pont [51] and Throne [54] recommend that smaller particles are included in a rotational moulding powder because they improve the flow of particles by their lubricating action. However in this polymer, because the smaller particles have hairs and tails, they have been shown to actually reduce the flow properties of the polymer.

The results of this study are in agreement with Paquette [21] who reports that the flow properties of the polymer should improve with increasing bulk density of the polymer powder.

4.2. Heating cycle of the standard moulding

The moulding was examined at 1 ± 0.5 minute intervals during the heating cycle and the observations tabulated in Table 3. The moulding was assumed to be complete after 12 ± 0.5 minutes when no bubbles could be observed in the moulding walls.

4.2.1. Scanning electron microscopy

Figure 19 to Figure 29 are scanning electron micrographs of mouldings starting from heating cycle of 2 ± 0.5minutes through to a heating cycle of 12 ± 0.5 minutes. Each Figure shows (i) the mould and (ii) the inner surface of the moulding.

4.2.2. Apparent density

Apparent density measurements are reported in Figure 30. The Figure shows the variation in the apparent density of the moulding with increasing length of the heating cycle.

4.3. Process variables in the heating cycle

Figure 31 shows the increase in the length of the heating cycle of the moulding with

TABLE 3

HEATING CYCLE OF STANDARD MOULDING BY VISUAL OBSERVATION

Heating Cycle (Minutes ± 0.5)	State of Moulding
1	No signs of particle fusion
2	Evidence that particle fusion has begun
3	Melt layer covering the inner mould surface, some polymer still unfused
4	Moulding nearly complete with very little unfused polymer
5	Moulding complete with no signs of unfused polymer, free surface of moulding uneven, air bubbles in wall of moulding
6	 Number of bubbles decreasing Inner mould surface becoming more even
7	
8	
9	
10	
11	
12	Inner mould surface even, no bubbles visible in wall of moulding

FIGURE 19

ELECTRON MICROGRAPH OF MOULDING SURFACE (LENGTH OF HEATING CYCLE = 2 MINUTES)

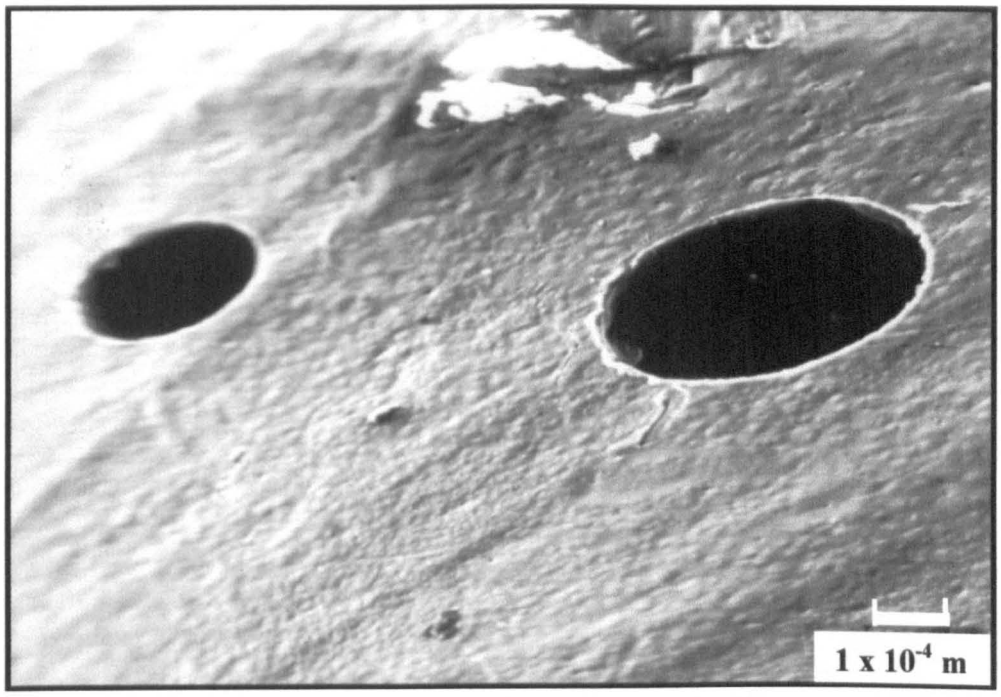

i) Mould surface x100

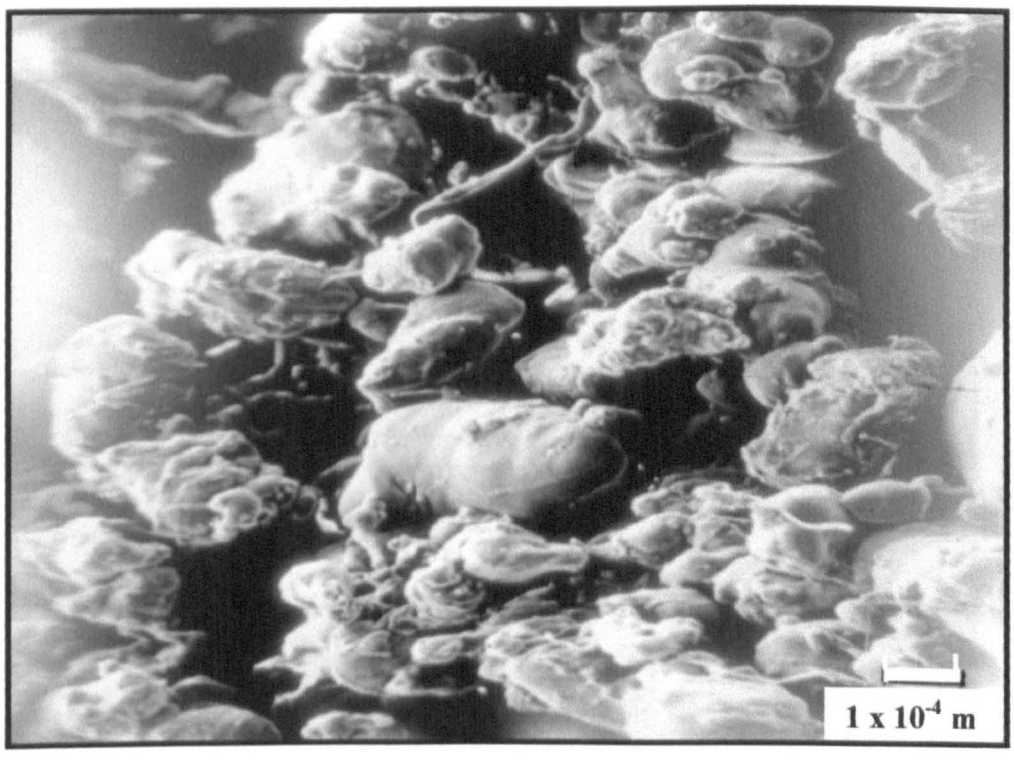

ii) Free surface x100

FIGURE 20

ELECTRON MICROGRAPH OF MOULDING SURFACE (LENGTH OF HEATING CYCLE = 3 MINUTES)

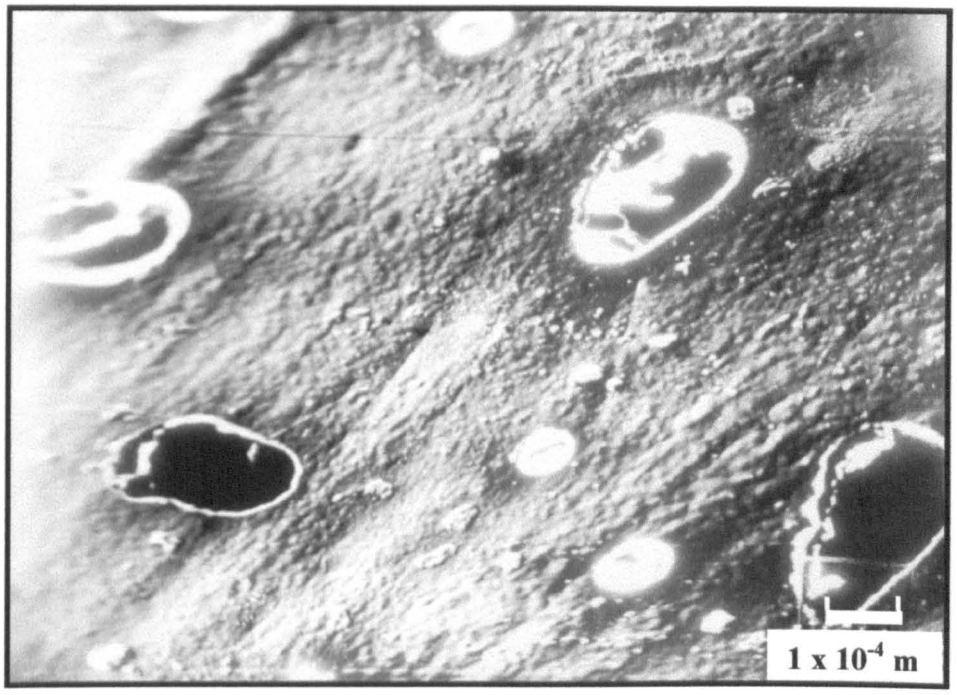

i) Mould surface x100

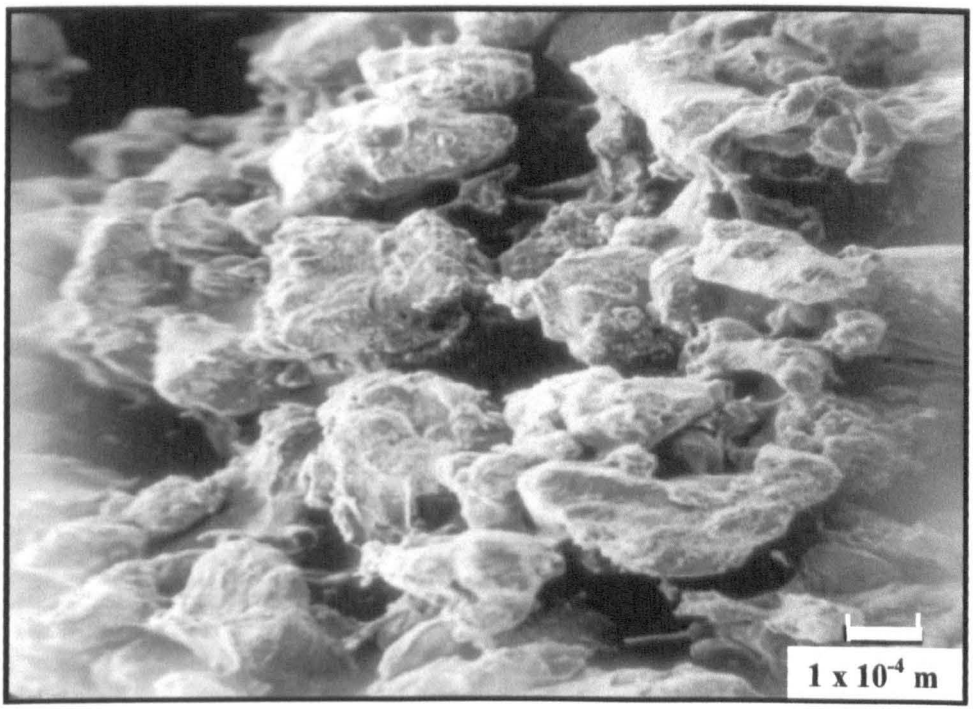

ii) Free surface x100

FIGURE 21

ELECTRON MICROGRAPH OF MOULDING SURFACE (LENGTH OF HEATING CYCLE = 4 MINUTES)

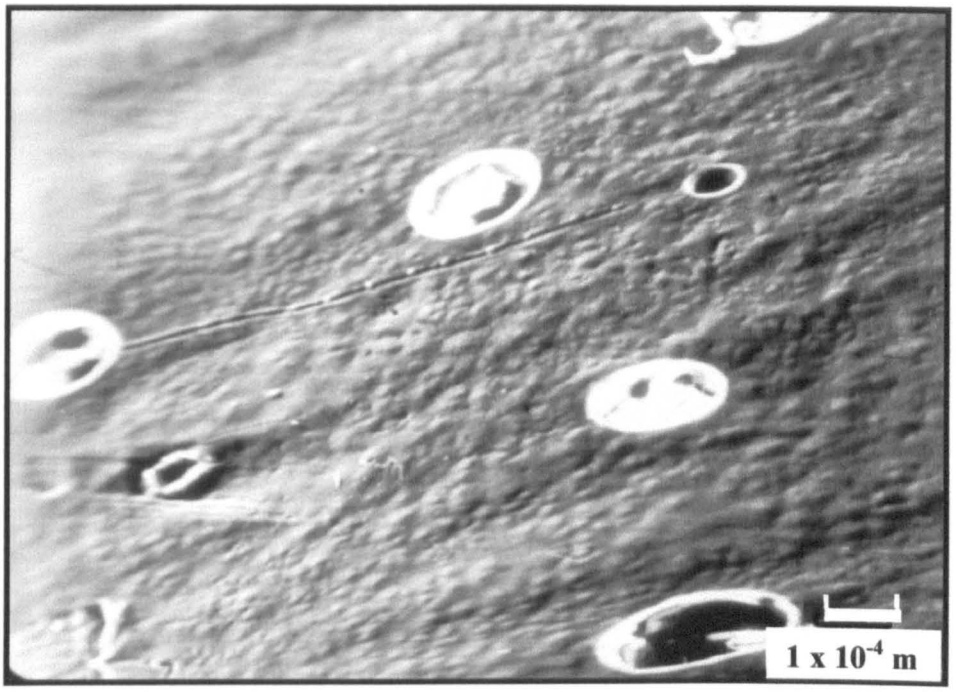

i) Mould surface x100

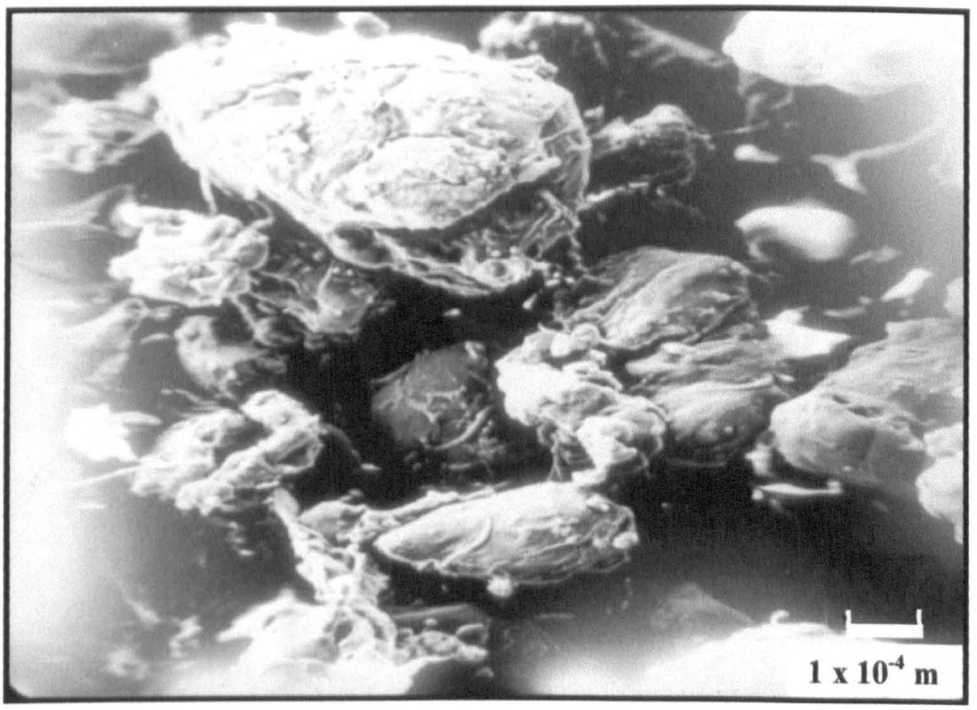

ii) Free surface x100

FIGURE 22

ELECTRON MICROGRAPH OF MOULDING SURFACE (LENGTH OF HEATING CYCLE = 5 MINUTES)

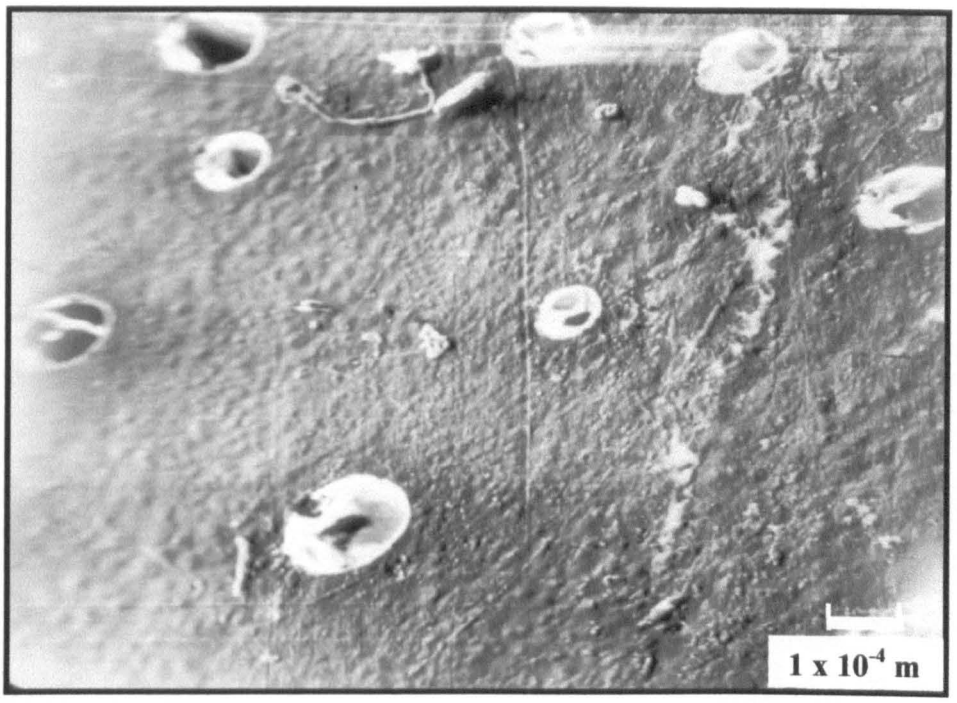

i) Mould surface x100

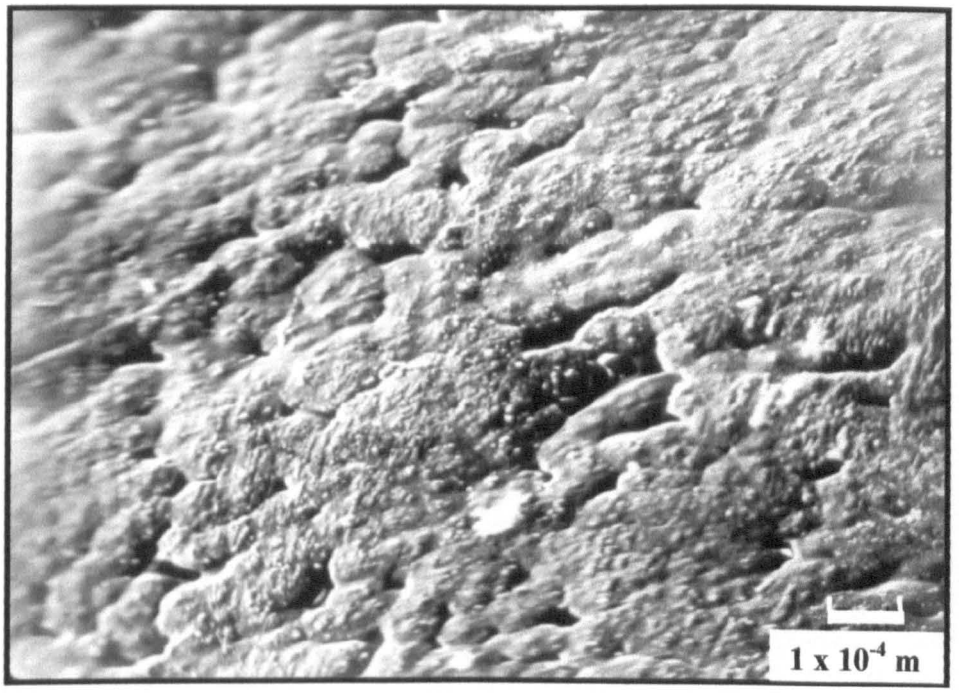

ii) Free surface x100

FIGURE 23

ELECTRON MICROGRAPH OF MOULDING SURFACE (LENGTH OF HEATING CYCLE = 6 MINUTES)

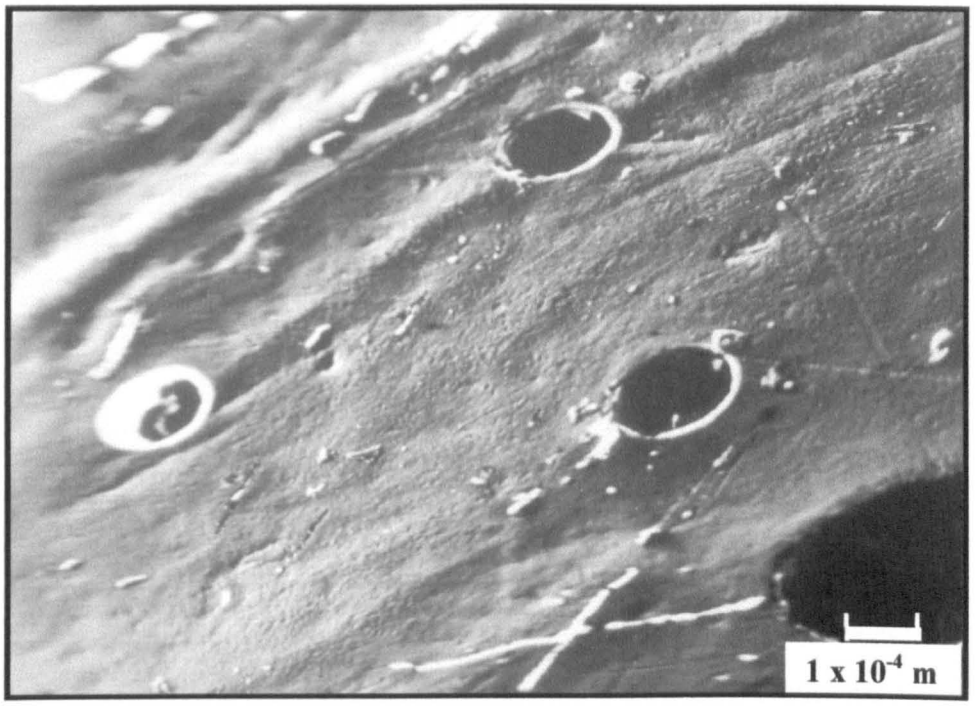

i) Mould surface x100

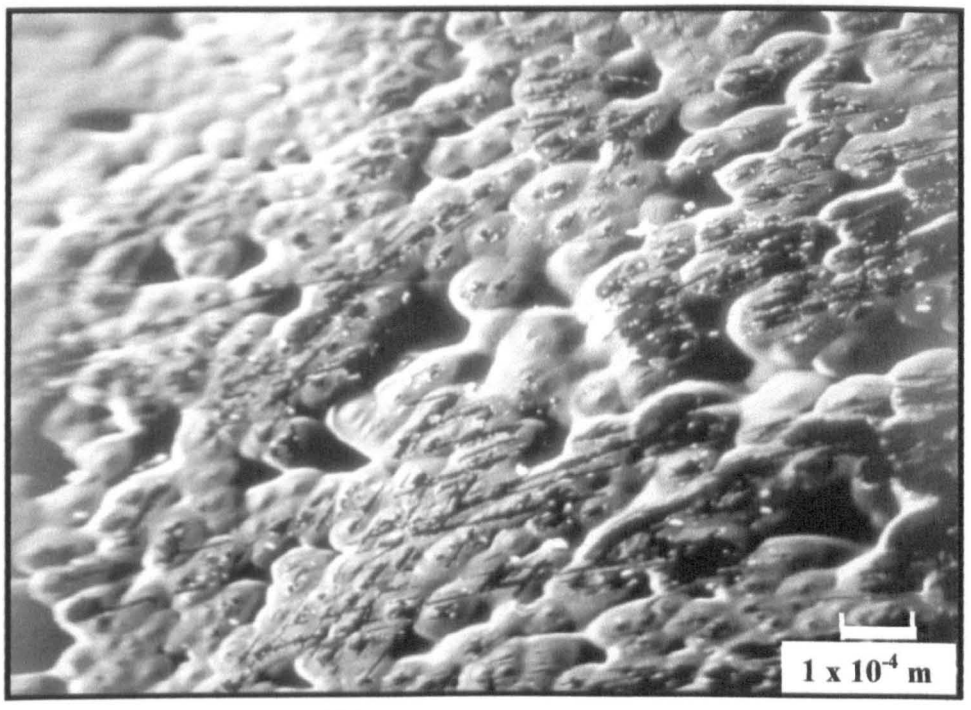

ii) Free surface x100

FIGURE 24

ELECTRON MICROGRAPH OF MOULDING SURFACE (LENGTH OF HEATING CYCLE = 7 MINUTES)

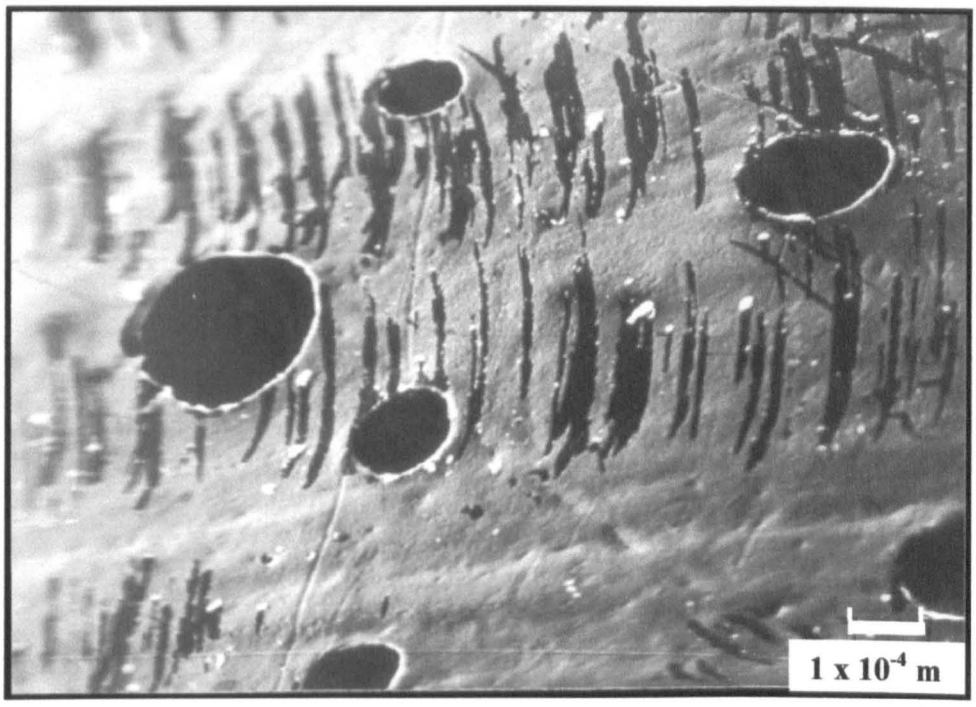

i)Mould surface x100

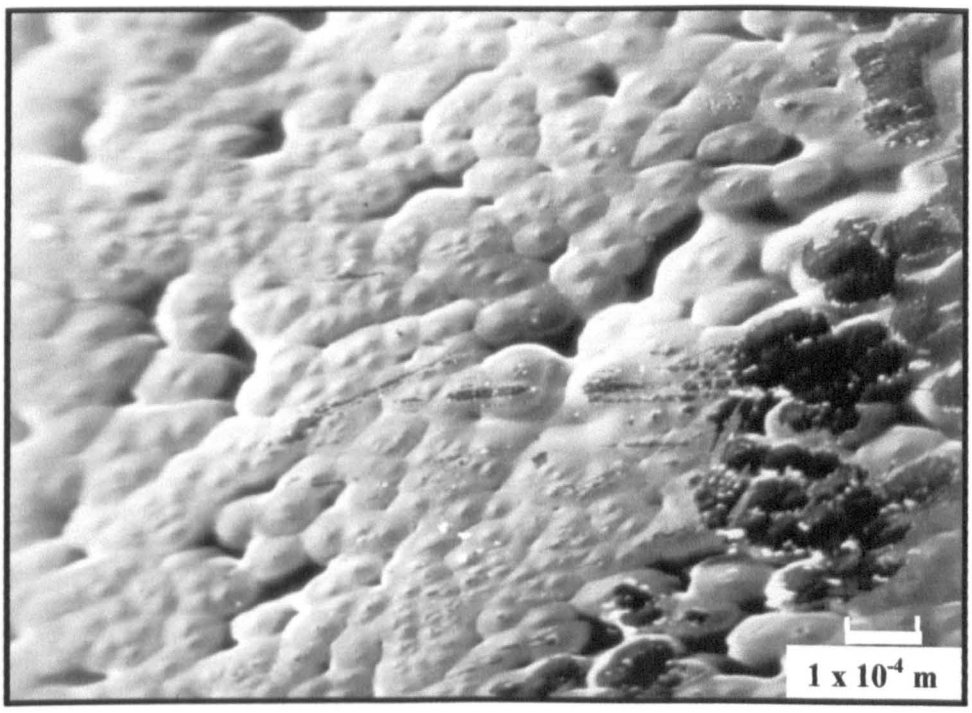

ii) Free surface x100

FIGURE 25

ELECTRON MICROGRAPH OF MOULDING SURFACE (LENGTH OF HEATING CYCLE = 8 MINUTES)

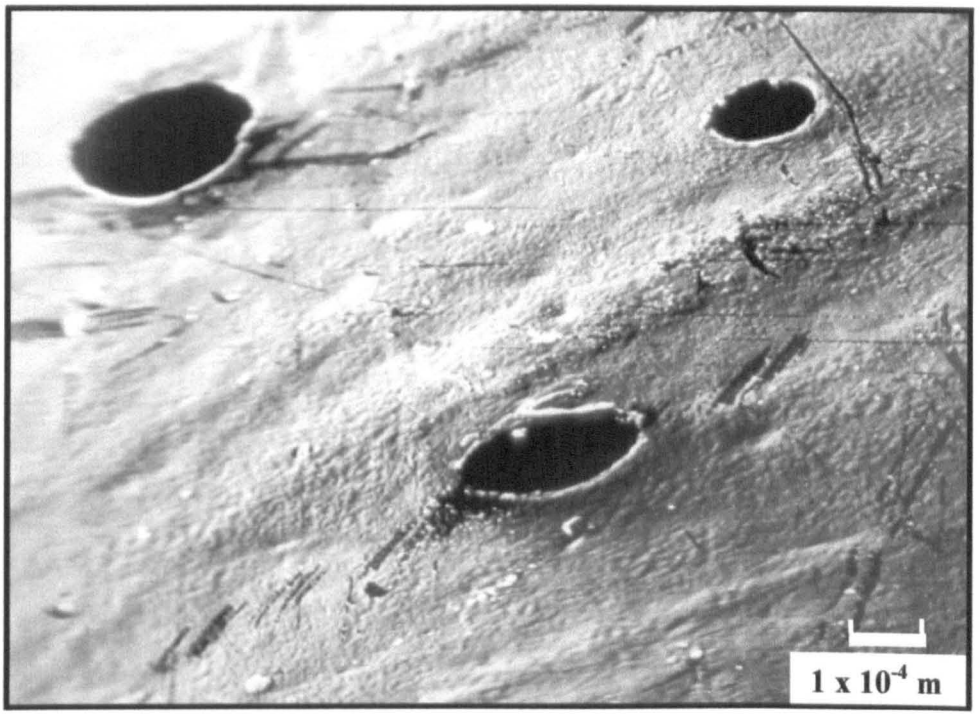

i) Mould surface x100

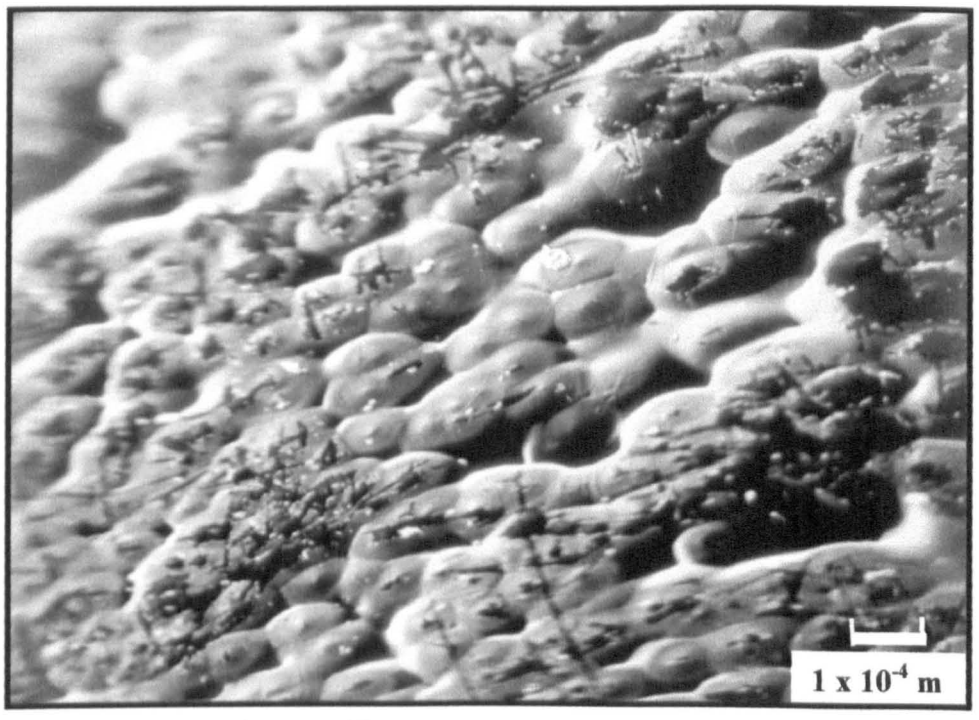

ii) Free surface x100

FIGURE 26

ELECTRON MICROGRAPH OF MOULDING SURFACE (LENGTH OF HEATING CYCLE = 9 MINUTES)

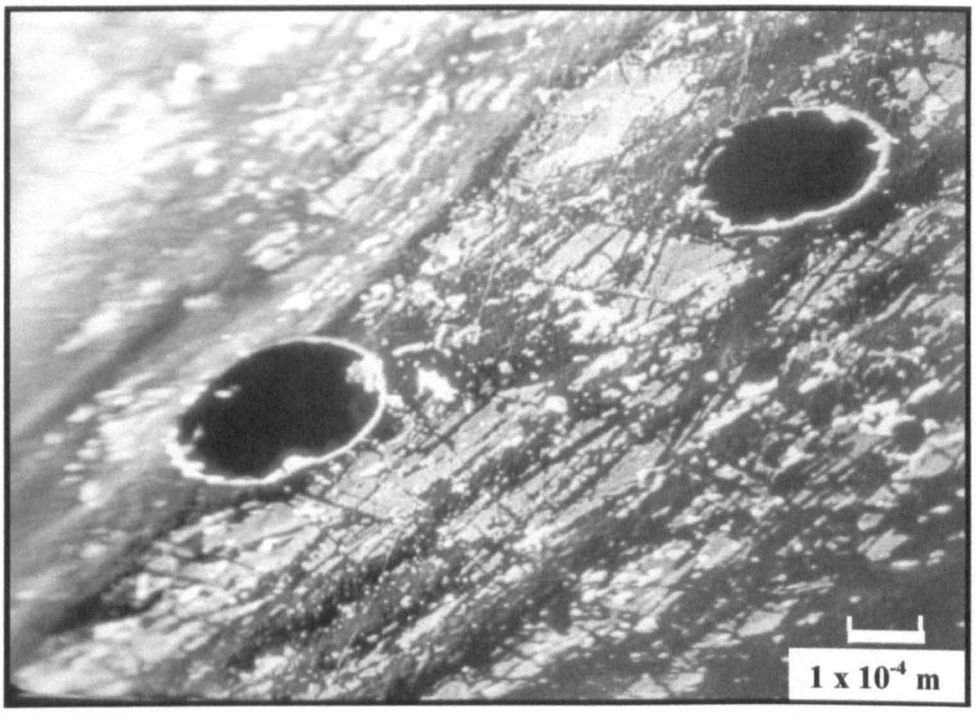

i) Mould surface x100

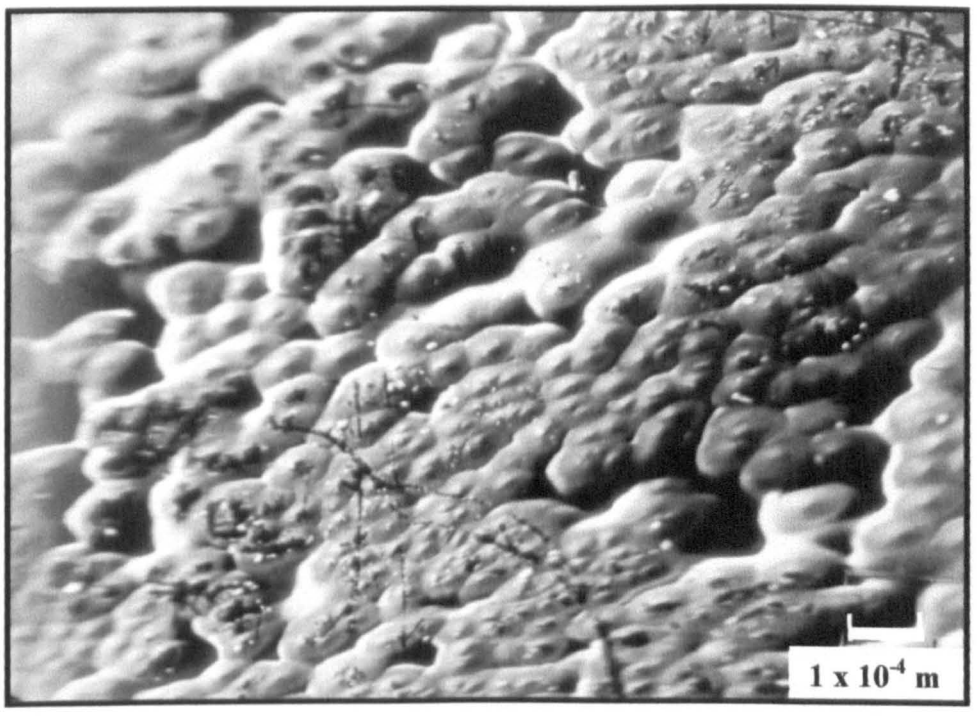

ii) Free surface x100

FIGURE 27

ELECTRON MICROGRAPH OF MOULDING SURFACE (LENGTH OF HEATING CYCLE = 10 MINUTES)

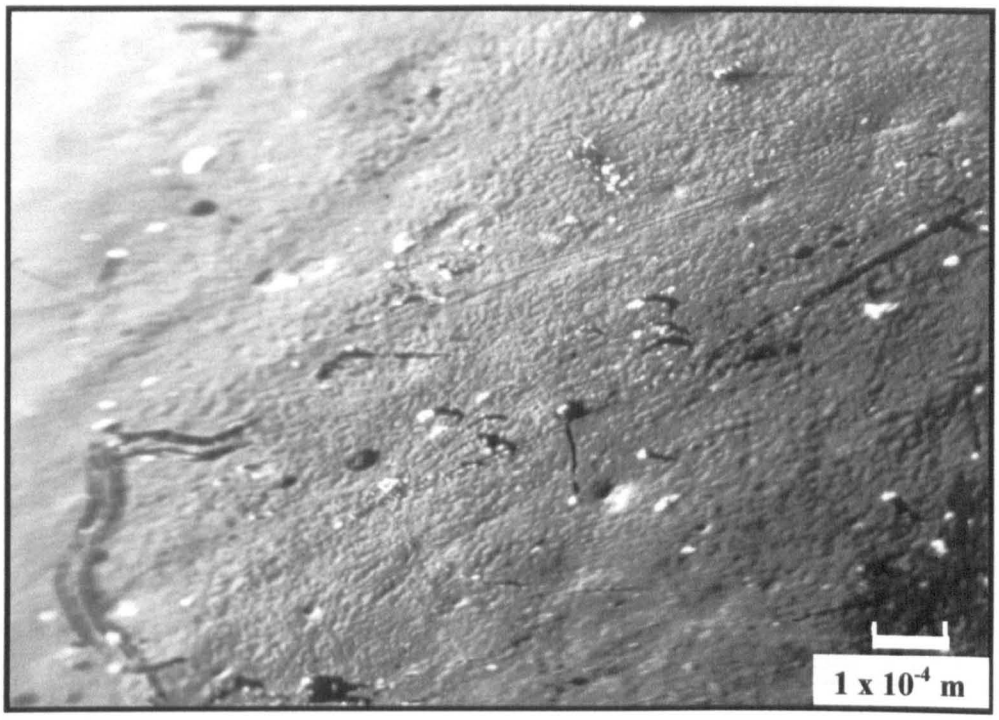

i) Mould surface x100

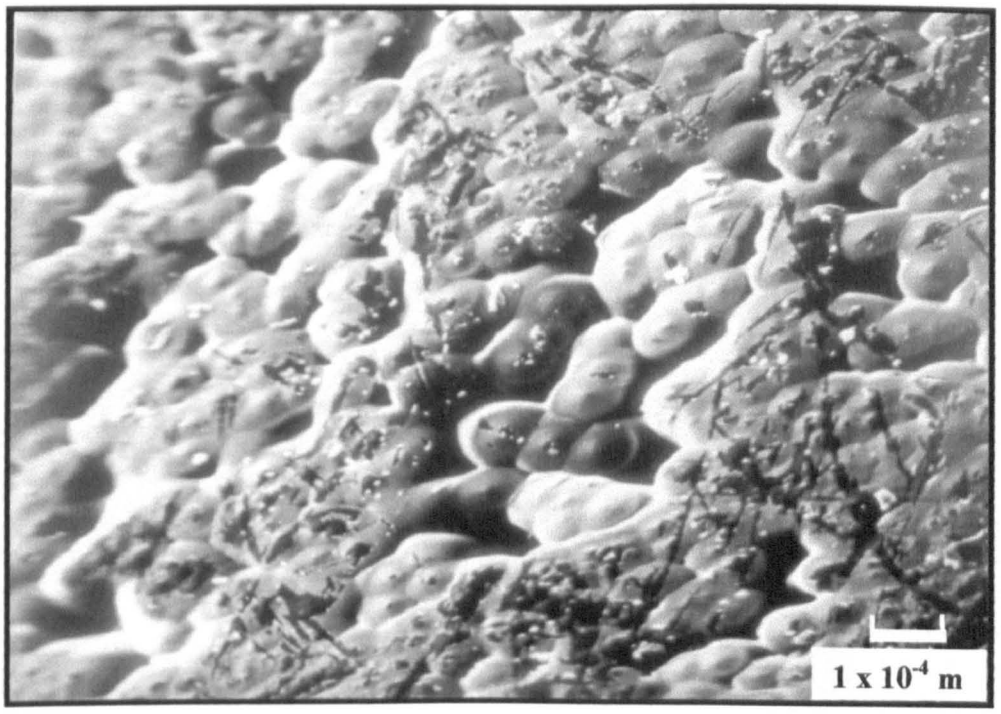

ii) Free surface x100

FIGURE 28

ELECTRON MICROGRAPH OF MOULDING SURFACE (LENGTH OF HEATING CYCLE = 11 MINUTES)

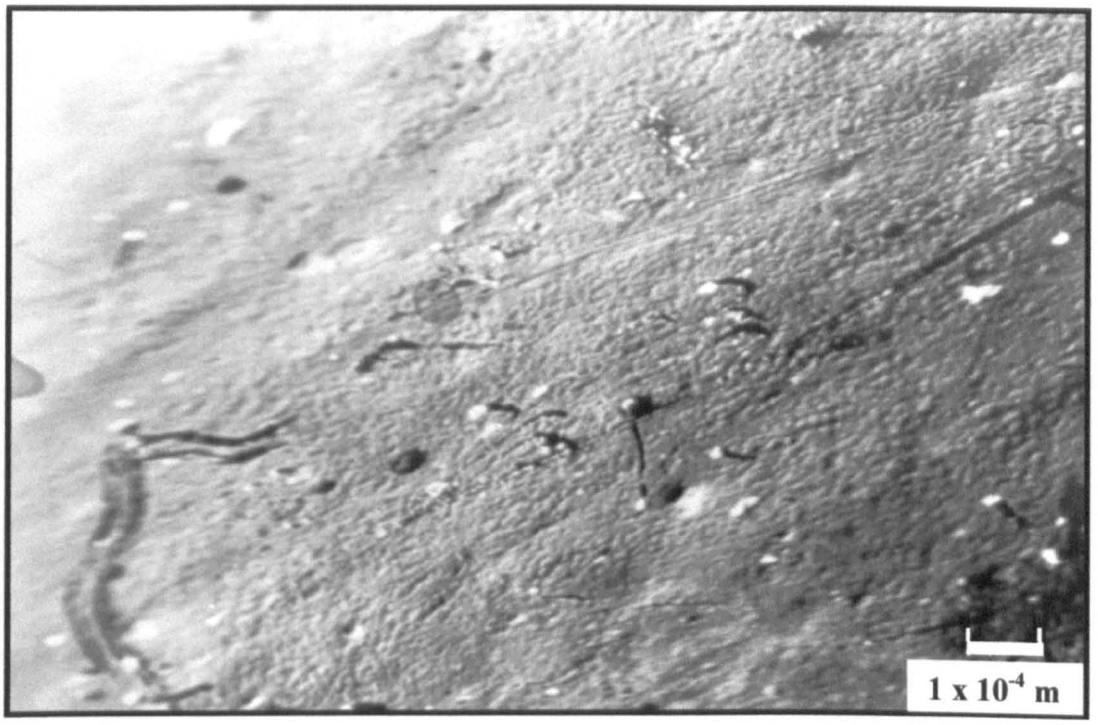

i) Mould surface x100

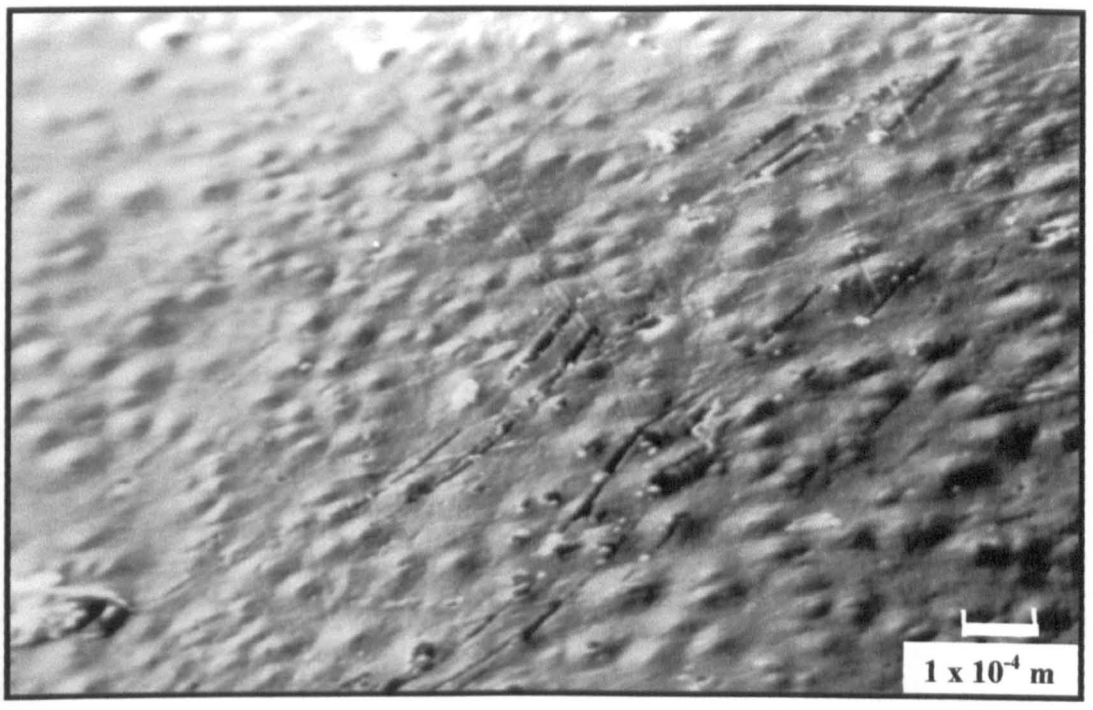

ii) Free surface x100

FIGURE 29

ELECTRON MICROGRAPH OF MOULDING SURFACE (LENGTH OF HEATING CYCLE = 12 MINUTES)

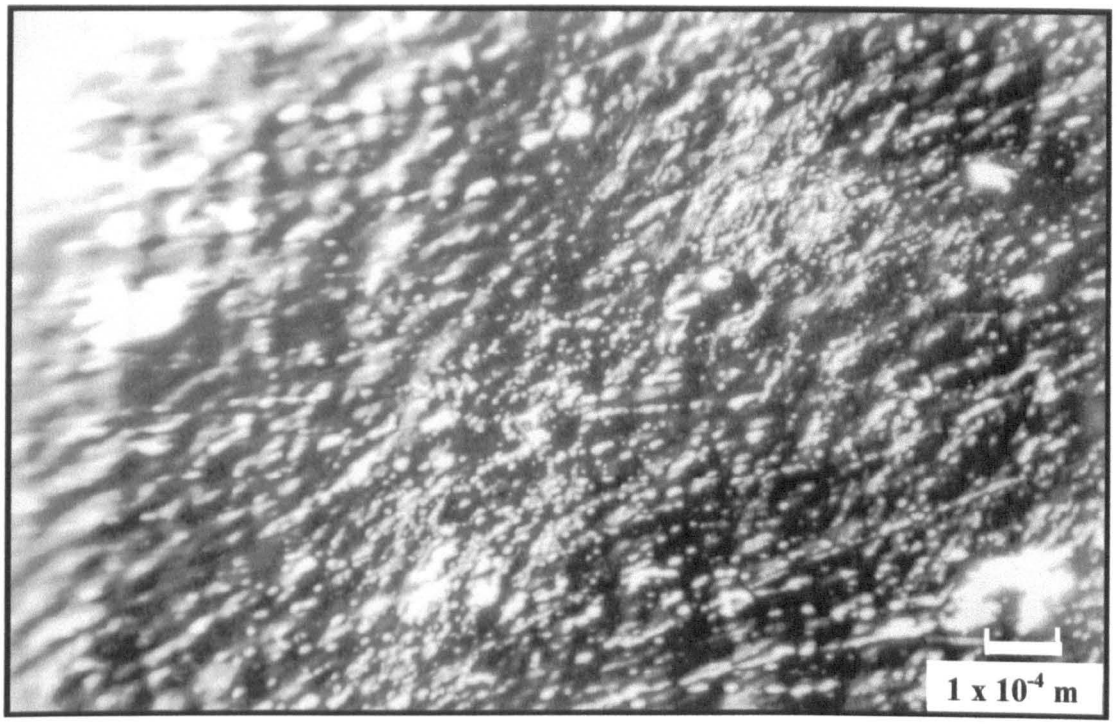

i) Mould surface x100

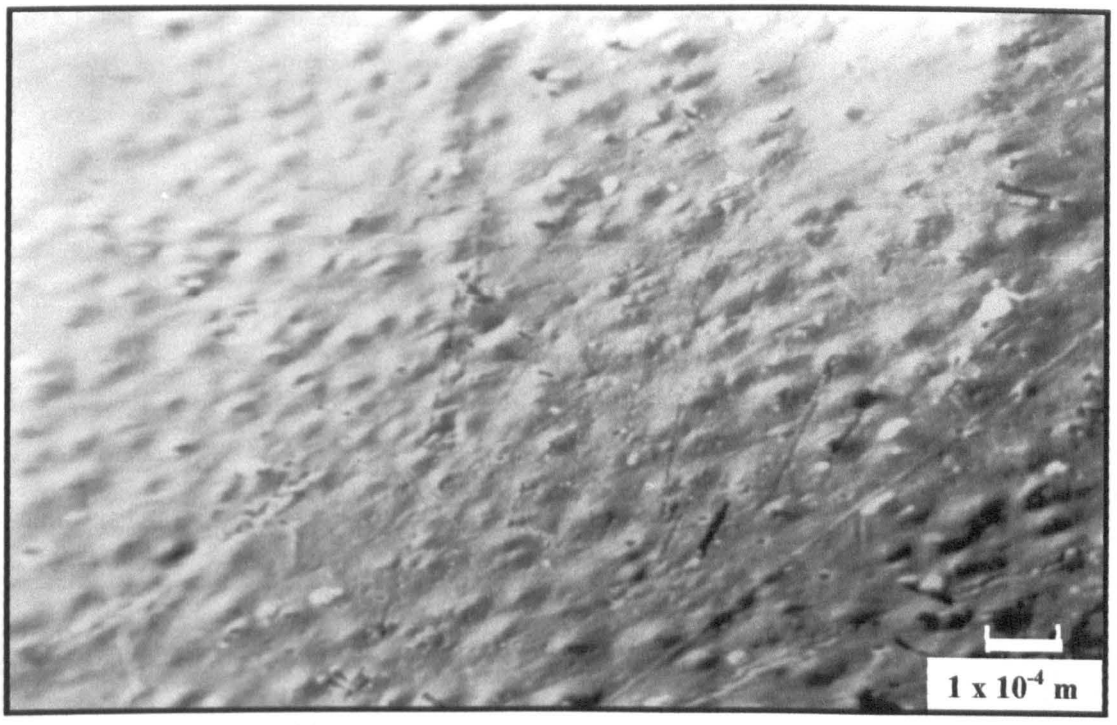

ii) Free surface x100

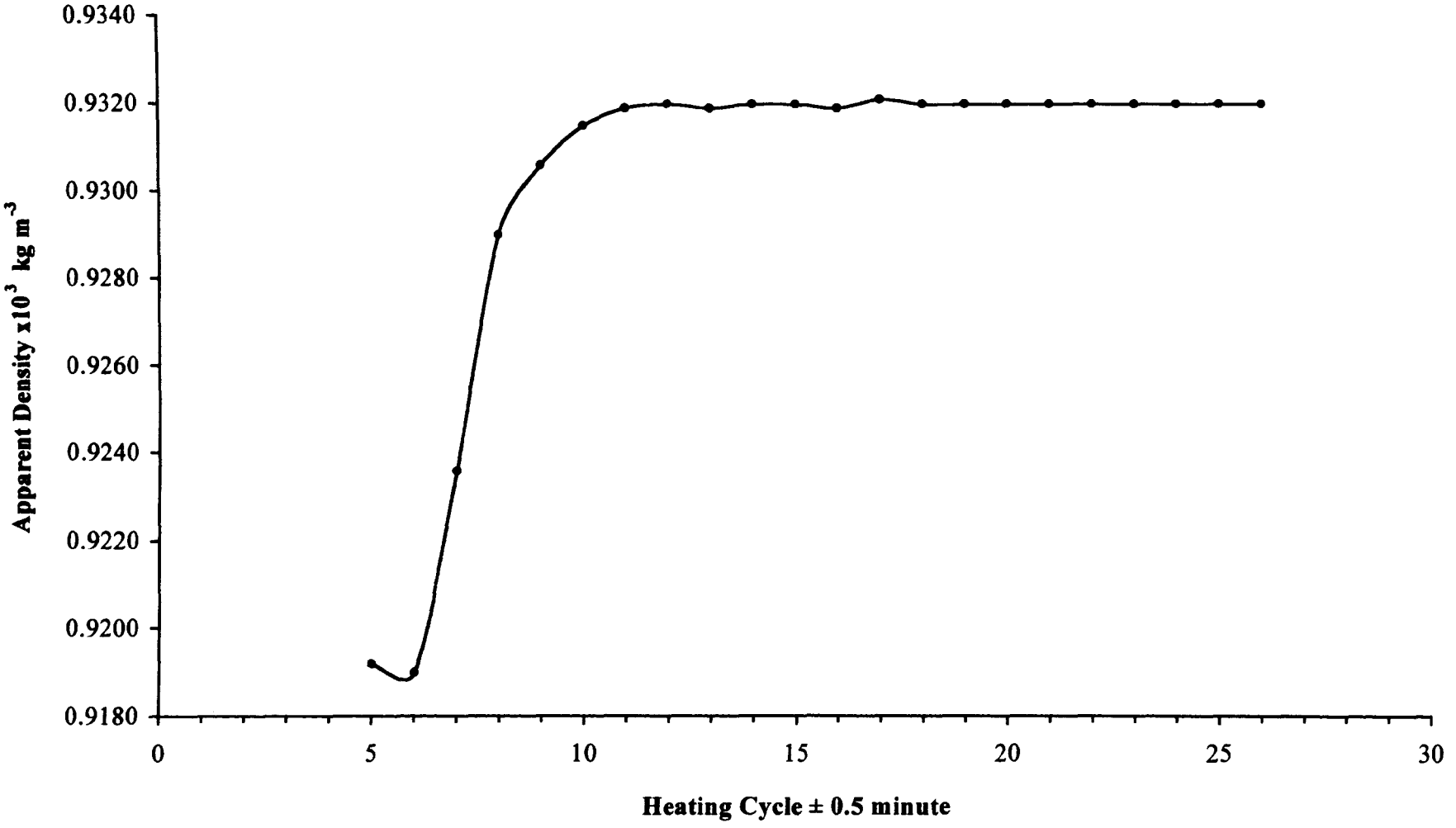

FIGURE 30

VARIATION OF APPARENT DENSITY WITH HEATING CYCLE

FIGURE 31

EFFECT OF POLYMER MASS ON THE HEATING CYCLE

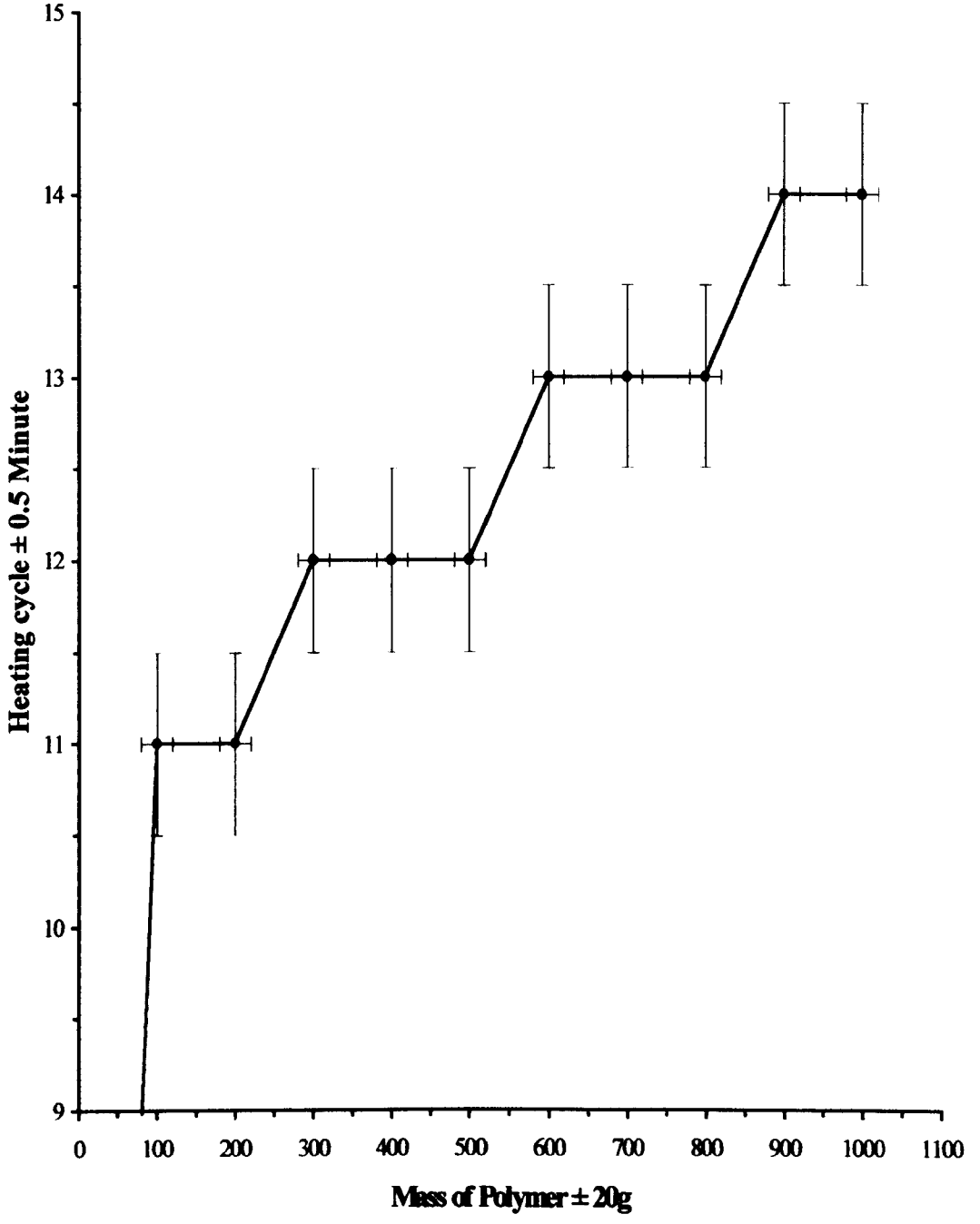

increasing mass or wall thickness.

The graph shows some mouldings of different mass having the same heating cycle. Possible reasons for this are related to the accuracy of the machine timer and are discussed in Section 5.2.1.

Figure 32 shows how, for a given moulding of mass 400g, the length of the heating cycle was found to decrease with increasing oven set temperature.

Examination of scanning electron micrographs of the mould and free surfaces in Figure 33 show that at 440° C oven set temperature, the moulding is complete after 4 ± 0.5 minutes. Compare this with the photomicrograph in Figure 29 which shows that at 220° C oven set temperature the moulding takes 12 ± 0.5 minutes to complete.

4.3.1. Mould induction phase

Results of the three methods used to measure the mould induction time are reported.

Figure 34 shows the results of the first method in which the mould was periodically removed from the oven and the temperature measured using a surface probe. The graph of the mould temperature against length of the heating cycle shows that the temperature of the mould reaches the polyethylene melt temperature range (120° C to 140° C) after a heating cycle of 1 ± 0.5 minutes. The mould induction time measured by this method is

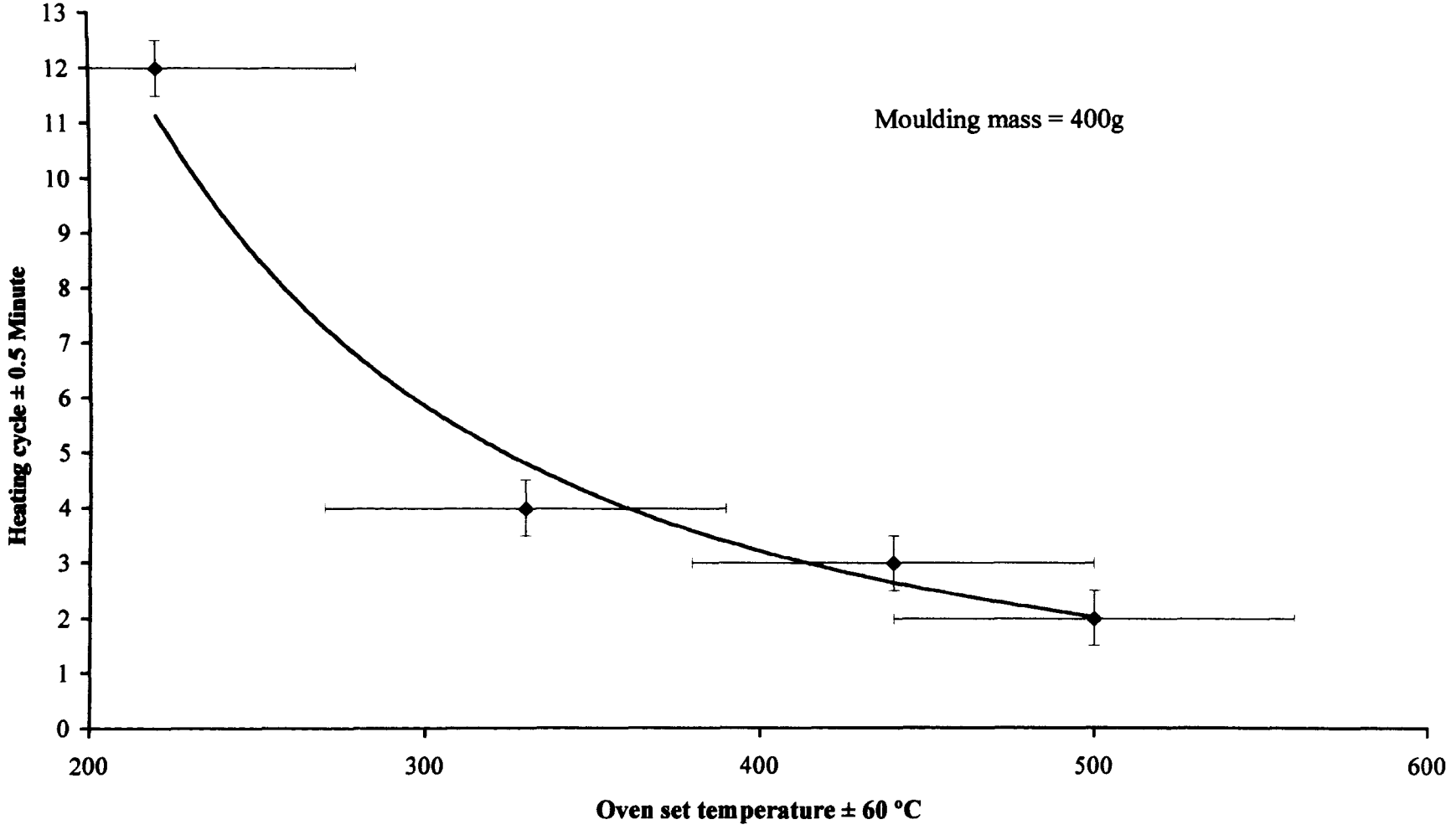

FIGURE 32

EFFECT OF OVEN SET TEMPERATURE ON HEATING CYCLE

FIGURE 33

SCANNING ELECTRON MICROGRAPHS OF INNER AND OUTER MOULDING SURFACES AT HIGHER OVEN SET TEMPERATURE
(Oven Set Temperature of 440° C ; Heating Cycle 4 ± 0.5 minutes Magnification = x100)

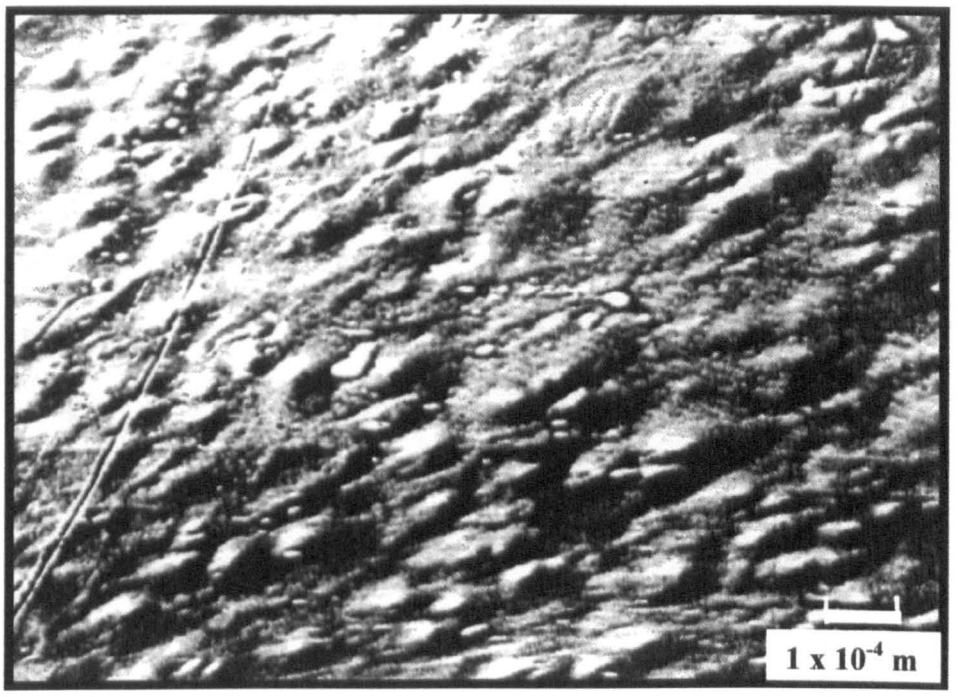

Mould Surface

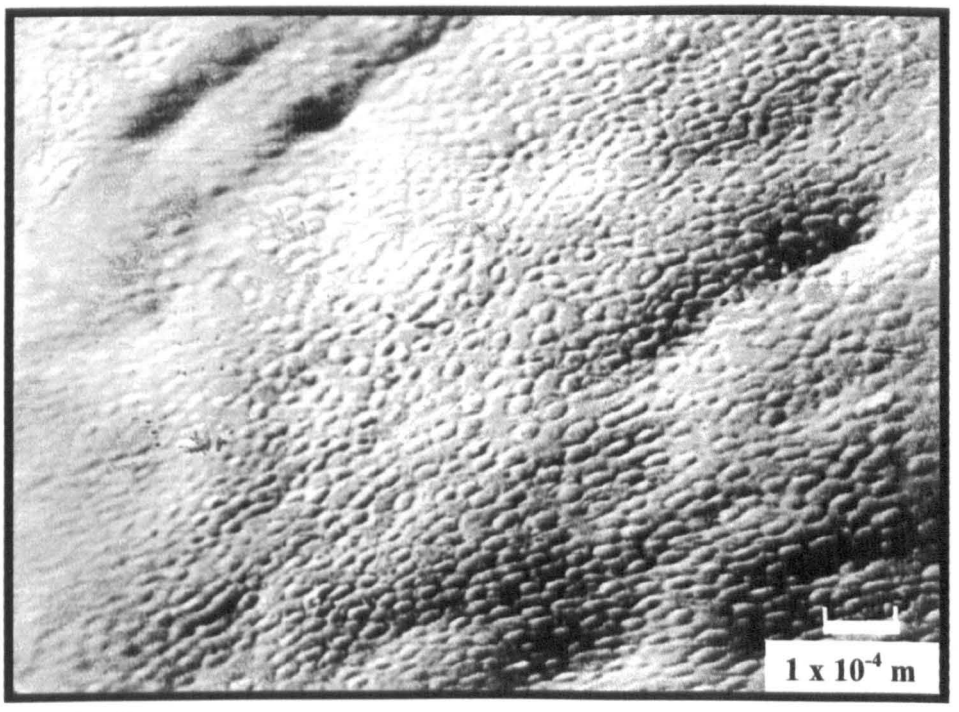

Free Surface

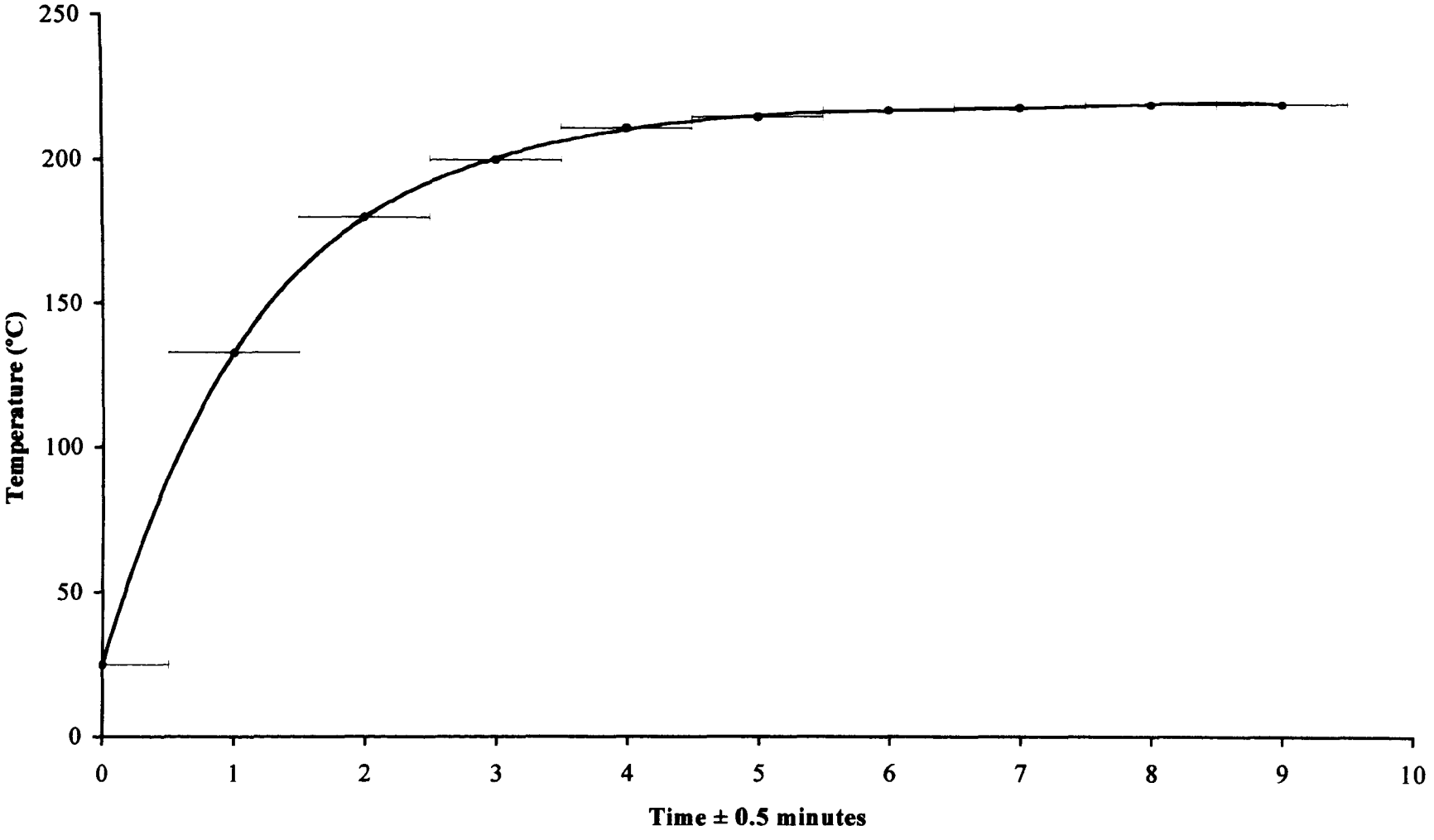

FIGURE 34

MEASUREMENT OF MOULD INDUCTION TIME

therefore 1 ± 0.5 minutes.

This result is supported by the second method in which a thermal image of the mould taken after 1 ± 0.5 minute heating cycle, Figure 35, which shows that the temperature of the mould is between 119° C and 142° C.

Results of the third method in which the temperature of the mould was continuously monitored during the heating cycle, disagree with the previous two measurements, see Figure 36. The mould induction time by this method is measured to be less than 0.5 minutes. However, from the previous observation in Section 4.2, that no polymer fusion occurs in the first 1 ± 0.5 min of the heating cycle (because the mould has not reached the polyethylene melt temperature), it can be assumed that the induction time of the mould cannot be less than 1 ± 0.5 minute. The discrepancy in this measurement can be explained by errors in temperature measurement, discussed further in Section 5.6.

Increasing the oven set temperature from 220° C to 440° C reduces the mould induction time from 1 ±0.5 min to less than 0.5 min, see Figure 37. The thermal image of the mould taken after a heating cycle of 1 ± 0.5 min at the higher temperature shows the temperature of the mould as between 213° C and 232° C. This is above the polyethylene melt temperature range of 120° C to 140° C.

4.3.2. Polymer fusion phase

The increase in fusion time of mouldings with increasing mass or wall thickness

FIGURE 35

MEASUREMENT OF MOULD TEMPERATURE USING THERMAL IMAGING

OVEN SET TEMPERATURE = 220° C
HEATING CYCLE = 1 ± 0.5 Minutes

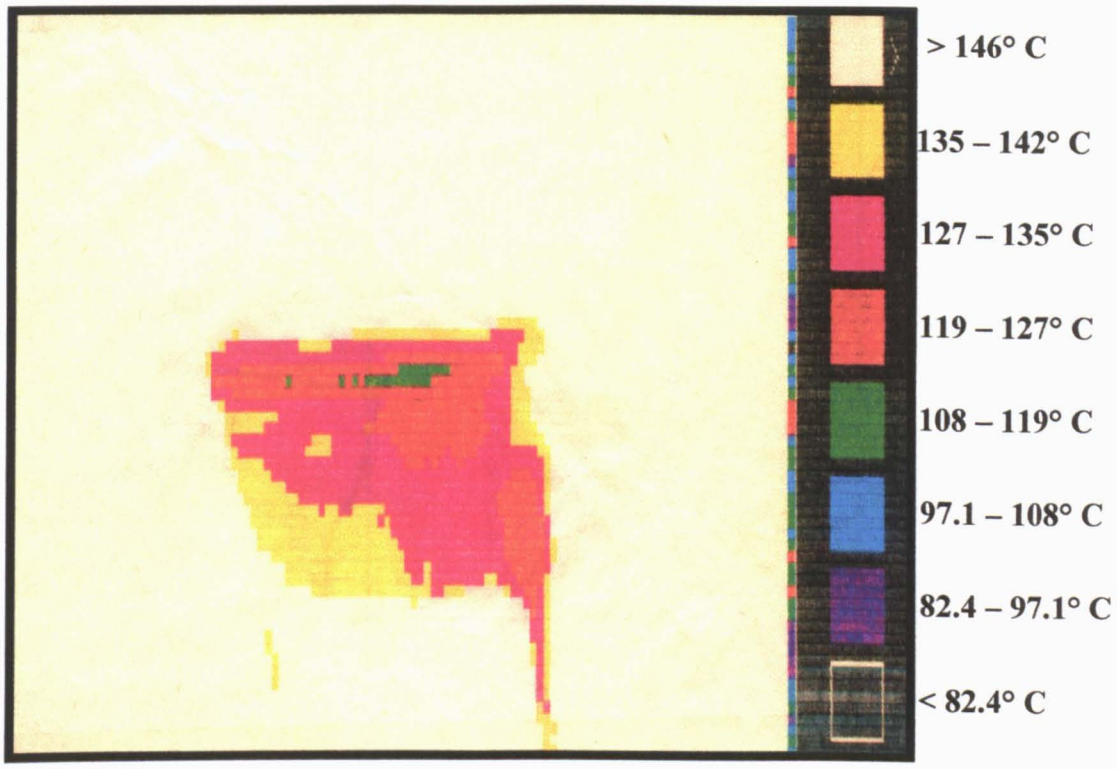

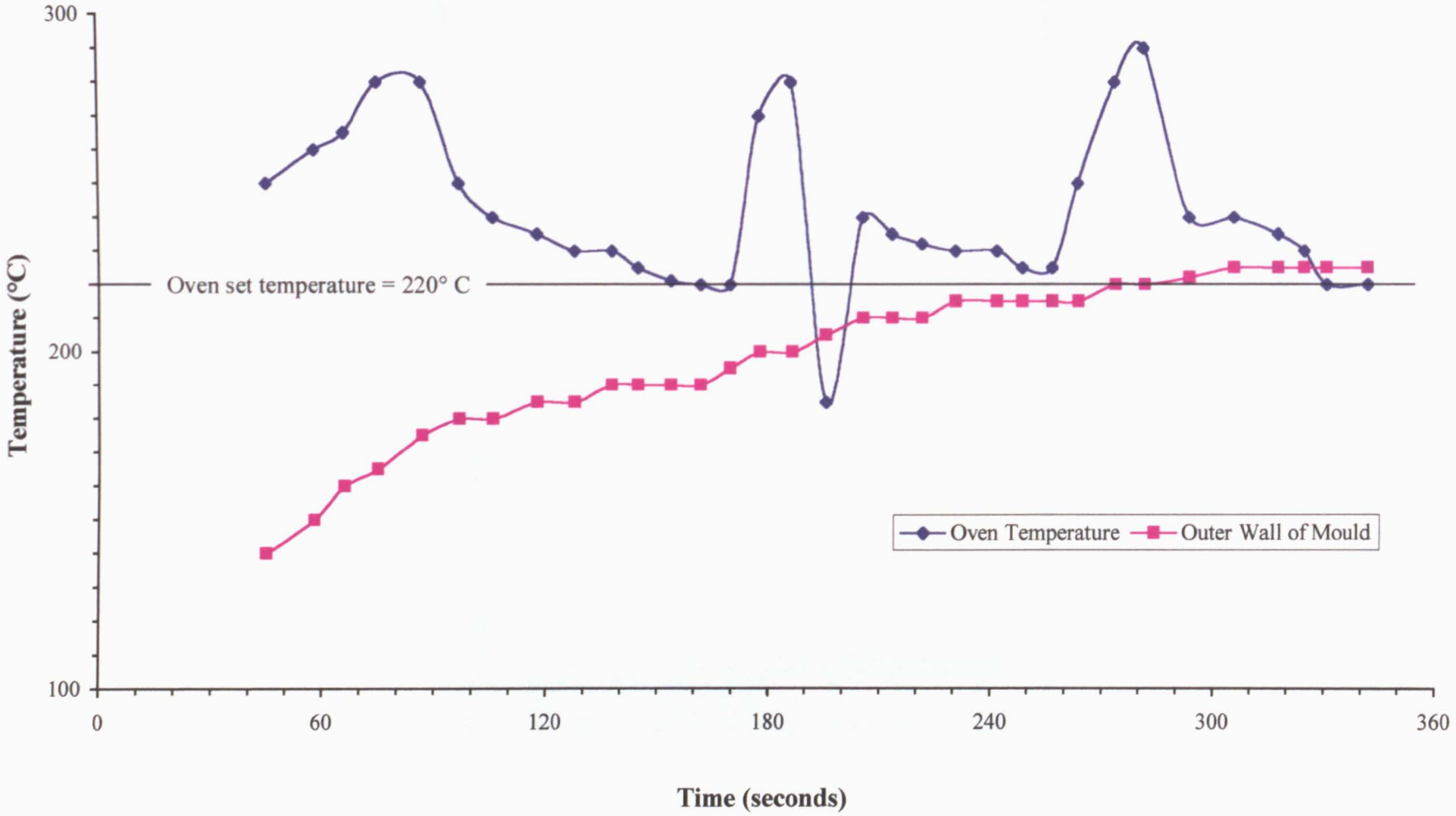

FIGURE 36

MOULD INDUCTION TIME

FIGURE 37

MEASUREMENT OF MOULD TEMPERATURE USING THERMAL IMAGING

OVEN SET TEMPERATURE = 440° C
HEATING CYCLE = 1 ± 0.5 Minutes

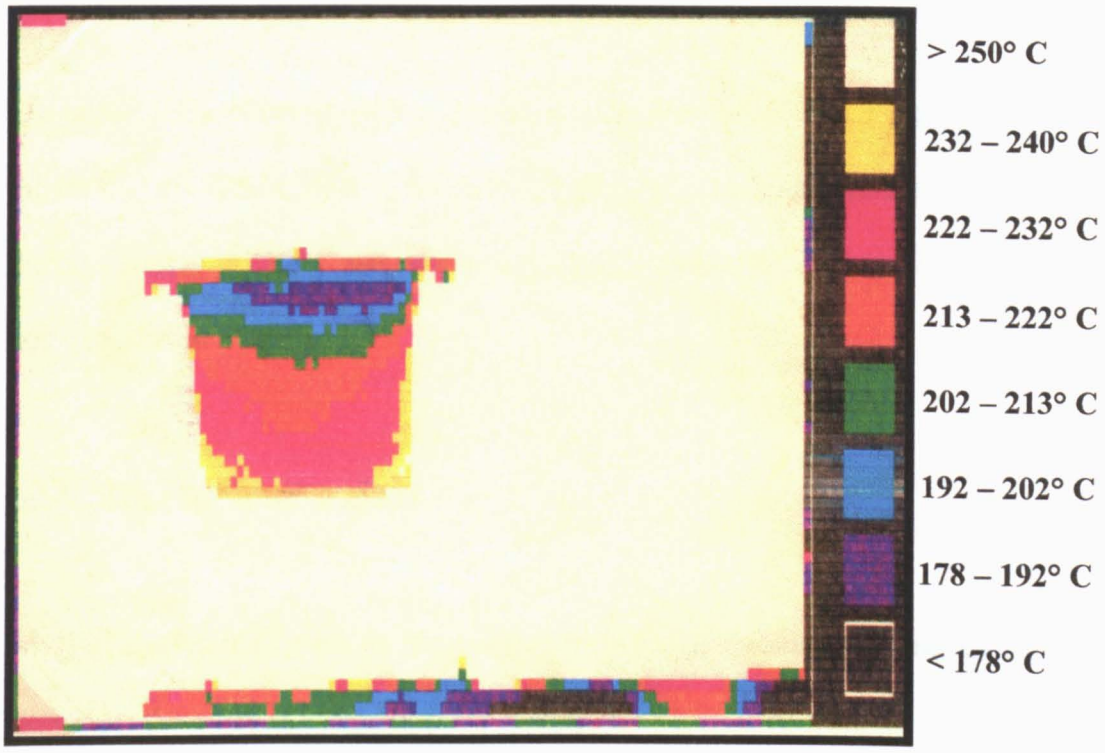

reported in Figure 38 is as expected. With the exception of the 600 ± 20g moulding, the graph is linear. This is discussed further in Section 5.2.1.2.

At the end of the fusion phase, the moulding wall contains many bubbles which results in uneven free surface of moulding as shown in Figure 39. This introduces large errors in measurement of moulding wall thickness and hence, for greater accuracy, the mass of the moulding instead of the wall thickness was recorded.

The study of the effect of oven set temperature on the fusion time, Figure 40 proves that the fusion time can be reduced by increasing the oven set temperature. Comparison of the fusion rates at 220° C and 440° C in Figure 41 shows the expected increase in the rate of fusion at 440° C.

4.3.3. Melt densification phase

Study of the effect of oven set temperature on the melt densification time, shows that increasing the oven set temperature from 220° C to 330° C reduces the melt densification time from 7 ± 0.5 min to 1 ± 0.5 min. Furthermore, increasing the oven set temperature beyond 330° C does not cause any further reduction in the melt densification time, see Figure 42.

The study of the effect of polymer mass on the melt densification time at 220° C shows that the densification time decreases with increasing mass, see Figure 43.

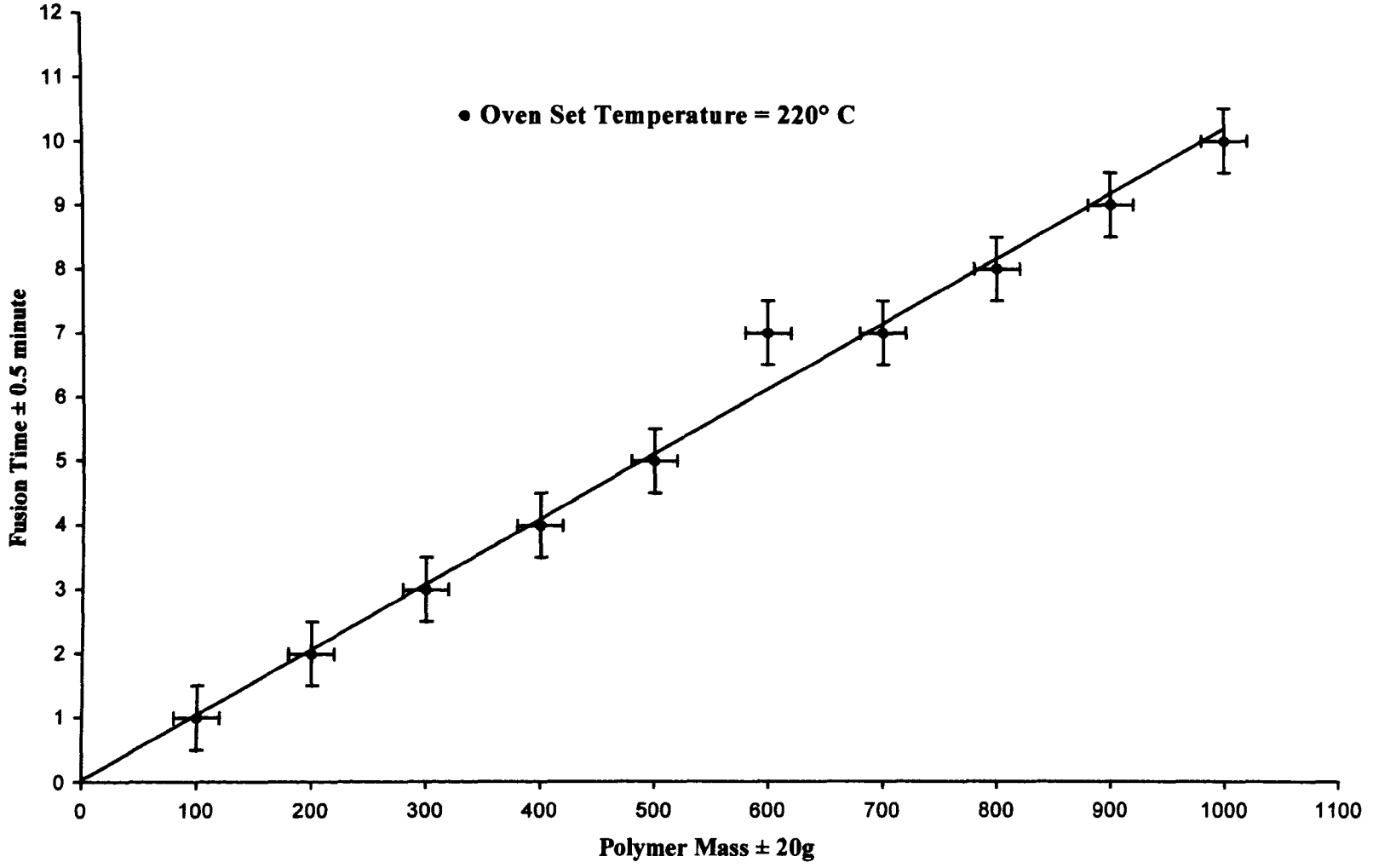

FIGURE 38

EFFECT OF POLYMER MASS ON THE FUSION TIME

FIGURE 39

CROSS SECTION OF MOULDING WALL

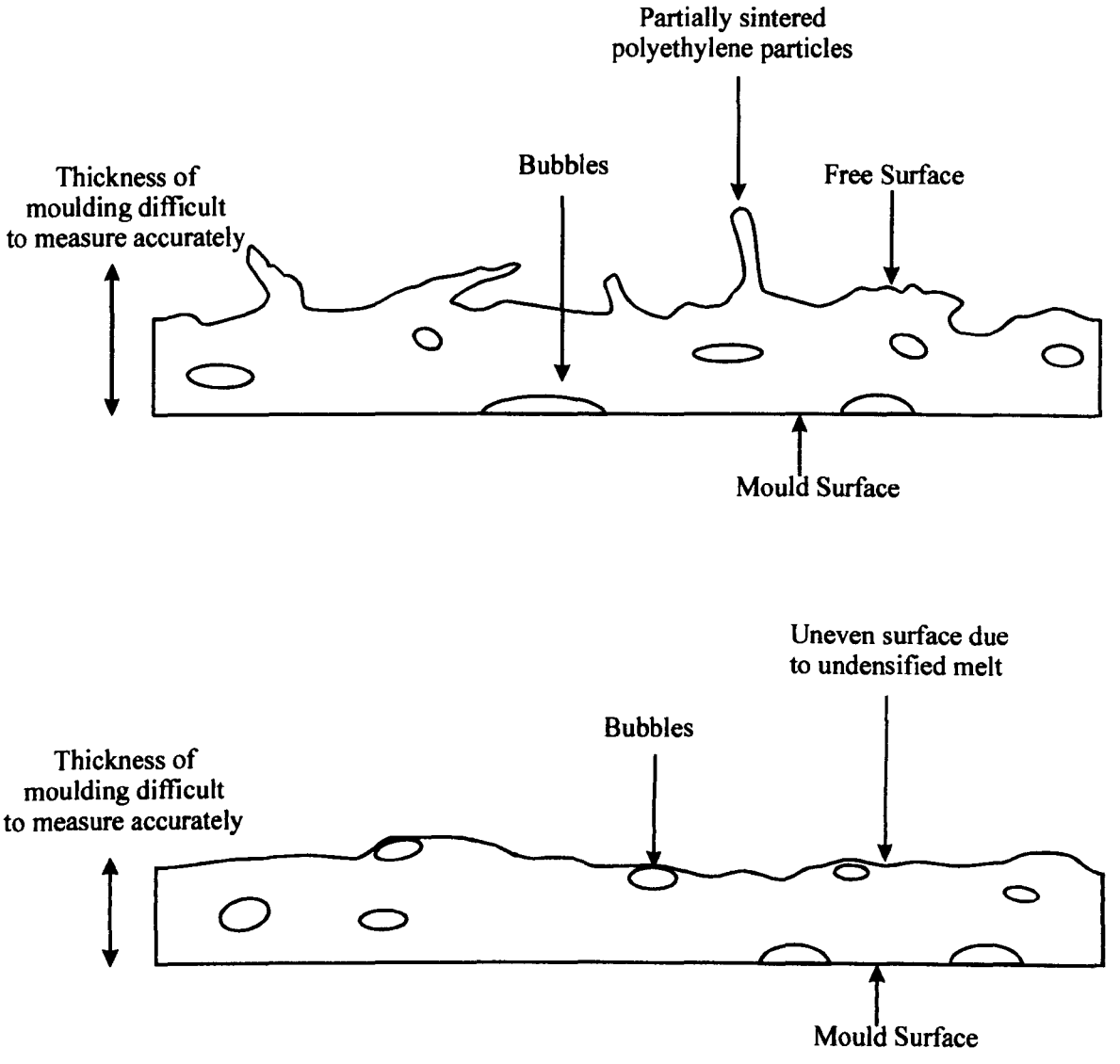

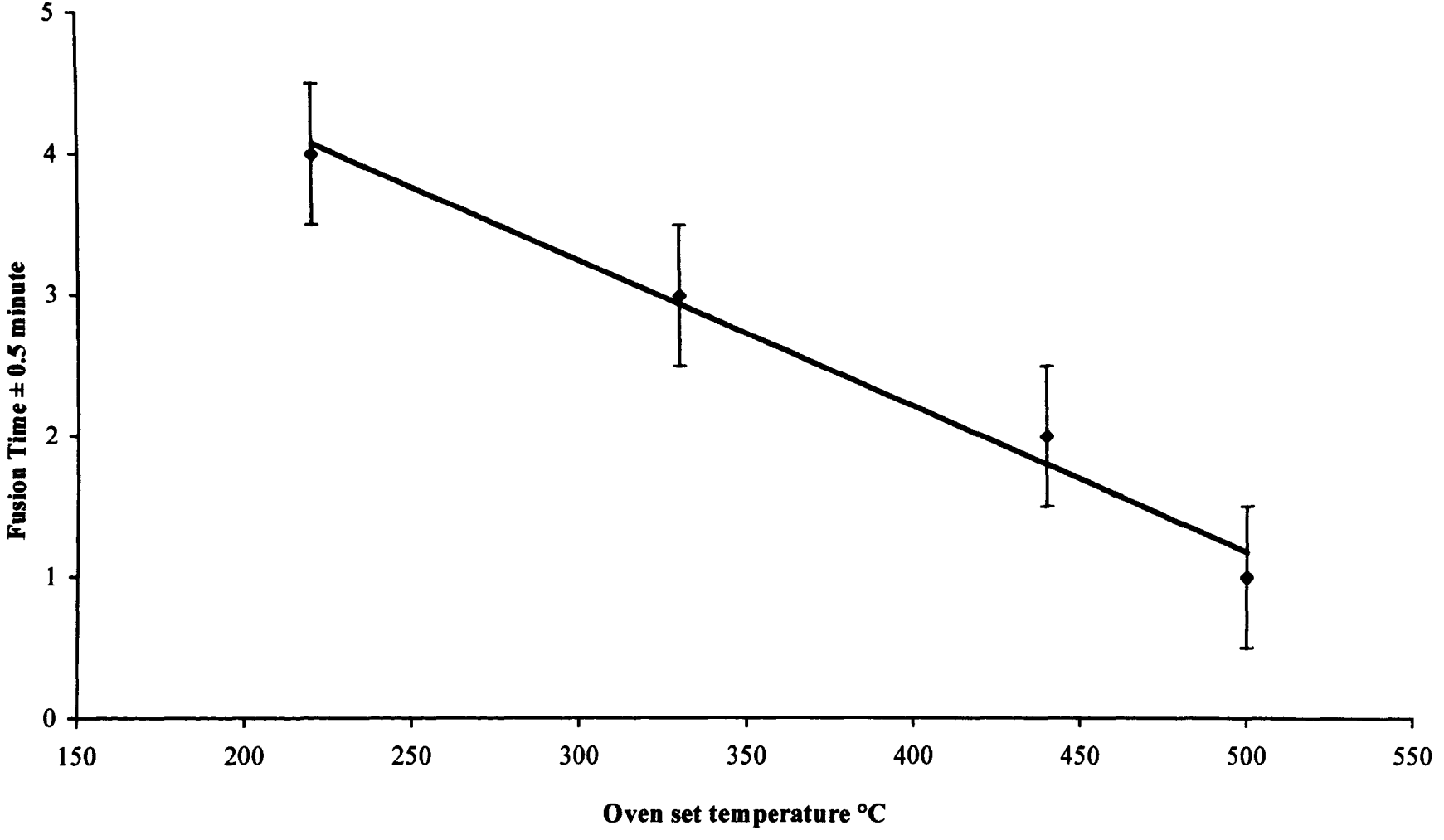

FIGURE 40

EFFECT OF OVEN SET TEMPERATURE ON FUSION TIME

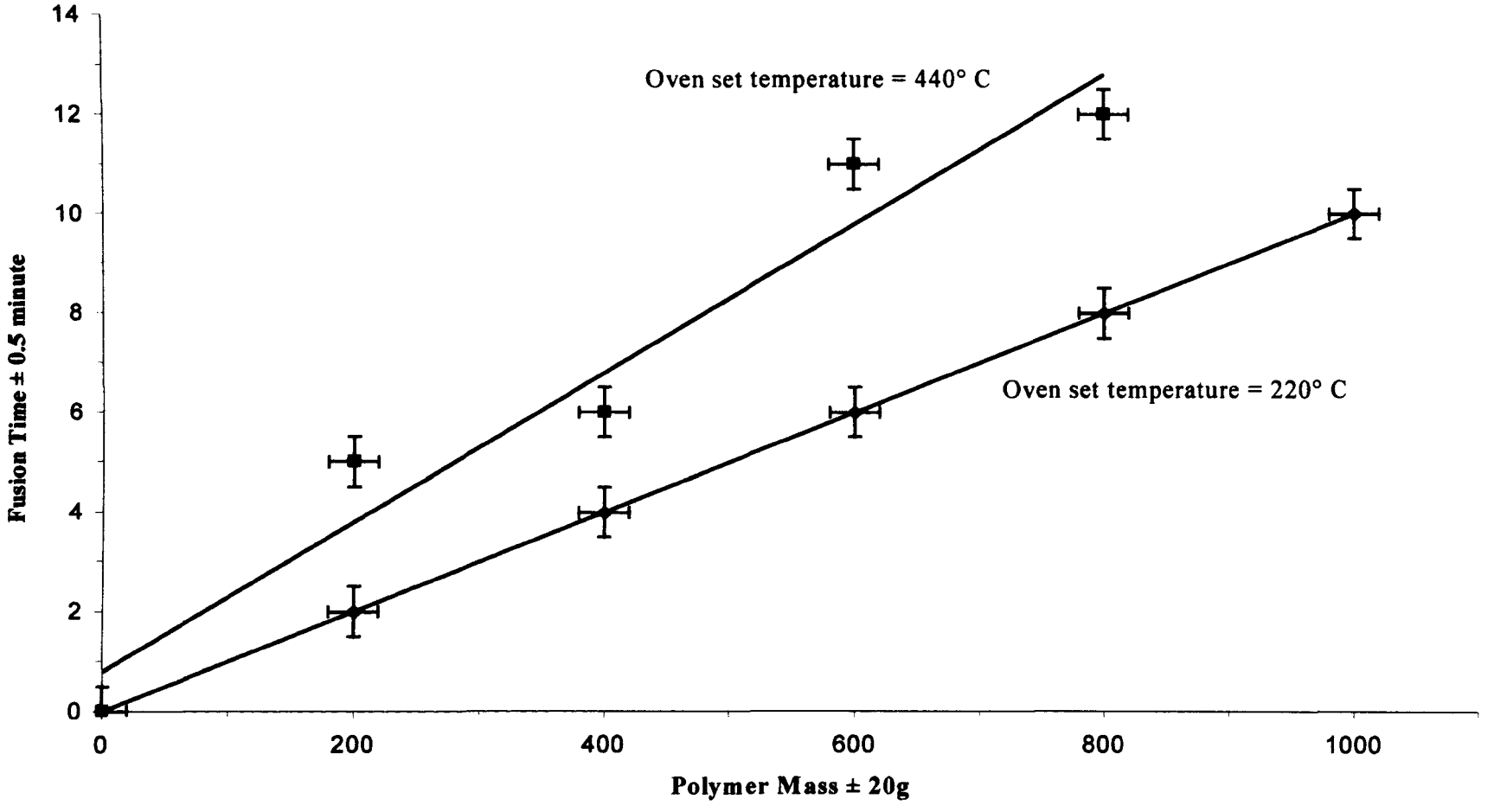

FIGURE 41

EFFECT OF POLYMER MASS ON FUSION TIME

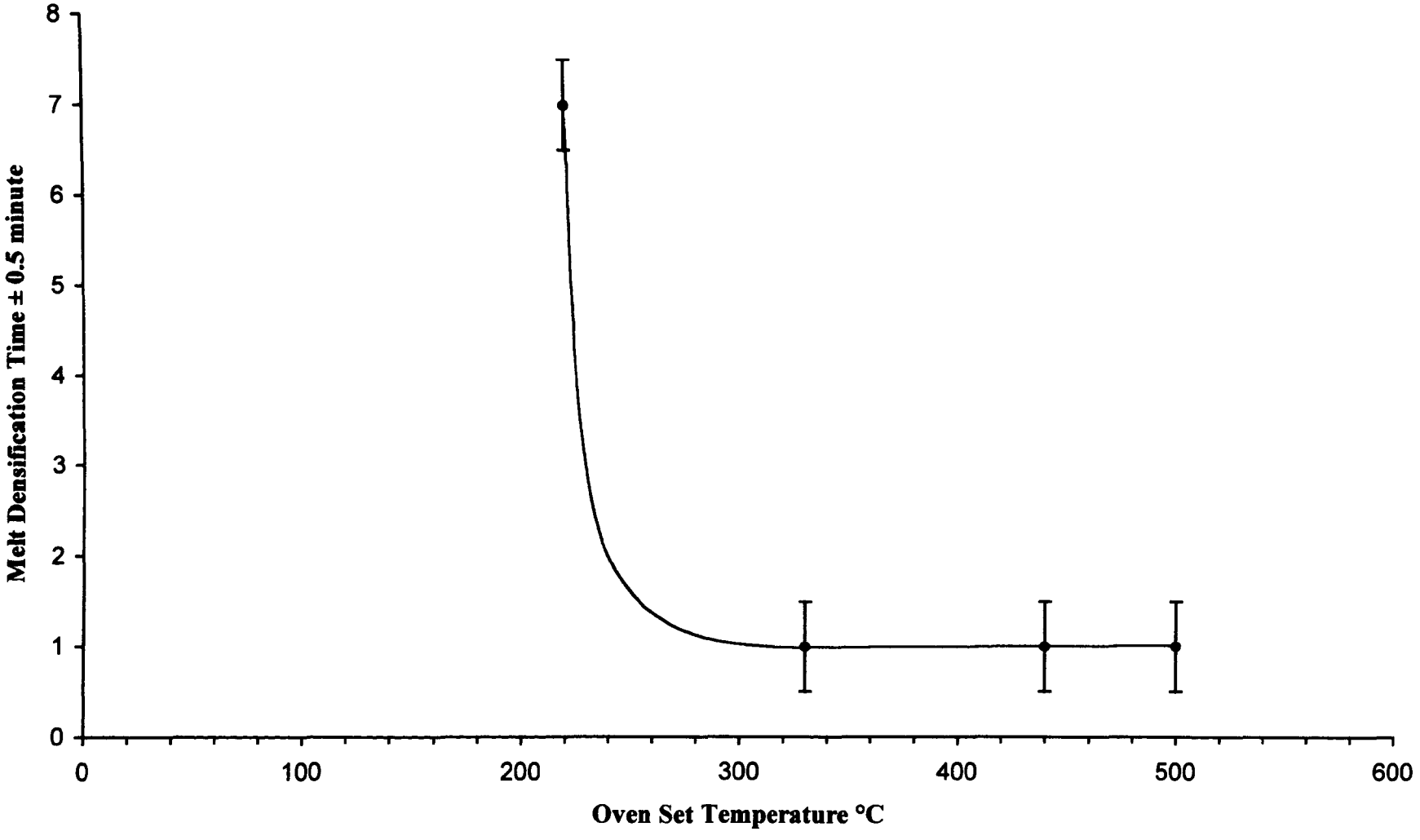

FIGURE 42

EFFECT OF OVEN SET TEMPERATURE ON MELT DENSIFICATION TIME

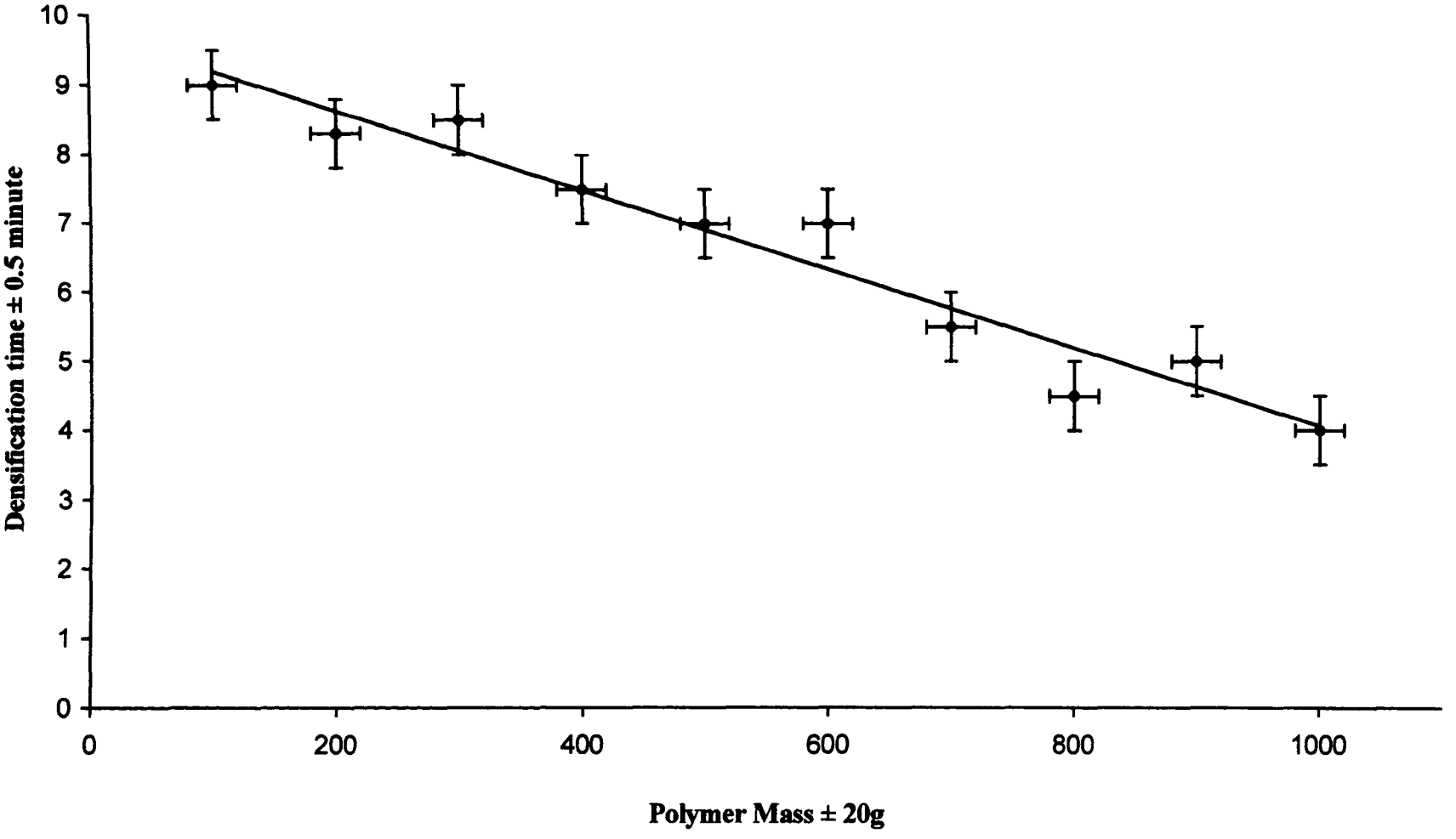

FIGURE 43

EFFECT OF MOULDING MASS ON MELT DENSIFICATION TIME

The effect of polymer mass on the melt densification at 440° C is shown in Figure 44. The graph shows that at this temperature, there is no increase in the melt densification time with increasing polymer mass.

The above results on the effect of the polymer mass and the ovens set temperature are very significant and are discussed further in Section 1.8.1, in conjunction with discussions on the mechanisms of bubble formation and dissipation.

4.4. Crystallinity in mouldings

4.4.1. Effect of cooling rate on spherulitic size

Microscopic examination of samples taken from different test mouldings, Figure 45, show how the spherulitic development is affected by the rate at which the polyethylene melt is cooled during the moulding process.

For an extended cooling time of 45 ± 0.5 minutes in ambient air conditions, the spherulites are large and well developed. The largest spherulite is measured as approximately 0.12mm, Figure 45B.

A fast cooling rate in the mouldings, achieved by spraying the mould with water at 20° C for 5 ± 0.5 minutes, results in smaller spherulitic size with uncrystallized polymer still apparent between the spherulites, Figure 45A.

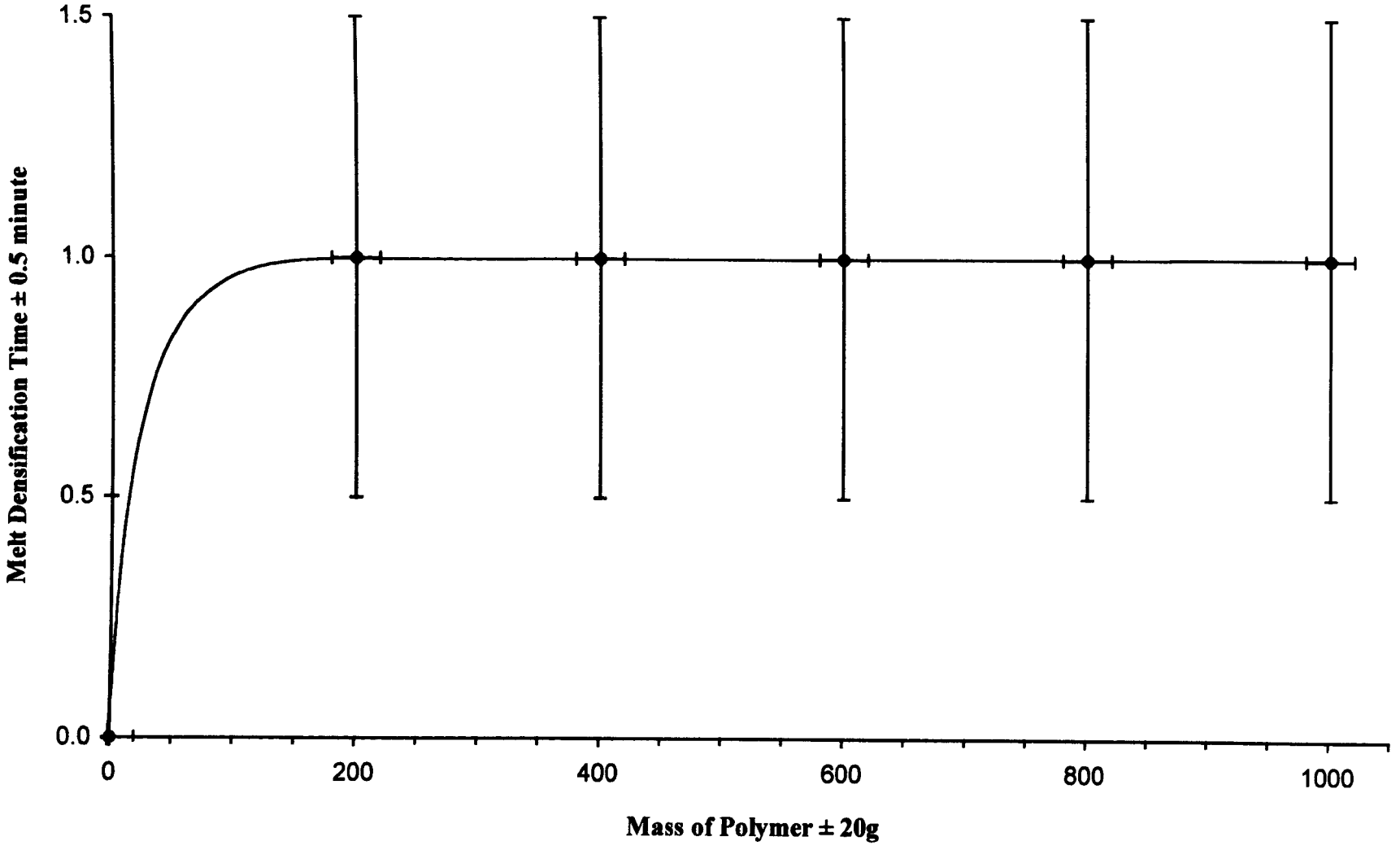

FIGURE 44

EFFECT OF POLMER MASS ON MELT DENSIFICATION TIME AT OST 440° C

FIGURE 45

EFFECT OF COOLING RATE SPHERULITIC MORPHOLOGY

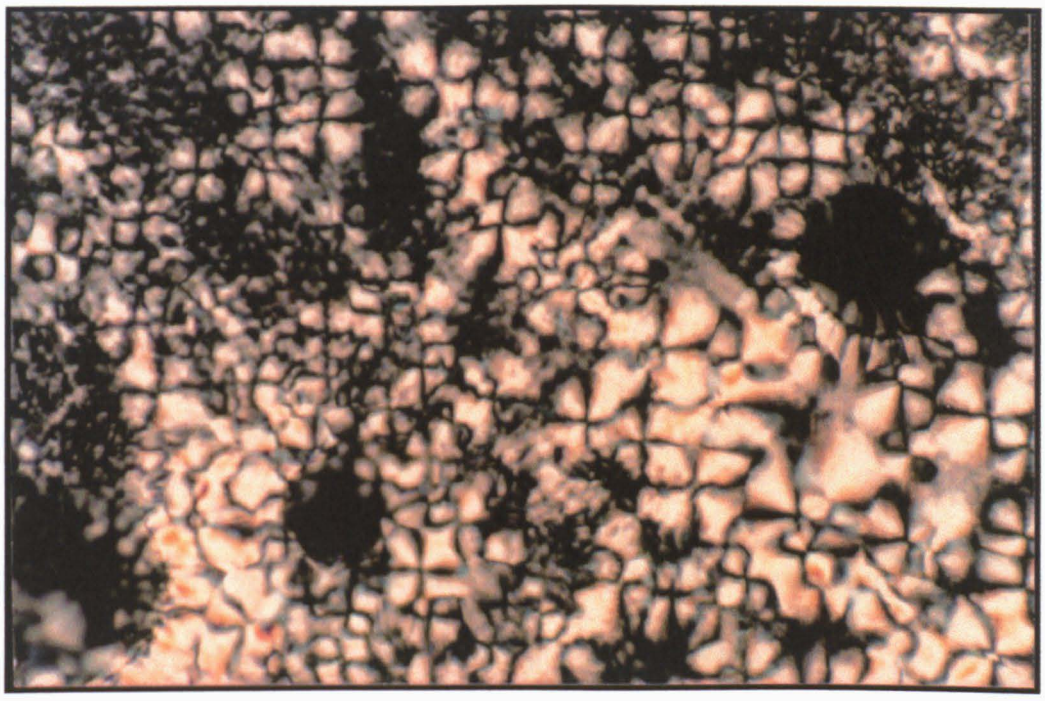

A. Fast Cooled Polyethylene: mould sprayed with water at 20° C for 5 ± 0.5 minutes

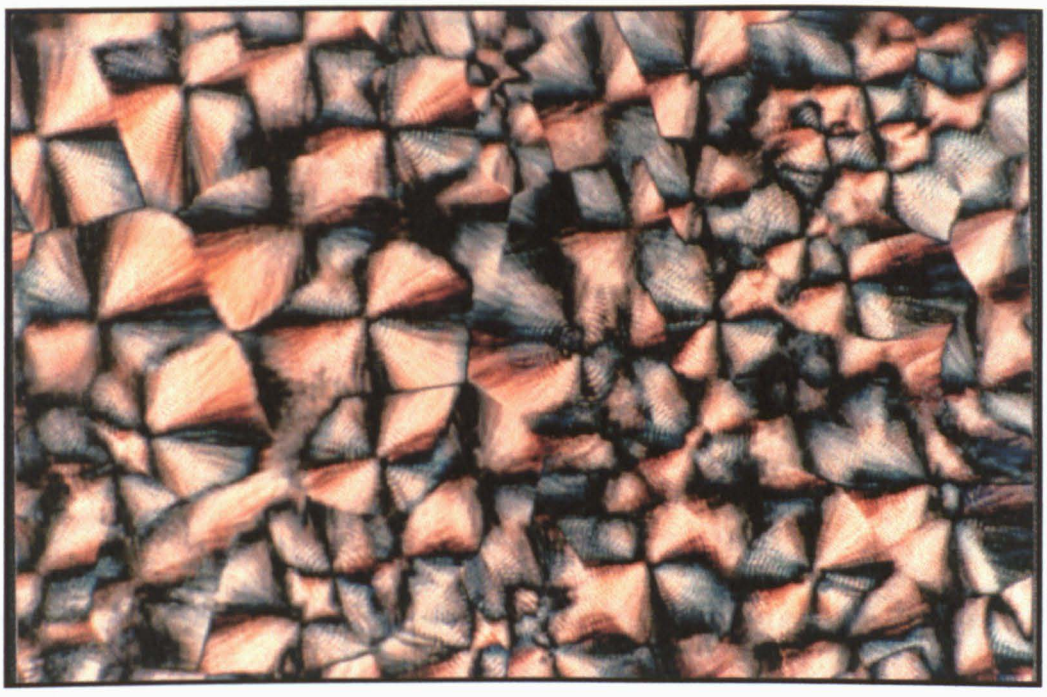

B. Slow Cooled Polyethylene: mould cooled in ambient air conditions for 45 ± 0.5 minutes

4.4.2. Degree of crystallinity

4.4.2.1. Effect of cooling rate

Table 4 shows that the average density of the slow cooled polyethylene - mould and polymer cooled in ambient air conditions for 45 ± 0.5 minutes - is higher than that of the fast cooled sample.

4.4.2.2. Effect of oven set temperature

The results show a slight increase in density at the higher oven set temperature of 440°C, compared to the oven set temperature of 220° C, see Table 5.

4.4.2.3. Variation with moulding surface

The results are given in Table 6. The average density of samples taken from the free surface of the moulding is measured higher than the density of samples taken from the mould surface.

4.5. Tensile properties

In the fusion phase, the stress at yield was found to increase sharply with increasing degree of fusion and reaches the almost maximum value of 13 x 10^6 N m^{-2} at fusion times

TABLE 4

EFFECT OF MELT COOLING ON POLYETHYLENE DENSITY

Rate of cooling of polyethylene melt	**Average Density x 10^3 kg m^{-3}**
Fast Cooled: Mould sprayed with water at 20° C for 5 ± 0.5 minutes	0.9219
Slow Cooled: Mould cooled in ambient air conditions for 45 ± 0.5 minutes	0.9320

TABLE 5

EFFECT OF OVEN SET TEMPERATURE ON THE DEGREE OF CRYSTALLINITY

Moulding Temperature	Average Density x 10^3 kg m^{-3}
440° C	0.9350
220° C	0.9334

TABLE 6

VARIATION OF DENSITY WITH MOULDING SURFACE

Moulding Temperature	Surface	Average Density x 10^3 kg m^{-3}
220° C	Mould	0.9350
	Free	0.9360

between 4 and 5 minutes, see Figure 46.

At this stage, the polymer is completely fused, but has a maximum number of bubbles. Continued heating of the polymer during the melt densification stage, Figure 47, increases the stress at yield from 13 x 10^6 N m^{-2} to 14 x 10^6 N m^{-2} over a period of 8 minutes, when the densification of the polymer is complete and all the bubbles have dissipated.

The effect of the heating cycle on elongation at break is reported in Figure 48. The elongation increases sharply during fusion, reaching a maximum value by the end of the fusion phase. The elongation decreases sharply again during melt densification.

Table 7 shows the effect of oven set temperature on the tensile properties. A slight increase in the apparent density and maximum yield stress is observed at the higher oven set temperature of 440° C, while the maximum elongation at break is found to decrease at the higher oven set temperature.

4.5.1. Isotropy in rotational mouldings

Table 8 shows that tensile test samples cut from mouldings at right angles to each other have approximately the same average yield stress. This indicates that there is no molecular orientation in the melt resulting in anisotropy of tensile properties in the mouldings.

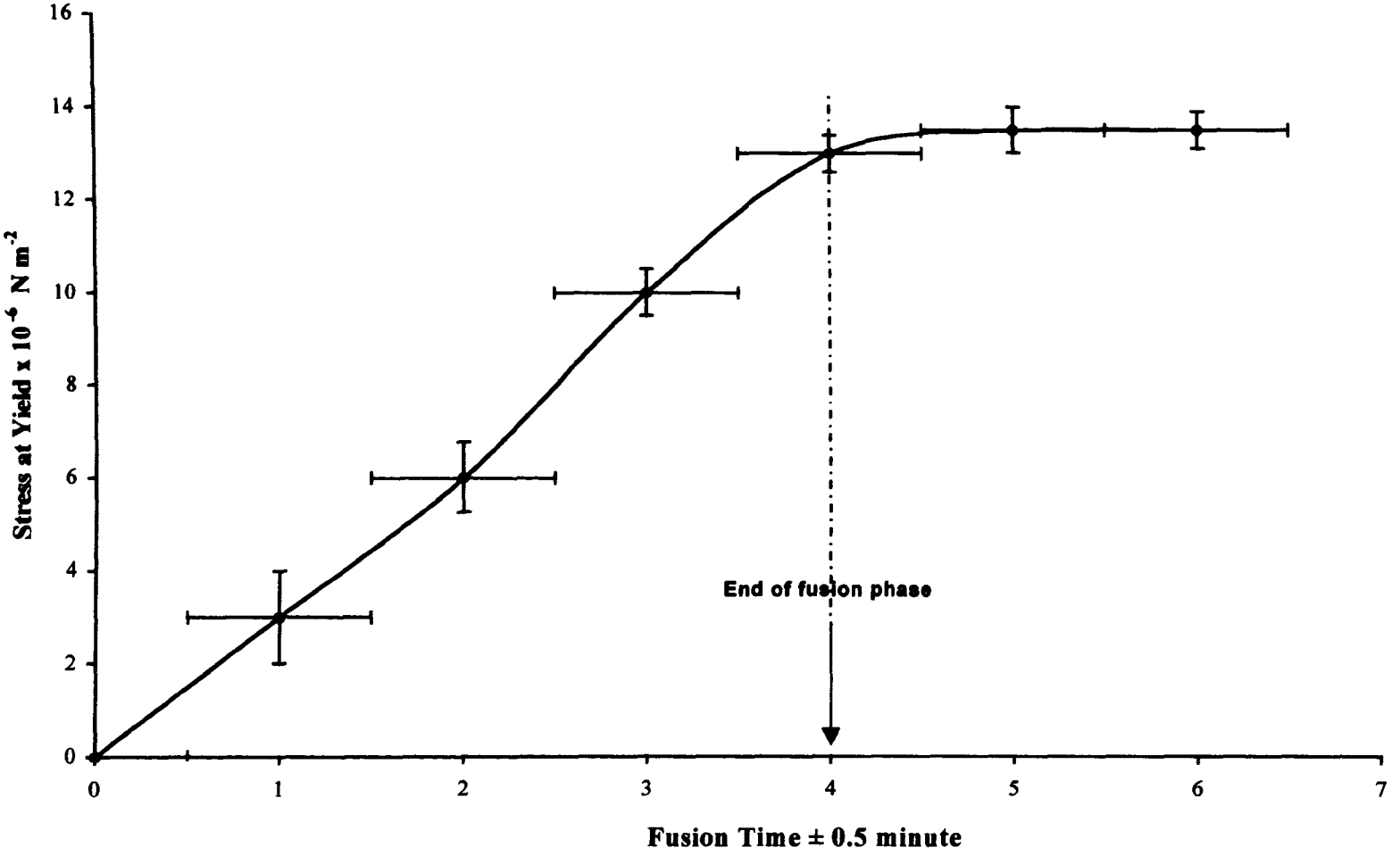

FIGURE 46

EFFECT OF FUSION TIME ON STRESS AT YIELD

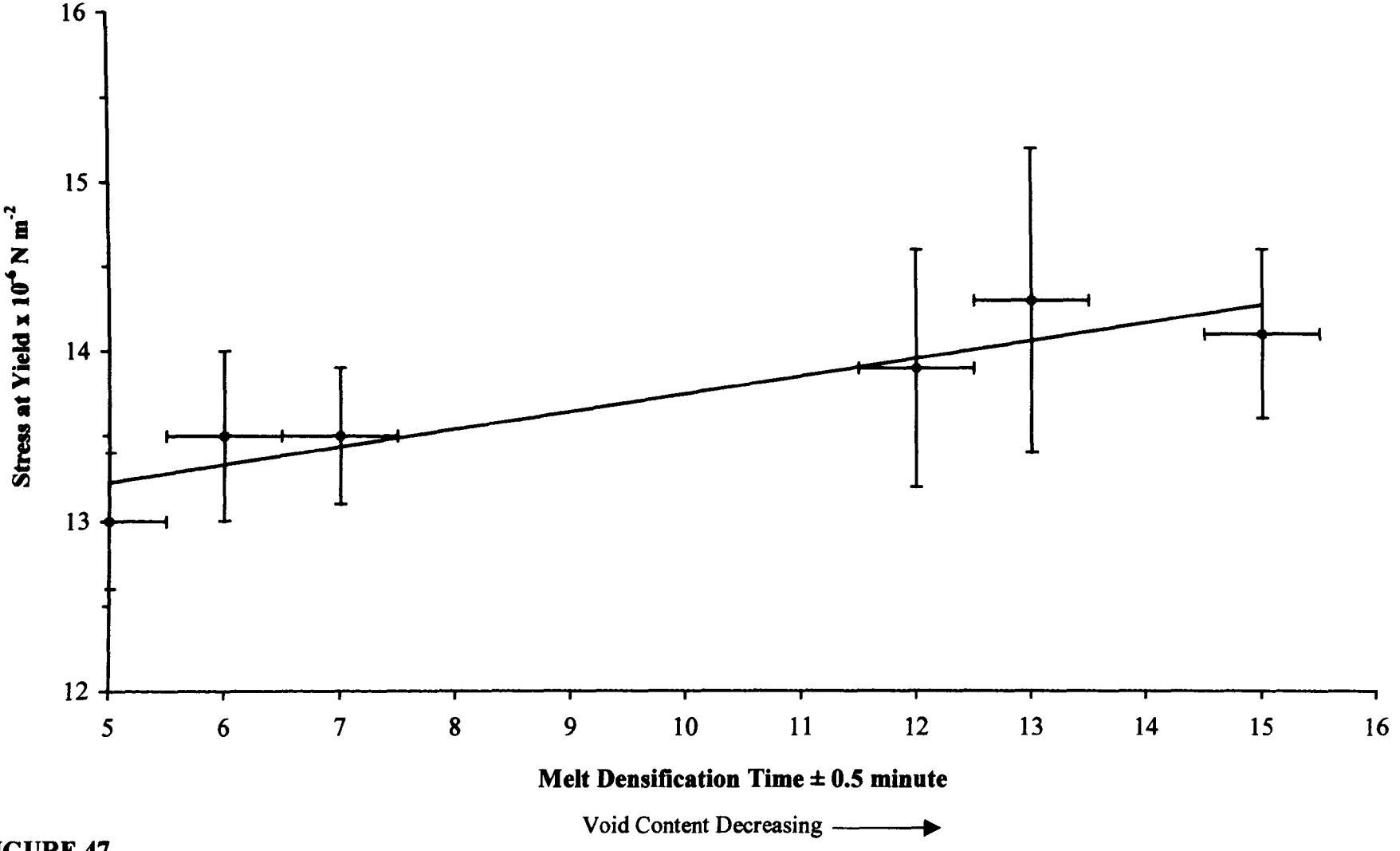

FIGURE 47

EFFECT OF BUBBLES ON STRESS AT YIELD

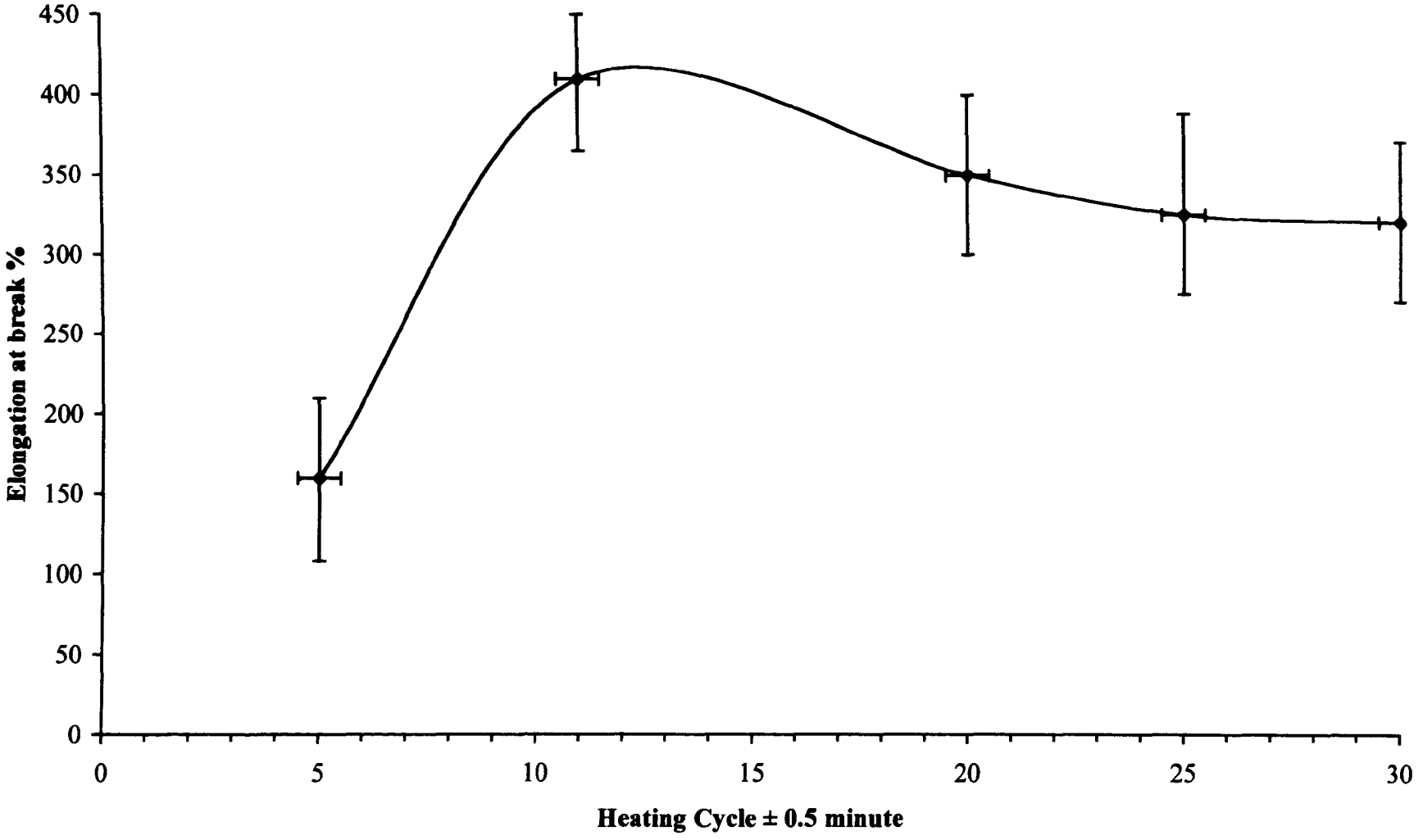

FIGURE 48

EFFECT OF HEATING CYCLE ON % ELONGATION

TABLE 7

EFFECT OF OVEN SET TEMPERATURE ON THE TENSILE PROPERTIES

Oven Set Temperature (°C)	Apparent Density x 10^3 (kg m^{-3})	Yield Stress (M Pa)	Maximum Elongation at Break (%)
220	0.9334	13.92	648
440	0.9350	16.16	365

TABLE 8

ISOTROPY OF YIELD STRESS

Yield Stress Samples Cut at 0° / M Pa	Yield Stress Samples Cut at 90° / M Pa
11.42	11.81
15.73	16.22
16.74	16.66
14.77	15.61
14.40	14.68
14.02	14.87
17.03	16.83
16.63	15.89
16.74	16.45
16.94	16.12
16.08	16.45
Average = 15.50	Average = 15.59

4.6. Thermal conductivity of polyethylene

Results reported in Table 9, show that the thermal conductivity of polyethylene in the solid state decreases with increasing temperature.

At constant temperature the thermal conductivity of polyethylene is observed to decrease with decreasing number of bubbles in the polymer.

Finally, as expected, the results also show that the thermal conductivity of polyethylene powder is lower than the solid.

TABLE 9

THERMAL CONDUCTIVITY OF POLYETHYLENE

Sample	Average Thermal Conductivity ($W\ m^{-1}\ K^{-1}$)	Temperature (°C)	Literature Value ($W\ m^{-1}\ K^{-1}$)
Solid Polyethylene	0.1194	34.6	
No Bubbles	0.114	39.0	
Solid Polyethylene Maximum Bubbles	0.098	34.6	
Polyethylene Powder	0.055	34.6	
Air	0.037		0.026
Polymer Methylmethracrylate (PMMA)	1.30		1.31

CHAPTER 5

DISCUSSION

5.1. Physical properties of polymer

5.1.1. Particle shape

The elongated shape of the particles in this grade of linear low density polyethylene is not the rounded shape recommended for rotational moulding by Ramazzotti [50] and Du Pont [51].

The elongations are commonly referred to as 'hairs, tails or fibrils' and are possibly caused by the partial melting of the polymer due to friction in the grinding process.

Paquette [21] reports that hair formation can be prevented or minimised by the careful control and monitoring of the grinding process. McDaid and Crawford [162] report grinding the polyethylene close to the softening temperature avoids the formation of fibrils or tails. Alternatively, once formed, the hairs can be removed by polishing the particles after grinding, by 'tumbling ' the powder against an abrasive surface. Heating the powder after grinding has also been shown to improve the powder quality [89, 162].

Despite a report by Du Pont [51] that mouldings from unpolished powder particles, or particles with a large length to diameter ratio are difficult to produce, no such difficulty was experienced in this study.

The effect of particle shape on the properties of a polymer powder has been increasingly reported to be an important parameter in the rotational moulding process. Two powders with identical size distributions and bulk densities and ground from the same polymer, can be shown to have quite different properties as a result of the variation in particle shape between the samples [88].

In rotational moulding, the shape of the polymer particle has also been shown to have an important effect on the heating cycle [51]. As discussed in Section 1.8.1, heat transfer to the polymer involves conduction through contact between the polymer particles and the inner mould surface. There is also some heat transfer by convection and radiation from the air inside the mould to the polymer. However, due to the low thermal conductivity of air and the polymer, this can be assumed to be negligible when compared to heat transfer by contact conduction with the mould wall.

Guillen-Castellanos [193] reports that particles with irregular shapes can affect the rate of heat transfer. This is because irregularities in the shape affect the degree of contact between the particles.

Du Pont [51] report that the rate at which the polymer powder melts can be shown to be a function of the shape of the particles. For a flat particle of thickness R, the surface to volume ratio (taken as a measure of the efficiency by which heat is transferred to the particle) has been stated as 1/R for air convection. For a cube of side R it is 6R and for a sphere of radius R, it is 3/R [51].

However, for contact conduction if only a small surface area of the particle is in contact with the heated surface, the surface to volume ratio becomes 1/2R for a flat particle, 1/R for a cube and zero for a sphere. Therefore, as the particle becomes more spherical, the area for conductive heat transfer becomes smaller.

As well as in heat transfer, the shape of the particles is also important in the flow of the polymer during rotation. Spherical particles obviously improve the flow properties of the powder. Paquette [21] reports that 'particle shape profoundly affects the flow characteristics of the powder in the mould.'

Thus the investigation in Section 4.1, and the above discussion highlight the need to find a balance between faster heat transfer through flat particles, and the improved flow properties of more spherical particle shapes.

Choosing a powder with flatter particles for improved heat transfer however, has a further disadvantage in that the rheology of flat particles is difficult to predict. This is due to the inevitable alternate slipping and sticking of the flat particles on the rotating surface. Therefore, trial and error would be necessary to determine flow patterns and cycle times for such polymers and particles.

5.1.2. Particle size distribution

The particle size distribution of the polyethylene powder (500 μm to below 150 μm), Figure 18, is outside the two ranges recommended by ICI [2], Ramazzotti [50],

Nickerson [24] and Soderquist [29] as the ideal for rotational moulding. The recommended ranges are 850 μm to 400 μm and 500 μm to below 297 μm. The distribution peak of 212 μm to 300 μm is lower than the 297 μm to 420 μm peak recommended by Du Pont [49] for low-density polyethylene.

As discussed in Section 2.1.1.1, in addition to the shape, the size of a polymer particle can also be shown to affect the rate of heat transfer.

Consider a flat particle of thickness R. As R increases, the surface to volume ratio of the particle also increases. A large surface to volume ratio will result in increased heat conduction by contact.

Thus as the particle size decreases, the heat transfer becomes more efficient. This is the main reason why particles in the 500 μm range, rather than extruder grade are used in rotational moulding.

An increase in the rate of heat transfer in the polymer powder means that the length of the heating cycle is reduced. This effect of the particle size on the length of the heating cycle is also observed by Ramazzotti [22, 50]. The author reports that as the particle size of the polymer is increased, additional heating time is required to develop a completely smooth interior surface in the moulding.

Another reported advantage of small particle size, is that it gives a better reproduction of the mould surface in the finished product [24, 50]. Soderquist [29] reports that a particle

size less than 297 μm is essential to achieve the desired quality in highly detailed mouldings. Larger particle size, when used with a high viscosity polymer is reported to result in poor surface reproduction [50].

There is however, a limit to which the size of the particle can be reduced. Very small sizes present moulding problems and increase grinding costs. Grinding of some polymers to between 149 μm and 100 μm has been found to result in excessive shearing and heating of the polymer, leading to loss of strength and undesirable characteristics such as discolouration in the moulding [113]. The rotation of very small particles (below 149 μm) within a mould has also been found to result in a build up of high electrostatic charges that result in an agglomeration of the particles [54]. This in turn is reported to lead to uneven melting and non-uniform wall thickness [50]. For hygroscopic polymers, surface absorption of moisture will also be increased which should result in powder agglomeration and hence, defects in the moulding.

Annechini at al [90] reports that powders of particle size less than 50 μm tend to fluidize excessively, causing bridging. Powders of particle size greater than 500 μm are reported to require long oven times and finished parts tend to have greater porosity than finer powders [113, 234].

McDaid and Crawford [162] have studied the effect of powder quality and particle size distribution on the bubbles in rotational moulding. The number and size of (surface and bulk) bubbles were found to decrease with improved powder quality.

Generally, studies have shown that that the shape, size and size distribution of the polymer powder affect both the rotational moulding cycle and the final product properties [193].

Finally, Crawford and McDaid [162] have investigated the effects of processing, cooling and post heating temperature on powder quality. During grinding, previous studies have shown that variables such as gap size and the number of teeth have a major effect on the particle size and size distribution [89].

5.1.3. Bulk density and rheology

Table 2 (Section 4.1.3) shows the bulk density of the unfractionated powder as measured is higher than the bulk density of the fractions below 300 μm. This demonstrates the closer packing expected in a powder with a wider size distribution - the smaller particles occupy the spaces between the larger particles.

Comparison of the bulk density of individual fractions however, shows the results are contrary to the expected. Due to the closer packing of smaller particles, the bulk density of the fractions would be expected to increase with decreasing particle size. However, the results show the opposite; the bulk density of the individual fractions decreases with decreasing particle size.

One explanation is that a greater number of smaller particles have tails or hairs, which reduce the degree of packing. This is supported by the fact that the flow of particles

below 300 μm is poor - hairs and tails must reduce the flow properties of the polymer. The results also show that the flow of particles decreases with decreasing particle size, with particles below 150 μm having no flow properties at all. The results thus suggest that the percentage of particles having tails and hairs increase with decreasing particle size.

Du Pont [51] and Throne [54] recommend that smaller particles are included in a rotational moulding powder because they improve the flow of particles by their lubricating action. However, the results of this study indicate that, because the smaller particles have hairs and tails, they actually reduce the flow properties of the polymer.

The results of this study are in agreement with Paquette [21], who reports that the flow properties of the polymer should improve with increasing bulk density of the polymer powder.

The melt flow index or MFI of a polymer was discussed in Section 2.1.3. The measured value of the linear low density polyethylene in this study, Table 2 (Section 4.1.3), is within the range recommended for rotational moulding by ICI [2].

The minimum MFI recommended for polymers used in rotational moulding is generally accepted as two. It is possible to use polymers with an MFI lower than two, but long heating cycles are required [2], with higher processing temperatures than average [3]. A higher MFI polymer will fuse easily into a uniform melt, resulting in mouldings with a smooth internal surface [21]. However, an upper limit on the MFI is set by the poor

resistance of these polymers to impact at low temperatures, and also a reduced resistance to environmental stress cracking. An increase in MFI above fifty is reported to give no further advantage in processing [3].

Most processing techniques involve some form of direct flow of polymer, in either the solid or the melt state, or both. In extrusion and injection moulding for example, the polymer pellets are fed to the screw from bins and hoppers, which have been designed to allow for maximum flow of powder. The success of the powder coating process depends on the flow characteristics of the polymer solids. The flow characteristics of polymer solids and polymer liquids are very different.

The flow behaviour of the polymer powder in the rotational moulding process is extremely important. Bulk density of the powder and its dry flow or pourability are two closely related polymer parameters which, as well as the particle shape and size distribution, affect the flow characteristics of the powder. However, the science of powder rheology is not as well investigated as the rheology of liquid materials.

Throne has discussed polymer flow during rotational moulding cycle [197]. The following are some factors reported to affect the way in which the polymer powders flow in the rotational moulds:

- Particle shape and size distribution.
- Particle smoothness.
- Particle surface adhesion.

- Smaller solid particle coating, such as ground pigments.
- Additives such as mineral oils.
- Mould surface roughness.

5.2. Heating cycle of the standard moulding

From the observations of the moulding surfaces in Table 3 (Section 4.2), the length of the heating cycle of the standard moulding was established as 12 ± 0.5 minutes. This is the length of the heating cycle as determined by visual examination, and commonly known as the 'trial and error ' method of the rotational moulding industry.

From Table 3, it is also possible to determine the length of each of the three phases of the heating cycle based on the following observations:

1. There is no polymer fusion in the first 1 ± 0.5 minutes of the heating cycle.
2. Fusion of the polymer is complete after a heating cycle of 5 ± 0.5 minutes.
3. All bubbles have dissipated after a heating cycle of 12 ± 0.5 minutes.

Thus, in the first 1 ± 0.5 minute, the mould temperature rises to the melt temperature range of the linear low density polyethylene. In the next 4 ± 0.5 minutes, the polymer fuses into a melt layer containing many air bubbles and covering the inner mould surface. This is followed by the final 7 ± 0.5 minutes in which bubbles in the melt dissipate.

The results can be summarised as follows, at 220° C oven set temperature:

Length of the mould induction phase = 1 ± 0.5 min.

Length of the polymer fusion phase = 4 ± 0.5 min.

Length of the melt densification phase = 7 ± 0.5 min.

Thus, total length of heating cycle = 12 ± 0.5 min.

The appearance of the moulding in this investigation at the various stages of the heating cycle is similarly observed by ICI [3], McAdams [6] and Rees [56].

The ICI [3] report is brief but also describes the appearance of the moulding after a heating cycle that is too long, causing oxidation of the moulding surface.

MacAdams [6] is more specific and has related the change in the appearance of the free surface and mould surface of the moulding to the heating time, see Table 10.

In this study, the longest (and hence the rate determining) step of the heating cycle of the standard moulding, was found to be the melt densification phase, which was measured as just over 58% of the heating cycle at 220° C oven set temperature, see Table 11. The mould induction phase and the polymer fusion phase are approximately 8% and 33% respectively.

Some sources [2, 63] make no distinction between the various phases of the heating cycle. Other sources [1, 22, 49, 50, 53] divide the heating cycle into two phases only: the

TABLE 10

ROTOMOULDED PART APPEARANCE VERSUS CURE TIME [6]

State of Cure	Way Under	Under	Slight Under	OK	Slight Over	Over	Way Over
Inside Colour Surface	← Same as outside →				Slight Yellow	Increasing Yellow to Brown	
Inside Colour Gloss	← Dull →			← Shiny →			
Inside Surface Appearance	Very Rough	Rough	← Smooth & Waxy →	Not Sticky	Slightly Sticky	Sticky	Very Sticky
Bubbles	Very Many	Many	Few to None	← None →			Few to Many Towards Outside Surface
Fill	Bridging	Less Than Best to Best		← Best →			
Tear Resistance	Poor	Less Than Maximum		← Maximum →			May Start to Decrease

TABLE 11

EFFECT OF OVEN SET TEMPERATURE ON THE THREE PHASES OF THE HEATING CYCLE

	Oven Set Temp. / °C	Mould Induction Time / Minutes ±0.5	Polymer Fusion Time / Minutes ±0.5	Melt Densification Time / Minutes ±0.5	Total Length of Heating Cycle / Minutes ±0.5
	220	1	4	7	12
% of the heating cycle		8.3	33.3	58.3	
	440	0.5	2.5	1	4
% of the heating cycle		12.5	62.5	25	
% reduction of heating cycle at 440° C		50	37.5	86	66

mould induction phase and the polymer fusion phase. The melt densification phase is considered to be part of the fusion phase, although Du Pont [53] recognise the point at which the fusion of the polymer is complete and the densification of the melt starts.

The US Army report [227] divides the heating cycle into four phases:

1. Mould induction time.
2. Time required for the polymer particles to reach the melt temperature range.
3. Polymer fusion time.
4. Melt densification time.

The additional phase is the time required for the polymer to reach the melt temperature range. However, it can be argued that this point overlaps with the mould induction phase and will be difficult to observe in practice.

There is therefore, no agreement in the literature concerning the number of phases of the heating cycle.

The results of this study however, show that the heating cycle can be divided into three phases, defined as follows:

1. Mould induction phase

At the start of the heating cycle, the mould is at room temperature. Thus in the first stage

of the heating cycle, heat is supplied to the mould primarily to raise its temperature. However, no polymer fusion can take place until the mould temperature reaches the melting point of the polymer. The time taken for the mould to reach the melting point of the polymer is defined as the mould induction time.

2. Polymer fusion phase

This begins when the polymer particles melt on to the rotating mould surface. At the end of the fusion phase, the inner mould surface is completely covered with the polymer melt. At this stage the melt contains many air bubbles.

3. Melt densification phase

This is the final stage of the heating cycle and is the time taken for the air bubbles in the melt to dissipate.

Contrary to the observations made in this study, Throne [54] reports that a fraction of the bubbles will always remain in the moulding even at long densification times.

The US Army report [227] divides the bubbles into two types; surface and bulk, and states that surface bubbles are intrinsic to rotational moulding. Unlike bulk bubbles, which can be eliminated or minimised by the judicious adjustment of the time and temperature of the polymer during the densification stage, surface bubbles cannot.

Both reports are contrary to the results of this study where photomicrographs of the moulding surfaces Figure 29 (Section 4.2.1), show both surface and bulk bubbles are eliminated by the end of a heating cycle of 12 ± 0.5 minutes.

Apparent density measurements, Figure 30 (Section 4.2.2) confirms the above results. At a heating cycle of 5 ± 0.5 min. (1 ± 0.5 min. mould induction time plus 4 ± 0.5 min. fusion time) the apparent density of the moulding is minimum, indicating a maximum number of bubbles in the moulding wall.

The apparent density then increases with increased heating time and reaches a maximum at a heating cycle of 12 ± 0.5 min. From this the melt densification time can be calculated as 7 ± 0.5 min. This is in agreement with previous results reported in Section 4.2 and Section 4.2.1.

The increase in apparent density with increasing cycle time is similarly observed by Dodge [192].

MacAdams [6] and McDonagh [5] support the observation that the presence of bubbles decreases the apparent density of the polymer.

5.2.1. Effect of process variables on the heating cycle

It can be assumed that thicker mouldings will take longer to form, and therefore, the increase in the heating cycle with increasing polymer mass reported in Figure 31 (Section

4.3) is as expected. This increase is also reported by various other sources [1, 22, 31]. Duncan and Zimmerman [1] found that the heating cycle is doubled as the wall thickness is doubled indicating a linear, directly proportional relationship.

However, the relationship found in this study is not linear. The graph in Figure 31 (Section 4.3) shows some mouldings of different mass have the same heating cycle. Examples are mouldings of mass 300g, 400g and 500g. These mouldings have the same heating cycle of 12 ± 0.5 minutes. Possible explanations for the lack of linearity in the graph are discussed as follows.

The first explanation relates to the accuracy of the machine timer. The design of the machine and timer do not allow measurement of fusion times less than 1 minute. For the same reason, it was not possible to improve the accuracy of the graph by increasing the polymer mass in 50g steps. The graph indicates that the fusion times of these mouldings would have fallen beyond the accuracy of the timer.

Secondly, it is possible that the relationship between the heating cycle and the mass, or the wall thickness of the moulding, is not linear. The three phases of the heating cycle; mould induction, polymer fusion and melt densification were investigated separately in Section 4.3.2. The investigation of the moulding mass or wall thickness on the fusion and melt densification times yielded some surprising results.

The fusion time of the moulding was found to increase linearly with the polymer mass, Figure 38 (Section 4.3.2). However, the melt densification time, Figure 43 (Section

4.3.3), was found to decrease with increasing polymer mass. These results are discussed further in Section 5.2.1.2 and Section 5.2.1.3. The implication for the present discussion is the possibility that the graph in Figure 31 (Section 4.3) is the combination of these two effects. The inclusion of the melt densification time with the fusion time (as a complete heating cycle) Figure 31, contributes to the shape of the graph. Therefore, contrary to what is is generally known, the results of this study would indicate that the fusion time of a moulding is not the same as the heating cycle, and distinction between the two needs to be made.

Continuing with the effects of process variables on the heating cycle, Figure 32 (Section 4.3) shows that, for a given moulding of mass 400g, the heating cycle decreases with increasing oven set temperature. The greatest reduction in the heating cycle is recorded when the oven set temperature is reduced from 330° C to 220° C. At higher temperatures, the rate at which the heating cycle is reduced appears to slow down. This can be explained by referring to Figure 42 (Section 4.3.3). This figure shows how the melt densification time is reduced as the oven set temperature is increased from 220° C to 330° C. Increasing the temperature to higher than 330° C does not cause any further corresponding decrease in the melt densification time. In the study of the heating cycle in Figure 32, this will contribute to the reduction of the overall heating cycle at temperatures higher than 330°C, and explains why the rate at which the heating cycle is reduced slows down.

The temperature range investigated in Figure 32 was between 220° C and 500° C. However, 500° C was too high for practical use, as the polyethylene started degrading at

temperatures higher than 440° C. Apart from thermal degradation, high temperatures also encourages oxidative degradation of the polymer, and increases the effects of thermal shock to the mould when sprayed with water in the cooling cycle [58].

McDonagh [5] reports problems with moulding thicker parts at high temperatures, where the mould surface of the moulding can degrade before fusion of the moulding is complete. Neidinger [25] and Ramazzotti [22] report that low moulding temperatures are necessary for thermally unstable polymers. The need for shorter cycle times at lower temperatures has led to the development of the jacketed mould design, in which heat transfer at lower temperatures can be improved by making it more uniform and providing better control.

Duncan and Zimmerman [1] report that it is possible to eliminate all particle boundaries in high density, but not low density polyethylene. The explanation given is that longer heating cycles are possible for high density polyethylene due to the higher thermal stability of the polymer. However in this study, scanning electron microscopy reveals no evidence of polymer boundaries remaining in the linear low density polyethylene at the end of the heating cycle, see photomicrographs in Figure 28 (Section 4.2.1).

As already stated, in this study 440° C was the highest oven set temperature before degradation was noticed in the polymer. Increasing the oven set temperature from 220°C to 440°C reduced the heating cycle of the standard moulding from 12 ± 0.5 minutes to 4 ± 0.5 minutes. This is shown in photomicrographs of the mouldings in Figure 29 (Section 4.2.1) and Figure 33 (Section 4.3).

The decrease in the length of the heating cycle with increasing oven set temperatures is widely reported in the literature [23, 28, 53]. Ramazzotti [22, 23] reports a 30% reduction in the length of the heating cycle when the oven temperature is increased by 52%.

Results of this study show a 66% reduction in the length of the heating cycle, when the oven set temperature is increased from 220° C to 440° C , see Table 11 (Section 5.2). This table is a summary of the effect of oven set temperature on the three phases of the heating cycle. At 220° C, the melt densification phase is the longest phase of the heating cycle (58%.) Increasing the temperature to 440° C reduces this to just 25 % of the heating cycle. Gogos [166] reports approximately 40% of the rotational moulding cycle is dedicated to the removal of bubbles from the polymer melt.

5.2.1.1. Mould induction phase

Table 11 shows how the mould induction time is reduced from 1 to 0.5 minute, when the oven set temperature is increased from 220° C to 440° C. However, because the overall length of the heating cycle is also reduced at 440° C, the mould induction time as a percentage of the heating cycle increases from 8.3% to 12.5%.

The reduction in the mould induction time with increasing oven set temperature is as predicted by Throne [55]. According to Equation 5.3.1.1.2, increasing the oven set temperature increases the heat transfer coefficient and this has the effect of reducing the mould induction time. This is discussed further in Section 5.3.1.1.

5.2.1.2. Fusion phase

Table 11 (Section 5.2) shows how at oven set temperature of 220° C, the fusion time of the moulding is four minutes. This is the second longest phase and 33% of the heating cycle.

Figure 38 (Section 4.3.2) shows how the fusion time of the moulding varies with increasing mass of the polymer. The graph is linear, indicating that (unlike the heating cycle), the fusion time of the moulding is directly proportional to the mass. The exception is the 600g ± 20g moulding. The fusion time of this moulding was consistently measured as 7 ± 0.5 min.

One explanation is that the actual fusion time is between 6 ± 0.5 min. and 7 ± 0.5 min. However, as discussed in Section 5.2, the design of the machine and timer do not allow measurement of fusion times less than one minute. For the same reason, it was not possible to improve the accuracy of the graph by increasing the polymer mass in 50g steps. The graph indicates that the fusion times of these mouldings would have measured beyond the accuracy of the timer.

The linear relationship between the heating time and the moulding wall thickness in the fusion phase (Figure 38) fits Equation 1.8.1.1.6, established by Cogswell [259], see Section 1.8.1.1.

$$t = \frac{3\,\eta_o\,x_m}{s} \qquad \text{(Equation 1.8.1.1.6)}$$

where:

t	=	time /s
η_o	=	viscosity of polymer melt at zero shear
x_m	=	depth of melt at time t
s	=	surface tension of polymer melt

During sintering, this equation predicts a directly proportional relationship between melt thickness and time. However, the equation assumes isothermal conditions when the viscosity and surface tension of the polymer remain constant. As discussed in Section 5.3, heat transfer in rotational moulding is unsteady and the temperature of the polymer cannot be assumed to remain constant, although the rise in the temperature may be small enough not to affect the overall equation.

Investigation of the effect of oven set temperature on the fusion time of the polymer, confirm that increasing the oven set temperature reduces the fusion time of the moulding. Table 11 (Section 5.2) shows how fusion time of the moulding is reduced from 4 min. to 2.5 min. when the oven set temperature is increased from 220° C to 440° C . The results fit Equation 1.8.1.1.2, established by Kuczynski et al [102], see Section 1.8.1.1.

$$\left(\frac{X^2}{a_s^{1.02}} \right)^n = K(T_s)\, t_s \qquad \text{(Equation 1.8.1.1.2)}$$

Where K is an experimental constant, T_s is the temperature, t_s is the sintering time, X is the radius of the interface and a_s is the radius of the PMAA sphere.

This equation suggests that, at constant sintering time, the rate of polymer fusion is directly proportional to the temperature.

This is shown in Figure 41 (Section 4.3.3), where the fusion time of the moulding is investigated at two oven set temperatures, 220° C and 440° C. The graph for 440° C has a higher gradient, indicating a higher rate of fusion at this temperature.

Table 11 (Section 5.2) summarise the effect of oven set temperature on the fusion time of the moulding. At the lower oven set temperature of 220° C, the fusion time of the moulding at 4 minutes is the second longest phase, and 33.3% of the heating cycle. Increasing the temperature to 440° C reduces the fusion time to 2.5 minutes, but at the higher temperature because the longest (62.5%) and rate determining phase of the heating cycle.

5.2.1.3. Melt densification phase

The melt densification time of the standard moulding at 220° C, was measured as 7 ± 0.5 minutes. Table 11 shows that at this temperature, the melt densification time is the longest and hence the rate determining phase of the heating cycle.

Study of the effect of oven set temperature on the melt densification time, shows that increasing the oven set temperature from 220° C to 440° C, reduces the densification time of the standard moulding from 7 to 1 ± 0.5 minutes. This is a reduction of almost 86%. At the higher temperature, the melt densification time is no longer the longest phase, but reduces from 58.3% to 25% of the heating cycle. This reduction in the melt

densification time with increasing temperature, is as predicted by Equation 5.2.1.3.1 established by Frenkel [100] to model the densification process, and is discussed below.

Following on from his equation for the growth of the web in the sintering material, Equation 1.8.1.1.1, Frenkel went on to establish an expression for the densification process in which the air bubbles are eliminated.

$$r_0 - r_t = \frac{S\, t_c}{2\, \eta_0} \qquad \text{Equation 5.2.1.3.1.}$$

r_0 = initial bubble radius
r_t = radius of bubble of time t
S = surface tension
η_0 = viscosity of polymer at zero sheer
t_c = time

Since S and η_0 are temperature dependent, Equation 5.2.1.3.1 suggests that the densification rate is temperature and time controlled. If the temperature is increased, the polymer melt viscosity η_0, increases. This would result in a decrease in the melt densification rate, and vice versa.

Figure 42 (Section 4.3.3) also shows that increasing the oven set temperature beyond 330° C does not cause any further reduction in the melt densification time. One explanation is that at 330° C, the polymer melt at the end of the fusion phase, is at the temperature at which the rate of bubble dissipation is so fast that it appears instantaneous. Thus any increase in the rate of bubble dissipation will be difficult to

observe. This is confirmed in Figure 42 (Section 4.3.3) where at 440° C oven set temperature, bubble dissipation is spontaneous.

Surprisingly, at 220° C oven set temperature, the melt densification was also found to decrease with increasing polymer mass, see Figure 43 (Section 4.3.3). One explanation is the increase in polymer fusion time with increasing polymer mass. This means that the polymer is exposed to the oven set temperature for longer times. Longer exposures to the moulding temperature means higher polymer melt temperature at the end of the fusion phase. This would result in increased rate of bubble dissipation.

Crawford and Xu [121], although using a different mathematical model (see Section 1.8.1.1) also concluded that the removal of bubbles from the polymer melt is influenced by the melt temperature.

In a later study, Spence and Crawford [122] again conclude that as the polymer melt temperature increases, the bubbles decrease in size and finally disappear.

The elimination of bubbles by increasing the oven set temperature and/or the length of the heating cycle is also reported by the United States Industrial Chemical Company [12] and McKenna [260, 261].

ICI [2] report a critical length of heating cycle after which most bubbles dissipate, and that any further increase in the heating time does not remove any remaining bubbles.

As stated before, the US Army [227] and Throne [54] divides the bubbles into two types; surface and bulk, and it is stated that surface bubbles are intrinsic to rotational moulding. Unlike bulk bubbles, which can be minimised or eliminated by controlling the time and temperature of the heating during densification, surface bubbles cannot.

This is supported by Paquette [21] who reports surface bubbles can only be minimised by a highly polished inner mould surface.

These reports are contrary to the results of this study where Figure 29 (Section 4.2.1) show both surface and bulk bubbles are eliminated by the end of the melt densification phase.

5.3. Heat transfer in the rotational moulding process

Rotational moulding is an unsteady state heat transfer process [22, 49, 53]. This means that the temperature of the mould and polymer are subject to change and never reach a constant value. Rammazzotti [22] has summarised the temperature changes in a typical rotational moulding cycle in the form of a graph, see Figure 49. A successful moulding is thus achieved by knowing the correct time to remove the mould from the oven and not by keeping the mould temperature constant, as for other major processing techniques.

There are only very few, brief references in the literature concerning the heat transfer processes in a typical rotational moulding cycle. The following is therefore, an attempt to identify the heat transfer processes taking place in each phase of the heating and cooling

FIGURE 49

TEMPERATURE VARIATION IN A TYPICAL ROTATIONAL MOULDING CYCLE

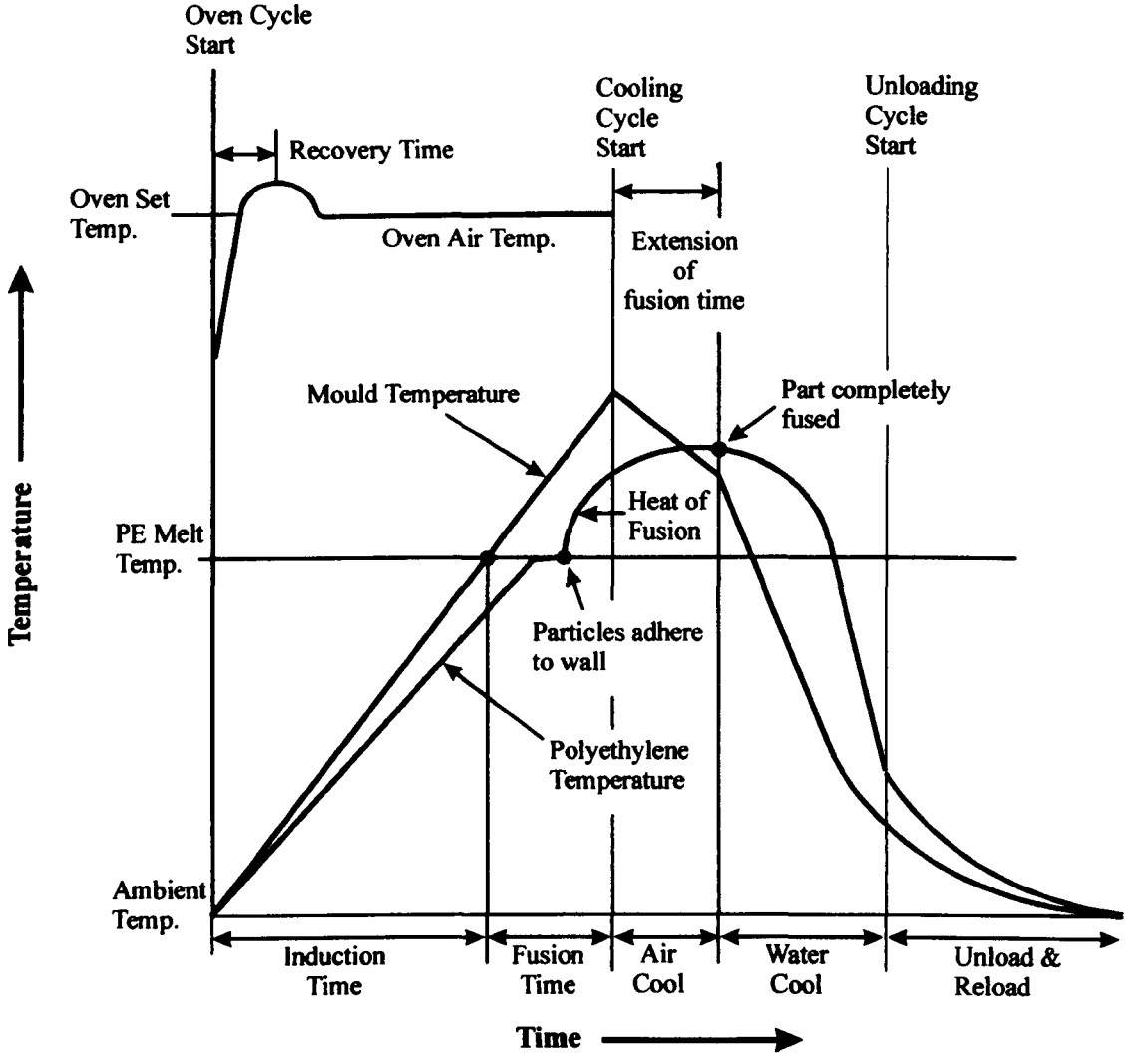

stage of the rotational moulding cycle.

5.3.1. The heating cycle

5.3.1.1. The mould induction phase

It is postulated that the following heat transfer processes, summarised in Figure 50, take place:

1. Heat transfer, mainly by forced convection from circulating air in oven to outer mould surface.
2. Heat transfer by conduction through the mould wall.
3. Heat transfer mainly by (contact) conduction from inner mould surface to polymer particles.
4. Heat transfer by convection from mould wall to air inside mould.

If the effects of mould rotation are ignored, then the above heat transfer considerations suggest that the temperature of the mould during the heating cycle will be determined by:

1. The thermal properties of the mould (thermal conductivity and heat capacity.)
2. The thickness of the mould wall.
3. The temperature of the circulating air.
4. The velocity of the circulating air.

FIGURE 50

HEAT TRANSFER PROCESSES IN THE MOULD INDUCTION PHASE

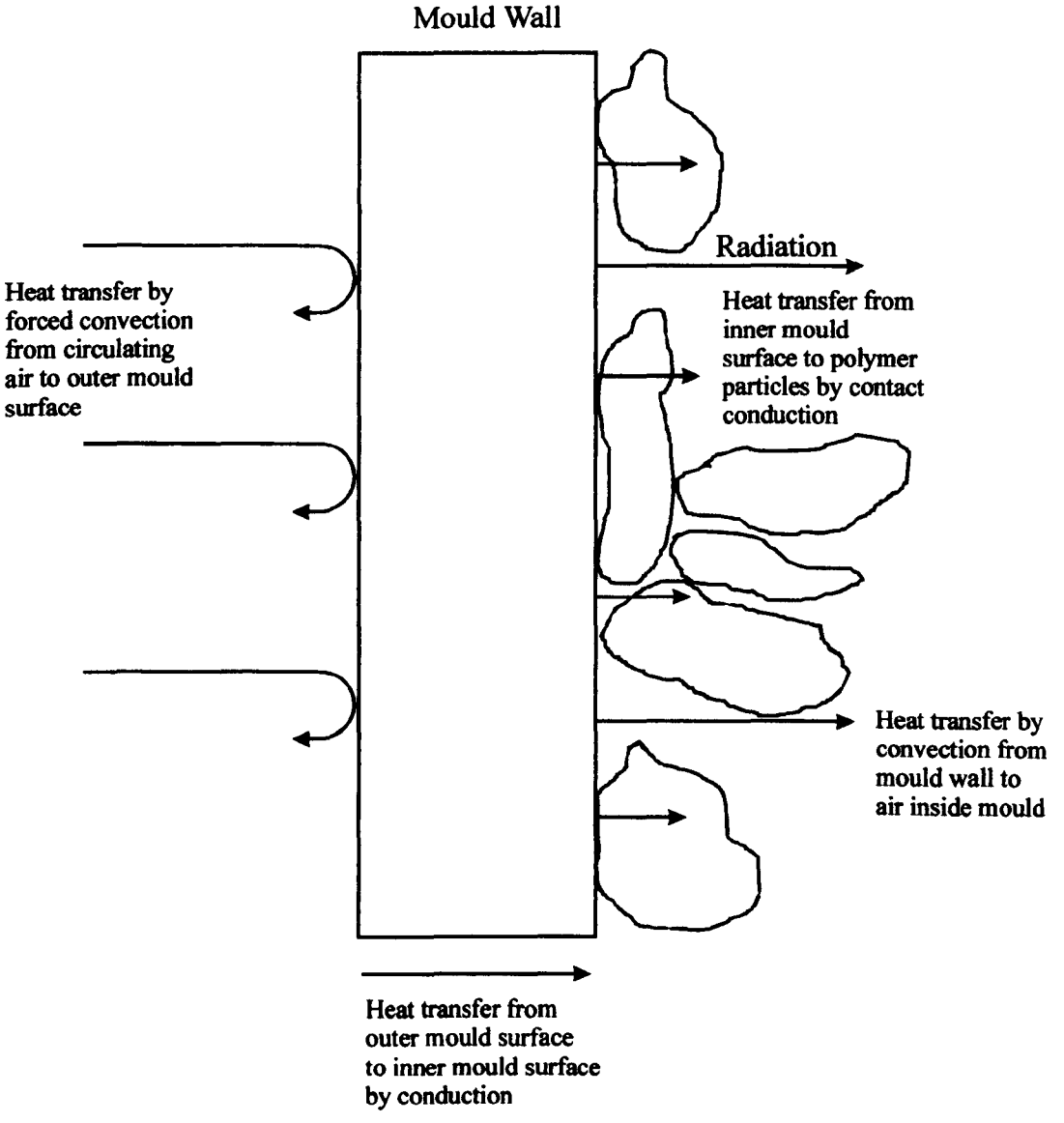

The last two factors, the temperature and velocity of the circulating air, define the heat transfer coefficient between the circulating air and mould;

$$h_c = \frac{q}{A\,(T_s - T_\infty)} \qquad \text{Equation 5.3.1.1.1.}$$

Where h_c is the convective heat transfer coefficient, q is the rate of heat transfer by convection, A is the heat transfer area, T_s is the surface temperature of mould and T_∞ is the temperature of circulating air at some specified location, far away from source. Some work on the theoretical determination of the heat transfer coefficient has been reported [103]. However, the mathematical approach assumes certain boundary conditions, which are rarely achieved in practice. It is thus best to assume the heat transfer coefficient is an empirical factor to be determined experimentally. Typical values of the heat transfer coefficient are given in Table 12.

In this study, the reduction of the mould induction time with increasing oven set temperature reported in Section 4.3.1 is explained by the increase in heat transfer coefficient at the higher oven set temperature.

Heat transfer across the mould wall can be assumed to be instantaneous, because of the high thermal conductivity of metals and the thin walls used in rotational moulding.

In this study, this assumption was experimentally verified by measuring the temperature of outer and inner mould surfaces during the mould induction phase, using

TABLE 12

TYPICAL VALUES OF HEAT TRANSFER COEFFICIENT

Medium	h ($W m^{-2} K^{-1}$)
Polymer to still air	10
Polymer to moving air at 25 km/h	30-40
Solid polymer to metal surface	250-500
Polymer to oil bath	400-600
Polymer to stirred water	1500-3000
Polymer melt at high pressure to metal surface	>10,000

thermocouples attached to the surfaces. The two temperatures were found to equalise instantaneously, with no measurable temperature gradient existing across the mould wall.

Due to the low thermal conductivity of air (0.43 W m^{-1} K^{-1} at 20° C), heat transfer by convection from the inner mould wall to the air inside the mould can be assumed to be negligible.

Transient heating of mould

Throne and Rao [55] has studied the variation of mould temperature with time. He applied the first law of thermodynamics to consider the change in the internal energy of the mould. Thus:

The change in the internal energy of the mould during time dt	=	The net flow into the mould from the environment during time dt

$$\rho_m \, c_m \, L \, dT_s = h_c (T_\infty - T_0) \, dt \qquad \text{Equation 5.3.1.1.2.}$$

Where ρ_m = density of mould material

c_m = specific heat capacity of mould material

L = thickness of mould wall

h_c = convective heat transfer coefficient

T_s = mould surface temperature at time t

T_0 = initial mould temperature

T_∞ = ambient temperature (oven temperature)

Rearranging and integration gives:

$$\frac{T_\infty - T_s}{T_\infty - T_0} = e^{[-h_c \alpha / L k_m] t} \qquad \text{Equation 5.3.1.1.3.}$$

Where $\alpha_m = \frac{k_m}{\rho_m C_m}$ = thermal diffusivity of mould.

k_m = thermal conductivity of mould.

Equation 5.3.1.1.3 shows that when all the mould parameters are kept constant, the temperature of the mould depends on the oven set temperature, and that when all mould parameters are known, the equation can be used to predict the mould induction time.

In this study, Equation 5.3.1.1.3 was used to predict the theoretical heating curve for the mould at an oven set temperature of 220° C, see Figure 51. Comparison with the measured values reported in Section 4.3.1, shows good correlation between the measured and the theoretical. (The theoretical graph can also be used to predict the induction time of the mould.)

5.3.1.2. Polymer fusion phase

Heat transfer in the fusion phase needs to be considered at several different stages.

FIGURE 51

MOULD TEMPERATURE DURING THE HEATING CYCLE – COMPARISON OF PREDICTED AND MEASURED VALUES

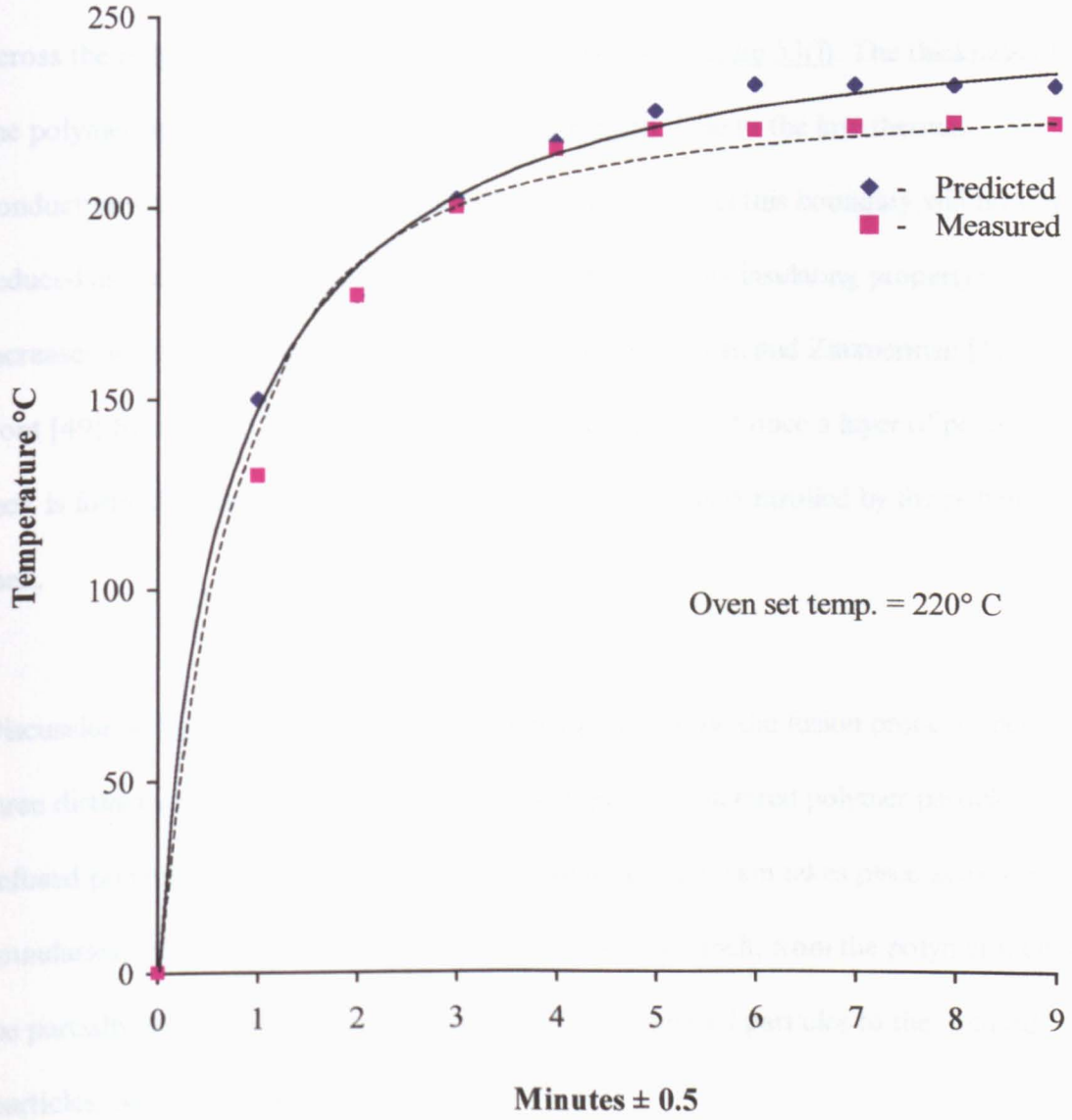

During mould rotation, as the polymer particles come into contact with the mould surface, heat transfer by contact conduction takes place across the mould surface/polymer particle boundary and the particles sinter and melt onto the mould surface, see Figure 52.

Once a layer of polymer melt is formed, continued rotation of the mould brings further polymer particles into contact with the polymer melt. Heat transfer now takes place across the polymer melt/polymer particle boundary, see Figure 53(i). The thickness of the polymer melt will increase with time, Figure 53(ii). Due to the low thermal conductivity of polyethylene, the rate of heat transfer across this boundary will now be reduced as the thickness of the polymer melt, (and hence its insulating property) increases with time. This assumption is also made by Duncan and Zimmerman [1], Du Pont [49] Ramazzotti [23] and Griffin [112] who report that once a layer of polymer melt is formed inside the mould, the rate of heat transfer is controlled by the polymer melt.

Discussion in Section 1.8.1 showed that at any point during the fusion process, there are three distinct zones in the mould; polymer melt, partially sintered polymer particles and unfused polymer. Thus heat transfer at any point during fusion takes place across three boundaries; from the inner mould surface to the polymer melt, from the polymer melt to the partially sintered particles and from the partially sintered particles to the unfused particles, see Figure 54.

From the basic heat transfer considerations, it can be assumed that the rate of heat

FIGURE 52

SIMPLE CYLINDRICAL MOULD MODEL FOR HEAT TRANSFER IN THE FUSION PHASE

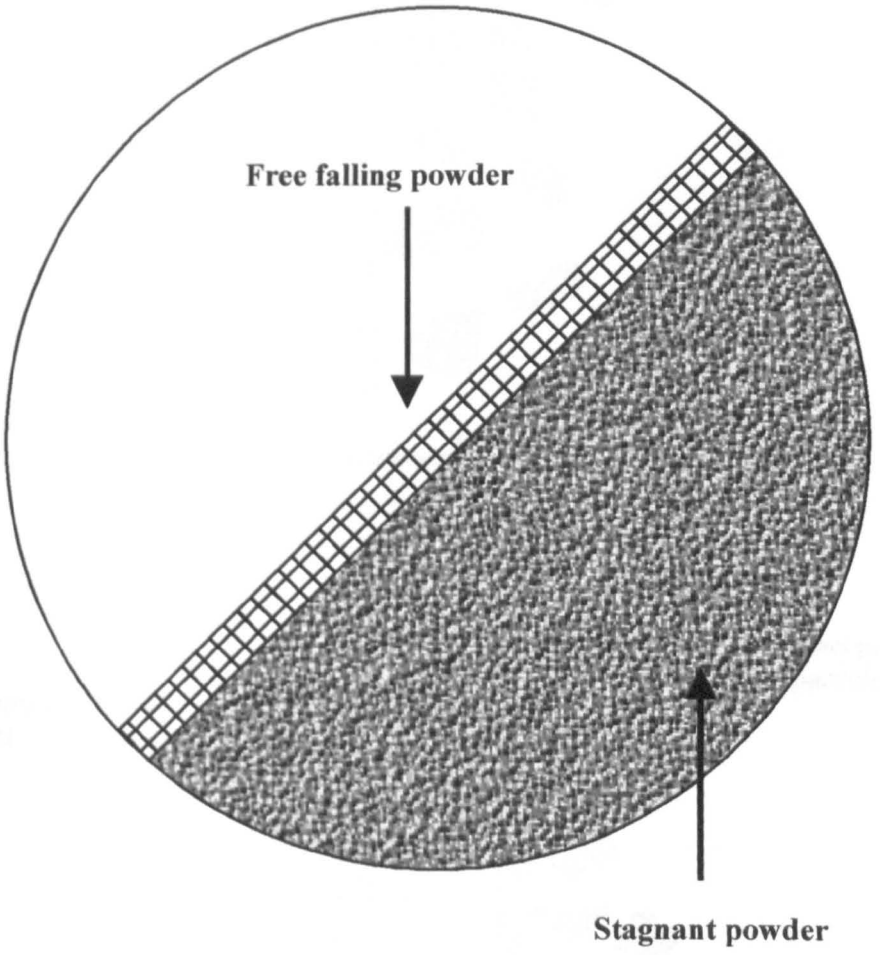

FIGURE 53 (i) & (ii)

HEAT TRANSFER DURING THE FUSION PHASE

(i) Heat transfer at the start of the fusion phase

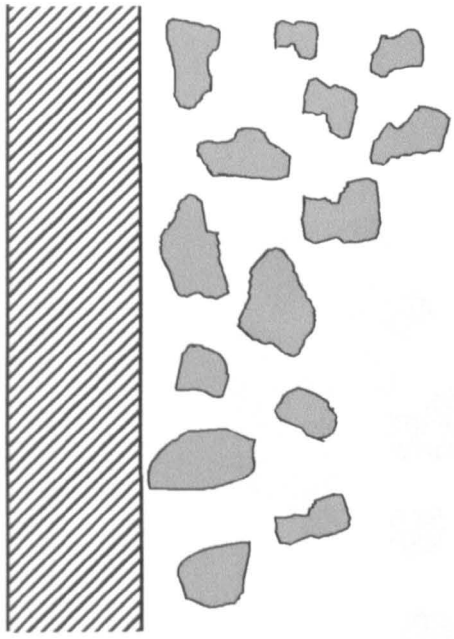

Heat transfer across mould wall / polymer particle boundary by contact conduction

Heat transfer across polymer melt / polymer particle interface

(ii) Heat transfer across mould wall / polymer melt interface

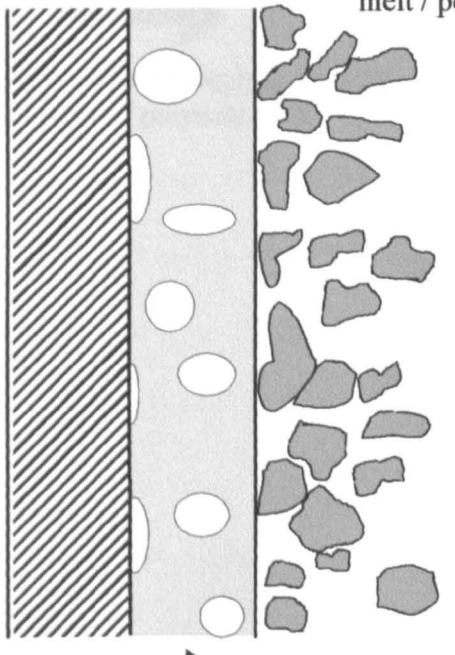

Heat transfer across mould wall / polymer melt interface

FIGURE 54

HEAT TRANSFER IN THE FUSION PHASE - CONTINUED

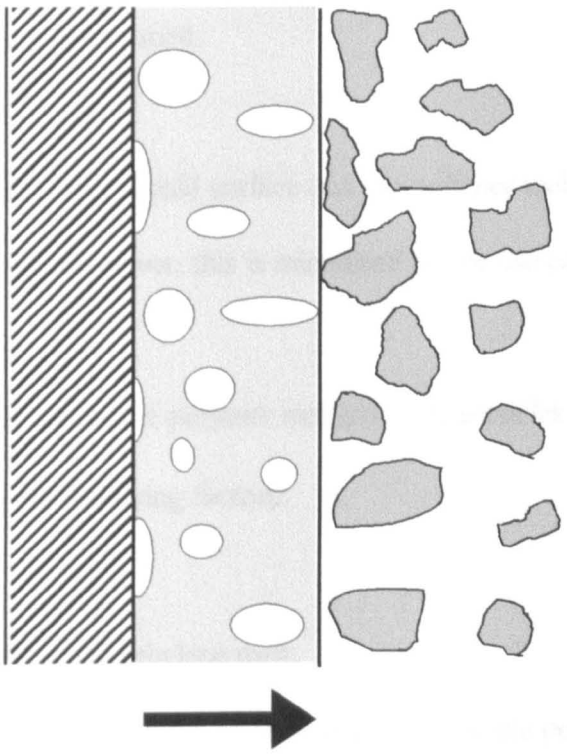

Heat transfer through increasing thickness of polymer melt

transfer across the inner mould surface/polymer particle boundary at any time t will be determined by the following factors:

1. The temperature of the mould [23].
2. The thermal properties of the mould and polyethylene [23].
3. The thickness of the polymer melt.

Poor contact between the inner mould surface and the polymer melt will increase the resistance to heat transfer. However, this is minimised by the use of a release agent.

The rate of heat transfer across the polymer melt/polymer particles boundary at any time t will be determined by the following factors:

1. The temperature of the polyethylene melt.
2. The degree of contact between the rotating particles and the polymer melt.

The rate of heat transfer across the sinter melt will be determined by the temperature of the sinter melt, and the degree of contact between it and the sinter melt. However, due to the low thermal conductivity of polyethylene, the temperature of the sinter melt will be low and heat transfer across this boundary can be assumed to be negligible.

Rao and Throne [55] have developed two models for the heat transfer during the fusion phase. The first one is based on a simple cylindrical mould. In the development of the

model, an assumption was made that the powder in contact with the cylinder moved with the cylinder by friction between the particles and rotating mould wall surface. On reaching a 50 degree dynamic angle of repose with the horizontal (the property that characterises the point at which the powder is released from the mould) the powder falls across the remaining static powder in free fall. This is shown schematically in Figure 52 (Section 5.3.1.2). Thus heat transfer to the polymer takes place by conduction from the inner mould surface during contact. As soon as the polymer reaches the melting point and adheres to the mould surface, it is considered to be removed from the powder mass balance.

The following equation was established to describe the heat transfer during the contact period:

$$\propto_{eff} \left(\frac{\partial^2 T}{\partial x^2} \right) = \frac{\partial T}{\partial t} \qquad \text{Equation 5.3.1.2.1.}$$

Where $\propto_{eff}$ = effective powder thermal diffusivity

T = mould temperature

X = distance from the initial powder contact with the mould surface

t = time

Using the equation to describe the temperature rise of the mould temperature, a temperature profile for the powder was derived:

$$T = T_{\infty} [\, 1 - \exp(-\beta t) \,] (1 - x / \delta)^3 \qquad \text{Equation 5.3.1.2.2.}$$

Where δ is the distance into the powder that the effects of mould heating can be felt.

δ is referred to as the penetration thickness.

β = time constant for mould

Throne [55] established that the penetration thickness can be calculated from:

$$\delta = \frac{2\sqrt{6\alpha_{eff}}}{T_\infty(1-e^{-\beta t_2})+T^0} \left\{ t_c\left[T_\infty^2 + 2T_\infty T^0 + (T^0)^2\right] + \left[\frac{2T_\infty^2}{\beta} + \frac{2T_\infty T^0}{\beta}\right]\left(e^{-\beta t_2} - e^{-\beta t_1}\right) - \frac{T_\infty^2}{2\beta}\left(e^{-2\beta t_2} - e^{-2\beta t_1}\right)\right\}^{1/2}$$

Equation 5.3.1.2.3.

Where t_c = total time the powder is in contact with mould surface

t_1 and t_2 = initial and final times of contact, respectively

Note: $t_c = t_1 - t_2$

T^0 = initial temperature

In 1976, a second model was proposed by Throne [236] in which the powder was assumed to be in continuous static contact with the inner mould surface, and that once a

layer of molten polymer had been formed, the rate of heat transfer was controlled by the melt.

The basic equations describing heat transfer through the mould and polymer are stated as follows:

$$\rho_m c_p (\partial T_s / \partial t) = k_m (\partial T_m / \partial x^2) \qquad \text{Equation 5.3.1.2.4.}$$

$$\rho_p c_p (\partial T_p / \partial t) = k_p (\partial^2 T_p / \partial x^2) \qquad \text{Equation 5.3.1.2.5.}$$

Where c_p = specific heat capacity of polymer

T_p = temperature of polymer

x = distance of heat transfer in time t

The boundary conditions that describe the heating of the polymer are:

$$-k_m \left(\partial T_m / \partial x \right)_{x=0} = h_c (T_m - T_\infty) \qquad \text{Equation 5.3.1.2.6.}$$

$$-k_m \left(\partial T_m / \partial x \right)_{x=x_0} = -k_p \left(\partial T_p / \partial x \right)_{x=x_0} \qquad \text{Equation 5.3.1.2.7.}$$

$$T_m (x = x_0) = T_p (x = x_0) \qquad \text{Equation 5.3.1.2.8.}$$

$$-k_p \left(\partial T_m / \partial x \right)_{x=L} = 0 \qquad \text{Equation 5.3.1.2.9.}$$

The first condition, Equation 5.3.1.2.6 describes convective heat transfer to the surface of the mould. Equation 5.3.1.2.7 and Equation 5.3.1.2.8 describe conditions at the interface between the inner mould surface and the surface of the polymer. Equation 5.3.1.2.9 represents an insulation condition for the inner surface of the polymer and suggests that heat transfer to the air inside the hollow moulding is zero.

5.3.1.3. The melt densification phase

Heat transfer in the melt densification phase takes place across just one boundary: the inner mould surface and polymer melt, see Figure 55. As in the fusion phase, the rate at any time **t** will be determined by the thermal conductivity of the melt at that temperature. The fact that the melt contains many air bubbles, and that the number will decrease with time also needs to be taken into account.

5.3.2. The cooling cycle

The heat transfer processes in the cooling cycle can be analysed as taking place across three boundaries, see Figure 56:

1. From the polymer melt to the air inside the mould.
2. From the polymer melt to the increasing layer of solid polymer.
3. From the solid polymer to the mould wall.

Due to the very low thermal conductivity of polyethylene melt and air, heat loss from the

FIGURE 55

HEAT TRANSFER IN THE MELT DENSIFICATION PHASE

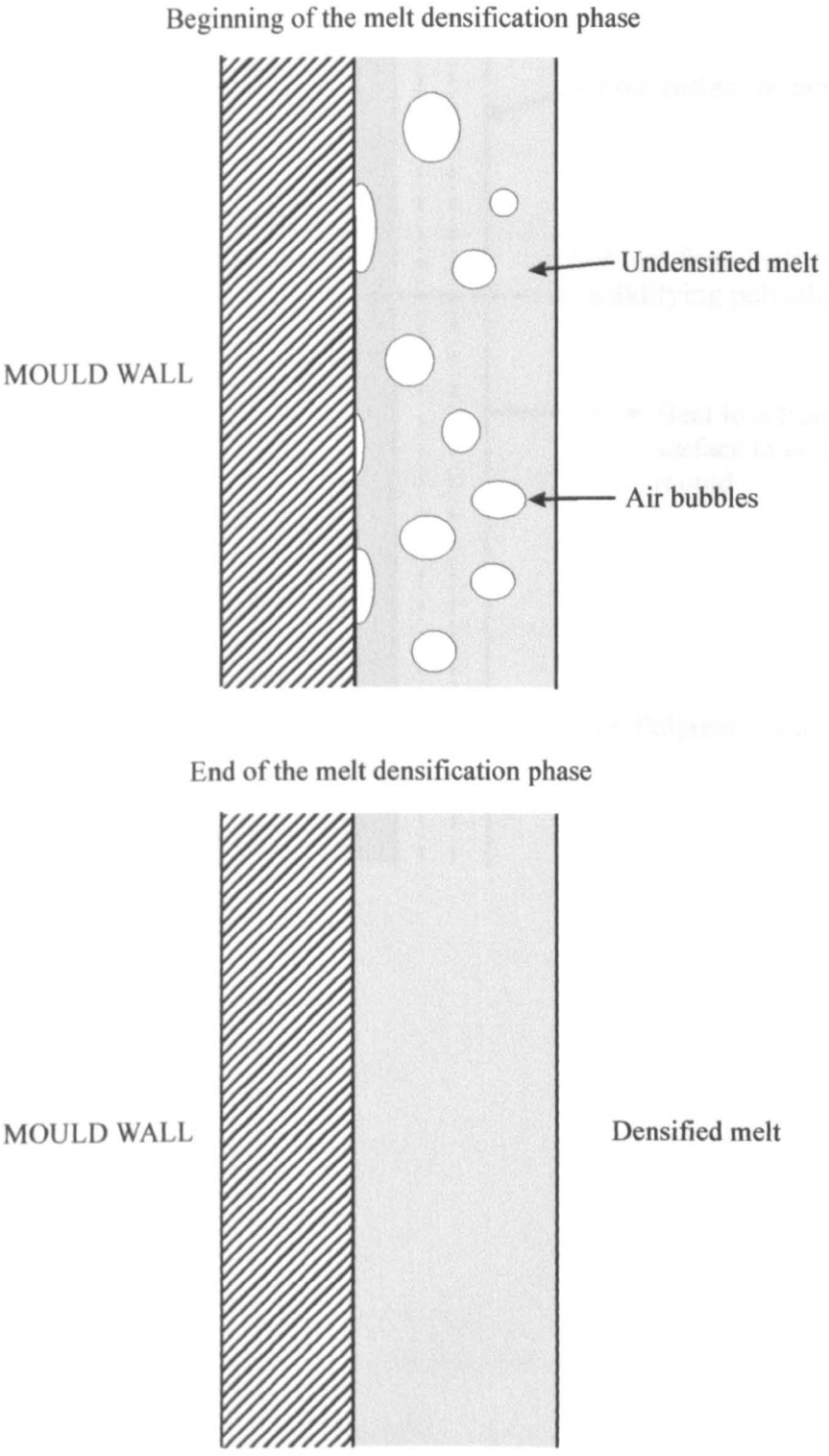

FIGURE 56

HEAT TRANSFER DURING THE COOLING CYCLE

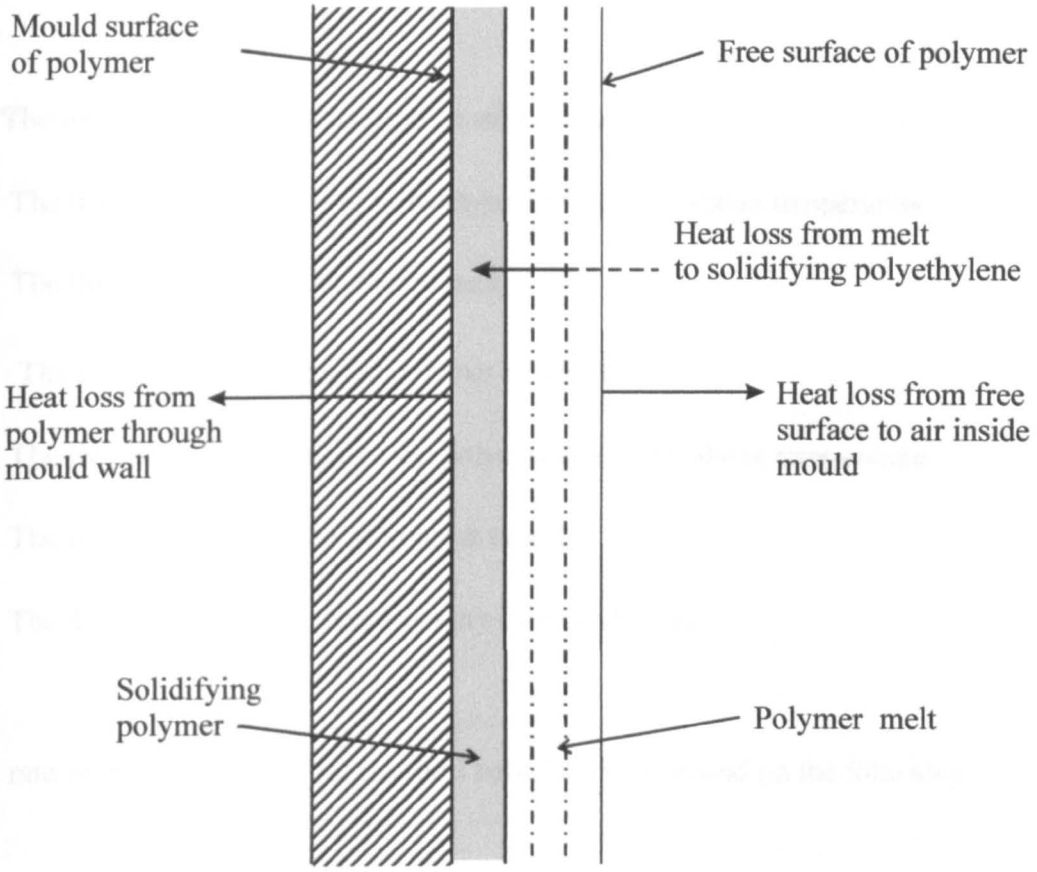

polymer melt to the air in the mould will be very small and can be ignored.

Basic heat transfer considerations show the rate of heat transfer across the second boundary will be determined by the following factors:

1. The temperature of the polyethylene melt at time **t**.
2. The thermal conductivity of polyethylene melt at the above temperature.
3. The thickness of the polyethylene melt at time **t**.
4. The temperature of the solid polymer at time **t**.
5. The thermal conductivity of solid polyethylene at the above temperature.
6. The thickness of the solid polymer at time **t**.
7. The density and specific heat capacity of polyethylene.

The rate of heat transfer across the third boundary will depend on the following:

1. The thermal conductivity of the mould.
2. The thickness of the mould wall.
3. The convective heat transfer coefficient.
4. The specific heat capacity of the mould.
5. The density of the mould.

Throne [236] has analysed some of the factors that influence the rate of heat transfer or the rate of cooling of an amorphous polymer in a metal mould. To simplify the

arithmetic, the following assumptions were made; the inner mould surface is at the same temperature as the outer mould surface, regardless of the mould thickness and the moulding wall thickness is large compared to the advancing 'freezing' front. These assumptions enable the use of an approximate method (known as the Goodman method) to solve the transient heat conduction equation that describes heat transfer from the molten polymer, discussed as follows:

The rate of heat loss from the mould

A heat balance equation for the mould material is derived by considering the change in the internal energy of the mould [237].

At **t = 0**, the mould at an initial of **T** is moved into an environment at an ambient temperature **T**. The heat balance becomes:

The change in internal energy of the mould during time dt	=	The net heat flow out of the mould into the environment during time dt

$$\rho_m \, c_m \, L \, T_s = h (T_s - T_\infty) \, dt \qquad \text{Equation 5.3.2.1.}$$

Where ρ_m = mould surface temperature

c_m = specific heat capacity of mould material

L = mould wall thickness

k_m = thermal conductivity of mould material

h = convective heat transfer coefficient

$\delta = \frac{k_m}{\rho_m c_m}$ = thermal diffusivity of mould

T_s = mould surface temperature

Rearrangement and integration of the above equation gives:

$$\frac{T_0 - T_s}{T_0 - T_\infty} = 1 - \exp^{-(h_c \propto_m / L\, k_m)\, t} \qquad \text{Equation 5.3.2.2.}$$

Where T_0 = initial mould temperaure

This equation is similar to the one describing the heating of the mould in Section 5.3.1.1, and is a classic first-order system response to a step change in the environmental parameter. This response is a strong function of the rate at which heat is removed from the mould surface, the thermal diffusivity and conductivity of the mould material, and the thickness of the mould wall. Thus for a given mould, the rate of heat loss from the mould will depend primarily on the heat transfer coefficient.

The rate of heat loss from the polymer melt

The transient heat transfer equation to describe the temperature profile in the polymer melt is established by Throne [236] as:

$$\frac{\partial}{\partial x}\left(k_p \frac{\partial T}{\partial x} \right) = \rho_p c_p \frac{\partial T}{\partial t} \qquad \text{Equation 5.3.2.3.}$$

Where k_p = thermal conductivity of polymer

ρ_p = polymer density

c_p = specific heat capacity of the polymer

According to Goodman [256], the temperature profile in the polymer melt can be approximated by:

$$\frac{T_0 - T}{T_0 - T_s} = (1 - x/\delta)^3 \qquad \text{Equation 5.3.2.4.}$$

Where x = distance into melt, measured from mould surface

δ = thermal penetration thickness

The thermal penetration thickness is obtained by substitution, with the appropriate boundary conditions. This is done in detail in Reference [236]. The form $\delta(t)$ for the penetration thickness, for a time dependent mould surface temperature $T_s(t)$ is given as:

$$\delta(t) = \frac{2\sqrt{6\,\alpha_p}}{(T_0 - T_s)} \left(\int_0^t (T_0 - T_s)^2 \, dt \right)^{1/2} \qquad \text{Equation 5.3.2.5.}$$

Where $\alpha_p = k_p / \rho_p c_p$ = the polymer diffusivity

The time dependent mould surface temperature is given by Equation 5.3.2.2. Substituting

this into Equation 5.3.2.5, the following expression for $\delta(t)$ is obtained:

$$\delta(t) = 2L\sqrt{\frac{6\alpha_s}{(Bi)\alpha_m}} \times \frac{1}{(1-e^{-vt})} \qquad \text{Equation 5.3.2.6.}$$

$$\times \left[vt - 2(1-e^{-vt}) + \tfrac{1}{2}(1-e^{-2vt}) \right]^{\frac{1}{2}}$$

where $Bi = hL / k_m$ the Biot number, representing the ratio of the heat transfer resistance in the convective fluid next to the mould surface to the resistance to conduction heat transfer within the mould material and $v = [h_c \alpha_m / k_m L]$.

Thus the above equation suggests that the penetration thickness is strong function of the ratios of the thermal diffusivities of the mould and the polymer.

5.3.3. Other heat transfer models

The first attempt at modelling heat transfer in the rotational moulding process was made in 1972 by Rao and Throne [55]. Since then several studies have been reported on improving the model [202, 237, 238, 239, 240]. These are summarised by Tiang and Bellehumer [191] and reported as follows.

Crawford and Nugent [203, 204] have developed a numerical simulation of the process. Improvement on this model by considering internal heating and cooling has been made by Sun and Crawford [238]. Bawiskar and White [239] have proposed an analytical

expression for heat transfer across the increasing melt depth in the heating cycle. Gogos et al [241] have presented the solution for heat transfer which uses lumped parameter for the heating cycle.

All the above heat transfer models report generally good correlation between predicted values and experimental data. However, Tiang and Bellehumer [191] report that these models are restricted to simple mould geometry, and do not allow the prediction of the final part porosity. The authors go on to propose a heat transfer model for the complete heating cycle, including the melt densification process. The model is based on the model proposed by Gogos et al [241]. To simplify the model, the heating cycle is divided into three phases. Phase I is the heating of the mould and polymer to the polymer melting point (T_m)

The time t_I required for the mould temperature T to reach the polymer melting point T_m is approximated as:

$$t_I = \frac{\rho_m c_m \delta_m}{h_m} \ln \left(\frac{T_0 - T_m}{T_0 - T_a} \right) \qquad \text{Equation 5.3.3.1.}$$

And the polymer powder temperature T_i at that time is given by:

$$T_i = T_0 - \frac{(T_0 - T_m)}{(K - 1)} \left[K - (T_0 - T_s)^{K-1} \right] \qquad \text{Equation 5.3.3.2.}$$

with $$K = \frac{h_i}{h_o} \frac{\rho_m c_m \delta_m}{\rho_p c_p \delta_p}$$

Where T_0 = Oven temp.

T_a = Air temp. inside mould

h_0 = Oven convective heat transfer coefficient

h_i = Powder convective heat transfer coefficient

ρ = Density

c = Heat capacity

δ = Thickness

Subscript m refers to mould

Subscript p refers to polymer

Phase II, the polymer fusion and melting phase, is modelled by considering the conservation of energy within the mould and the adjacent melt layer and is given by:

$$(\rho_m c_m \delta_m + \tfrac{1}{2} \rho_p c_p \delta_{pl}) \frac{dT}{dt} + \left(\tfrac{1}{2} \rho_p c_p \frac{d\delta_{pl}}{dt} + \frac{k_p}{\delta_{pl}} \right)(T - T_m) = h_o (T_o - T)$$

Equation 5.3.3.3.

And the rate of polymer melt deposition $\frac{d\delta_{pl}}{dt}$ is given by:

$$\frac{k_p}{\delta_{pl}} (T - T_m) = \rho_p \frac{d\delta_{pl}}{dt} [c_p (T_m - T_i) + \Delta H]$$

Equation 5.3.3.4.

$$+ h_i (T_m - T_i)$$

While the heat balance relation for the powder is:

$$\rho_p c_p (\delta_p - \delta_{pl}) \frac{dT_i}{dt} = h_i (T_m - T_i)$$ Equation 5.3.3.5.

Where δ_{pl} = melt deposition thickness

k_p = polymer melt conductivity

ΔH = polymer heat of fusion

Phase III, the final melt densification phase consists of further heating of the mould, polymer melt, and air inside the mould. The conservation of energy within the mould, polymer melt and air inside the mould is given by:

$$\rho_m c_m \delta_m \frac{dT}{dt} = h_o (T_o - T) - \frac{k_p}{\delta_p} (T - T_{p\delta})$$ Equation 5.3.3.6.

$$\rho_p c_p \delta_p \frac{dT_p}{dt} = \frac{k_p}{\delta_p} (T - T_{p\delta})$$ Equation 5.3.3.7.

$$\rho_a c_a \delta_a \frac{dT_a}{dt} = h_a (T_{p\delta} - T_a)$$ Equation 5.3.3.8.

Where $T_{p\delta}$ is the temperature at polymer melt front and the subscript **a** refers to air inside mould.

The equations describing polymer fusion and melt densification are solved numerically. The discrete solutions generated for mould temperature T, melt deposition δ_{pl}, powder temperature T_i, polymer melt temperature T_p and air temperature inside the mould T_a are correlated and expressed as continuous polynomial equations.

5.4. Crystallinity in rotational mouldings

5.4.1. Spherulitic morphology

Microscopic examination of the moulded polyethylene in Figure 45 (Section 4.4.1) reveals that unique microstructures are present in rotational mouldings. In this study, for linear low density polyethylene, this microstructure is observed to be spherulitic.

The spherulite is now recognised as an important unit of polymer morphology. The following discussion of spherulitic growth attempts to explain why the structure, as observed in this study, is unique to rotational moulding (when compared to other moulding techniques).

Spherulites contain fibrous sub units. It is now believed that fibrillar development is a fundamental process in spherulitic growth, with the fibrils extending radially out from a central nucleus, see Figure 57.

In rapidly grown structures such those obtained by fast cooling, Figure 45A (Section 4.4.1), the fibrils are usually of microscopic dimensions and so cannot be resolved.

During slow spherulitic growth, Figure 45B, the fibrils grow to between 10^{-8} and 10^{-6} m in cross sectional area. When fibrils reach these dimensions, it is very likely that they consist of aggregates of smaller, more fundamental microfibrils containing crystallites. Observations have shown that the crystallites are lamellar in structure. In highly crystalline samples the fibrils may be the crystallites having the expected dimensions, see Table 13.

The fibrils are punctuated along the length with defects that contribute to the amorphous content. However the 'real' amorphous regions are formed between the growing fibrils and spherulitic boundaries.

To summarise, polyethylene samples containing large spherulites have smaller amorphous regions between the spherulites, and therefore have a higher degree of crystallinity. Similarly, fast cooled polymers have smaller spherulites with bigger amorphous regions in between, and hence a lower degree of crystallinity.

An important feature of fibrillar development is that it involves branching and is the

FIGURE 57

STAGES IN THE DEVELOPMENT OF A SPHERULITE, AS PROPOSED BY BERNAUER AND SHOWING THE RADIATING FIBRILS

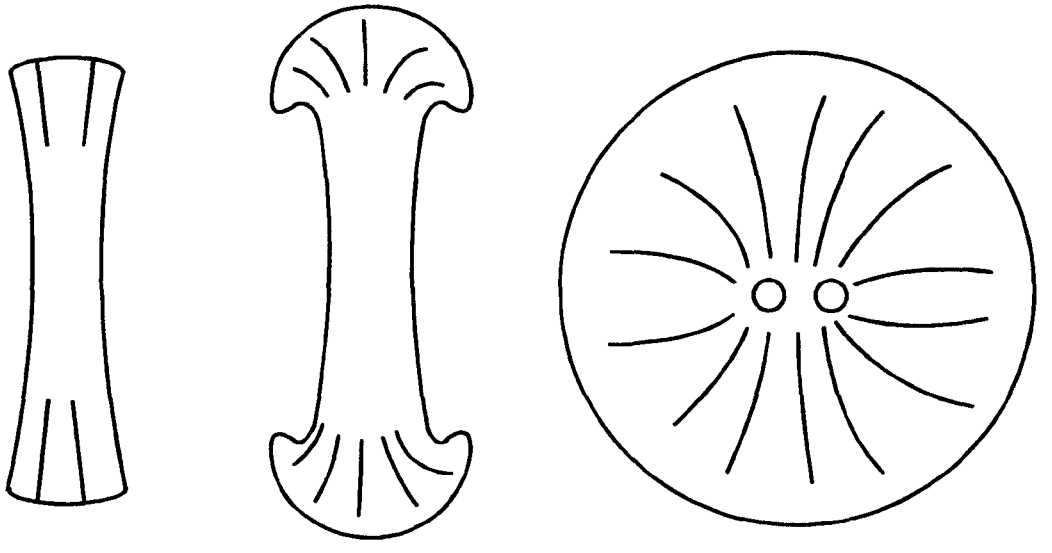

TABLE 13

APPROXIMATE DIMENSIONS OF STRUCTURAL UNITS IN POLYMERS

Spherulite (m)	Fibril (cross section) (m)	Crystallite (m)	Single Crystal (m)
$> 10^{-6}$	$10^{-8} - 10^{-6}$	5×10^{-9} - 20×10^{-9}	$10^{-8} - 10^{-6}$

process by which space is filled as the spherulite grows. During growth, the branching fibrils often twist, see Figure 58. In some structures, the twisting can take place co-operatively to produce periodic variations in the refractive index, which give rise to the ring structure observed in Figure 45B (Section 4.4.1). To date, the reason for the twisting is believed to be unknown.

Results indicate that the spherulitic structure in rotational mouldings is unique to the process.

Examination of photomicrographs in Figure 45 (Section 4.4.1), also show the spherulites are free from orientation; spherulitic growth appears to be equal in all directions. This is because during a moulding cycle, the mould rotation speeds are kept low, and hence the melt experiences only very low shear rates. There is no shearing of the melt or orientation of the molecules in any particular direction.

Apart from the effects of shear, other factors that affect spherulitic development have been reported.

In 1945, Bunn and Alcock [114] reported the first study of spherulitic development in polyethylene. This report also includes the effect of cooling rate on growth.

Other factors widely believed to affect spherulitic size in a given polymer are molecular weight, percentage crystallinity, the degree of branching, thermal history and mechanical working of the melt. The effects of these factors on spherulitic size can be summarised as

FIGURE 58

SCHEMATIC REPRESENTATION OF A POSSIBLE MODEL FOR TWISTED LAMELLAE IN SPHERUTIC POLYETHYLENE SHOWING CHAIN FIELDS ANDINTERCRYSTALLINE LINKS

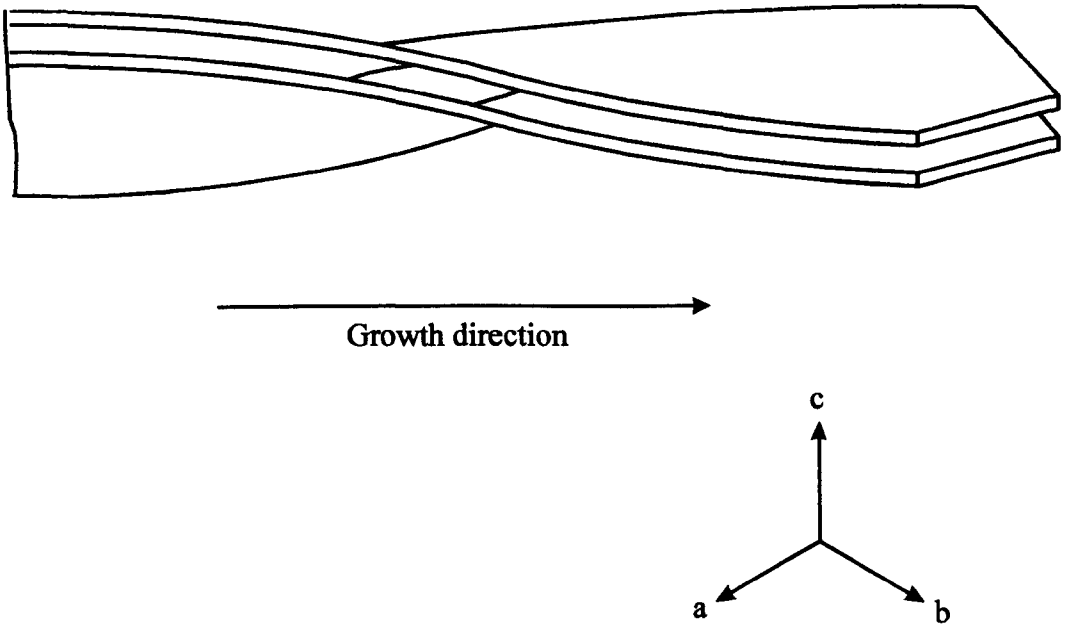

follows:

1. Slow cooling of melt through the melt temperature range produces large spherulites while sudden quenching to low temperatures results in smaller spherulites.
2. Polyethylenes with the least branching are observed to form the largest spherulites.
3. In linear polyethylene, generally, spherulitic size is found to increase with increasing molecular weight.
4. Cramez et al [161] report the addition of nucleating additives such as pigments results in a finer microstructure – many spherulites of small size.
5. Mechanical working of the melt (not relevant to rotational moulding) followed by shock cooling results in very small spherulitic size.

Also, if the processing temperatures are high enough to cause degradation of the polymer, then spherulites that grow freely at the free surface are replaced by a non-spherulitic or a transcrystalline texture, depending on the extent of the degradation.

Generally, spherulitic structure in low weight materials has been more extensively studied than in high molecular weight polymers. This is because although spherulites are present in the majority of semi crystalline polymers, the size is not always large enough to be resolvable in the optical microscope. No inherent upper limit on the size of spherulites has yet been observed [115].

The study of spherulitic structure is necessary because it has important implications for the mechanical properties of the moulding. Large spherulites are believed to act as stress

concentrators, inducing impact type fractures in the moulded polymer. The degree of crystallinity has also been shown to affect the mechanical properties. This is discussed in Section 5.5.

5.4.2. Degree of crystallinity

5.4.2.1. Effect of crystallisation temperature and cooling rate

As already noted, the photomicrograph of slow cooled polyethylene in Figure 45 (Section 4.4.1), shows large, well defined spherulites. The discussion in Section 5.4.1 would indicate that these samples contain a higher degree of crystallinity. Density measurements reported in Table 4 (Section 4.4.2). confirm this assumption; the average density of the slow cooled samples is measured higher than that of the fast cooled samples.

The degree of crystallinity in the processed polymer, in terms of the crystallisation process and the degree of supercooling, is explained as follows.

When a polymer melt is cooled to any temperature below its melt point, the melt is said to be supercooled. The lower the temperature the melt is cooled to below its melting point, the greater the degree of supercooling.

When the polyethylene melt is supercooled, molecules in the melt become aligned to form small ordered regions known as nuclei. This is nucleation and is the first step in the

crystallisation process. The second stage of crystallisation is when the nuclei grow by the addition of further polymer chains. The detailed study of crystallisation kinetics is reported in many standard textbooks.

In rotational moulding, in the heating cycle, the polymer is heated to a temperature above its melt temperature. The melt is said to be supercooled. The subsequent slow cooling of the polymer melt in the cooling cycle means that the polyethylene is kept at the super cooled temperature for a longer time. This allows more time for an ordered crystalline structure to develop, resulting in large spherulitic size with a higher degree of crystallinity.

In contrast, when the polymer melt is fast cooled in the cooling cycle, the polyethylene is only kept at the supercooled temperature for a short time, and not long enough for an ordered crystalline structure to form. This gives rise to the largely undefined type of crystalline structure observed in Figure 45A (Section 4.4.1). This has a lower degree of crystallinity as indicated by the lower density measurements reported in Table 4 (Section 4.4.2.1).

Thus the results of this study show how the temperature in the heating cycle, and the rate at which the polymer is cooled in the cooling cycle of the rotational moulding process, affects the morphology and the degree of crystallinity in the processed polymer.

The results show that the degree of supercooling and the rate at which the polymer melt is cooled, can affect the spherulitic size and the degree of crystallinity in the polymer.

These effects are summarised in Figure 59. At the end of the heating cycle, the polymer is at some temperature below the melting point (depending on the oven set temperature and the length of the heating cycle.) This is the crystallisation temperature. At low crystallisation temperatures, the nucleation rates are high. However, growth of nuclei at low temperatures is restricted and results in smaller spherulitic size and a lower degree of crystallinity in the polymer.

At high crystallisation temperatures the nucleation rates are slow. High melt temperatures reduce the viscosity of the melt, allowing greater mobility in the polymer chains. This encourages growth of the nuclei, resulting in larger spherulitic size and a greater degree of crystallinity in the polymer.

The rate of cooling in the polymer melt has a similar effect. A fast cooling rate reduces the crystallisation temperature, resulting in smaller spherulitic size and a lower degree of crystallinity. This effect is widely reported.

Similarly, a slow cooling rate has the same effect as a high crystallisation temperature.

With respect to rotational moulding, the process variables affecting crystallinity and morphology of the polymer can be summarised as; the length of the heating cycle, oven set temperature, rate of cooling of the polymer melt and the type of cooling medium.

FIGURE 59

EFFECT OF CRYSTALLINITY TEMPERATURE AND COOLING RATE ON THE DEGREE OF CRYSTALLINITY

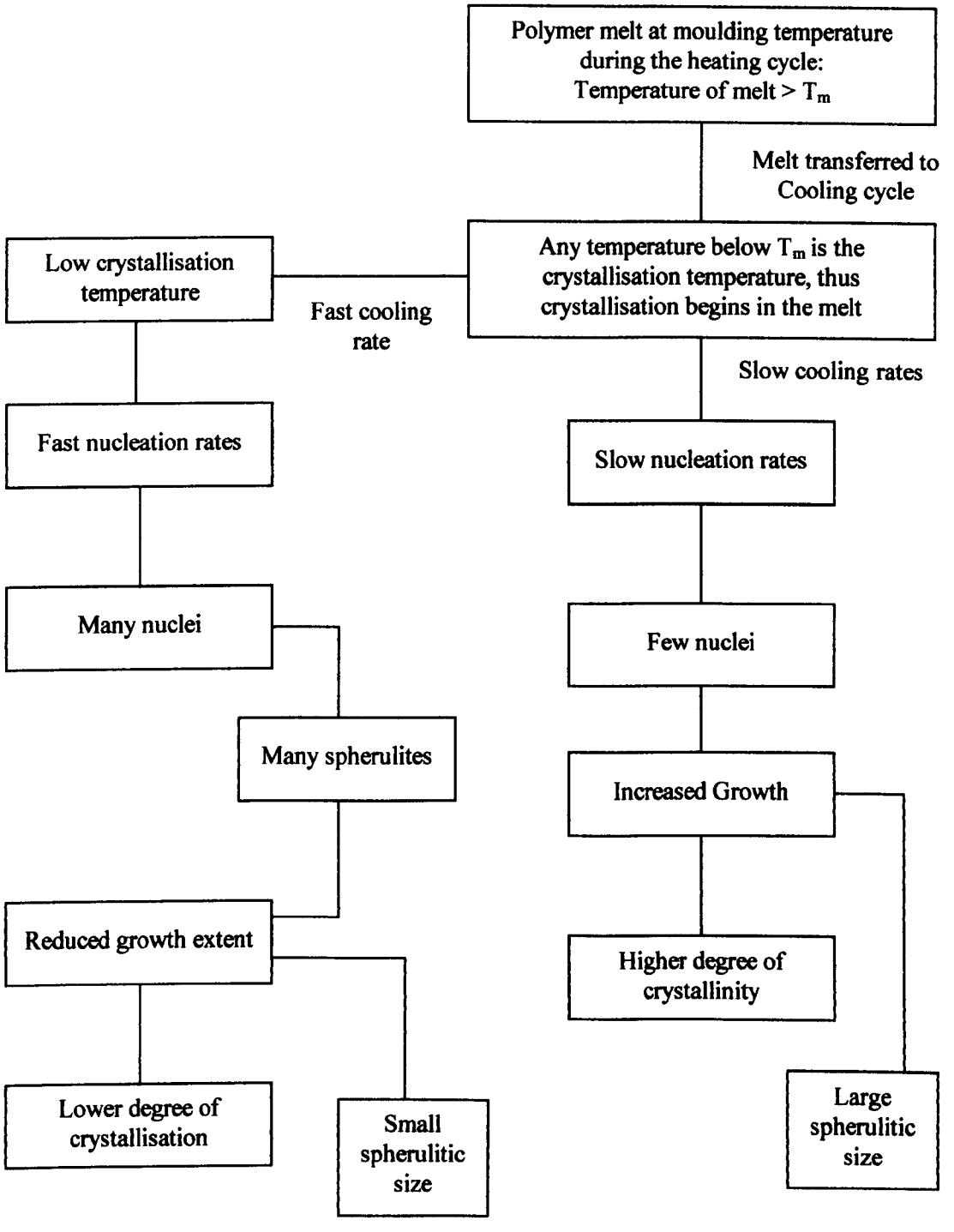

5.4.2.2. Variation of crystallinity with moulding surface

The results of this study are in line with the discussion in Section 5.4.2.1. The average density of samples taken from the free surface of the moulding, is higher than that of the mould surface. This indicates a higher degree of crystallinity on the free surface, compared to the mould surface of the moulding.

The free surface of the moulding cools by heat transfer to the air inside the mould, and by heat transfer through the melt. The mould surface cools by heat transfer out through the mould wall, see Figure 56 (Section 5.3.2).

However, because of the low thermal conductivity of air and the polymer melt, heat transfer from the free surface will be slow. Compared to this, heat transfer from the mould surface will be faster because of the high thermal conductivity of the metal mould, and the good thermal contact between the polymer and the mould wall. The use of release agents further improves the contact.

Thus the density measurement results are as expected, and in agreement with Kline [106]. The lower degree of crystallinity on the mould surface, is the result of a faster cooling rate of this surface compared to the free surface.

Callan et al [216] have measured a crystallinity gradient through the thickness of a fast cooled polyethylene moulding. The mould surface was typically found to have 33.9% crystallinity as opposed to 42.6% for the middle and 46.4 % for the free surface.

Soderquist [29] reports a higher impact resistance at the mould surface compared to the free surface. This is explained in terms of a greater degradation at the mould surface. However, reduction in impact resistance has been related to an increase in crystallinity. The larger spherulites are thought to act as stress concentrators reducing the impact strength of the polymer.

Callan et al [216] report that fast cooling reduces the degree of crystallinity and increases the amorphous regions, which offer a greater resistance to impact force. Soderquist [29] recommends the addition of internal cooling to the normal external cooling of the polymer, in order to minimise the crystallinity in the free surface of the moulding. This has the added advantage of reducing warpage.

Finally, Callan et al [216] have observed a higher degree of crystallinity in the corner regions of a moulding, compared to the flat sides. This is because the corners are thicker and cool slower than the rest of the moulding.

Cramez et al [161] have reported the changes in microstructure in polyethylene when the polymer is overheated. As the temperature inside the mould was increased to above a critical value, the morphology at the inner mould surface was observed to change. The size and perfection of the spherulites reduced, and an inward growing layer of columnar type structure started to appear. At very high temperatures, the spherulitic structure disappears completely on the inner surface and is replaced by a dark ribbon of material without any texture. Fluorescence microscopy that detects double bands in the polymer chains, showed that the altered microstructure was due to the thermo-oxidative

degradation of the polymer.

Godinho et al [185] have similarly observed a difference in microstructure and texture between the inner free surface and the outer mould surface.

5.5. Effect of processing conditions on tensile properties

Du Pont [53] report that the tensile strength of the moulding at the end of the fusion phase will be low, as the polymer is not fully densified. This is supported by McDonagh [5], who concludes that the presence of bubbles lowers the tensile strength of the polymer.

However, results of this study reported in Figure 46 and Figure 47 (Section 4.5) show that the polymer achieves over 90% of its final yield stress at the end of the fusion phase. Continued heating of the polymer to the end of the melt densification phase increases the yield stress by only another 10%.

The study of the effect of the heating cycle on the percentage elongation, Figure 48 (Section 4.5), shows that at the start of the melt densification phase (heating cycle of 5 minutes), when there is a maximum number of bubbles in the polymer, the percentage elongation has a minimum value. This is explained by the bubbles acting as stress concentrators during a tensile load, Figure 60, causing cracks to appear and spread during the load, thereby reducing the elongation at break.

FIGURE 60

EFFECT OF BUBBLES ON ELONGATION OF POLYETHYLENE UNDER A TENSILE STRESS

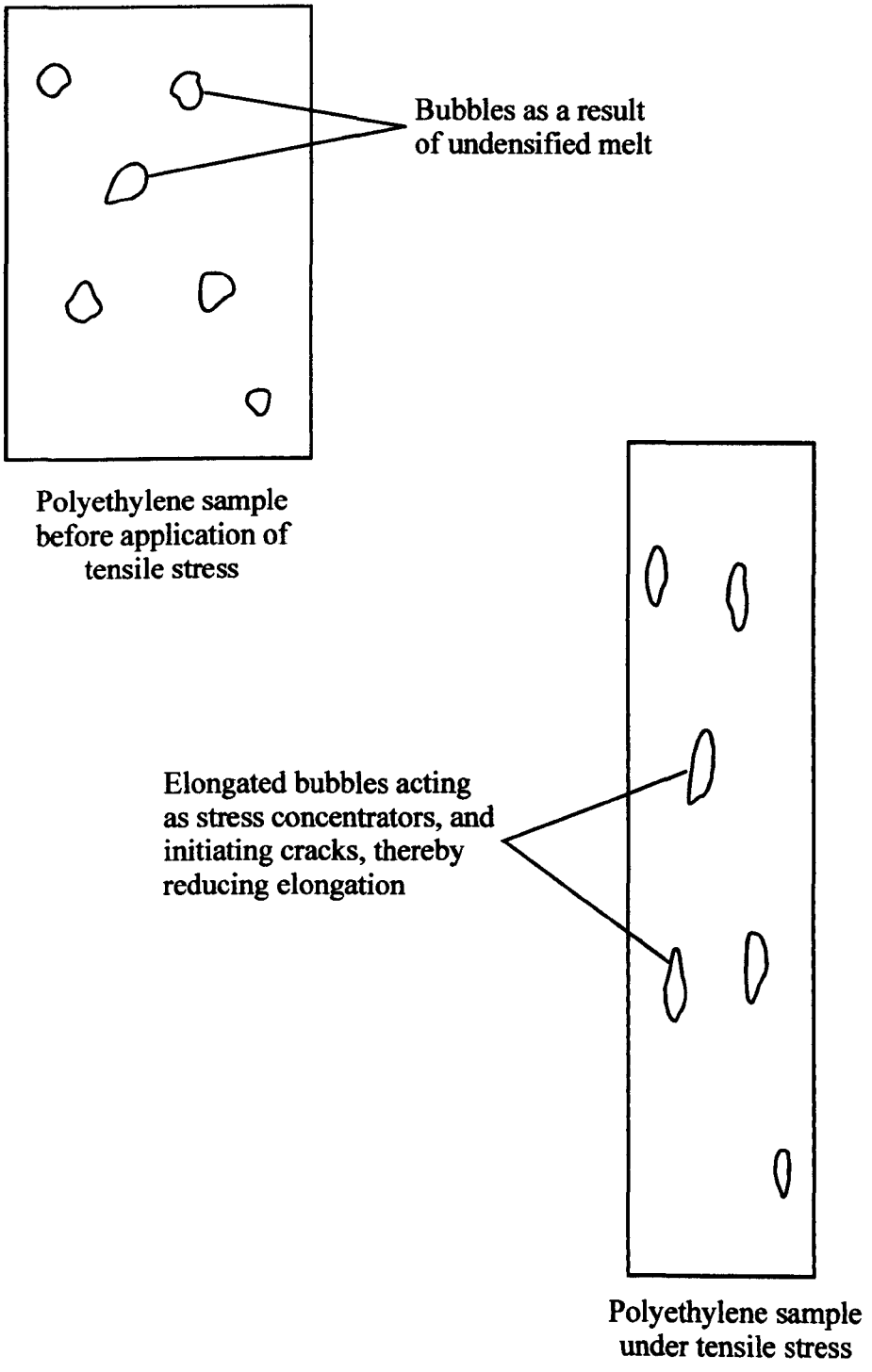

As expected, the elongation at break has a maximum value at end of the melt densification phase, when the bubbles have dissipated.

At high rates of strain, the bubbles can also be assumed to act as stress concentrators to initiate impact type failures. This is confirmed by Rees [56], who reports that the impact strength of both high and low density polyethylene increases as bubbles are eliminated from the wall of the moulding.

The increase in the yield stress of rotational mouldings with increasing degree of polymer fusion reported, in Figure 46 (Section 4.5), is explained by consideration of the fusion mechanism of polymer particles. Discussion in Section 5.2.1 suggests that in the processed polymer, the length of the fusion phase determines the extent to which interparticle boundaries are eliminated. At short heating cycles particle fusion is incomplete, and the boundaries between the particles are therefore weak, and can act as weak points during a load bearing process. The effect of this is to reduce the yield stress of the polymer. This also explains why the elongation at break during fusion is low.

The increase in tensile strength with increasing heating time is also reported by Liu and Lai [150], although the heating temperature (surprisingly), is reported to be relatively insignificant. The most significant parameter to affect the tensile properties found by the authors is the particle size. The cooling method is also reported to affect the tensile strength.

The large variation in the percentage elongation of samples during fusion, can be

explained by the large variation in the number of bubbles in the test samples.

After densification, the large variation in percentage elongation can be explained by the variation in the extent to which strain hardening occurs in the polymer during the tensile load.

Strain hardening is observed after the tensile test piece has passed the yield point. The cross sectional area starts to decrease more rapidly at one particular point along the gauge length, as the 'neck' starts to form. The nominal stress is observed to fall after yield and settles at a constant value as the neck extends along the specimen. Eventually the whole specimen is necked, strain hardening occurs and the stress rises until the sample eventually fractures. The process whereby the neck extends is known as cold drawing. Cold drawing was originally attributed to local heating of the specimen by the energy expended during deformation. However, detailed measurements have shown that a neck can form even at very low strain rates, when the heat is easily dissipated.

5.5.1. Isotropy in rotational mouldings

Results reported in Section 4.5.1, show that there is no anisotropy of tensile properties in rotational mouldings, indicating an absence of molecular orientation in the polymer. These results support the observations made of the spherulitic structures in Section 4.4. However, the disadvantage of unorientated polymers, is that the elastic modulus and stress at break can be low, since the strain in the unorientated polymer is due largely to relative movements of the polymer chains, rather than the stretching of the polymer

chains themselves, as in orientated polymers. Orientation or alignment of polymer chains increases these forces, and the elastic modulus and tensile strength are observed to increase significantly. The effects of orientation can be seen in Figure 61.

Compared with an isotropic moulding, the modulus is increased when tensile stresses is applied along the principle direction of orientation or melt flow, and the stress is decreased perpendicular to the direction. Certain shear moduli are also decreased and the elastic modulus, the stiffness and toughness of the polymer may also be affected. Advantage is taken of orientation in the production of orientated synthetic fibres and films. In most cases, however, orientation is less pronounced and an unwanted consequence of fabrication.

Godinho et al [185] suggests that stresses can be set up in rotational moulding during the cooling stage, due to the temperature differentials across the relatively thick walls which can be used for some rotationally moulded products. A study to measure the differences in properties across the wall thickness of rotationally moulded polyethylene is reported. It was found that the tensile strength varied by typically 10% and the stress modulus by up to 15% across the moulding wall.

Fast cooling of the moulding can also generate internal stresses in the wall, resulting in warpage or shrinking.

An alternative method of obtaining rapid and uniform cooling, is to use a combination of external and internal cooling. Cooling the polymer from both sides not only increases the

FIGURE 61

VARIATION OF STRENGTH WITH DIRECTION OF ORIENTATION OF MOLECULES

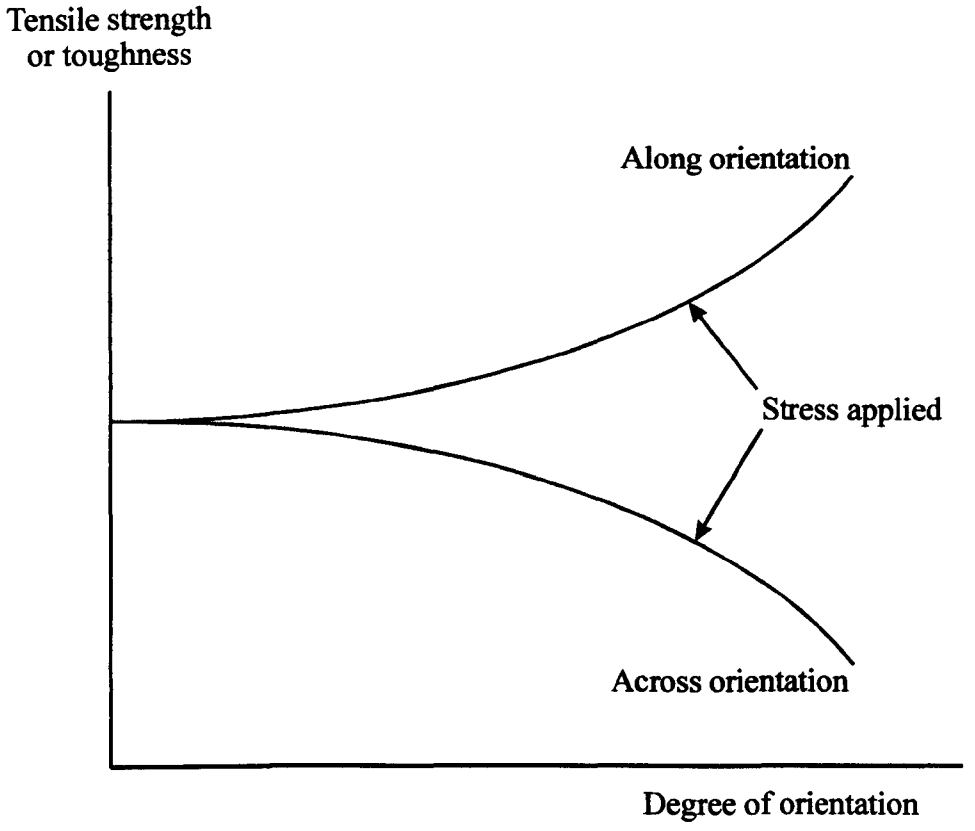

rate, thereby improving the physical properties, but gives better dimensional control by promoting uniform shrinkage.

Internal cooling is achieved by introducing chilled air or water into the mould through the machine arm [23, 24] and is also important in minimising oxidation in polymers such as polycarbonate, polypropylene and Nylon 6 [25]. The technique has not been widely applied because of its potential difficulties [23, 24]. With water cooling, there is the possibility of steam generation as the water is heated, resulting in internal pressure that can damage the mould. However, internal pressure when properly controlled, holds the moulding against the mould and improves the heat transfer from the moulding as it is cooling [23].

Experiments have been performed using liquid carbon dioxide as the internal cooling medium. The high pressure generated as the liquid vapourises inside the mould, appear to be excessive for most moulds in use and the method is not recommended at present [24].

5.6. Principal sources of error

The main source of error in the heating cycle investigations, comes from the temperature of circulating air in the oven. Figure 36 (Section 4.3.1) shows how the measured oven temperature does not correlate with the temperature set, and can be 30° C lower and up to 70° C higher than the set temperature. This is due to insufficient control over the temperature of the gas flame.

Errors in the mould induction time investigations are due to heat losses from the mould during the temperature measurement, from not allowing the mould to rotate during the measurement and from a lack of good thermal contact between the thermocouple junction and mould wall.

In the continuous temperature measurement, the thermocouple bead was attached to the surface of the mould. The top of bead is exposed to the air in the oven, and therefore records not only the mould temperature, but also the air temperature in the oven.

In the determination of the length of the heating cycle of mouldings, errors come from the accuracy of the machine timer. The smallest time interval that could be measured was one minute.

In the investigation of the effect of fusion time on the yield stress, the main source of error was the thickness measurement of the tensile test samples. For fusion times between one and three minutes, partially sintered polymer attached to the fused polymer making thickness measurement difficult, see Figure 39 (Section 4.3.2).

In completely fused moulding samples, accurate thickness measurement was made difficult by uneven moulding surface due to undensified melt, see Figure 39.

Throne [197] notes that the funnel test for measuring flow properties of the polymer, does not take into account the effects of air and mould temperature on the flow or MFI of polymer. In addition, the melt index test is carried out under some shear stress and the

shear flow experienced by the polymer melt is significantly higher than during the rotational moulding process.

Finally, errors were possible in the investigation of the effects of heating temperature on density measurements. The length of the heating cycle for the oven set temperature of 440° C was set at three minutes, and twelve minutes for 220° C. For greater accuracy, the length of the heating cycle should have been kept constant for both mouldings. However, this proved to be impossible as previous results on the study of the heating cycle had shown that at an oven set temperature of 220° C, a minimum heating cycle of twelve minutes was necessary for complete fusion and densification. A shorter heating time would result in an undensified melt with air bubbles in the moulding that would affect the density measurements. The alternative was to heat the 440° C temperature mouldings for twelve minutes. However at this temperature, a heating cycle longer than three minutes resulted in the degradation of the polymer.

5.7. Conclusions

5.7.1. Physical properties of the polymer

a) The flow properties of the polymer are improved by increasing the size distribution of the particles.

b) Grinding the polymer to a very small particle size (below 150 μm) is an advantage only when hairs and tails, present in a greater number of smaller particles, are

removed.

5.7.2. Heating cycle

a) Determination of the heating cycle of a moulding by visual examination, as used by the rotational moulding industry, is accurate.

b) The heating cycle can be divided into three phases; mould induction, polymer fusion and melt densification.

The three phases are clearly distinguishable and can be defined in terms of mould heating, sintering of polymer particles and densification of the melt.

The length of each phase of the heating cycle is determined by the oven set temperature. For the test moulding used in this study, at the lower oven set temperature of 220° C, the longest and hence the rate determining step of the heating cycle is the melt densification stage. At the higher oven set temperature of 440° C, the longest phase changes to the polymer fusion phase.

Increasing the oven set temperature reduces the length of each of the phase of the heating cycle. However, the greatest effect is on the melt densification stage. For the test moulding used, 330° C is a critical oven set temperature when the melt densification time is reduced to 1 ± 0.5 minute. This is not reduced by any further increase in the oven set temperature.

c) Contrary to reports [1, 5] the relationship between the moulding wall thickness and the length of the heating cycle is not perfectly linear.

d) The mould induction time can be predicted from Equation 5.3.1.1.3, established by Throne and Rao [55] to model the heating of the mould during processing.

e) The fusion time of the moulding is directly proportional to the mass of polymer.

f) The rate of polymer fusion increases directly with increasing oven set temperature.

g) Particle boundaries can be completely eliminated during the fusion phase. This is contrary to reports by Duncan and Zimmerman [1] who state complete boundary elimination is possible only in high density polyethylene, not low density polyethylene.

h) As predicted by Frenkel in Equation 5.2.1.3.1, the melt densification phase is time controlled at constant temperature, and temperature controlled at constant time.

i) The melt densification time decreases with increasing polymer mass.

j) The end of the melt densification phase can be checked by apparent density measurements.

5.7.3. Crystallinity

a) Spherulitic size in the solid polymer is affected by the rate of cooling of the polymer

melt. Fast cooling rates result in small spherulitic size; slower rates of cooling increase spherulitic size.

b) Hence cooling rates of polymer melt affect the degree of crystallinity in the solid polymer. A fast cooled polymer has a lower degree of crystallinity compared to a slow cooled polymer.

c) In addition to the cooling rate, the degree of crystallinity is also affected by the oven or crystallisation temperature; the degree of crystallinity increases with increasing oven temperature during the heating cycle.

d) Finally the degree of crystallinity is affected by the moulding surface. The mould surface has a lower degree of crystallinity compared to the free surface.

5.7.4. Tensile properties

a) Yield stress increases with increasing fusion time and reaches a maximum at the start of the melt densification phase.

b) Elongation at break passes through an optimal level, with the maximum value at the end of the fusion phase.

c) Mouldings at the higher oven set temperature of 440° C have slightly improved yield stress. However, the elongation at break is reduced.

d) Rotational mouldings are isotropic with regard to tensile properties.

5.7.5. Thermal properties

a) Thermal conductivity of solid polyethylene decreases with increasing temperature.

b) At constant temperature, the thermal conductivity of the undensified solid decreases with decreasing numbers of bubbles in the polymer.

c) Thermal conductivity of polyethylene powder is lower than that of the fully densified solid.

5.8. Further work

Commercially, the results of the heating cycle investigations are of great significance. The heating cycle is a critical aspect of the rotational moulding process, affecting capital and operating costs of equipment, production rates and product quality.

Short heating cycles increase production rates, and the reduction in the heating cycle by increasing the oven set temperature is of commercial advantage to the rotational moulding industry.

Higher heating temperatures increase the heat transfer rates to the polymer, allowing

powders of larger particle size to be used. As larger particles are easier and cheaper to grind, this offers economic advantages. Further work could be carried out to determine the largest particle size distribution that could be used at higher temperatures, without impacting product quality.

Work on the mechanical properties of the moulding, showed how elongation at break passes through an optimal level as the heating cycle increases. The elongation at break may be taken as a measure of the toughness of the polymer. Further work could be carried out to measure the actual impact strength of the moulding and quantify its variation with the bubble content

References

1. Duncan, R.E., Zimmerman, A.B., "Rotational Moulding Of High Density Polyethylene", Society of Plastics Engineers, Regional Technical Conference, March 1976, p50-55.

2. Anon., " Rotational Moulding of Alkathene Polyethylene Powders", Technical Service Note A110, Second edition, Polyolefins Group, ICI Plastics Division, Welwyn Garden City, Herts.

3. Anon., "Factors Affecting the Properties of Rotational Mouldings" Alkathene Technical Service Note A122, Polyolefins Group, ICI Plastics Division, Welwyn Garden City, Herts.

4. Carrow, G.E., "Crosslinkable Rotational Moulding High Density Polyethylene Resins and Applications" Society of Plastics Engineers, Regional Technical Conference, Polyolefins 2: Feb 1978, p177 – 190.

5. McDonagh, J. M., "Rotational Casting of Acetal Copolymer", Society of Plastics Engineers, Regional Technical Conference, March 1969, p35 – 41.

6. MacAdams, J.L., "How to Predict Physical Properties of Rotomoulded Parts", Society of Plastics Engineers, Regional Technical Conference, Injection and Rotational Moulding, 1975, p64 – 71.

7. Tatar, S.L., "Nonferrous Moulds for Blow Moulding and Rotational Moulding", Society of Plastics Engineers, Regional Technical Conference,, Feb 1971, p 5-7.

8. Anon., "Rotomoulders Ready for More Growth", Plastics and rubber Weekly, No 935, May 1982, p3

9. Coucourakis, G., "Plastics Get Tough – Rotational Moulding Offers Low Mould Costs", Plastics and Rubber news, Jan 1979, p9

10. Plastics and Rubber weekly, " PE Resins Added to DuPont..." No957, Oct 1982, p6

11. Duncan, R.E., Ellis, D.R., McCord, R.A., "Rotational Moulding", US Industrial Chemicals Company.

12. Anon, "Rotational Moulding of Microthene Polyethylene", Booklet NoPL 23 – 865, US Industrial Chemicals Company.

13. Johnson, W.C., "Economic Evaluation of Rotational Moulding", Symposium on Rotational Moulding, US Industrial Chemicals Company.Nov 1963

14. Sowa, M.W., "Rotational Moulding of Glass Reinforced Polyethylene" Society of Plastics Engineers, 28th Annual Technical Conference, May 1970, p 703-707

15. Anon. "Resins Debut at Rotomoulding..", Plastics World, No6, May 1983, p11-12

16. Shearer, P., "Rotmoulding is Getting Bigger", Modern Plastics, Oct 1970, p86-89

17. Merril,R., "Pilot installation confirms the effectiveness of heat conservation...", Plastics Engineering Aug 1979, p 30-33.

18. Anon., Vistron Corporation, "Machinery and Equipment", Modern Plastics, Aug 1969 p 122-136

19. Anon., "Dual Shuttle Rotational Moulding Machine", Rotodyne Manufacturing Corporation, Building 12, Brooklyn Navy Yard, Brooklyn, New York.

20. "New Rotomoulding Machine Offers Liquid Heating and Cooling", Modern Plastics, Aug 1968 p123.

21. Paquette, S.R., "A Guide for Selecting Rotational Moulding Powders", Society of Plastics Engineers, Regional Technical Conference, March 1969, p 13-23.

22. Ramazzotti, D. J., "Rotational Moulding", Plastics Engineering, June 1976, p33-35.

23. Ramazzotti, D. J., "Rotational Moulding", Plastics Engineering, Dec 1975, p32-34.

24. Nickerson, J.A., "Rotational Moulding", Modern Plastics Encyclopedia, 1968-1969, p 806-885.

25. Neidinger, W.K., "Rotational Casting – State of the Art from a Custom Moulder's Viewpoint", Society of Plastics Engineers, 28th Regional Technical Conference, May 1970, p700 –702.

26. Wright, V., "Big Push Starts in Powder Moulding", Modern Plastics, March 1968, p64-70.

27. Crawford, R. J., "Rotational Moulding", Queens University, Belfast.

28. Anon., "Rotational Moulding Systems", Plastics Engineering, June 1974.

29. Soderquist, R. E., "Rotational Casting of Powders", Society of Plastics Engineers, Regional Technical Conference, Plastics Powders, March 1967, p59-65.

30. Emnrich A., "What's New in Rotomoulding", Plastics Technology, Oct 1978, Vol 24, Pt 11, p 87-91.

31. Rees, R.L., "Rotational Moulding", Modern Plastics Encyclopaedia, 1968-1969, p 884-885.

32. Ramazzotti, D.J. "Rotational Moulding: A Process Whose Time Has Come", Plastics Engineering, Oct 1979, p 47-49.

33. Nickerson, J.A., "Rotational Moulding", Modern Plastics Encyclopaedia, 1968, p 825-833.

34. Anon., "Polyethylene Rotomoulding Markets: New Uses", Plastics World, Vol42, 2, Feb 1984.

35. Anon., "Polyethylene Trailer Body", Plastics and Rubber weekly, No996, 16July 1983.

36. Anon., "New Rotomoulding Material – Polystyrene", Modern Plastics, Oct 1976, p98-99.

37. Eigo,M., "Where's the Action in ABS?", Modern Plastics, Feb 1968, p 79-83.

38. Sneller, J., "Rotational Moulding has New Values for Foams and Thermosets", Modern Plastics, Nov 1979, p 46-49.

39. Titterton, W., "Corrosion Resistent Linings by Rotational Moulding", Machine Design, Vol.56, No.10, may 1984, p 106-111.

40. Petrucelli, F., "Rotomoulding Nylon 6", Plastics Technology, Vol 28, No6, June 1982, p 73-76.

41. Carrow, G. E., "Crosslinkable Rotational Moulding High Density Polyethylene" Society of Plastics Engineers, 30th Regional Technical Conference, Plastics Powders, May 1972, p 762-765.

42. Crater, W., "Rotational Moulding of Nylon 11", Society of Plastics Engineers, Regional Technical Conference, Plastics Powders, March 1967, p59-65.

43. Kaufman, W. J., Jackson, D.P. "Plastisol Moulding", Modern Plastics Encylopedia, Vol 41 part 1A, 1964, p.676-682.

44. Robertson, A. B. Toelcke, G. A., "Rotolining with E-CTFE Fluoropolymer", Modern Plastics, Dec 1973, p.74-75.

45. Anon "Polyolefins Tanks", Plastics and Rubber Weekly, No. 964, 20th November 1982, p.6.

46. Anon "Emergency Milk Tank", Plastics and Rubber Weekly, No. 976, 26th February, 1983, p. 16.

47. Anon "Alkathene Polyethylene", Technical Data Sheet, ATD 316, Polyolefins Group, ICI Plastics, Welwyn Garden City, Herts.

48. Anon "Mould Release Agents", Du Pont of Canada Limited, PO Box 660, Montreal, Canada, H3C 2V1.

49. Anon "Rotational Moulding Process Va. riables", Du Pont Company, Plastics Department, Wilmington, Delaware 1989.

50. Ramazzotti, D., "Rotational Moulding – the State of the Art", Society of Plastics Engineers, Regional Technical Conference, October 1975, p.43-65.

51. Anon "Powder Characteristics", Du Pont of Canada Limited, PO Box 660, Montreal, Canada, H3C 2V1.

52. Rees, R. L., "Polyethylene and Crosslinked Polyethylene for Rotational Moulding", Society of Plastics Engineering, ANTEC 83, 40th Annual Technical Conference, 10-13th May, 1982, p.621-626.

53. Anon "Process Variables", Du Pont Pont of Canada Limited, PO Box 660, Montreal, Canada, H3C 2V1.

54. Throne, J. L., Plastics Process Engineering, Marcel Dekker Inc.

55. Rao, M. A., Throne, J. L., "Principles of Rotational Moulding", Polymer Engineering and Science, July 1972, p.237-339.

56. Rees, R.L., "Rotational Moulding of High Density Polyethylene", Society of Plastics Engineering, 27th Annual Technical Conference, May 1969, p.567-571.

57. Martino, R., "Rotomoulding: On the Brink of Something Big", Modern Plastics, September 1976, p.69-71.

58. Obstfeld, F. A., "When to Rotomould and When Not To", Modern Plastics, March 1968.

59. Anon "Rotational Moulding – The Unique Plastics Process", Association of Rotational Moulders, 221 North La Salle Street, Chicago, Illinois 60601.

60. Sanada, M., "Economics of Plastic Moulding Processes", Society of Plastic Engineers, 31st Annual Technical Conference, May 1973, p.237-240.

61. Dreger, D. R., "Selecting a Process for Plastic Parts", Machine Design, February 1980, Vol.52, part 4, p.76-80.

62. Beau, G. L., Caren, S., "Engineers Guide to Designing Rotationally Moulded Plastic Parts", Society of Plastics Engineering, 41st Annual Technical Conference, 2-5 May 1983, p.226-229.

63. Krau, T.J., "Rotational Moulding", Modern Plastics Encyclopedia, Vol. 60, October 1983.

64. Ogorkiewicz, R. M., "Thermoplastics: Effects of Processing", Iliffe Books Ltd.

65. Ogorkiewicz, R. M., "Thermoplastics: Properties and Design", John Wiley and Sons.

66. Anon., "Effects of Fusion on the Physical Properties of Rotomoulded Parts", Du Pont of Canada Limited, , PO Box 660, Montreal, Canada, H3C 2V1.

67. Throne, J. L., "Rotational Moulding of Reactive Liquids", Society of Plastics Engineering, 32nd Annual Technical Conference, 1974, p.367-370.

68. Anon., "Alkathene Polyethylene", Technical Data Sheet A TD315, Polyolefins Group, ICI Plastics Division, Welwyn Garden City.

69. "Rotational Moulding Equipment", Du Pont of Canada Limited, , PO Box 660, Montreal, Canada, H3C 2V1.

70. "Ideas for Using Rotational Moulding", Association of Rotation Moulders.

71. "Rotational Moulds", Du Pont of Canada Limited, , PO Box 660, Montreal, Canada, H3C 2V1.

72. "New Dimensions in Rotomoulding", Modern Plastics, April 1966.

73. Ward, T. K., "Linear Low Density Polyethylene", Modern Plastics Encyclopedia, Vol.60, October 1983.

74. "HDPE Rotomoulding Resin", Modern Plastics, Vol.60, March 1983, p.74.

75. "Production of Rotationally Moulded Hollow Articles by Activated Anionic Polymerisation of Lactams", Modern Plastics, May 1968, p.70.

76. "Latch for Rotomoulds", Simmons Fasteners Corporation, PO Box 693, Albany, New York 12201.

77. Kamal, M. R. et al, "Anisotropy and Dimensions of Blow Moulded Polyethylene Bottles", Polymer Engineering and Science, Vol.22, No.5, April 1982.

78. "Rotationally Moulded Storage Tanks", B P and R, October 1982.

79. "New Ways to Make Big Plastic Parts", Machine Design, September 1982.

80. Ward, N. M., "The International Market for Rotational Moudling", DSM Rotational Moulding Seminar, 25-27th April 1982, Holland.

81. Harkin-Jones, E., Crawford, R.J.,"Guidelines for the Rotational Moulding of Liquid Polymers", Society of Plastics Engineers, Annual Technical Conference, 1998.

82. Restiano, M. C., "Try Linear Low Density Polyethylene Parts for Faster, Tougher Rotomoulded Parts", Plastics Engineering, July 1981, p.39-42.

83. Rabe, W. P., "An Introduction to Linear Low Density Polyethylene", Plastics and Rubber News, November 1981, p.42-52.

84. Tomo, D., "Rotational Moulding of Polyethylene Powders", Society of Plastics Engineers, Annual Technical Conference, May 1971, Chicago, Illinois.

85. Kraus, T. J., "Formulating Plastisols for Rotational Moulding", Society of Plastics Engineers, Annual Technical Conference, May 1971.

86. Stepaneck, G., "Rotational Moudling of Plastisols", Society of Plastics Engineers, Annual Technical Conference, May 1971.

87. Hickey, H. F., "Rotationally Cast Products from Caprolactam", Society of Plastics Engineers, Annual Technical Conference, May 1971.

88. Nickerson, J.A., "New Dimensions in Rotomoulding", Modern Plastics, April 1966, p86-89.

89. Stufft, T.J., strebel, J., "How Grinder Variables Affect Bulk Density and Flow Properties of Polyethylene", Plastics Engineering, p 29-31, Aug 97.

90. Annechini, D. Takacs, E.,, Vlachopoulos, J., "Some New Results On Rotational Moulding of Metallocene Polyethylenes", p 1291- 1293, ANTEC 2001.

91. Lontz, J. F., Sintering of Polymer Materials, Fundamental Phenoma in the Materials Sciences, Vol.1, Bonis, L. J. and Hasner, H. H.

92. Rosenweig, N., Narkis, M., Sintering behaviour of PMMA, Poly. Eng. Sci., 21, p988, 1980.

93. Rozenweig, N. and Narkis, M., Dimensional Variations of Two Spherical Polymeric Particles During Sintering, Poly. Eng. Sci, 21, 1981.

94. Rozenweig, N. and Narkis, M., Sintering Rheology of Amorphous Polymers, Poly. Eng. Sci., 21 (17) 1981.

95. Rozenweig, N. and Narkis, M., Newtonian Sintering Simulator of Two Spherical Particles. Poly. Eng. Sci. 23 1983.

96. Rao, M. A. and Throne, J. L., Theory of Rotational Moulding: Part III. Sintering and Degradation, Soc. Of Plastics Engineers, May 1972.

97. Progelhof, R. C., Cellier, G. and Throne, J. L., New Technology in Rotational Moulding: Powder Densification, Society of Plastics Engineers, Annual National Tech. Eng. Conf., 1982.

98. Kelly, P. Y. A Microscopic Examination of Rotomoulded Polyethylene. Du Pont, Canada. Undated.

99. Tadmor, Z. and Gogos, C. G., Principles of Polymer Processing, John Wiley and Sons, Toronto, 1979.

100. Frenkel, J. Viscous Flow of Crystalline Bodies Under the Action of Surface Tension, J. Phys. (USSR) 1945.

101. Kuczynki, G. C. and Zaplatynskyj, J., Sintering of Glass, J. Am. Ceramic Soc. 39. 1956.

102. Kingery, W.D., Berg., M., J. Appl. Phys., 26, p1205, 1955.

103. Holman, J. P., Heat Transfer, 2nd Ed., McGraw-Hill, New York, 1968.

104. Michaels, A. S. and Bixler, H. J., Solubility of Gases in Polyethylene, J. Poly. Sci., 1961.

105. Michaels, A. S. and Bixler, H. J., Flow of Gases Through Polyethylene, J. Poly. Sci., 1961.

106. Kline, G. M., Permeability of Polymers to Gases, Vapours and Liquids, Modern Plastics, March 1966.

107. Ramazzotti, D., "Rotational Moulding – The State of the Art", SPE., Regional Technical Conference, Oct 1975, p 43-65.

108. McKelvey, J. M., "Heat Transfer and Thermodynamics", Processing of Thermoplastic Materials, E. C. Bernhardt, Ed.

109. Sundstrom, D. W., Young, C., "Melting Rates of Crystalline Polymers Under Shear Conditions", Polymer Engineering and Science, Jan 1972, Vol 12, No.1.

110. Griffin, O. M., "Thermal Transport in Contact Melting of Solids", Polymer Engineering and Science, July 1972, Vol.12, No.4.

111. Ross, T. K., Chemical Engineering Science, Vol.1, No.212, 1952.

112. Griffin, O. M., "Heat Transfer to Molten Polymers", Polymer Engineering and Science, March 1972, Vol.12, No.2.

113. Rao, M. A., Throne, J. L., "Theory of Rotational Moulding: Part 1, Heat Transfer", Society of Plastics Engineers, 30th Annual Technical Conference, 1976, p.752-756.

114. Bunn and Alcock Bunn, C. W. and Alcock, T. C., Trans Farad Soc., 11, 317, 1945.

115. Personal communication, Dr. Hemsley, School of Polymer Technology, University of Loughbrough.

116. Nielsen, L. E., "Mechanical Properties of Polymers", Reinhold, Chapter 5, 1962.

117. Ritchie, P. D., Op. Cit. Chapter 2, 1965.

118. Alfrey, T. J., "Mechanical Behaviour of High Polymers", Interscience, Chapter F, 1948.

119. Ogorkiewicz, R. M., et al, SPE Journal, 25, (3) 43, 1969.

120. Ferry, J. D., "Viscoelastic Properties of Polymers", 2nd ed. Wiley, 1970.

121. Xu, L. and Crawford, R. J., J. Mat. Sci., Vol.28, 2067, 1993.

122. Spence, A. G. and Crawford, R. J., "The Effect of Processing Variables on the Formation and Removal of Bubbles in Rotationally Moulded Products", Poly. Eng. Sci., Vol.36, No.7, April 1996.

123. Kucznski, G. C., Neuville, B. and Toner, H. P., J. App. Poly. Sci., Vol.14, 2069, 1970.

124. Lontz, J. F., "Sintering of Polymer Materials", Fundamental Phenomenon in Materials Science, Bonnis, L. J. and Hanser, H. H., Plenum Press, New York, 1964.

125. Crawford, R. J. and Scott, J. A., Plast. Rubb. Proc. Appl., Vol.7, 85, 1987.

126. Scott, J. A., PhD thesis, Queen's University of Belfast, 1986.

127. Bellehumeur, C. T., Bisaria, M. K., and Vlachopoulos, J., "An Experimental Study and Model Assessment of Polymer Sintering", Poly. Eng. Sci., Vol.36, No.17, 1996.

128. Hornsby, P. R. and Maxwell, A. S., J. Material Sci., Vol.27, 2525, 1992.

129. Eshelby, J. D., Metals Trans., Vol.185, 806, 1949.

130. Hopper, R. W., J Fluid Mech., Vol.230, 355, 1991.

131. Mackenzie, J. K. and Shuttleworth, R., Proc. Phys. Soc., Vol.62, 833, 1949.

132. Cosgrove, G. J., Strozier, J. A., Seigle, L. L., J. Appl. Phys., Vol.47, 1258, 1976.

133. Scherer, G. W., J. Am. Ceram. Soc., Vol.60, 236, 1977.

134. Jagota, A. and Scherer, G. W., J. Am. Ceram. Soc., Vol.78, 521, 1995.

135. Ross, J. W., Miller, W. A. and Weatherly, G. C., J. Appl. Phys., Vol.52, 3884, 1981.

136. Kuiken, H. K., J. Fluid Mech., Vol.214, 503, 1990.

137. Van der Vorst, G. A. L., PhD thesis, Eindhoven University of Technology, The Netherlands, 1994.

138. Martinez-Herrera, J. I. And Derby, J. J., AIChE, J., Vol.40, 1794, 1994.

139. Jagota, A. and Dawson, P. R., J. Am. Chem. Soc. Vol.73, 173, 1990.

140. Jagota, A. and Dawson P. R., Acta Metall., Vol.36, 2551, 1988.

141. Mazur, S., "Coalescence of Polymer Particles", Polymer Powder Technology, Narkis, M. and Rosenzweig, Eds, John Wiley and Sons, New York, 1995.

142. Mazur, S. and Plazek, D. J., Prog. Org. Coat., Vol.24, 225, 1994.

143. Siegmann, A., Raiter, I., Narkis, M. and Eyerer, P., J. Mat. Sci., Vol.21, 1180, 1986.

144. Barnetson, A. and Hornsby, P. R., J. Mat. Sci., Lett., Vol.14, 80, 1995.

145. Bellehumeur, C. T. and Vlachopoulos, J., SPE, ANTEC, 1998.

146. Pokluda, O., Bellehumeur, C. T. and Vlachopoulos, J., AichE J., 1997.

147. Kontopoulou, M. and Vlachopoulos, J., "Bubble Dissolution in Molten Polymers and its Role in Rotational Moulding", Poly. Eng. Sci., July 1999, Vol. 39, No.7

148. Beall, G. L., "Rotational Moulding, Today and Tomorrow", Pg.3178, ANTEC 1997.

149. Wright, J., Spence, A. G. and Crawford, R. J., "Analysis of Heating Efficiency in Rotational Moulding", Pg.3184, ANTEC 1997.

150. Liu, J., Lai, C. "Using the Taguchi Technique to Optimize the Rotational Moulding Process", Pg. 3189, ANTEC 1997.

151. Dority, Howard, H., "Colour For Rotational Moulding – The Challenges We Face", Pg.3194, ANTEC 1997.

152. Xu, L., Crawford R. J., "The Development of the Computer Simulation Program for the Rotomolding Process", Pg.3205, ANTEC 1997.

153. Attaran, M. T., Wright, E. J., Crawford, R. J., "Computer Modelling of the Rotational Moulding Process", Pg.3210, ANTEC 1997.

154. Gogos, C. G., Olson, L., Liu, X., Pasham, V. R., "Computational Model for Rotational Moulding of Thermoplastics", Pg.3216, ANTEC 1997.

155. Kontopoulou, M., Takacs, E., Bellehumeur, C. T., Vlachopoulos, J., "A Comparative Study of the Rotomolding Characteristics of Various Polymers", Pg.3220, ANTEC 1997.

156. Crawford, R. J., "Reducing Cycle Times in Rotational Moulding – A Challenge", 56th Annual Technical Conference of the Society of Plastics Engineers, Plastics on My Mind, , ANTEC 1998, p 1108

157. Bellehumeur, C. T., Vlachopoulos, J., "Polymer Sintering and Its Role in Rotational Molding", Pg.1112, ANTEC 1998.

158. Spence, A., "Roto-Blow Moulding, a Rotational Moulding Hybrid", ", 56th Annual Technical Conference of the Society of Plastics Engineers, Plastics on My Mind, , ANTEC 1998, p 1108

159. Rake, W.P.J., "An Introduction to Linear Low Density Polyethylene", Plastics and Rubber News, Nov 1981, p 42-52

160. Gogos, C. G., Liu, X., Olson, L. G., "Cycle Time Predictions for the Rotational Molding Process with and without Mold/Part Separation", Pg.1133, ANTEC 1998.

161. Cramez, M. C., Oliveira, M. J., Crawford, R. J., "Relationship between the Microstructure and the Properties of Rotationally Moulded Plastics", Pg.1137, ANTEC 1998.

162. McDaid, J., Crawford, R. J., "The Grinding of Polyethylene Powders for use in Rotational Molding", Pg.1152, ANTEC 1998.

163. Liu, S.-J., Ho, C.-Y., "Experimental Investigation of the Warpages in Rotationally Molded Parts", Pg. 1156, ANTEC 1998.

164. Liu, S.-J., Tsai, C.-H., "An Experimental Study of Foamed Polyethylene in Rotational Molding", Pg.1161, ANTEC 1998.

165. Kontopoulou, M., Takacs, E., Vlachopoulos, J., "Polymer Melt Formation and Densification in Rotational Molding", Pg.1428, ANTEC 1999.

166. Gogos, C. G., "Bubble Removal in Rotational Molding", Pg.1433, ANTEC 1999.

167. Wright, E. J., Crawford, R. J., "Computer Simulation of the Rotational Moulding of Plastics", 57th Annual Technical Conference of the SPE on Plastics Bridging the Millenia, ANTEC 99, May 02-06, 1999.

168. Bellehumeur, C. T., "Combined Effect of Polymer Sintering and Heat Transfer in Rotational Molding", Pg.1446, ANTEC 1999.

169. Wright, M. J., Crawford, R. J., "A Comparison between Forced Air Convection Heating and Direct Electrical Heating of Moulds in Rotational Moulding", 57th Annual Technical Conference of the SPE on Plastics Bridging the Millenia (ANTEC 99), May 02-06, 1999. Pg.1452.

170. Weber, M., Gonzales, R., "Viscoelastic Properties of Rotational Molding Resins", Pg.1468, ANTEC 1999.

171. Abu Fara, D. I., Kearns, M. P., Crawford, R. J., "System Modelling for the Control of the Rotational Moulding Process", Pg.1471, ANTEC 1999.

172. Robert, A., Crawford, R. J., "The Effect of Fillers on the Properties of Rotationally Moulded Polyethylene", 58th Annual Technical Conference of the Society of Plastics Engineers, May 07-11, 200, ANTEC 2000; Society of Plastics Engineers Technical Papers, Conference Proceedings, Vols I-III, 1399-1403, 2000

173. O'Neil, F.M., McDonagh, J.M., "Rotational Moulding of Celcon Acetal Copolymer" Society of Plastics Engineers, Annual Technical Conference, May 1971, Chicago, Illinoise.

174. Spence, A., "Investigation of the Rheological Properties of Rotomolding Resins", Pg.1482, ANTEC 1999.

175. Wisley, B. G., "The Rotational Molding of Glass Fibre Reinforced Polyethylene", Pg. 1487, ANTEC 1999.

176. Throne, J. L., "The Foaming Mechanism in Rotational Molding", Pg.1304, ANTEC 2000.

177. Liu, S.-J., Yanh, C.-H., "Rotational Molding of Polyethylene Foam by Pellets", Pg.1309, ANTEC 2000.

178. Pop-Iliev, R., Park, C. B., "Processing of Polypropylene Foams in Melt Compounding Based Rotational Foam Molding", Pg.1314, ANTEC 2000.

179. Wang, X., Harkin-Jones, E., Crawford, R. J., Fatnes, A. M., "Investigation of Rotational Moulding Characteristics and Mechanical Properties of Metallocene Polyethylene", 58th Annual Technical Conference of the Society of Plastics Engineers, May 07-11, 200, ANTEC 2000; Society of Plastics Engineers Technical Papers, Conference Proceedings, Vols I-III, 1326-1330, 2000.

180. Takacs, E., Annechini, D., Vlachopoulos, J., Kontopoulou, M., "An Investigation of the Rotomoldability of New Generation Polyethylene", Pg.1331, ANTEC 2000.

181. Rangarajan, P., Huang, J., Baird, D., "Studies on the Rotomolding of Liquid Crystalline Polymers", Pg.1338, ANTEC 2000.

182. Cramez, M. C., *Oliveira, M. J., Crawford*, R. J., "Optimisation of Rotational Moulding of Polyethylene by Predicting Antioxidant Consumption", *Polymer* Degradation and Stability, 2002, Vol 75, no2, p321-327

183. Bellehumeur, C. T., Tiang, J. S., "Modelling of Bubble Formation in Rotational Molding", Pg.1356, ANTEC 2000.

184. Kearns, M. P., Corrigan, N., Crawford, R. J., "A Comparison between Open Flame and Hot Air Heating Methods for the Rotational Moulding of Plastics", 58th Annual Technical Conference *of the Society of* Plastics Engineers, May 07-11, 200, ANTEC 2000; Society of Plastics Engineers Technical *Papers, Conference* Proceedings, Vols I-III, 1360-1365, 2000.

185. Godinho, J., Cunha, A.M., Crawford, R.J., "Property Variations in Polyethylene Articles Produced by a Variety of Moulding Materials", ANTEC 1997, Plastics Saving Planet Earth, Conference Proceedings, p 2829-2833.

186. Beall, G. L., "The What, How and Why of Rotational Molding", Pg.1368, ANTEC 2000.

187. Bothun, G., "Aesthetics, Industrial Designers, and Designing for Rotational Molding", Pg.1372, ANTEC 2000.

188. Fawcett, J., "Computer Aided Design for Rotationally Molded Parts", Pg.1385, ANTEC 2000.

189. Bickerton, S., Crawford, R. J., "Investigations into Rotational Moulding of Short Fibre Reinforced Thermoset Resins", Pg.1276, ANTEC 2001.

190. McDowell, G. W. G., Orr, J. F., Kissick, J., Crawford, R. J., "A Preliminary Investigation into the Use of Wood Fibers as a Filler in the Rotational Molding of Polyethylene", Pg. 1281, ANTEC 2001.

191. Tiang, J. S., Bellehumeur, C. T., "Non-Isothermal Melt Densification in Rotational Molding", Pg.1307, ANTEC 2001.

192. Dodge, P. T., Perry, J. L., "Rotomolded Part Density and Its Relationship to Physical Properties", Pg.1317, ANTEC 2001.

193. Guillen-Castellanos, S. A., Bellehumeur, C. T., Weber, M., "Polyethylene Powder Characteristics: Impact on Polymer Sintering and Rotational Molding", Pg.1321, ANTEC 2001.

194. Van Hooijdonk, J. P. F., Kearns, M. P., Armstrong, C. G., McCann, B., Coey, L., Crawford R. J., "The Influence of Different Processing Parameters on the Properties of Polypropylene for Rotational Moulding", Pg.1326, ANTEC 2001.

195. Kissick, J., Wang, X., Harkin-Jones, E., Crawford R. J., "Falling Weight Impact Testing Analysis of Rotationally Moulded Polyethylene", Pg.1331, ANTEC 2001.

196. Vasudeo, Y. B., Nabar, S. M., Kapadia, J., Rangaprasad, R., "Studies in Rotational Moulding of Linear Polyethylene Modified with Elastomers and Fillers for Automotive Exteriors", Pg.1336, ANTEC 2001.

197. Throne, J. L., "Powder Flow During Rotational Molding", Pg.1230, ANTEC 2002.

198. Pick, L. T., Harkin-Jones, E., "An Investigation of the Impact Behaviour of Rotomoulded Polyethylenes Over a Wide Temperature Range", Pg.1245, ANTEC 2002.

199. Crawford, R. J., Cramez, M. C., Oliveira, M. J., Spence, A., "The Importance of Monitoring Mold Pressure During Rotational Molding", Pg.1250, ANTEC 2002.

200. Pop-Iliev, R., Park, C. B., "Single-Step Rotational Foam Molding of Skin-Surrounded Polyethylene Foams", Pg.1276, ANTEC 2002.

201. Spence, A., "Roto-Blow Moulding, A Rotational Moulding Hybrid", Centro Incorporated, Society of Plastics Engineers Incorporated, ANTEC 1998.

202. Ahlgren, E., Tuel, D., Goodman., "Electric Infrared versus Gas Fired Rotational Moulding", Society of Plastics Engineers Incorporated, ANTEC 1998.

203. Crawford, R.J., Nugent, P., Plast.Rubb.Proc.Appl., 11, 107, 1989.

204. Crawford, R.J., Nugent, P., Xu, L., Adv., Polym. Tech., 11, 181, 1992.

205. Syler, State Industries Inc., 500 By Pass Rd, Ashland City., Tenesse 37105.

206. The Graphics Systems Company, 999 Highway 89A, Claksdale, Arizona 86324.

207. Progelhof, R.C., Throne, J. L., "The Role of Transient Heat Transfer in Plastics Processing", Society of Plastics engineers, 34th Annual Technical Conference, April 1976, pages 532- 6.

208. Birley, A.W., "Polymer Crystallinity and the Engineer", Journal of Polymer Science, No 62, 1978, Pgs 343-351.

209. Whitehead, J., "Dow PE Expert Urges Caution On Growth rate", Plastics and Rubber Weekly, No 962, Nov 1982.

210. Clark, N., Durney, T.E., "Recent Advances in Particle Shape Characterisation", Journal of Powder and Bulk Solids, Technology, Vol 8, 1984, Page 21 – 24.

211. Crawford, R., J., "Rotational Moulding", RAPRA Review Reports, 1993, Vol 6, No 11, Issue 71.

212. Anon., "Sclair 8307 Linear Low Density Polyethylene – Two Decades of Experience" DuPont of Canada Ltd, PO Box 660, Montreal, Canada H3C 2V1.

213. Tanaka, A., "Rotational Moulding of ABS Resin", Japan Plastics, p16., Jan 1974.

214. Scott., J., "Rotational Moulding", PhD thesis, Queens University, Belfast, 1985.

215. Liu., Shih-Jung, Chen, Chi-Feng, "Optimisation of Bubble Size in Rotationally Moulded Parts", Plastics, Rubber and Composites, Vol 29, No8, 2000.

216. Callan, N., Kearns, M.P., Spencer, H., Crawford, R.J., "Effects of Cooling Rate on the Mechanical Properties of Rotationally Moulded Parts", Queens University, Belfast.

217. Xu, L., Crawford R. J., "Computer Simulation of the Rotational Moulding Process", Plastics, Rubber and Composites and Processing and Applications, Vol. 21, No5, 1994, p257-73.

218. Crawford, R.J., "Design of Stiffening Features in Rotationally Moulded Plastic Parts", ANTEC 2000, Society of Plastics Engineers, p 1388-1392, 2000.

219. Robert, A., Orr, J.F., "Influence of Mica and Talc Fillers on the Poperties Of Rotationally Moulded LLDPE", ANTEC 2000, Society of Plastics Engineers, p1399-1403.

220. Henwood, N., "Adding Value to Rotational Mouldings with Colour and Special Effects", ANTEC 2000, Society of Plastics Engineers, p1404-1409.

221. Ferrari, G., Andreola, P., Bianchin, E., Valcarenghi, A., "CFC- free Integral Skin Polyurethanes Made by Rotational Moulding", Polyurethanes World Congress, 1993, p 540-545.

222. Zimmerman, A. B., "Fundamentals, Growth and Future of Rotational Moulding", Basic Principles of Rotational Moulding, Ed. P.F. Bruins, Gordon and Breach, 1971.

223. USI Chemicals Symposium on Rotational Moulding, Chicago, Nov 1963.

224. USI Chemicals Symposium on Rotational Moulding, Chicago, Nov 1964.

225. Cramez, M., C., Oliveira, M. J., Crawford, R.J., "Effect of Nucleating Agents and Cooling Rate on the Microstructure and Properties of a Rotational Moulding Grade of Polypropylene", J of Mats Sci, 36, 2001, p2151-2161.

226. Anon., "Rotational Moulding – Choice of Release Agent; Alkathene Polyethylene"
ICI Plastics Division, Technical Data Sheet A. TD 317, Welwyn Garden City, England, 1980.

227. Anon, " Rotational Moulding of Plastic Powders", Engineering Design Handbook, US Army Report, Department of the Army Head Quarters, United Sates Army, 5001 Eisenhower Ave, Alexandria, VA 22333, April 1975.

228. Crawford, R.J., Nugent, P.J., "A New Process Control System for Rotational Moulding", Plastics, Rubber and Composites, Processing and Applications, 17, 1992.

229. Martin, D., Halley, P., Truss, R, Murphy, M., Meusburger, S., "The Development of Nanocomposites to Enhance Functionality of materials for Rotational Moulding", ANTEC 2002, Society of Plastics Engineers, p 1292-1294.

230. Crawford, R.J., "Introduction to Rotational Moulding" Rotational Moulding of Plastics, John Wiley and Sons, New York, 1992.

231. Murphy, M.J., Martin, D. J., Truss, R.., Haley, P., "Improving Polyethylene Performance – The Use of Nanocomposites in Ziegler-Natta Polyethylene for Rotational Moulding", ANTEC 2002, Society of Plastics Engineers, p1286-1290.

232. Archer, E., Harkin-Jones, E., Kearns, M.P., "Investigation of the processing Characteristics and Mechanical Properties of Metallocene Polyethylene Foams for Rotational Moulding", ANTEC 2002, p 1281- 1285.

233. Takacs, E., Vlachopoulos, J., Rosenbusch, C., "Foaming with Microspheres in Rotational Moulding", ANTEC, 2002, p 1271-1273.

234. Throne, J. L., Sohn, M.S., Adv. Polym. Tech., 9, 1989, p181.

235. Corrigan, N., Harkin-Jones, E., Crawford, R.J., "Rotational Moulding of a Dicyclopentadiene Reactive Liquid Polymer", ANTEC 2002, Society of Plastics Engineers, p1261-1263.

236. Throne, J. L., "Rotational Moulding Heat Transfer – An Update", Polymer Engineering and Science, Vol 16, No4, 1976.

237. Throne, J. L., "Some Factors Influencing Cooling Rates of Rotationally Moulded Parts", Polymer Engineering and Science, Vol 12, No 5, 1972.

238. Sun, D.W., Crawford., R.J., Polym. Eng. Sci., 33, p 132, 1993.

239. Bawiskar., S., White., J.L., Intern. Polym. Proc., 10, p 62, 1995.

240. Xu, L., Crawford, R.J., Plast. Rubb. Comp. Proc. Appl., 21, p 257, 1994.

241. Gogos, C. G., Olson, L.G., Liu., X., Pasham, V. R., Polym. Eng. Sci., 38, p 1387, 1998.

242. Draus, T.J., "Formulating Plastisols for Rotational Moulding", Society of Plastics Engineers, Annual Technical Conference, May 1971, Chicago, Illinois.

243. Rao, M.A., Throne, J. L., "Theory of Rotational Moulding – Part II: Fluid Flow", Society of Plastics Engineers, 30th ANTEC, 1972, p 757 – 758.

244. Schneider, M., "Dry Blend Polyvinyl Chloride", Society of Plastics Engineers, Annual Technical Conference, May 1971, Chicago, Illinois.

245. McDonagh, J.M., "Process Variables in Rotomoulding"Basic Principles of Rotational Moulding, Ed., Bruins, P.F., Gordon and Breach, 1971.

246. Meril, R., "Pilot Installation Confirms the Effectiveness of Heat Conservation Even in a Small Rotational Moulding Oven", Plastics Engineering, Aug 1979, p 30-33.

247. Anon., "Now Clear PC Rotomoulded Parts", Modern Plastics International, p30, Nov 1980.

248. Crawford, R.J., Queens University, Belfast, Nothern Ireland.

249. Hands, D., PhD Thesis, University of Bradford, 1976.

250. Majurey, M.J., "The Demand and the Availability of Thermal Conductivity Data for Polymers", Plastics and Rubber Institute, Vol 2, No3, p111, May/June 1997.

251. Hands, D., Horsfall, F., "The Thermal Diffusivity and Conductivity of Natural Rubber Compounds", Rubber Chemistry and Technology, Vol 50, May/June 1977.

252. Shoulberg, R.H., "The Thermal Diffusivity of Polymer Melts", Journal of Applied Polymer Science, Vol 7, p 1597-, 1963.

253. Hands, D., "The Thermal and Transport Properties of Polymers", J. of Applied Polymer Science, Vol 7, p 1597 – 1611, 1963.

254. Sheldon, R.P., Lane, S.K., "Thermal Conductivity of Polymers – Polyethylene", Polymer Research Laboratories, Department of Chemical Technology, Institute of Technology, Bradford.

255. Hansen, D., Bernier, G.A., "Thermal Conductivity of Polyethylene; the Effects of Crystal Size, Density and Orientation on Thermal Conductivity", Polymer Engineering and Science, Vol. 12, May 1972.

256. Goodman, T. R., Advances in Heat Transfer, Vol. 1, Ch 2, Academic Press, New York, 1964.

257. Eiermann, "Thermal Conductivity of High Polymers", J. of Polymer Science, Polymer Symposium, No6, p 157-

258. Yagi, S., Kunii., D., A.I.Ch.E.J., Vol. 3, p373, 1957.

259. Cogswell, F.M., Polymer Melt Rheology, 1981, George Golwin Ltd., London.

260. McKenna, L.A., "The Properties of Rotationally Moulded Polyethylene" Society of Plastics Engineers, Annual Technical Conference, Oct. 1965, p33-

261. McKenna, L.A., "The Properties and Economics of Rotationally Moulded Polyethylene", Progressive Plastics, Vol 7, p 24-, Dec 1965.